The development and characterisation of biocompatible emulsion templated foams for additive manufacturing

The University Of Sheffield.

Thesis submitted to the University of Sheffield for the degree of Doctor of Philosophy

Colin Sherborne

Department of Materials Science and Engineering

November 2015

ACKNOWLEDGMENTS

I would like to thank my supervisor Dr Frederik Claeyssens, whose optimism, persistence and guidance helped shape this project and open up new opportunities for my future career. Thank you for giving me both the opportunity to work on this project and being given the freedom to explore additional research areas of interest and direction.

I would like to thank the financial supporting bodies that enabled me to undertake this PhD, the Engineering and Physical Sciences Research Council (EPSRC). I would not have been able to complete this work without you.

I would like to thank and acknowledge the following collaborators for the joint publications. Professor Neil R. Cameron, Dr David W. Johnson, Matthew P. Disbury Christopher Pateman. Robert Owen, Thomas Paterson, Nicola H. Green and Gwendolen C. Reilly.

Naturally I owe a huge thanks to everyone who has helped me throughout my work here at Sheffield University. My friends and colleagues: Joe Lemmens, for his useful insight into the details I might have overlooked, as well as always looking at the problem from the correct angle. Tom Paterson, for help throughout the project up until its end. Hossein Bahmaee, for your enthusiasm and helping hand near the end. Shweta Mittar, for providing guidance throughout the project. Nii Armah, for your laughter and friendship throughout. Lindsey Dew, for the collaboration work. Christopher Pateman and Richard Plenderleith, for both your advice and company.

I would like to thank Dr Ihtesham Rehman for allowing me to use his equipment, without it I would not have been able to do post process the PolyHIPE material. Thank you to Dr Nicola Green for all the technical assistance on the confocal microscope

To my partner Natalie. Words cannot express my gratitude and thanks for always being there and not only being patient, but being supportive throughout the late nights and long weekends. You put up with me throughout this project, and I wouldn't be here today without you.

Finally my parents, you have made me who I am today. I appreciate everything you have done for me. I look up to you both and I try to have the same attitude and values that you have.

An optimist sees the glass as being half full.

A pessimist sees the glass as being half empty.

However. An engineer sees the glass as being twice as big as it needs to be.

Acronyms

%	Percentage
µg	Microgram
µl	Microlitre
2D	Two dimensional
3D	Three dimensional
$CHCl_3$	Chloroform
DCE	Dichloroethene
DCM	Dichloromethane
DMD	Digital Micromirror Device
DMEM	Dulbecco's Modified Eagle's Medium
E	Young's modulus
EHA	2-Ethylhexyl acrylate
EtOH	Ethanol
F	Fungizone
FDA	Food and Drug Administration
g	Gram
HDF	Human dermal fibroblast
HIPE	High Internal Phase Emulsion
HLB	Hydrophilic-lipophilic balance
IBOA	Isobornyl acrylate
M	Molar
MeOH	Methanol
mg	Milligram
MG63	Human osteosarcoma cells

ml	Millilitre
mm	Millimetre
MP	Multiphoton
MTT	3-(4,5-dimethylthiazol-2-yl)-2,5-diphenyltetrazolium bromide
NaOH	Sodium hydroxide
PBS	Phosphate Buffered Saline
PLA	Polylactic acid
PolyHIPE	Poly(High Internal Phase Emulsion)
P/S	Penicillin/streptomycin
PCL	Poly ε-caprolactone
PP	Polypropylene
PTFE	Polytetrafluoroethylene
PVC	Polyvinyl chloride
SEM	Scanning electron microscopy
TCP	Tissue culture plastic
TE	Tissue engineering
TPP	Two Photon Polymerisation
TMPTA	Trimethylolpropane triacrylate
Wt %	Weight Percent

Abstract

A High internal phase emulsion (HIPE), contains a high volume ratio between two immiscible liquids which form an emulsion comprising of a droplet phase, and a continuous one. The water volume ratio has to exceed 74% to be classified as a HIPE. When the continuous phase is a polymerizable monomer, a porous polymeric material can be created by emulsion templating of the HIPE to create a highly porous foam called a PolyHIPE.

This thesis will address the growing need to manufacture complex 3D tissue engineering scaffolds from synthetic biocompatible polymeric materials. The PolyHIPEs inherent porous nature is an attractive material for this application. The highly porous interconnected network of the PolyHIPE architecture can provide the basic cellular support, porosity and interconnectivity for cell ingrowth and nutrient/waste removal. The ability to tailor these features by altering the conditions of the initial emulsion, or adjusting the monomer formulation means that the scaffold can be tuned to control the cell material interaction and mimic the native physiological environment of the cells. The development of a Poly ε-caprolactone (PCL) based PolyHIPE opens up another material that can be used for this application, and may be more suitable for future cell based studies.

In this thesis I demonstrate the incorporation of both additive, and subtractive manufacturing techniques to the PolyHIPE material. This is used to introduce a secondary, macroscopic level of porosity on top of the inherent micro-porosity from the templating of water droplets. Projection and scanning stereolithography polymerises the HIPE in a layer-by-layer fashion to produce bespoke porous 3D scaffolds. Laser etching is used to introduce a macro porosity within a PolyHIPE sheet, this is a technique that can be adapted to a range of biomaterials for a high throughput fabrication process. The underlying methodology, characterisation and logistics of using these advanced fabrication techniques to customize the PolyHIPE into novel bespoke porous structures is demonstrated. This method of processing the HIPE has not previously been reported on in the literature to the best of my knowledge, therefore the characterisation presents the groundwork for this structuring methodology for the PolyHIPE.

The first section of this thesis I introduce the stereolithographic fabrication of the PolyHIPE material. This is a hybrid technique where the micro porosity is dictated by the initial emulsion conditions, such as water volume ratio, and the macro structure is dictated by the selective polymerisation of the HIPE. Adjusting the laser intensity has an effect on both the size and structural stability of the polymerised structures, and a fabrication time for basic structures takes only seconds. Proof of concept designs are initially fabricated to demonstrate this approach and characterise the processing parameters. The PolyHIPEs internal morphology is unaffected by the stereolithography fabrication process over its bulk polymerisation counterpart.

The second section focuses on the identification, characterisation and elimination of a surface skin effect that forms around the outside of the polymerised PolyHIPE surfaces. The generation of the surface skin was experimentally shown to occur during the washing stages as the outer surface collapses upon itself. The underlying mechanism behind this comes from the gradual scattering and decrease in polymerizable energy of the Ultraviolet Light (UV) as it is absorbed.

Separate polymerised regions that overlap formed connecting bridges from this UV scattering effect and the addition of a light absorber is shown to significantly increase both the surface porosity and increase the achievable resolution of the stereolithography approach.

The mechanical properties of the PolyHIPE are tailored by altering either the monomer blend or water volume ratio. This demonstrated the tunability of the PolyHIPEs so that it can potentially be tailored for specific cellular applications.

Finally the last chapter focuses on the methodical development of a PCL based PolyHIPE. This is the first example of a photocurable PCL PolyHIPE in the literature to my knowledge. This section is presented as a systematic methodology to identify the key emulsion stability parameters for a stable PCL based emulsion though experimental means, and tailor them to increase emulsion stability. A blend between the PCL and thiolene was initially used as a stepping stone for the pure PCL PolyHIPE. The emulsion stability was found to be highly sensitive to a solvent blend, as well as a particular surfactant. The protocol for a stable PCL based HIPE was eventually established for the now routine development of a PCL PolyHIPE.

Statement of originality

The work presented in this document is entirely my own work, except where I have stated. Where Masters Students' work has been used, the results have been reanalyzed by me.

Publications

(1) David W. Johnson*, Colin Sherborne*, Matthew P. Didsbury, Christopher Pateman, Neil R. Cameron, Frederik Claeyssens. "Macrostructuring of Emulsion-templated Porous Polymers by 3D Laser Patterning." *Advanced Materials* **25**, 3178-3181 (2013). (* joined first author)

(2) Robert Owen, Colin Sherborne, Thomas Paterson, Nicola H. Green, Gwendolen C. Reilly, and Frederik Claeyssens. "Emulsion Templated Scaffolds with Tunable Mechanical Properties for Bone Tissue Engineering." *Journal of the Mechanical Behavior of Biomedical Materials* **54**, 159–172 (2016).

Conference Presentations

(1) Stereolithography of High Internal Phase Emulsions for Tissue Engineering Applications. Colin Sherborne[1], David W. Johnson[2], Matthew P. Didsbury[2], Chris Pateman[1], Neil Cameron[2] and Frederik Claeyssens[1]. [1]The Kroto Research Institute, University of Sheffield, UK and [2,]Department of Chemistry & Biophysical Sciences Institute, Durham University, UK. **TERMIS-EU, Genova, Italy 2014 (Oral)**

(2) Photostereolithography of High Internal Phase Emulsions for Tissue Engineering Applications. Colin Sherborne[1], David W. Johnson[2], Matthew P. Didsbury[2], Chris Pateman[1], Lindsey Dew[1], Neil Cameron[2] and Frederik Claeyssens[1]. 1, The Kroto Research Institute, University of Sheffield, UK and 2, Department of Chemistry & Biophysical Sciences Institute, Durham University, UK. **USES 2014, University of Sheffield (Oral)**

(3) Stereolithography of High Internal Phase Emulsions for Tissue Engineering Applications, Colin Sherborne[1], David W. Johnson[2], Matthew P. Didsbury[2], Chris Pateman[1], Neil Cameron[2] and Frederik Claeyssens[1]. 1, The Kroto Research Institute, University of Sheffield, UK and 2, Department of Chemistry & Biophysical Sciences Institute, Durham University, UK. **TCES 2014, Newcastle (Poster)**

(4) Laser Writing of Neural Tissue Engineering Scaffolds for Biohybrid Devices**,** The Kroto Research Institute, Colin Sherborne. **USES 2013, University of Sheffield (Poster) *Competition winner***

(5) Laser Writing of Neural Tissue Engineering Scaffolds for Biohybrid Devices, Colin R. Sherborne, Christopher J. Pateman and Frederik Claeyssens. The Kroto Research Institute, University of Sheffield**. Living Machines, Barcelona, Spain 2012 (Poster)**

Scientific Image Competitions within the Kroto Research Institute

The Kroto Research Institute is named after Sir Harry Kroto, who was awarded the Nobel Chemistry Prize in 1996 from his discovery the Bucky ball form of carbon, the "buckminsterfullerene". These images were viewed by Sir Harry Kroto during his yearly visits to The Kroto Research Institute.

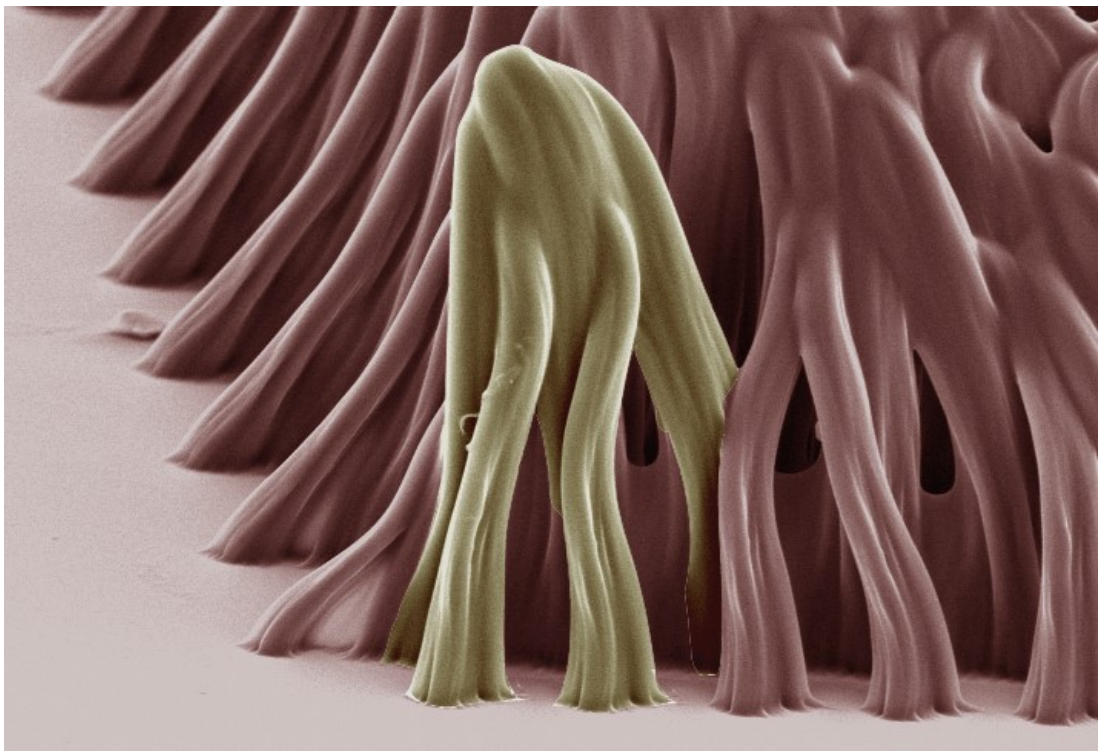

Figure 1: Standing Man. 2013- Winner – *Kroto Research Institute*

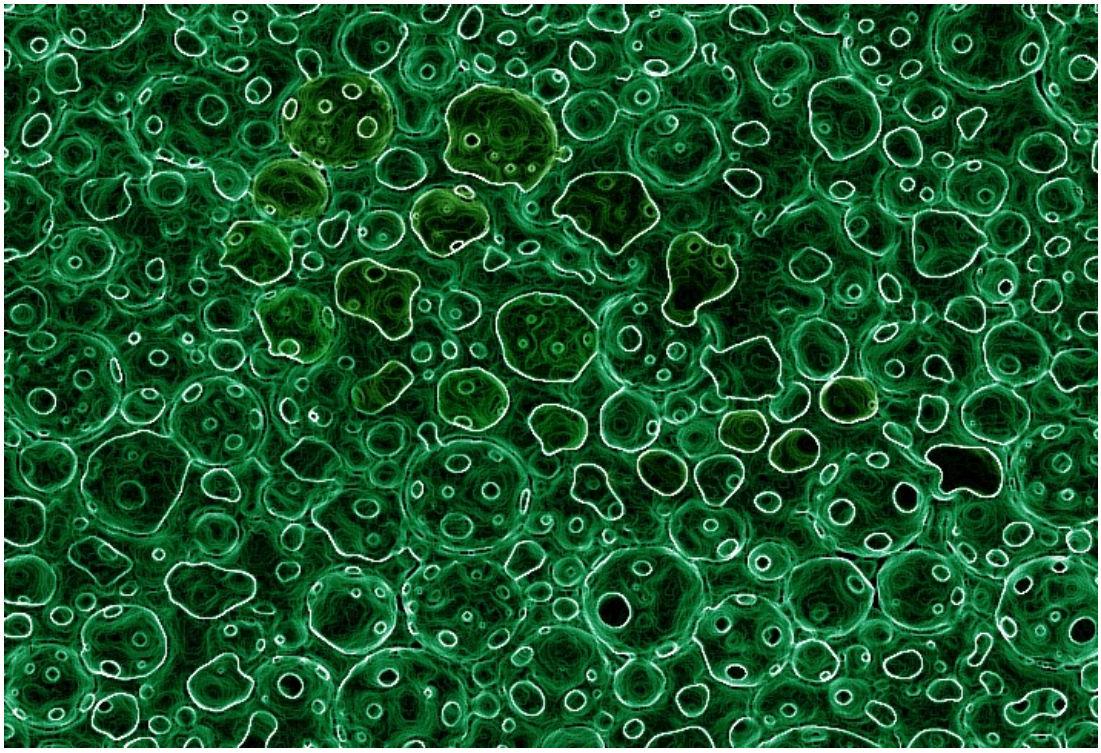

Figure 2: Can you see the fish: 2013-Winner– Kroto Research Institute

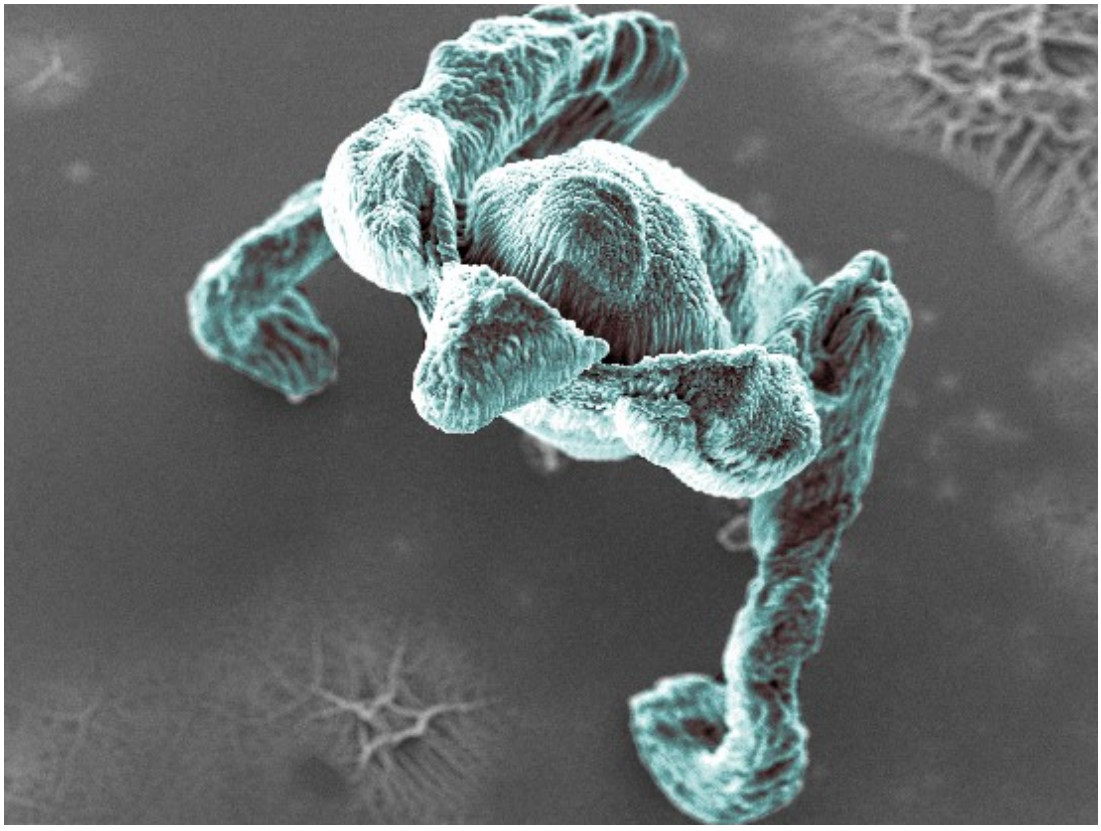

Figure 3: Monster. 2013- Winner– Kroto Research Institute

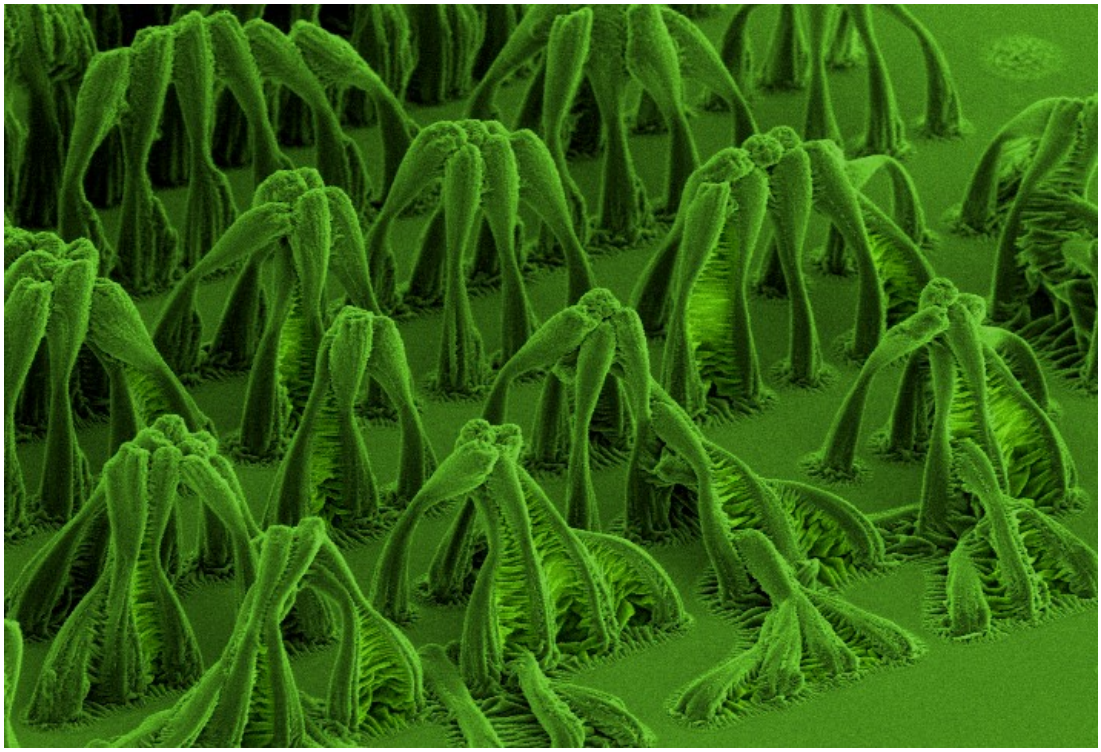

Figure 4: Carnivorous Plant: 2014- Image competition winner in the Materials Science and Engineering department, Sheffield University.

Outreach Scheme: collaboration with local artist Kate Sully

Figure 5: Art exhibition at the Winter Gardens, Sheffield. 2015

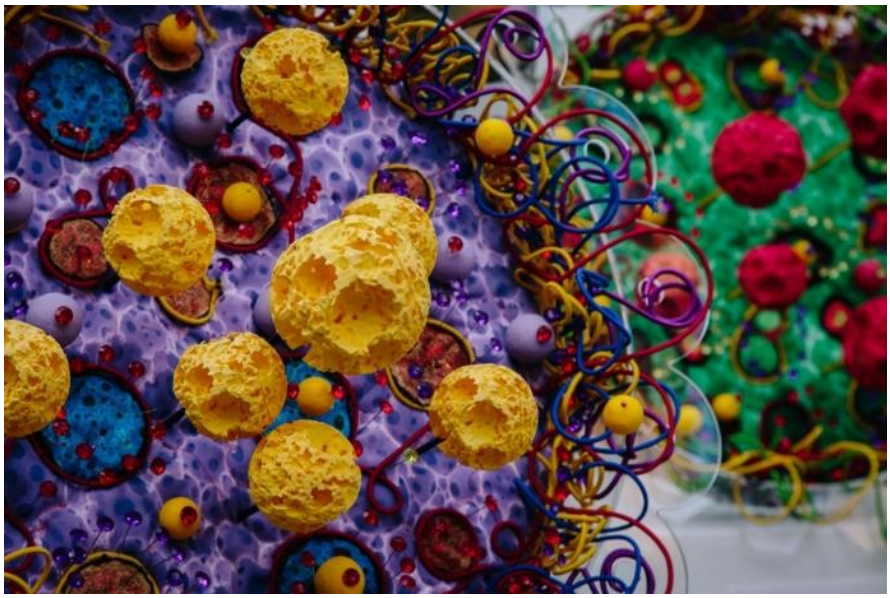

Figure 6: The local artist drew inspiration from my PolyHIPE work to create these sculptures. False colour SEM images of the PolyHIPE are printed on the fabric. 3D printed porous spheres were produced using a 3D file I obtained by imaging the PolyHIPE using a micro-CT. These printed PolyHIPE spheres were spray painted and incorporated into the sculpture.

Contents

List of Figures

1. CHAPTER ONE: Literature review of the PolyHIPE material

Emulsion templating involves preserving the internal shape, and structure, of an emulsion to produce a porous polymer. This fabrication technique requires a thorough understanding of the emulsion conditions and the respective parameters. These have a significant effect on the properties of the final material. The subject of emulsion templating has been well-documented and there are a number of excellent reviews about the PolyHIPE material Silverstein [1], Pulko et al. [2], and Cameron [3]. These reviews offer both a comprehensive review of the PolyHIPE materials and applications that will be outside of the scope of this thesis.

An emulsion is defined as a liquid containing two immiscible liquids; such as oil and water, wherein one of these liquids is in a dispersed phase within the continuous one. In this thesis, the word continuous will be used to describe the liquid phase that is fully connected throughout the entire emulsion, and the discontinuous phase is used to describe the suspended droplet phase; these droplets are isolated from each other within the emulsion as these are surrounded by the thin film of the continuous phase

The stability of the emulsion is dictated by the interfacial tension between the droplet and continuous phase, and this relates to the total interfacial area (the outer surface area of the droplet phase that is in contact with the continuous phase) of the droplet phase. The two liquids are immiscible, and the reduction in this surface area of contact is a thermodynamically driven process, this is achieved by an increase in the average droplet size, which causes a decrease in the interfacial area. The emulsion stability is dependent on its ability to resist this destabilization.

The stability of an emulsion is brought about by using an emulsifying agent. An emulsifying agent is an amphiphilic compound which contains both hydrophobic and hydrophilic ends which enables it to orient itself at the oil/liquid interface thereby preventing the two phases from contacting with each other. It forms a barrier between them, and is an essential requirement for the stability of the emulsion. The emulsion stability is also dependent on a range of factors namely interfacial tension, viscosity, volume fraction ratio and temperature during both the emulsion formulation and the temperature of the polymerisation stage for making a PolyHIPE of the emulsion [4].

Emulsions have been classified into two types depending on which phase is the continuous or discontinuous phase i.e. water-in-oil (W/O) or an oil-in-water emulsion (O/W) depending on which is the droplet phase [5]. A W/O emulsion will contain water droplets suspended in the continuous oil phase, and O/W is the opposite. In an W/O emulsion the oil phase is in turn referred to as the organic phase and the droplet water phase as the aqueous one. Splitting of droplets from larger to smaller ones requires energy input and this is provided by the mechanical force from a stirrer. The mechanical force from the stirrer provides the stress energy to deform, and subsequently breakup the droplets into smaller ones [5]. As the droplets get smaller, more energy is required to break them up hence more shear energy required. Viscosity plays an important part in the droplet formation as the greater the viscosity the more resistance the fluid will have against being broken up.

It is often difficult to visually determine the emulsion type, so a dilution test can be used to do so. An easy method to determine the emulsion type is to add it to water. If a W/O emulsion is added to water then the emulsion will form emulsion droplets suspended with the water, which is referred to as a W/O/W emulsion, whereas a O/W emulsion will spread out. In most cases the emulsion is white. The whiteness of the emulsion is caused by the suspension of droplets scattering the light.

Emulsion templating is a structuring technique were the continuous phase of the emulsion is polymerised around a non-polymerisable droplet phase to produce a porous foam like material [6]. In this process the droplets act like a ‘template’ for the pore formation, and are subsequently removed afterwards to leave behind the hollow voids [7]. A review on the range of different W/O and O/W emulsions that have been used to create these porous foams from a variety of different materials can be found in the feature article by Pulko et al [2]. If the continuous phase contains a polymerisable monomeric solution. Then upon polymerisation the name of the produced porous material will be reflected in the original name for the emulsion used to create it.

The acronym PolyHIPE refers to porous foam created by polymerisation the continuous phase of a high internal phase emulsion (HIPE). The emulsion is classified as being a high internal phase one when the droplet fraction exceeds 0.74 [8], although this can be as high as 0.99 [9] as the classification for HIPE has to be above 74% of the droplet phase. The HIPE has a very high ratio of its water to oil phase, and the

emulsion type and subsequent classification is determined by this value. Low and medium internal phase emulsions LIPE/MIPEs (Low/Medium Internal Phase Emulsions) have water volumes less than 30wt% and between 30-74 wt% respectively [2, 10]. The 0.74 minimum droplet ratio requirement is the maximum packing density of uniform non-deformable packing of spheres, above this percentage the water droplets are deformed into non-uniform polyhedrons, which results in a more efficient packing density [11], and also increases the viscosity of the emulsion. This polyhedral shaped water droplet has been observed experimentally when the HIPE was frozen in liquid nitrogen to preserve the morphology of the emulsion at the gel point of the polymer and then imaged by cryo-SEM [12], and is shown in **Figure 7**.

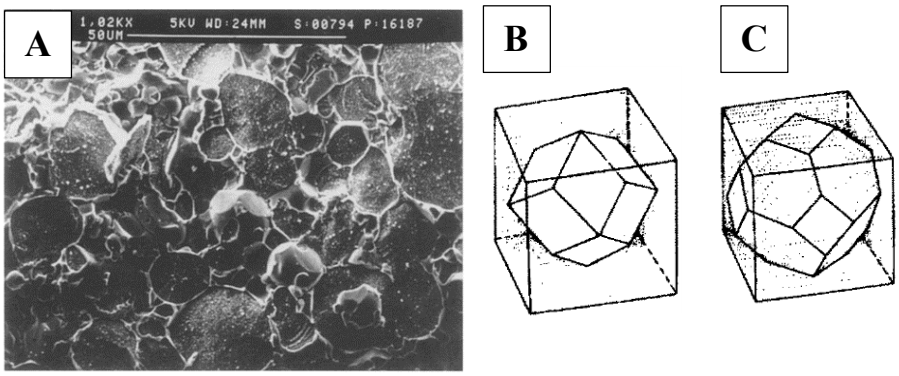

Figure 7: (**A**) SEM image of a non-polymerised styrene/DVB HIPE from Cameron et al [12]. A frozen polyhedral shaped water droplet can be seen in the centre of this image. The drawings B and C represent different droplet deformations caused by the packing arrangement of the HIPE [13]. (**B)** A Rhomboidal dodecahedron, (**C**) A tetrakaidecahedron.

1.1.1. The PolyHIPE material

The following section of this Thesis will focus on the PolyHIPE as a material and then the emulsion aspect used in the templating process used to create it. The main factors used to control the morphology will be discussed, and then the logistics behind the initial emulsion aspect.

I will start by defining the terminology that is used in this thesis to describe the PolyHIPE morphology. By voids or pores I am referring to the large spherical spaces in the PolyHIPE that are created by the water droplets from the initial emulsion. The hollow gaps in the polymer that connect the adjacent hollow spherical voids are called

connecting windows, when discussing the level of interconnectivity between the pores I am referring to these connecting windows. When I use the word morphology; I am broadly referring to the pore volume, size, degree of interconnectivity and the overall packing arrangement of the PolyHIPE. An understanding of the parameters that influences all of the above features are required in order to both control, and manipulate them for specific requirements.

The rapid change of state from the liquid monomer to a rigid polymer upon polymerization preserves the morphology of the initial HIPE up until the gel point. Therefore the pre-processing conditions of the HIPE template dictate the final morphology of the PolyHIPE [6]. The emulsion is a liquid-liquid system where one phase exceeds 74%, so by this nature the emulsion can easily poured and solidified into a variety of moulds prior to solidification. The remaining aqueous droplets are simply removed during post processing steps such as washing in a suitable solvent and then evaporating off the remaining solvent.

1.1.2. Thermal polymerisation of the PolyHIPE

PolyHIPEs can be created by thermally polymerizing the continuous phase of the HIPE. A variety of organic monomers have been used in this way to create PolyHIPEs. The majority of publications use the monomers styrene and divinylbenzene [3] [14]. The PolyHIPE is formed from the polymerisation of the aromatic hydrocarbon styrene (STY) often with the crosslinking agent divinylbenzene (DVB), a radical initiator and a suitable emulsifier; Span 80 being the most common surfactant used for these water in oil emulsions [1]. Other acrylates have been incorporated into the PolyHIPE as a blend, including 2-ethylhexyl acrylate (EHA) [3] [11] [14] [15] and the popular aqueous soluble initiator potassium persulphate is mostly used. For example, the monomer EHA has been used in 2013 as monomer blend for the thermal polymerisation of the PolyHIPE with the initiator sodium persulphate (NaPS) [11].

All these monomers are water immiscible and have been shown to be rigid enough to support the growth of cells. Acrylic acid (Aa) has been incorporated into the droplet phase to adjust the functionality of styrene based PolyHIPEs to improve the cell attachment [6]. EHA has been shown to reduce the brittleness of the polymeric material [6], the hydrophobic EHA monomer also lowers the interfacial tension

between the two phases which creates a smaller void diameter [16]. The polymerized version Poly (2-ethylhexyl acrylate) (PEHA). is regarded as a biocompatible polymer has been blended with PCL to be used in tissue engineering based applications [17]. Nevertheless the styrene and EHA/IBOA materials have a non-degradable carbon backbone and can only be used for *in vitro* applications. Pickering PolyHIPEs have also been thermally cured, often the water soluble thermal initiator, potassium persulphate ($K_2S_2O_8$) is used as the radical source [18].

1.1.3. Photo polymerisation of PolyHIPE

The first example of a PolyHIPE material being produce by photocuring an acrylate based monomeric HIPE in the literature was in 2006 [8]. This study used a blend of the monomers 2-ethylhexyl acrylate (EHA) and isobornyl acrylate (IBOA), with the crosslinking agent Trimethylolpropane triacrylate (TMPTA) to control the elasticity of the material, finding that 10wt% IBOA had a more elastic nature whereas 40wt% IBOA had a brittle one, similar uses for these two monomers have also been reported for the PolyHIPE preparation [19]. The crosslinker Trimethylolpropane triacrylate (TMPTA) is used to increase the degree of crosslinking with these monomers and Span 80 as the surfactant [8]. The surfactant Hypermer B246 has also been used to make emulsions of these acrylate based monomers [19, 20], including degradable PolyHIPE [21]. The addition of EHA is known to increase the elasticity of the polymer matrix [22]. The fast rate of polymerisation of the PolyHIPE has been used to create porous beads using a water in oil in water emulsion (W/O/W) using EHA as part of the monomer blend [23].

Photocurable PolyHIPEs can be polymerised within a matter of seconds as opposed to their thermally cured counterparts, which can take up to 24 hours to polymerise depending on the thermal initiator [19]. Despite the HIPE being a white opaque material, thick sheets up to 35mm deep have been UV polymerised, this is achievable because the free radicals are able to propagate through the emulsion [19]. This fast cure time period means that less stable emulsions can be cured that might destabilise with the increase in temperature, this increases the range of materials for HIPE templating [19, 21, 24]. The transition from thermally cured to photo initiated requires changing the radical initiator [25]. The photocurable process can be used at low

temperatures, and from a material perspective, it opens the possibility to use a wide range of new materials for the preparation of the PolyHIPE structure.

1.1.4. The initiators locus of initiation

The location of the initiator has a significant effect on the morphology and interconnectivity of the PolyHIPE [15] [18]. The example of a W/O emulsion where the cross-linkable organic phase is the continuous phase (oil phase) will be used to illustrate the difference. A schematic illustrating the effect different loci of initiation is shown in **Figure 8** from the publication by Robinson et al [26].

The solubility of the initiator will determine the point of initiation for the crosslinking reaction, and depending on what the solubility is, will determine the level of interconnectivity between the adjacent pores. By comparing the difference between the respective volumes between the two phases, the organic phase is the minor one and the droplet phase; with its high volume percentage of the total emulsion, is the major one. In two emulsions a set amount of initiator can be added to either the organic or droplet phase. The organic phase, with its lower volume of liquid, will reach its gel point more rapidly during polymerisation and have a greater amount of interconnectivity if an oil soluble initiator is used, as opposed to a water soluble one. Water soluble initiators will initiate the crosslinking reaction from the water/monomer boundary and then propagate throughout the monomer phase. This will create an initial strong barrier film between the adjacent droplets which will be more resistant to the polymer contraction process that has been shown to causes the interconnectivity between the pores. Therefore as a result, a closed pored PolyHIPE will be created. The organic phase initiation on the other hand will polymerise to a greater extent in the boundary between 4 water droplets, which will cause the monomer to contract during the polymerisation process, this contraction will also be pulling on the thin film surrounding the water droplets, causing it to be pulled apart, creating a more interconnected PolyHIPE morphology.

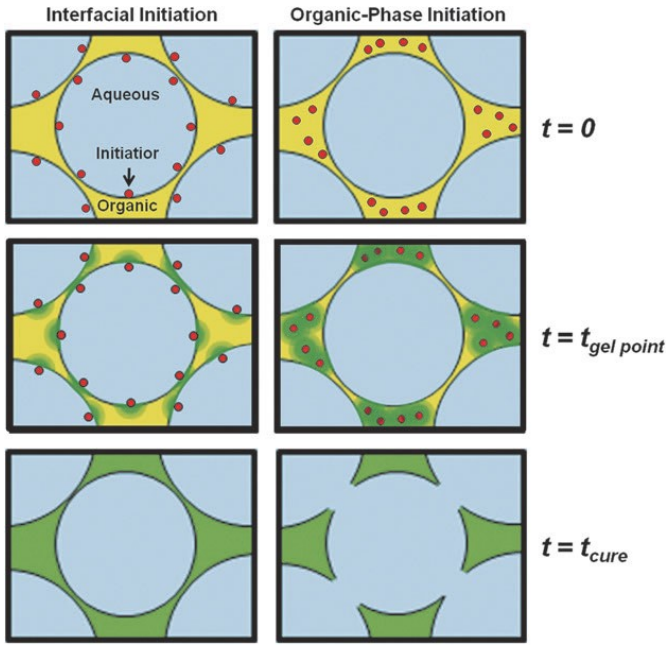

Figure 8: Schematic drawing of the different mechanisms forming the PolyHIPE based on the loci of the initiator. **Right**: organic phase initiator, **Left**: droplet phase initiator. The red indicates the initiator, yellow the photocurable material, and **green** is the initial regions that are crosslinked by the initiator. The organic phase initiation causes more interconnectivity as the contracting polymer tears the thin film connecting adjacent droplets. paper from [26].

The effect of the solubility of the initiator has a significant effect on the morphology for thermally initiated Pickering PolyHIPEs. The organic phase initiator such as benzoyl peroxide (BPO) caused coalescence of the emulsion before the monomer is fully polymerised, the slow polymerisation reaction cannot lock the morphology quick enough, and resulted in a degree of destabilisation of the emulsion during the polymerisation reaction, leading to droplet coalescence [18]. The water soluble thermal initiator Potassium Persulphate KPS, in the Pickering HIPE results in a more PolyHIPE morphology.

1.1.5. PolyHIPE interconnectivity

The PolyHIPEs interconnectivity was found to occur when the material started gelling, which suggests the interconnecting windows are formed as the monomer contracts during its polymerization from the liquid state to a solid one. This was observed experimentally by imaging the transition of the isolated droplets to an interconnected foam, this was achieved by freezing the HIPE at different time points of the polymerisation reaction as it forms the PolyHIPE, these samples were imaged using a

Cryo-scanning electron microscope [12]. The monomeric film is thinnest in the region between adjacent droplets, and at this location it's most susceptible to the effects of the contraction during the polymerisation process.

An alternative theory has been presented for the interconnecting pores. Bismarck et al [27] argued that the interconnecting windows are formed by a mechanical effect during the post processing conditions, such as the solvent wash and drying conditions. And that the films remain intact during the polymerisation stage. There are a range of factors that affect the interconnectivity, such as the water volume fraction, surfactant concentration and the nature of the polymer formation. Silverstein has imaged a PolyHIPE structure that has not been dried or washed in the Soxhlet extractor, and has a porous interconnected structure, indicating that the interconnectivity was created during the polymerization process [15] and not by post processing. However, in my opinion, there will be examples where the post processing can introduce additional interconnectivity within the PolyHIPE.

1.1.6. The effect of water volume on the PolyHIPE

The internal phase volume ratio (the volume of water added to the emulsion), is an important component that can be controlled to tailor the final porosity and interconnectivity of the PolyHIPE, and is a classic example of how the pre-processing conditions of the emulsion dictates the PolyHIPEs morphology.

Water volume plays an important role in the open or closed interconnectivity and the PolyHIPEs density [28], generally speaking, a lower water volume will produce a closed pored high density structure, and increasing the water volume ratio can be used to create a very low density highly interconnected foam. A HIPE can be created with a water volume ratio up to 99%, although the resulting PolyHIPE was very fragile and collapsed during the drying process, but a 98.5% PolyHIPE was stable enough to survive the drying process [9].

In relation to the water in oil emulsion, i.e. droplets of water suspended around a continuous film of oil (the organic monomer). When the water volume ratio is increased, then the finite amount of the oil phase will be stretched around an increasing surface area of the water droplets. As long as the emulsion stability is sufficient

enough, this will result in an ever thinner monomer film surrounding the droplet phase. This effect is highlighted in the schematic shown in **Figure 17** and **Figure 9** and which was taken from the publication [29]. This thin film will increase the final interconnectivity of the resulting PolyHIPE, this is because it is more prone to the effects of contraction as the monomer is converted to a polymer, thus resulting in more connecting windows between the adjacent voids [12].

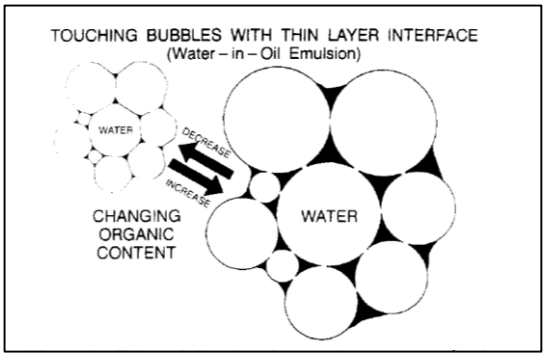

Figure 9: Schematic drawing showing the effect of increasing and decreasing the organic phase of the emulsion. Image taken from [29].

The difference between a low organic volume and a high one is shown above in **Figure 9** . Lowering the organic volume has the same effect as increasing the aqueous volume. A transaction from the spherical water droplet packing arrangement to a more polyhedron shaped one can be seen in the figure, as well as a decrease in the thickness of the organic phase separating the water droplets. The corresponding SEM images from this schematic is shown in **Figure 17**.

1.1.7. Surface active agents: The Surfactant

The surfactants main role is to reduce the interfacial tension of the emulsion; this in turn enables a smaller droplet size that can be supported, and is an essential requirement for the emulsion stability [5]. The surfactant is the most important component of an emulsion. An emulsion between two immiscible liquids are inherently unstable due to the surface tension, which can lead then to separate out into two separate layers of liquid. This separation is driven by the interfacial tension created between the two liquids, as the two liquids do not want to be in contact with

each other. The surface tension of water arises from the hydrogen binding; water molecules are more energetically stabilised in the bulk as compared to on the surface. A surfactant reduces this tension enabling a uniform wetting over the surface. Decreasing the size of the spherical droplets in an emulsion increases the surface area of contact between these two liquids and therefore increases the emulsions interfacial tension, which leads to a higher degree of instability, eventually leading to separation into the two layers; oil and water. To prevent this phase separation surface active agents are incorporated into the emulsion to both increase the stability and prevent separation by essentially creating a barrier between the phases. Increasing the surfactant will increase the stability only to a certain extent, as too much will cause the surfactant to self-assemble into micelles.

The surfactant is an amphiphilic compound, it is a molecule with a hydrophobic tail (water hating) and hydrophilic head-group (water loving) that allows it to adsorb and accumulate at the interface between the two liquids [5]. The addition of the surfactant reduces the interfacial tension, or lowers the surface energy between the two liquids by acting as a barrier preventing the two phases from coming in to contact with each other. Generally speaking the higher the emulsion stability the smaller the achievable droplet size [30]. The surfactant stabilises the continuous film that surrounds the droplet phase [31]. For both O/W and W/O emulsions, the only difference in relation to the surfactant is its orientation, due to its hydrophobic and a hydrophilic end [5].

If the initial emulsion contains a large amount of surfactant then its removal after polymerization can be difficult, and residual surfactant could remain. One alternative is to formulate an emulsion which is stabilised by particles that arrange themselves at the interface between the two liquid phase to prevent coalescence, these are known as a Pickering emulsion [18]. In this emulsion the particles act as surfactants by migrating to the interface between the two phases.

1.1.8. Effect of the surfactant on the PolyHIPE morphology

When HIPE templating is used to produce porous PolyHIPEs, the component that determines the interconnectivity is the surfactant concentration, more so than the volume of water. For example a closed pored PolyHIPE can be created using a low amount of surfactant, despite having a 97% nominal volume of water [32].

The type of surfactant is very important for determining the emulsions stability, its morphology and its interconnectivity [33]. Surfactant concentrations between 2-6% produces a closed pored system, whereas 7-50% concentrations will form an open pored structure in the resulting PolyHIPE [12]. It is also observed that increasing the surfactant concentration produced smaller pore sizes, and an increased level of interconnectivity [34] [2]. This effect is attributed to the increased thinning of the polymer film surrounding the droplet phase as the surfactant amount is increased. SEM images of this can be seen in the below **Figure 10**.

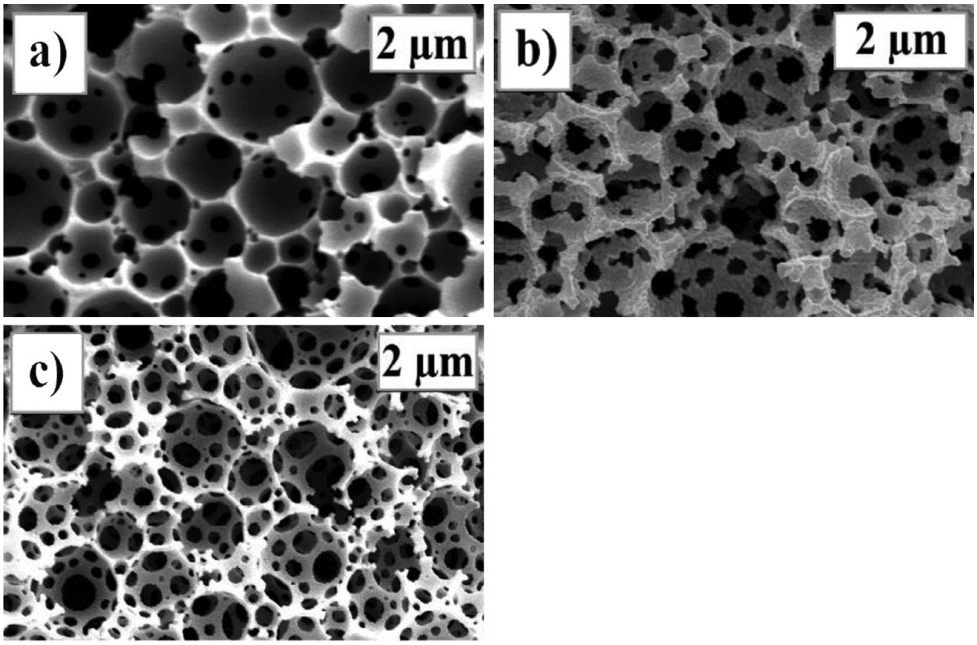

Figure 10: a) 75% water 5% surfactant, (**b**) 75% water 15% surfactant and (**c**) 90% water, 15% surfactant. SEM images taken from [34].

The effect of increasing the surfactant from 5-15% can be seen in **Figure 10** [34]. The SEM images **(a)** and **(b)** show the effect of increasing the surfactant concentration from 5- 15% on the PolyHIPEs interconnectivity when the water volume ratio is kept at the same 75%. Image C shows the effect of also increasing the water volume to 90% as well as the higher 15% surfactant. Image **(c)** has a higher level of interconnectivity and porosity than compared to the other two images.

Increasing the surfactant in the HIPE increases the interconnectivity of the PolyHIPE, **Figure 10**. The increased amount of surfactant can support a thinner monomer film surrounding the droplet phase, this thin film is more prone to contraction, and thus

tearing during the polymerisation stage [3]. Increasing the surfactant concentration will lower the interfacial tension more thus increasing the stability of the emulsion. This increased stability means that a smaller droplet size can be supported and will result in a smaller pore size in the resulting PolyHIPE. so increasing the surfactant concentration will decrease the pore diameter as the emulsions stability is increased [3]. Nevertheless there is a finite amount of surfactant that can be added to increase the emulsion stability, as anything above 50% will produce a weak porous material [3]. It has been reported upon that the surfactant has a greater effect on the pore structural than the droplet phase volume ratio with a styrene/divinylbenzene PolyHIPE [32]. This is because the surfactant ratio will affect the way the oil surrounds the water molecules. The surfactant and monomer in the continuous phase are not soluble in water but are miscible with each other, so their ratio will be important in determining the final structure of the foam produced [32].

This study reports that there is a limited range of useful monomer/surfactant formulations for their 1:1 ratio of styrene/divinylbenzene monomer mixture foams, with 20-50% surfactant being the most useful for the porous structure. Nevertheless the optimum surfactant ratio will have to be experimentally determined for any other monomer ratio used.

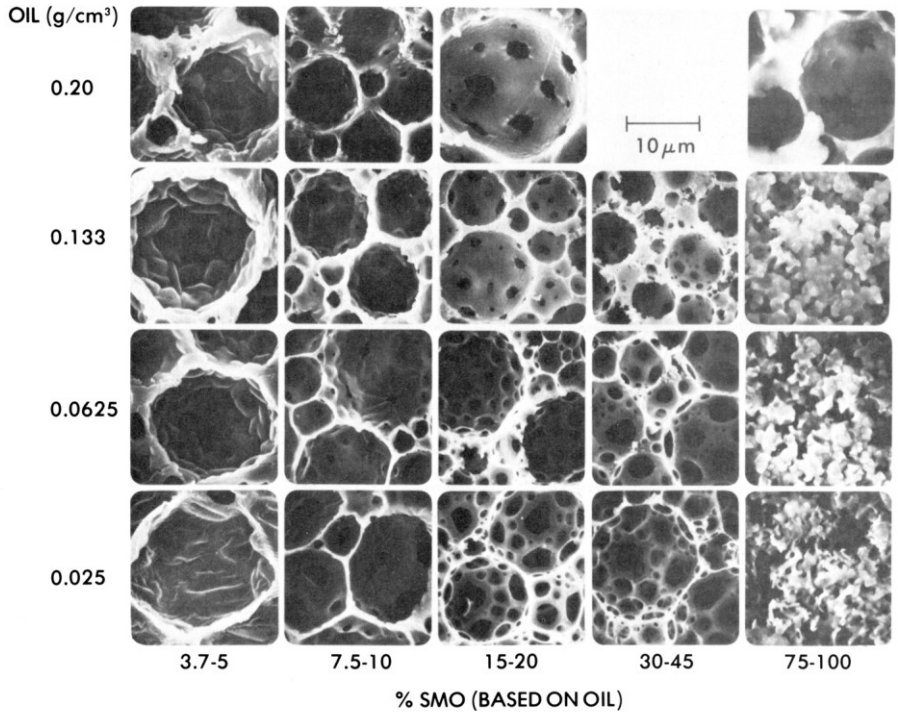

Figure 11: SEM images of the different microstructures formed with the polymerised emulsion with different ratios of the oil and surfactant [32].

Figure 11 from [32] shows the effect of varying the oil and surfactant concentration on the morphology of the final polymerised foams. Low surfactant ratios up to 5% have a closed morphology, 7-10% surfactant foams have a small amount of interconnectivity between adjacent droplets. This is caused by the thin film retracting during the polymerisation stage. The degree of interconnectivity is more pronounced in the 15-20% surfactant concentrations, increasing the surfactant ratio above this caused the spherical porous wall morphology to gradually form more of a network of interconnecting struts, which eventually collapsed during the drying process as the surfactant was increased to 75-100% ratio, this can be seen in **Figure 11**.

Surfactants such as Span 80 do not react during the polymerisation process [15] therefore any residue amount should be removed during post processing stages. Soxhlet extraction can be used to remove these non-polymerised components such as the surfactant and salts that could be used in the initial emulsion preparation [19].

1.1.9. The HLB scale

Non –ionic surfactants have been classified by their HLB (Hydrophile-Lipophile Balance) number. This number relates to the difference between the hydrophilic and lipophilic ends of the surfactant molecule. The three sections of the HLB relate to the water (hydrophile), the oil (lipophile) and the' balance' refers to the ratio between these two components. The HLB calculation includes the division of the molar mass of the hydrophilic end, by the molecular mass of the surfactant molecule to get the ratio between the two. The HLB range is given as a number between 1-20. The lower numbers in the scale (less than 10) represent oil soluble surfactants, these can form water in oil emulsions (W/O) as they are more hydrophobic. The higher numbers (greater than 10) are water soluble and can form oil in water emulsions (O/W) as they are more hydrophilic. This list is described in more detail below:

1 - 3: Used create a mixture between dissimilar oils, and as an antifoaming agent

4 - 6: Used to form water in oil emulsions (W/O)

7 - 9: Good to wet powders into an oil, often used as a wetting agent

8 – 16: used to form oil in water emulsions (O/W)

13 – 15: Can be used to create a detergent solution

13 – 18: Can be used to solubilize oils into water.

The HLB number relates to the surfactants solubility, low values correspond with a hydrophobic surfactant and higher values with more hydrophilic ones, so the table goes from highly oil soluble to highly water soluble. This numbering system is used as a reference guide to determine the correct surfactant that should be used to create the desired emulsion. As the phase in which the surfactant is most soluble will be the emulsions continuous phase. An example of the different types of surfactants and co-surfactants are shown with their respective HLB value by J.M Williams [35]. For example, One of the most widely used surfactants is sorbitan monoleate (Span 80) [30] for the preparation of a Water in Oil emulsion (W/O) due to its low HLB value of 4.2. The surfactant Hypermer B246 has a HLB value of 5.6, both surfactants are insoluble in water (as low HLB value surfactants are hydrophobic). The continuous phase of the emulsion is the phase which the surfactant is preferentially soluble [12], and the type of emulsion can be predetermined by the appropriate choice of surfactant. Low HLB

surfactants reside in the oil phase for W/O emulsions [5], and high HLB surfactants are more water soluble therefore they will create an O/W emulsion.

1.1.10. Soxhlet extraction

Soxhlet extraction is an effective method to extract any residual monomer and surfactant, as well as any porogen solvent that could otherwise remain trapped within any closed pores with the PolyHIPE. Nithitanakul et al [36] demonstrated that the soxhlet extraction duration affected both the surface area and mechanical properties of a Poly(Divinylbenzene)PolyHIPE. Soxhlet extraction was shown to Soxhlet increase the surface area by 107%, and that after a 12 hour wash cycle the mechanical properties of the PolyHIPE was reduced. TEM analysis of samples washed by Soxhlet extraction have been shown to have an increased surface area by removing the residue materials trapped within the pores. A low 1-3 hour wash time was insufficient to remove this material, while the longer 6-12 hour time was shown to remove all the residue material in the PolyHIPE and was shown to be the optimum time for the highest surface area and mechanical properties [36].

1.1.11. Destabilising mechanisms of the emulsion

The addition of energy into the emulsion can be used to create a smaller droplet size, the reverse of this process involves the gradual coarsening and destabilisation of the emulsion which eventually leads to the remerging of the droplet phase and eventual separation of the two phases. There are a variety of different destabilising mechanisms and paths that contribute to this coarsening and destabilising of the emulsion; these are illustrated in **Figure 12,** these will be described in more detail in the following section. An understanding of the origins behind the emulsion instability can be used to prevent the breakdown of the emulsion, and lead to an improvement in the stability. For example it has been shown that the emulsion can destabilise by Ostwald ripening even if the surfactant quantity was increased, even though this increase prevents coalescence of the emulsion [37].

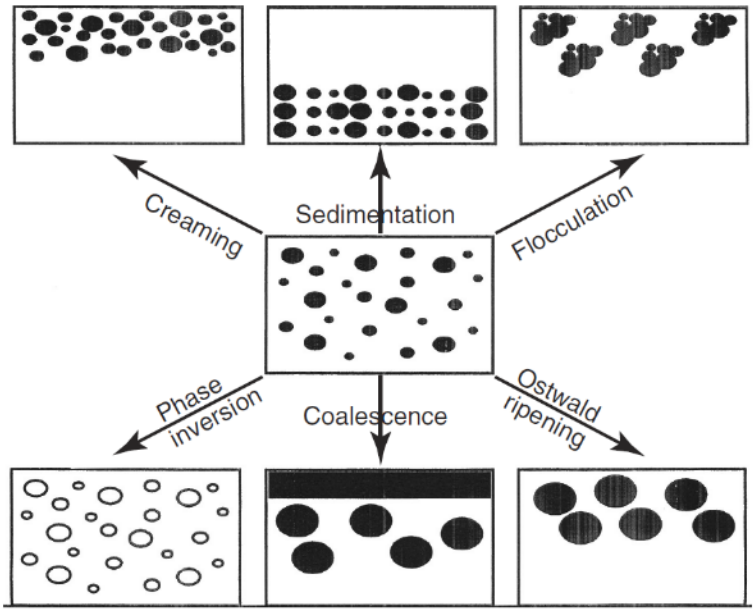

Figure 12: The different destabilising mechanisms for the emulsion from [5].

1.1.12. Ostwald Ripening

Ostwald Ripening involves the gradual increase in the droplet size distribution caused by the smaller droplets gradually merging together to create larger ones. The process involves the migration of the droplet molecules though the continuous phase causing larger droplets to form at the expense of the smaller ones [3]. Over a sufficiently long enough time period this will eventually lead to the complete breakdown of the emulsion, therefore by preventing Ostwald ripening, or by limiting it, a more stable emulsion can be created.

The driving force behind the Ostwald ripening and droplet growth is that it results in a lowering of the systems free energy, this is because it causes a reduction of the interfacial area between the two phases [31]. The rate of Ostwald ripening is dependent on the solubility difference between the different sized droplets. Smaller droplets have a greater solubility than larger ones, therefore the dissolved matter will diffuse from the smaller ones to the larger ones [5], this diffusion of the molecules through the continuous phase causes gradual coarsening of the emulsion. The two droplets do not need to be in contact for this to happen as the matter is transported though the continuous phase [31]. This will result in the growth of the larger droplets at the expense of smaller ones, and is an irreversible process [37]. One method for example

to reduce Ostwald ripening is to add an insoluble component to the droplet phase that cannot diffuse through the continuous barrier film. As the smaller droplets gradually lose their molecules to the larger ones, this component remains in the smaller droplets and creates a chemical potential difference [5].

If the oil phase of the emulsion cannot be changed or altered then additional components can be added to the droplet phase to increase the emulsions resistance to Ostwald ripening. One method is to add an additive to the droplet phase that is completely insoluble in the oil phase, as other molecules transfer through the continuous phase to the larger droplets, the immiscible additive will remain behind and create a concentration gradient against further ripening [38]. This could be a useful method to increase emulsion stability for biomaterial applications, without altering the material in the continuous phase.

1.1.13. Flocculation

Flocculation is caused by van der Waals attraction between the particles or droplets into the emulsion, the overall size of the droplets does not change, but the droplets all clump and aggregate together resulting in their non-uniform distribution [5]. This will occur if there is insufficient repulsion between the droplets to keep them apart

1.1.14. Coalescence

As the thin film between adjacent droplets gradually gets thinner and thinner it can eventually split, this disruption of the film causes the adjacent droplets to merge and fuse together to form larger ones, in a process called coalescence [5]. Therefore this process is heavily dependent on any fluctuations within the continuous thin film between the droplets. Increasing the surfactant concentration can reduce the likelihood of this destabilisation mechanism [37], and the majority of the emulsion collapse is by this mechanism.

1.1.15. Phase Inversion

Phase inversion involves a change in the emulsion classification. A water in oil emulsion can become an oil in water emulsion. The once water droplets that were suspended in the continuous phase of the oil, can become the continuous phase within a suspension of droplets of oil. There is often an intermediate transition period between these two extremes where both emulsion types are present [5].

1.1.16. Creaming and sedimentation

Creaming and sedimentation can be caused if there is a density difference between the two phases [5] and effects the droplet distribution of within the emulsion, it can be controlled by subjecting the emulsion to an external force, for example; Gravity could can the droplets to build up on the bottom of the emulsion, and low density droplets could build up on the top surface in a process known as creaming. Both of these generally do not affect the size of the droplets, only their distribution within the emulsion.

1.1.17. Emulsion stability: electrolyte addition

Emulsion stability is defined as the emulsion maintaining its droplet size distribution, and overall structure over time without any significant change. One way to increase the stability of the emulsion is by adding an electrolyte to the aqueous phase. When the electrolyte is added to the aqueous droplet phase it reduces the rate of Ostwald ripening, which involves the joining together of smaller droplets to form larger ones by the molecule diffusion through the continuous. The addition of salt decreases the miscibility between the two phases, which enhances the emulsion stability and it also affects the surfactant adsorption at the phase boundary [39]. Over time the emulsion will have an increased amount of larger droplets and will result in a decrease in the scattering and consequently the white appearance of the emulsion, a decrease in the droplet size will increase the white appearance as the smaller droplets will scatter the light more.

The addition of electrolytes to the aqueous phase has been shown to increase the stability of the emulsion, its storage stability, reduced coarsening rate and greater

resistance to coalescence. Electrolytes such as KCl, K_2SO_4, $ALCl_3$ $MgSO_4$ (magnesium sulphate), $MgCl_2$ and NaCl (Salt) can be used [40].

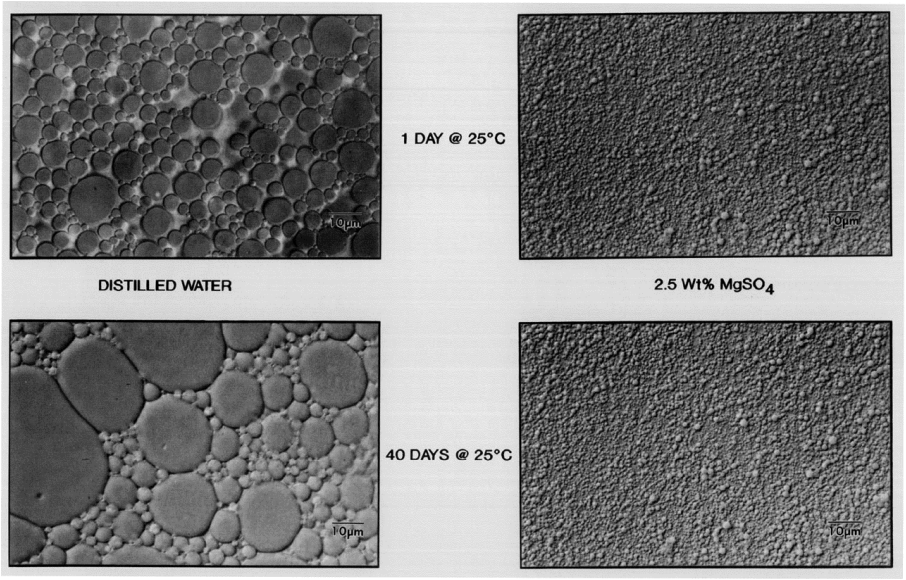

Figure 13: Photographs of two emulsions to show the effect of the electrolyte M_gSO_4 on emulsion stability. Both emulsions are 91% droplet phase with 15% surfactant. Images taken from [40].

As shown in **Figure 13** increasing the concentration of the electrolyte potassium sulphate, (K_2SO_4), from 10^{-6} g to10 g/100 ml caused a significant decrease in the pore diameter from 50 to 5µm, with the thermally cured PolyHIPE [3].

The electrolyte acts as a co-surfactant between the surfactant molecules, by this it acts as an addition to the surfactant, and further reduces the surface tension. The addition of the electrolyte potassium sulphate with a styrene DVB based emulsion has been shown to produce a 10 fold reduction in the pore size [33]. One of the theories behind its ability to increase the stability of the emulsion is that it affects the surfactant packing at the interface [40], this would cause a reduction in interfacial tension and consequently increase the resistance to coalescence.

When NaCl is added to the solution is depresses the cloud-point of the micelles. The cloud point is the temperature when the surfactant is no longer soluble in the liquid and precipitates out, resulting in a cloudy appearance, and the addition of the electrolyte increases the cloud point temperature. This is caused by a salting-in/salting-out effect, causing a lower solvation of the surfactant as the surrounding water is removed from the surfactant monolayer [1]. The addition of the electrolyte can have

an effect by increasing the hydrophobic interaction of the surfactant molecules, this relates to the hydration around the surfactant molecules. Salt (NaCl) is also water soluble, and is more polar than water. When it is added to water it will make the liquid more polar, which is what increases the polarity difference between the two phases of the emulsion [1]. The salt ions are associating with the surfactant, and essentially shielding them more from the surrounding water molecules.

2. CHAPTER TWO: 3D structuring of PolyHIPEs via Stereolithography

2.1 Aims and Objectives

The aim of this chapter is to develop and characterise the selective structuring of an emulsion based material to produce porous structures. Two techniques will be explored: An additive manufacturing stereolithography approach as well as a subtractive manufacturing laser etching one. This is achieved by:

1. Creating a water in oil emulsion using photocurable monomers.
2. Investigating the effect of bulk and selective polymerisation of the HIPE by controlling light exposure using both a scanning and projection based stereolithography system.
3. Characterisation of both the polymerisation methods in terms of porosity, potential, limitations and mechanical properties.
4. Post processing the PolyHIPE into bespoke structures by laser etching.

2.2 Introduction

There is an ever increasing range of materials and techniques that can be used with the stereolithography additive manufacturing approach. This fabrication method involves the gradual building up of an object by the addition of material, this is typically done layer-by-layer. The technology behind this fabrication process at its heart is very versatile, and can be specifically tailored depending on the materials requirement. This fabrication techniques has become ever more accessible. It has found an ever increasing application in the field of tissue engineering [41]. However the challenge associated with the majority of the additive manufacturing technologies is that it becomes ever more challenging to produce structures within the 10-100 μm range [42]. This has been partially overcome with the use of light to polymerise the material, although as the minimum feature size decreases then the overall fabrication time increases.

In this chapter the combination of HIPE templating and micro-stereolithography (μSL) will be explored for the production of porous scaffolds. The micro porosity of the scaffolds is controlled by HIPE templating, while the macro porosity is controlled by the selective polymerisation of stereolithography. The combination of these two fabrication techniques, which has been unexplored in the literature until recently [25] [43], opens up the potential to independently structure materials on different length scales (hierarchical structuring). This work was initiated in collaboration with Neil Cameron's group in Durham University which was published in Advanced Materials [43]. The work presented in this chapter reports on this initial work, and then its development, optimisation and characterisation of the initial experimental conditions. The differences in PolyHIPE processing via the spatially controlled polymerisation by microSL, and the traditionally used bulk polymerisation method for the PolyHIPE material will be discussed. Finally, the potential of this material for tissue engineering based applications will be highlighted.

2.3 Literature Review on the additive manufacturing of PolyHIPE

2.3.1. Stereolithography: an introduction

Stereolithography is a solid freeform technique which builds up a 3D object in a layer-by-layer process to create an object. To achieve this a light sensitive photo-polymerisable liquid is exposed to light. The absorption of the light initiates a change of stage from a liquid state to a solid one. This is a photochemical reaction, in that the absorption of a photon of light results in a chemical reaction causing the monomer units to crosslink together to form a solid polymer. This reaction can be initiated by the absorption of Ultraviolet light, other light sources can be used although typically a laser light source is used due to its superior beam quality and wavelength uniformity. The fabrication process typically involves exposing either the top or bottom of a small vat of photocurable resin, recoating the surface and then repeating the process.

The polymerising light can either be scanned across the material (scanning stereolithography) to create 3D objects in a line-by-line fashion, or via a single surface exposure of a pattern of UV light (projection stereolithography), where the top or

bottom surface is uniformly exposed [44]. Both methods form a 3D objects in a layer by layer-by-layer process

The two different stereolithography techniques of the HIPE are shown in **Figure 14**

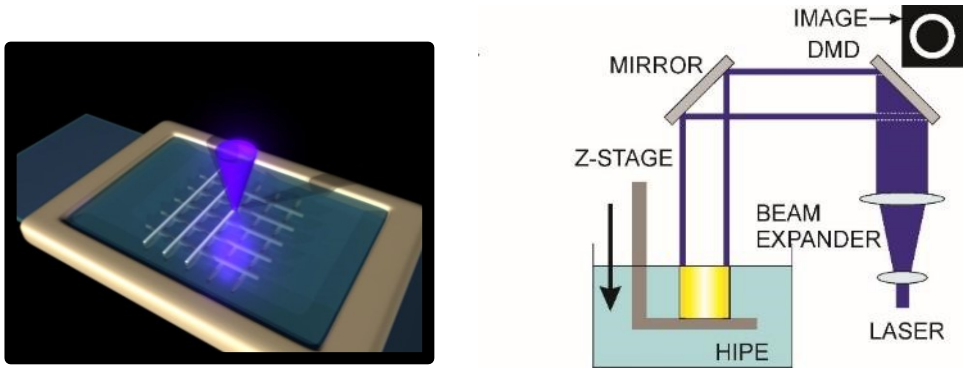

Figure 14: **Left,** computer generated image of the scanning stereolithography technique. **Right**, a schematic of the projection polymerisation technique [43].

Projection stereolithography is a faster process in comparison to scanning stereolithography since a 2D image is projected into the resin compared to scanning the image pixel-by-pixel. To produce a high resolution structure a very small scanning spot is required, which will mean that more scans are required to polymerise the same area. So there is a trade-off between achievable resolution and the fabrication time with the direct laser write method

2.3.2. Stereolithography of High Internal Phase Emulsions

Both HIPE templating and stereolithography offer great potential for fabrication of a porous material. The former produces a porous foam with a very good degree of control over the porosity by polymerizing the monomer or pre-polymer around suspended water droplets to form a polymer network. Whereas the latter (stereolithography) has exceptional control of the porosity by spatially controlled polymerisation.

The combination of HIPE templating and stereolithography addresses the trade-off seen between the fabrication process and achievable resolution, and at the same time it greatly decreases the fabrication time while maintaining microscopic resolution.

The pre-processing conditions to create the emulsion can be used separately to control the micro porosity (1-100 μm), while the stereolithography controls the macro porosity beyond 100 μm [43].

In the literature HIPE templating and additive manufacturing have been combined together to produce a large gyroid structure of the PolyHIPE material by a projection based method [25]. Computer controlled layer-by-layer stereolithography is used to produce the structure. The larger user controlled porosity is controlled by the HIPE regions exposed to the initiating light, the spaced between these regions creates the macroscale porosity. In this study trimethylolpropane triacrylate (TMPTA) was used to build 3D structure of PolyHIPEs. To photo cure these acrylate based HIPEs a photo initiator (Irgacure 819) was used.

Microfabrication techniques such as Two Photon Polymerisation (TPP) can produce well defined 3D structures with a very high degree of resolution within the micron and sub-micron range. This fabrication techniques has been explored previously in our group [45, 46]. However there is a trade-off between achievable resolution and the speed of fabrication, the TPP technique takes prohibitively long to fabricate even small macroscopic objects with this high level of precision. Other techniques such as HIPE templating rely on the processing parameters to determine the 3D architecture, and can have a high degree of control over a pore distribution that is within a controllable range. Large volumes of HIPE can be polymerised and the internal porosity will be very similar throughout the PolyHIPE. Therefore HIPE templating allows for good control over porosity and interconnectivity, with the ability to produce larger sample volumes, furthermore the development of the selective polymerisation technique of HIPEs further increases the controllable architecture [43].

As a standalone technique HIPE templating can be used to create a bulk sheet of a porous foam called a PolyHIPE. This is achieved by using a monomeric material for the continuous phase of the emulsion, which can undergo a crosslinking process to solidify it from its liquid state to a solid one. The mechanism for this can either be thermal or light initiated, the latter significantly reduces the time for polymerisation [19].

Bulk polymerisation process does not readily allow for 3D structuring of the 3D foam, HIPEs are normally set within a mould via bulk curing. Depending on the radical

initiator used the polymerisation reaction can initiated by either light (photons of light) or temperature (thermal). For example the thermal initiated reaction involves transferring the HIPE into a plastic tube or mould, and then heated to 60^{o}C for 2 hours to polymerise it. The entire HIPE is cross-linked in a single step process to produce the PolyHIPE

Photocurable HIPEs were first reported in the literature in 2006 [8]. The difference between the thermal and light initiated polymerisation reaction is the initiating method. The polymerisation reaction remains the same for the monomer to polymer conversion. Thermal initiators that can be used include AIBN and potassium persulphate, and photo initiators such as diphenyl (2,4,6-trimethylbenzoyl) phosphine oxide/2-hydroxy-2-methylpropiophenone blend can be used. [25]

The use of UV light to initiate the photochemical polymerisation reaction has distinct advantages over its thermally cured counterpart. Both in terms of the fabrication time; the polymerisation reaction goes from a few hours to a matter of seconds, and itself allows for less stable materials to be used as the emulsion can be preserved before it destabilizes, which is very important as an unstable emulsion may destabilise during the heating process to polymerize it.

A disadvantage with bulk photocuring of the HIPE is the low depth of penetration of the UV light due to the high light scattering nature of an emulsion. Indeed, the penetration depth of the light is determined by the Beer-Lambert law and the suspended droplets within the emulsion act as scattering sites greatly reducing the penetration depth of the light within the emulsion

The aforementioned publications indicate that additive manufactured PolyHIPEs have an excellent potential in the field of tissue engineering amongst other additive manufacturing methods for the development of a new generation of tissue engineering scaffolds [47]. The use of photocurable materials is of particular interest as it increases the range of (bio) materials that can be used that were previously unexplored for this emulsion templating technique.

2.4 Materials and Methods

2.5 Materials

Monomers isobornyl acrylate (IBOA), 2-ethylhexyl acrylate (EHA), crosslinker trimethylolpropane triacrylate (TMPTA) and Photoinitiator diphenyl (2,4,6-trimethylbenzoyl) phosphine oxide/2-hydroxy-2-methylpropiophenone blend were used without modification from Sigma Aldrich. Potassium Persulphate was purchased from Fisher Scientific and used without modification. The surfactant Hypermer B246 was purchased from Croda Industrial, and the surfactants Span 80 and Tween 20 were purchased from Sigma Aldrich. All materials were used without further purification.

2.6 Methods

2.6.1. Scanning Electron Microscopy

The morphology of the PolyHIPEs was investigated using a scanning electron microscopy (SEM), a Philips/FEI XL30 SEM operating at 25 kV was used to image the morphology of the PolyHIPE. Samples were mounted on carbon pads adhered to aluminum stubs and then gold sputter-coated using (SC500, emscope) to increase the conductivity for imaging.

2.6.2. PolyHIPE void measurement

Image J Version 1.44p was used to calculate the average void size and interconnectivity from the SEM images. A statistical correction factor was used account for the non-equal fracturing of the PolyHIPE. The fracture will occur at the weakest areas around the hollow pores and not centrally to produce the largest diameter. The measured images will be an underestimate of the actual pore size, therefore the measured values are multiplying by $(\frac{2}{\sqrt{3}})$ [48] to give a more accurate representation of the pore size. This value is obtained from the average ratio between the pore size and the measured pore size [14] [30].

2.6.3. Glass functionalisation

Piranha solution was prepared using a 3:1 mixture of sulphuric acid (95%-98% H_2SO_4, Sigma Aldrich) and hydrogen peroxide (30 wt % solution in water, Sigma Aldrich. This is a powerful oxidizing agent and for our application it has the dual advantage to remove any organic matter or residue from the glass surface from the manufacturing stage, as well as exposing surface hydroxyl groups (–OH) for the functionalization step. 13 mm glass coverslips were washed for 30 minutes in Piranha solution, then rinsed in deionised water, then washed in methanol to remove any water residue during drying. The coverslips were submerged in an alkoxysilane coupling agent solution of 10% 3-(methacryloxy) propyltrimethoxysilane (MPTMS, Polysciences Inc) in Toluene (Sigma) to introduce methacrylate groups onto the glass surface, to which the polymer attaches to upon polymerisation. Alternative silanes are available that can be used to coat the glass surface [18]. The container is wrapped in foil to prevent light exposure, and left for 24 hours. The treated glass was washed with a 70% isopropanol solution to remove any excess MPTMS / toluene solution, and dried prior to use.

2.6.4. Silicone PDMS sheet fabrication

Flat sheets of silicone were produced and used to create temporary wells to contain the HIPE during the stereolithography process. A silicone elastomer kit (Sylgard) was used to create these sheets of silicone. The elastomer and curing agent were thoroughly mixed in a 10:1 ratio in a disposable container. This introduced bubbles which were removed by either two techniques. The liquid was either put in a vacuum oven (Heraeus Vacutherm, Thermo Scientific) or then cycled from under vacuum to normal atmospheric pressure to draw the bubbles to the upper surface and then pop them. The other technique is to centrifuge the silicone (MSE Mistral 1000) at 1000 rpm for 3 minutes, which was the predominantly chosen method because of its fast speed at removing the air bubbles. The silicone was then poured into a round petri dish and left for 2 hours at 60^{o}C to fully set. A 11 mm cork puncher was used to cut holes into the sheet of silicone, and a larger 20 mm cork puncher around the first hole to give adequate space to both adhere to the 13 mm functionalised glass coverslips and the glass holder slide beneath it.

2.6.5. HIPE preparation

For the HIPE preparation the compositions used were based on the initial publication [43]. The ratio between the organic monomer components EHA and IBOA were varied to alter the elasticity of the Polymer, EHA is an elastomer whereas IBOA increased the brittleness of the polymer, [8], in each case the crosslinking agent TMPTA is added at a constant percentage. A typical HIPE formulation involved mixing the respective monomers EHA and IBOA monomers in a 50 ml glass beaker (Fisher Scientific). The surfactant Hypermer B246 is added to the monomer mixture and allowed to slowly dissolve, increasing the temperature and mixing rate at this stage increases the rate the surfactant dissolves. The photoinitiator (a 50:50 blend of diphenyl(2,4,6-trimethylbenzoyl)phosphine oxide and 2-hydroxy-2-methylpropiophenone,) was added at 5% of the organic weight, the weight percentage was predominately used because the photo initiator is very viscous, and pipetting out by volume alone proved to be an unreliable method for reproducibility. The mixture was subjected to gentle agitation with an overhead stirrer (Pro40, SciQuip), which is increased to 350 rpm while the water is added dropwise over 5 minutes. The use of an overhead stirrer to agitate the oil and water phases is a typical method used to prepare the HIPE on the laboratory scale [2]. The resulting HIPE was allowed to stir for an extra 2 minutes to ensure complete mixing, and then transferred to a glass vial wrapped in foil to prevent premature polymerization.

2.6.6. Bulk polymerisation of the HIPE by UV light

The HIPE was photo polymerised originally using both procedures. A Light Hammer® 6 variable power UV curing system with LC6E benchtop conveyor from Fusion UV Systems Inc.® A 200 W cm^{-2} mercury bulb at 100% intensity settings was used, here the initial HIPE preparation was placed into a PTFE cylindrical mould (20mm, Ø = 25mm) secured between two glass plates using adhesive tape. This was then passed under the UV bulb numerous times using the conveyor belt (3.5 speed setting). The resulting PolyHIPE samples were washed in acetone for 18 hours before being vacuum dried at room temperature.

Bulk photopolymerisation was also carried out using a UV belt curer (GEW Mini Laboratory, GEW engineering UV) with a 100 W cm^{-2} UV bulb. The HIPE sample was passed several times under the UV lamp at 5m/min on both sides. The resulting monoliths were immersed in acetone (100 ml, 24 h), or washed in a Soxhlet apparatus for 24 h with ethanol to remove any residue surfactant on the PolyHIPE surface [19]. The samples were dried in vacuum oven and dried under vacuum afterwards until constant mass.

2.6.7. Microstereolithography of the HIPE

A schematic of the microstereolithography experimental set-up is shown in **Figure 15** and the corresponding photos in **Figure 16.**

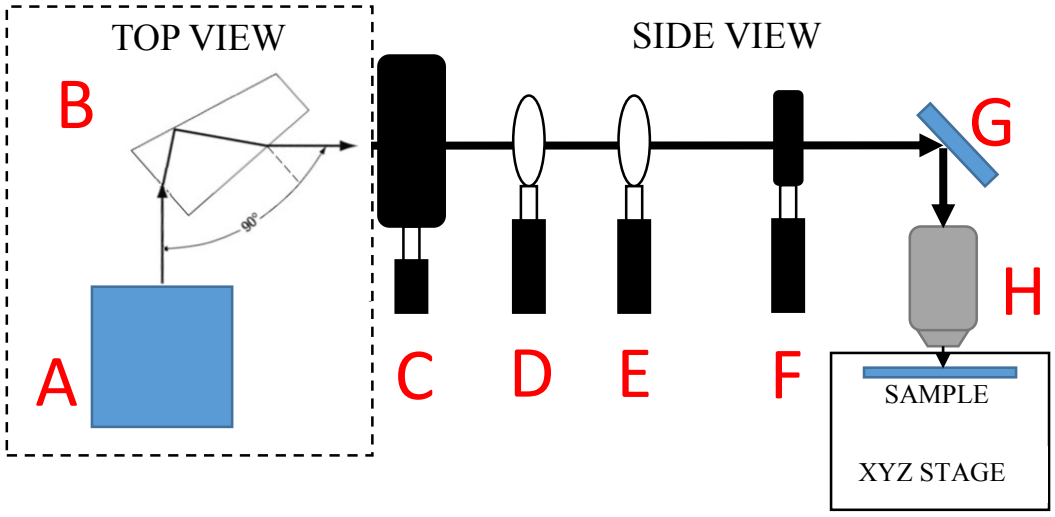

Figure 15: Schematic of the microstereolithography experimental setup for the direct laser write structuring of the HIPE. The Arrows show the laser direction. The corresponding photos are shown in **Figure 16**. A, microchip laser. B, Pellin Broca Prism. C, Shutter. D and E Galillean beam expander. F, adjustable pin hole. G, mirror. H, objective.

To fabricate the PolyHIPE structures a passively Q-switched microchip laser, Pulselas P-355-300 sub-nanosecond pulsed was used (Alphalas, Gottingen, Germany). This laser emits at wavelengths 1064, 532 and 355nm through frequency doubling and tripling, with a 0.5 ns pulse width and maximum power of 12mW at 355nm (16.6 kHz repetition rate. The 355 nm wavelength was separated from the 1024 and 532 nm using a Pellin Broca Prism (ADB-10, Thorlabs, Germany), **Figure 15** part B. A shutter (UNIBLITZ LS6, VincentAssociates) linked to a shutter driver (VCM-D1, VincentAssociates) was used to control the ON/OFF state of the laser.

The beam was expanded through a Galilean beam expander to ~8 mm beam diameter. An adjustable pin hole is used to create a circular beam that is reflected by a silver mirror before focusing through a 10× objective (Carl Zeiss, EC Plan-Neofluar 10×, Numerical Aperture 0.3). A 13 mm round coverslip which was previously surface functionalized with methacryloxypropyltrimethoxysilane (MPTMS) to provide surface methacrylate groups which ensured surface attachment of the written structure was placed into a sample holder attached to a high precision xyz-stage **Figure 15**, (Aerotech ANT130XY base for XY-translation and PRO115 for z-translation). A temporary well for the HIPE material was created using A PDMS sheet with a hollow circle cut out to house the coverslip and to create a temporarily water tight seal against the glass surface. The HIPE was pipetted into the PDMS well and the objective focused just above the glass-HIPE interface. The PolyHIPE lines, square structures and woodpile structures were fabricated using this setup by scanning the laser light over the top surface of the HIPE. After every sequence of laser scans, the shutter closed and the stage moved away from the objective to allow me to pipette the next layer of HIPE into the well, before automatically returning to the new focal spot at the top of the HIPE.

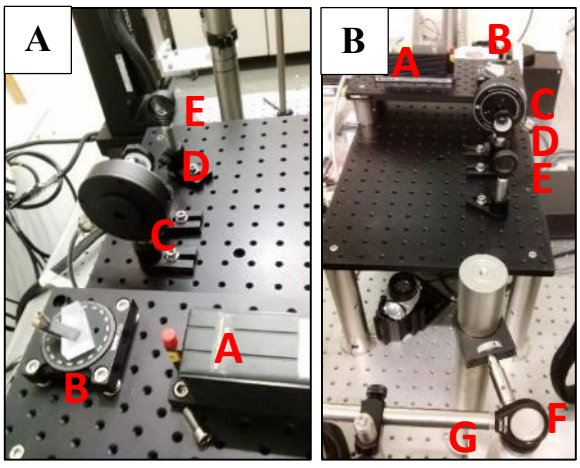

Figure 16: A, microchip laser. B, Pellin Broca Prism. C, Shutter. D and E Galillean beam expander. F, pin hole. G, mirror. H, objective.

The projection µSL used as a laser source a 150 mW, 405nm laser source was used (Vortran Laser Technology Inc, Sacramento, CA, USA). The laser output expanded to a 5 mm diameter beam and was reflected from a Digital Micromirror Device (DMD) (Texas Instruments Incorporated, TX, USA), which acts as a programmable mask for

the projection stereolithography set-up. The image projected from the DMD device was directed by a silver coated mirror into a cylindrical receptacle containing the photo curable HIPE. The receptacle was placed on a computer controlled motorised z-axis translation stage apparatus (Thorlabs Ltd, Cambridge shire, UK) to enable building 3D objects with this setup. The laser power was set to 5 mW for the experiments. A flat-bottomed vial containing 2 ml of the HIPE was placed on an L-shaped copper lip mounted on a z-translation stage as writing platform. This copper lip was slowly lowered in the solution until the HIPE just covered the platform. From this position the laser was switched on and the platform was translated at constant speed to obtain a solid object. A schematic of this setup is shown in **Figure 24**.

2.6.8. Laser cutting of the PolyHIPE sheets

Sheets of PolyHIPE were photocured and placed onto the stage of the laser cutter Mini 18 Laser, Epilog Laser) the laser power was varied from 5% to 40% depending on the thickness of the PolyHIPE, and the PolyHIPE was exposed to multiple laser passes to cut through it. The stage speed was varied from 5-70% and a laser frequency of 2,500Hz was kept constant throughout. The laser cutter only allowed for speed and laser power to be adjusted as a percentage.

2.6.9. Tensile testing of the PolyHIPE

A BOSE EnduraTEC ELF 3200 extensometer was used, a 450 N load cell with an extension rate of 0.02mm/sec was used to grip the sample. The distance between the grips was kept at a constant 10mm apart. The force and displacement was measured to give the Young's Modulus (E), the Ultimate Tensile Stress (UTS) and the Percentage Elongation before Failure. An electronic micrometer (2046F, Mitutoyo) was used to measure the thickness of the samples accurate to 1 μm.

The Ultimate Tensile Stress was calculated by dividing the maximum applied force by the measured cross sectional area, the initial length between the grips was kept at a constant 10mm for all samples. Using the gradient of the linear elastic region of the force displacement curve the young's Modulus was calculated. The equations relating to the Young's Modulus calculations are shown below.

$$\boldsymbol{E = \frac{\sigma}{\varepsilon}} \qquad Youngs\ Modulus = \frac{Stress}{Strain} \qquad \text{Eq 1}$$

Equation 1: Young's Modulus Equation

$$Stress\ = \frac{Force\ (F)}{Area\ (A)}\ \&\ \ Strain = \frac{Change\ in\ length\ (\Delta L)}{Original\ length\ (Lo)} \qquad \text{Eq 2}$$

Equation 2: Two equations that can be merged into equation 1

Eq 3

$$E = \frac{F * L_O}{A * \Delta_L}$$

Equation 3: Eqn.1 and Eqn.2 merged together

The gradient of the force-displacement curve is the same as the force divided by the change in length in Eqn.3. Substituting in the original length of the sample (10 mm) into L_O leaves the area remaining. The width was kept at a constant 6 mm throughout all the samples, so the area is simply 6mm* the sample thickness, resulting in ***Equation 4.***

$$E\ (MPa) = Gradient\ of\ the\ linear\ region * \frac{10mm}{Sample\ Thickness\ (mm) * 6mm} \qquad \text{Eq 4}$$

Equation 4: calculation to determine the Young's Modulus from the gradient of the force-displacement curve

2.6.10. Cell culture

Human dermal fibroblast cells were isolated from tissue samples obtained from consenting patients undergoing either elective abdominoplasty or breast reduction surgery. The tissue collected was used under the requirements stipulated by the Research Tissue Bank Licence 12179 and fibroblast cells were isolated by the lab technician staff. The fibroblast cells were cultured and expanded in T75 culture flasks until they were ~80% confluent, then they were transferred to new flasks to continue the cell expansion. Cell culture was done in a tissue incubator hood at 37°C, 5% CO_2. The cell medium was changed every 3 days. Prior to use the cells were detached from the tissue culture plastic surface by first washing them in 10ml of Phosphate Buffer Solution (PBS) and then incubating them with 2.5 ml of trypsin (Trypsin-EDTA solution, Sigma). 10 ml of media was added to the flask which was then tapped several times against the table edge to detach the cells. The cell suspended media was pipetted into a 50 ml centrifuge tube and spun at 1000 rpm for five minutes. The resulting pellet

of cells was isolated and re-suspended in 2 ml of media prior to seeding the scaffold with cells.

Sterile scaffolds were transferred to a 24 well plate and washed in PBS 3 times to remove any remaining alcohol. 75,000 cells were seeded onto the scaffolds within a 40 µl media droplet and were left in the incubator for 20 minutes to give time for the cells to attach to the sample before 1ml of media was added to the wells.

2.6.11. PicoGreen DNA Quantification Assay

A PicoGreen dsDNA assay kit (Invitrogen^{TM}) was used on the PolyHIPE samples to quantify cell viability. The DNA was extracted from the cells by a repeated freeze thawing cycle, then the DNA was bound with a fluorescent marker so that it can be quantifiably determined using a fluorescence reader. Comparison between cell experiments are determined by comparing the fluorescence of the samples, a higher intensity indicates a greater amount of cells. After cell culture the samples were treated with a Triton X-100 solution in 1% carbonate buffer, then freeze thawed three times from room temperate to -80ºC. The PicoGreen protocol was then followed, this involved preparing 500µl of trypsin-EDTA (1:20 ratio in water) then the PicoGreen Dye stock was dissolved 200 hundred fold in the trypsin-EDTA solution. The fluorescence was measured at 530 nm using an excitation of 480 nm. The fluorescence reader was a BIO-TEK ELx 80 plate reader.

2.6.12. Confocal imaging

For staining, the cells were first washed with PBS to remove any excess media, then the samples were fixed by submerging in 1 ml of 3.7% formaldehyde solution onto the scaffolds and left for 20 minutes. Afterwards the cells were washed twice with PBS. The samples were submerged in a 1% BSA, 0.1% Triton-X100 solution for 20 minutes. To image the cell's nucleus they were submerged in 1 ml of DAPI solution from a stock solutiBon containing 10 µg/ml, and left in a foil container for 20 minutes. The DAPI solution was removed and samples washed in PBS 3 times. To image the F-actin filaments were stained with FITC-labelled phalloidin from a stock solution containing 0.5 mg/ml in dimethyl sulfoxide (DMSO), and left for 30 minutes in a foil

container. The sample was washed twice in PBS. The samples were stored in PBS wrapped in foil in the fridge prior to imaging.

2.6.13. Confocal microscopy

Images were obtained using an upright confocal microscope (LSM510 Meta upright laser-scanning confocal microscope (Carl Zeiss MicroImaging, Germany). The light source was from a Chameleon Ti: sapphire multiphoton laser (Coherent, CA, USA) DAPI was imaged using λ_{ex} = 400 nm and λem = 461 nm (blue). FITC was imaged using λ_{ex} = 495 nm and λ_{em} = 519 nm (green). 3-D images of the cells are produced by taking multiple images at different heights and stacking them in sequence to form a 3D image. The images were processed using the Carl Zeiss Laser Scanning Systems LSM 510 software.

3. CHAPTER THREE: Results of Scanning Stereolithography of PolyHIPE

3.1 HIPE formulation

Different acrylate based PolyHIPE samples were created with varying the monomer ratios and water volumes. The two monomers Ethylhexyl Acrylate (EHA) and Isobornyl Acrylate (IBOA) were chosen as these monomers are both hydrophobic and the mechanical properties can be altered by varying the respective ratios between the two monomers [8]. EHA is an elastomer whereas the IBOA monomer produces a more brittle polymer. EHA based PolyHIPE (EHA 75, 80 and 90) refer to the elastic PolyHIPE formulation with respective porosities of 75, 80 and 90% dictated by the monomer to water ratio. The IBOA PolyHIPEs (IBOA 75, 80 and 90) are rigid in comparison to the EHA PolyHIPE formulations. The crosslinking agent trimethylolpropane triacrylate (TMPTA) is used in all cases, this is because the EHA and IBOA monomers are monofunctional acrylates [8], and will not form a high enough degree of crosslinking on their own to form a solid polymer.

The acrylate monomer blend of EHA, IBOA and TMPTA has been used in the literature previously to bulk polymerise sheets of PolyHIPE [8]. This was the first example of a photocured PolyHIPE. They reported that increasing the ratio of EHA to IBOA increased the elasticity of the PolyHIPE, although no quantifiable data was shown. We used the surfactant Hypermer B246, although Span 80 has been used previously with this monomer blend [8]. EHA has been used for thermally cured pickering PolyHIPE formation with the crosslinker divinyl benzene (DVB) [18]. The crosslinker increases the interconnectivity between the growing polymer chains to create a 3D network.

Table 1: Monomer values for initial stereolithography structuring. Respective void (**a**) and window diameters (**c**) were measured from SEM images, the standard deviation (**b**) was determined from (**a**).

Sample	EHA [mL]	IBOA [mL]	TMPTA [mL]	Hypermer B246 [g]	Initiator [mL]	Water [mL]	Average void diameter (<D>) [μm] [a]	Std [μm]	Average window diameter (<d>) [μm] [c]
EHA75	4.1	1.6	1.3	0.21	0.38	21	24	9	2.5
EHA80	4.0	1.6	1.3	0.21	0.35	28	23	12	4.1
EHA90	4.1	1.6	1.2	0.18	0.35	63	20	7	5.4
IBOA75	1.1	4.6	1.2	0.21	0.34	21	11	4	1.6
IBOA80	1.2	4.5	1.3	0.20	0.36	28	14	4	1.8
IBOA90	1.2	4.6	1.3	0.21	0.37	63	19	8	3.4

Table 1 shows the different mixing ratios used for making the original set of PolyHIPEs, as well as the average void diameter of the resulting PolyHIPEs produced, which will be discussed later in the chapter. The crosslinking agent trimethylolpropane triacrylate (TMPTA) is used to improve the crosslinking and is added to the monomer mixture in the same percentage (18%) for all samples. In these experiments the total monomer volume for the oil phase of the HIPE was set to 7 ml.

To prepare the organic phase the relative weights of the monomers were calculated from the density, and all the monomers were weighed out (density of EHA is 0.885 g/cm^3, IBOA 0.99 g/cm^3 and Triacrylate 1.10 g/cm^3). To calculate the volume of water required for the set nominal porosities the water addition is added respective to the monomer volume only, i.e. the surfactant Hypermer B245 (3-5 wt %) and initiator diphenyl (2,4,6-trimethylbenzoyl) phosphine oxide/2-hydroxy-2-methylpropiophenone blend (5wt %) are not taken into consideration when calculating the respective monomer to water ratios. The droplets of water have to be slowly added to the oil phase while it is being mixed to give sufficient time for them to be broken up into smaller droplets that will become dispersed within the oil phase. If the water was added too quickly it resulted in an Oil in Water (O/W) emulsion; this is where the oil droplets are suspended within the water, and the sample was subsequently disposed of. We require the oil or monomer phase to be the continuous one to produce the PolyHIPE structure upon polymerisation.

After polymerisation the PolyHIPE is washed in acetone and then air dried. More extensive wash cycles have been used in the literature, for example the PolyHIPE can be washed at 60ºC in a 1:1 acetone/water solution, and then sample frozen at -80ºC and freeze dried to minimize sample shrinkage [8]. For our application we found that washing in a water miscible solvent was adequate for this preliminary work.

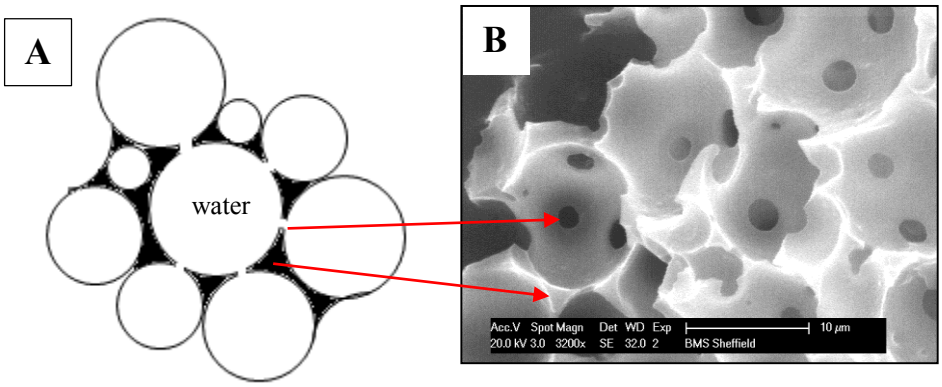

Figure 17: (**A**) Schematic of a water in oil emulsion showing a 2D representation of the water droplets surrounded by the oil phase. **(B**) SEM image of the polymerised PolyHIPE structure (EHA75) showing where the oil phase has polymerised around the water droplets. Red arrows are pointing towards the interconnecting windows between the pores, and the polymer cured between 3 adjacent water droplets.

A schematic of the HIPE emulsion can be seen in the above **Figure 17** image **A**, and a typical example of the PolyHIPE morphology is shown in image **B**. The red lines show where the schematic drawing matches up to the corresponding areas of the PolyHIPE. The interconnecting windows between adjacent pores are created by the thinnest region of the oil phase between adjacent droplets can be seen, as well as the spherical voids that were originally templated by the water droplets.

3.2 Scanning stereolithography of the PolyHIPE

A focused laser beam is scanned over the HIPE surface so the structure is 'written' directly on its surface. An in house built stereolithography fabrication rig was used for the structuring experiments. This is shown in **Figure 16**. UV light from a passively Q-switched DPSS microchip laser is collected and collimated through a Gaussian lens set-up and then focused onto a sample holder attached to a xyz high precision Aerotech stage.

The emulsion was originally housed in a temporary well created using several layers of adhesive tape with a hole cut in the middle, this was adhered on top of a functionalized glass coverslip. The tape created a seal around the coverslip preventing any material loss, and was a cheap and effective method for creating a temporary well to house the photocurable HIPE. Nevertheless this was soon replaced with a thin 1-2 mm thick sheet of polydimethylsiloxane **(**PDMS) with a 11 mm circular hole bored using a hole puncher, the PDMS was adhered to a glass coverslip ontop of a glass slide to create a temporary seal around the coverslip to house the HIPE during the experiment. The glass coverslips were washed in the highly oxidising piranha solution, and then pretreated with MPTMS solution to functionalise its surface with methacylate groups, which the polymerizing polymer then covalently binds to ensuring firm attachment to the glass substrate, binding the polymer to the glass [45]. The binding of the PolyHIPE to the glass coverslips made the sample handling easier for the post processing washing stages, which involving submerging the PolyHIPE into a water miscible solvent such as acetone, which dissolves all the uncured monomers while the crosslinked polymer remains unaffected.

3.2.1. PolyHIPE square structures

When these experiments were carried out there were no previous reports on the stereolithography of HIPE to use as a point of comparison for the initial UV exposure settings. Therfore for simplicity the initial structures produced were chosen to be arbitrary squares and lines, these are easy to program within the stage software, and

offer an extra degree of complexity over using just straight lines. These square structures were imaged by SEM images (**Figure 18).**

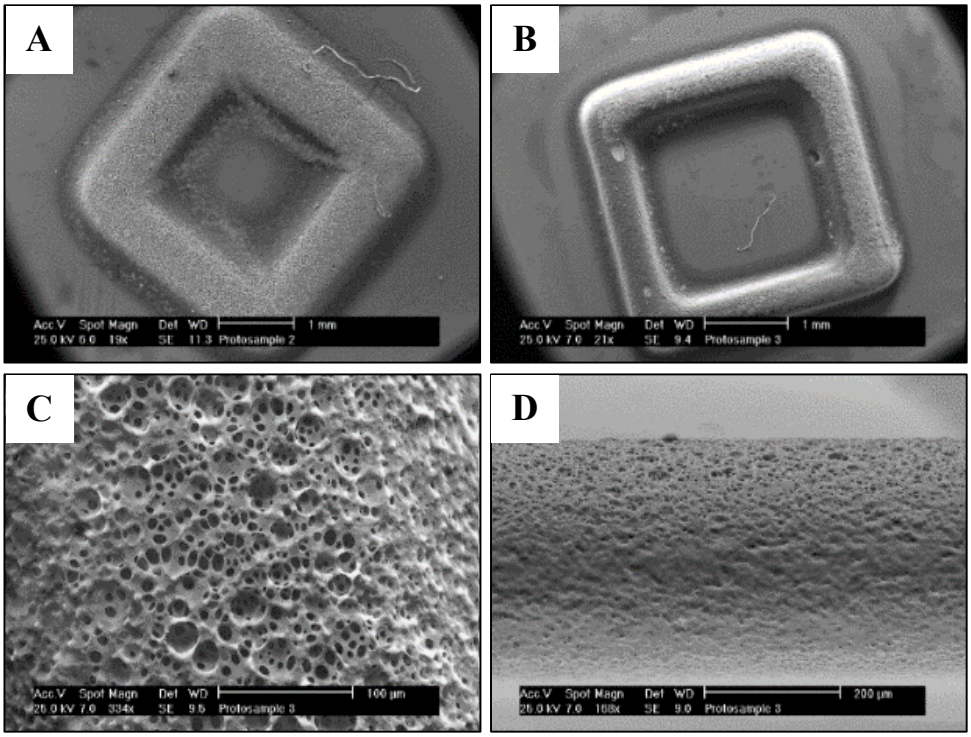

Figure 18: SEM images of a polymerised PolyHIPE square with different magnifications. (**A and B**), Initial square structures of PolyHIPE. **C**, shows the Top view of the square with a more open surface. **D**, side view of the PolyHIPE square, the side appears to have a closed outer surface.

These initial PolyHIPE structures demonstrated the potential of stereolithography of PolyHIPE materials, and defined the laser write parameters for more complex structures. The initial square structure in image **A** in **Figure 18** have thicker sides than image B. This was caused by a slower scan speed of the laser causing an increased amount of polymerisation around the focal spot. The PolyHIPE squares appeared white as expected of a porous foam, as the pores will scatter the light. However it was only from SEM images seen in **Figure 18,** was it noticed that the outer surface had a more open pored morphology on the top surface than its side, which appears to have a closed pored rough texture.

Throughout this thesis I will refer to the closed pore like nature around the PolyHIPEs outer surface as a surface skin. This closed outer pored surface skin has been mentioned previously in the literature, where the outer surface of the HIPE was shown

to destabilise to form a surface skin when it was polymerised against Polyvinyl chloride (PVC). An open surface was observed when the authors polymerised the HIPE against Polytetrafluoroethylene (PTFE) [3].

Given that the emulsion cured readily with the scanning stereolithography set-up, the next question was whether or not the internal structure of the produced PolyHIPE squares retained its classic PolyHIPE morphology, or if the closed pored morphology seen on the outer surface occurred thought the material. To answer this question one of the larger PolyHIPE squares was broken and the internal morphology analysed by SEM image analysis **Figure 19**. The internal morphology of the squares retained the PolyHIPE morphology, and the surface skin was found to be confined, as the name suggests, to the outer surface.

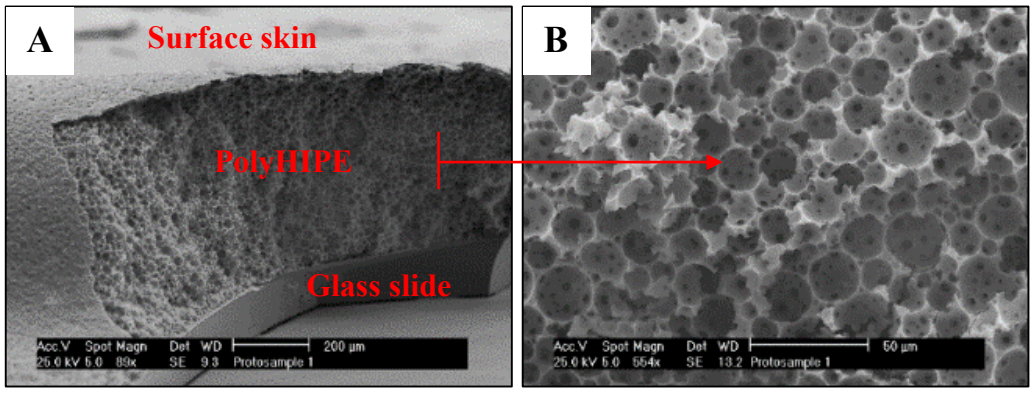

Figure 19: SEM image of PolyHIPE with surface skin 80% porous, EHA formulation UV cured at 355 nm. **A**, an overview of the cracked PolyHIPE square structure shown in ***Figure 18***. **B**, a close up of the internal porous morphology within the original PolyHIPE square.

To produce more complex structures the effect of different laser processing parameters needed to be determined. To do this, a series of lines were scanned each with an increased scanning speed from 1 to 5 mm/s to establish the effect of the polymerisation time on the internal structure of the PolyHIPE. The lines produced at the lower scan speeds were noticeably thick, and as the scan speed increased the lines gradually decreased in size until the produced material had a gel like appearance and no internal porosity as seen in the SEM images in **Figure 20**.

One explanation on the size difference in the PolyHIPE lines is that the emulsion droplets scatter the UV light, so a slower write speed will be thicker as a result. The

collapsed lines with the faster speeds indicates that there is an upper limit on the achievable write speed, image **D** in **Figure 20.** Their collapsed nature may be due to there being insufficient UV light absorption to fully polymerise the monomers at the fast speed, the mechanically weak partially polymerised monomer would collapse during the washing stages as it may not be able to support itself. This demonstrates that both the quality of the polymerised features and their respective size is heavily dependent on the write speed settings and the amount of UV light these materials are exposed to.

The PolyHIPE lines have a different shape depending on the laser scanning sped, the slower speeds produced thicker lines than the faster ones, and this can be seen in **Figure 20**. During the polymerisation process the laser was focused from the base of the glass slide upwards into the HIPE. The lines shape could be attributed to the scattering of the UV light as it passes into the HIPE. Image C shows the minimal width structure produced by this original experiment, which is ~100 μm.

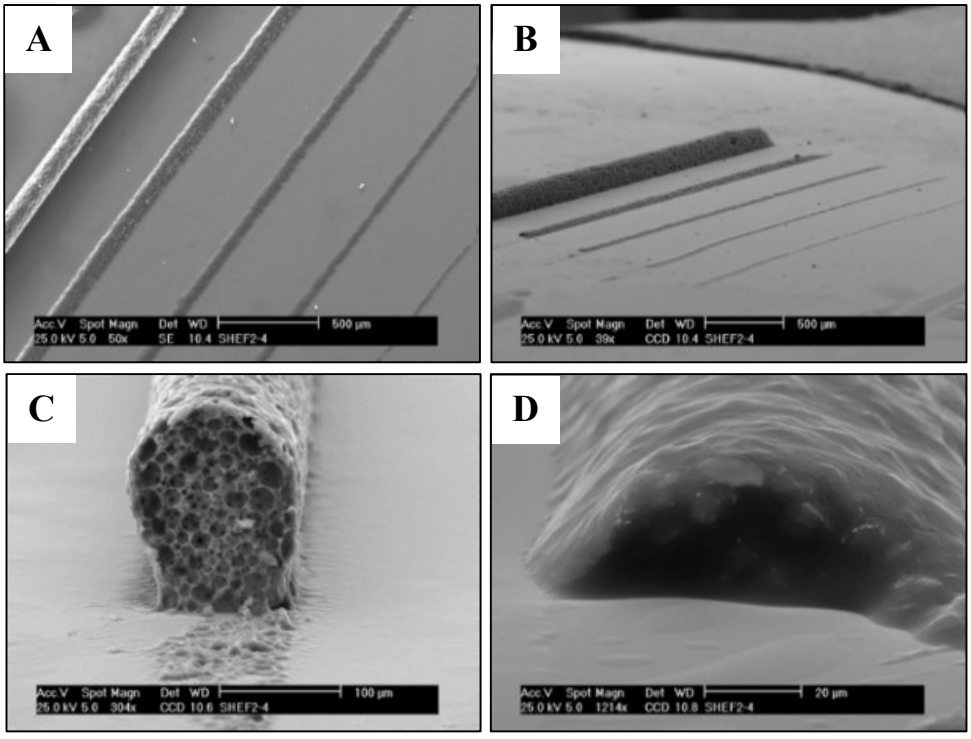

Figure 20: PolyHIPE lines polymerized with increasing laser write speed. EHA 80 HIPE formulation used. **A,** direct laser write speeds of 1-5mm/s in increments of 1mm/s from left to right. **B** shows image **A** from a different angle to show the surface shape. **C**, internal morphology of the PolyHIPE line. **D**, the destabilised polymer line written at the higher write speed

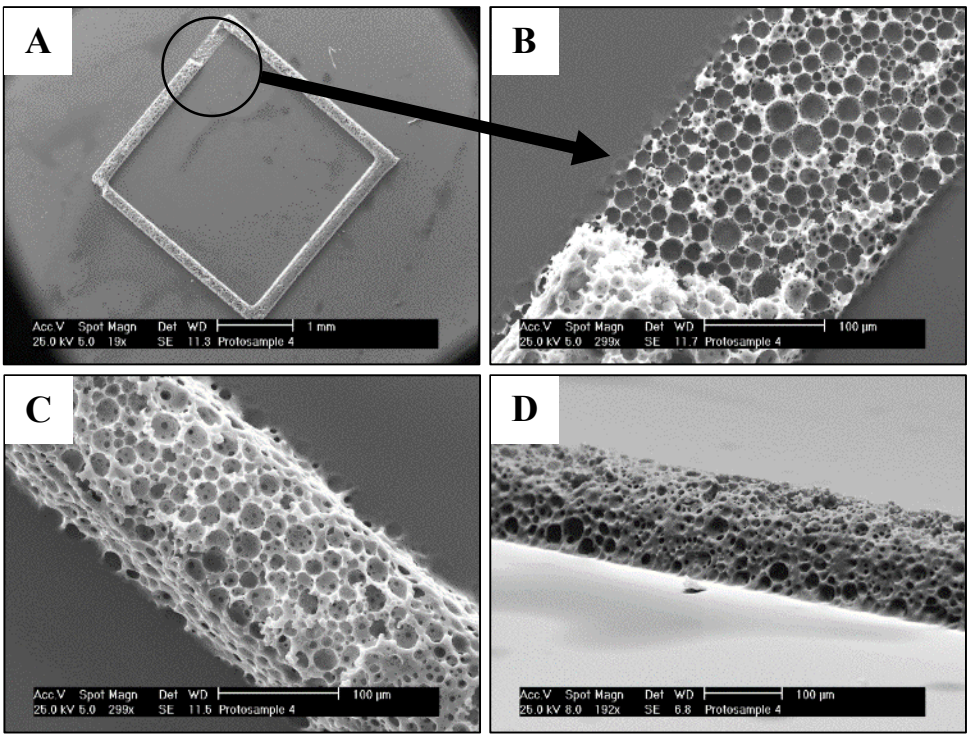

Figure 21 SEM images of a 3D printed square. **A**, PolyHIPE square, **B,** broken off section of the PolyHIPE line adhered to the glass. **C,** top surface. **D**, side view.

The internal morphology of the PolyHIPE is maintained at the glass/polymer boundary, this can be observed in image **B** in **Figure 21**. In this image the initial square structure had a section cut off to expose the inner morphology of the PolyHIPE. The edge of the PolyHIPE line shown in Image **B** also shows small areas where the monomer has polymerised around half of a spherical droplet, hence leaving larger pores around the outside of the PolyHIPE square. Some partial surface skin can be seen around the edges which is not observed at the top surface.

3.2.2. PolyHIPE: grid lattice

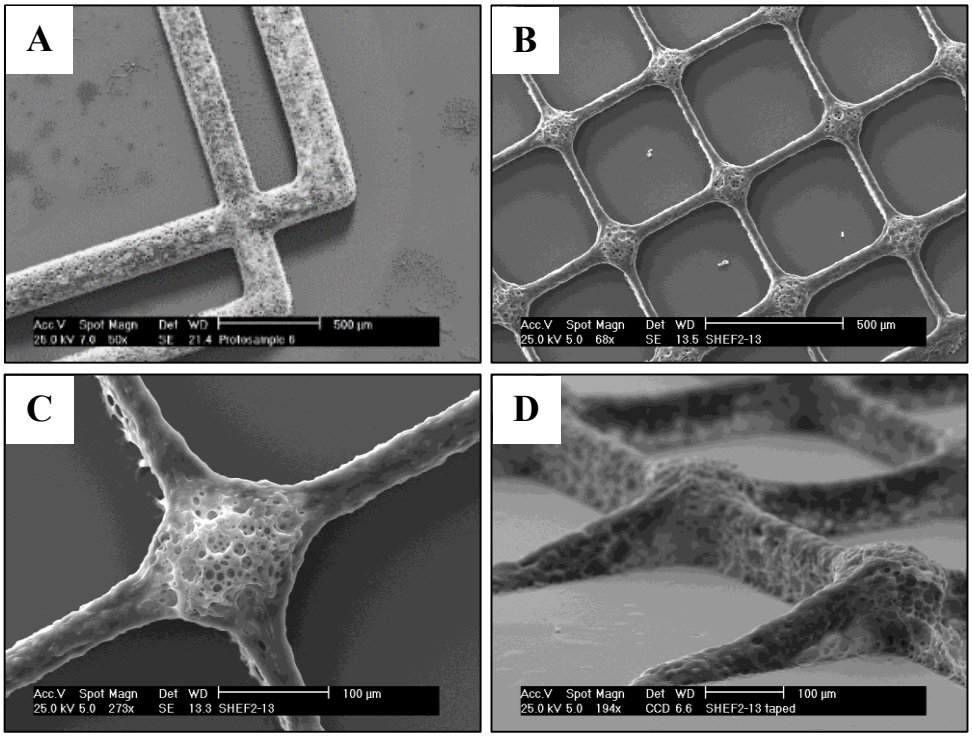

Figure 22: example of a printed grid. Top left crossover of two lines, top right grid array, EHA80 HIPE formulation regular grid pattern Bottom left shows the overlapping regions. Bottom right side view of the lines to show surface

The initial PolyHIPE structures, both the lines and squares have demonstrated that the confinement of the polymerisation region can be sufficient enough to structure the HIPE in a spatially controlled manner. A more complex grid lattice was produced with 30 µm thick lines overlapping each other in **Figure 22**. This more complex structure was produced by scanning the focused UV laser first in the horizontal 'X' direction, then in the vertical 'Y' direction. The intersecting regions where the two lines cross over were thicker than the individual lines. This is because the 'Y' scan of the UV light had to pass over the previously cured lines from the initial 'X' directional scan. The thicker regions at the interface between the two lines relates to the degree of UV exposure, as the UV light is scattered by the previously cured PolyHIPE lines, which causes a larger area of polymerisation. This larger overlapping region has been seen with other stereolithography processes that have produced a similar pattern [49].

The PolyHIPE structure deteriorates completely towards the very edge of the grid lattice. This can be seen in image **D** in **Figure 22**. The surface skin can be seen covering

the top of these lines. A provisional explanation for this is that the outer region of the lines did not have a sufficient amount of UV light exposure at these edges to crosslink the polymer to the same extent as the rest of the lines.

A combination of two squares and the grid lattice was polymerised over each other to observe the effect that multiple passes of the laser has on the sample, as well as the effect different cured regions would have on each other. First the large squares were structured, then the grid lattice was polymerised over it. There is a large amount of excess polymerisation around the square structures caused by scattering of the UV light. This can be seen by the increased degree of polymerisation around the larger square regions, which have a partially closed surface skin shown in image **B** in **Figure 23**. Image **B** also shows a defect within the large line caused by a large water droplet, this shows the internal PolyHIPE morphology is maintained within these structures.

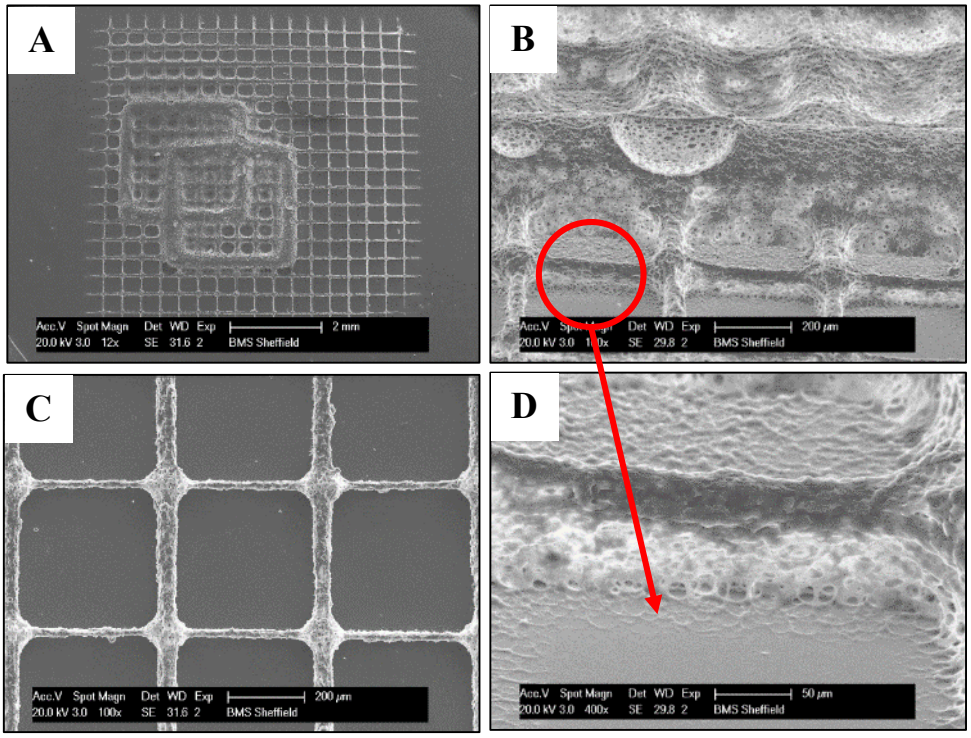

Figure 23. (**A**) An overview SEM image of a slowly polymerized square structure and faster polymerized grid lattice around it. (**B**) Close up of the square showing where an air bubble or large water droplet created a concave defect, (**C**) top view of the grid lattice, (**D**) open porosity can be seen on the side of the grid lattice lines.

An interesting observation to be made is the glass surface surrounding the polymerised line in Image **D** in the above **Figure 23**. There is a small amount of polymer on the glass surface that uniformly surrounds the cured PolyHIPE line, this effect is not

present around the lines in image **C**. This excess cured region only exists around the lines near the larger polymerised square structure, which indicates that it is either present because of the excess UV scattering, or another mechanism involving the crosslinking of the monomer units is taking place. Also a very faint outline of the PolyHIPE structure can be partially made out in this polymer region on the glass slide, as if the HIPE has partially cured and then collapsed on itself nearest to the glass surface, perhaps this is caused by the glass scattering the UV light at the HIPE/glass boundary.

3.3 Projection stereolithography of HIPE

One of the advantages of using photocurable monomers for the PolyHIPE production is that the photo-initiated free radical polymerisation process can be tailored to match different wavelengths of light, therefore a range of different light sources can be used to polymerise the HIPE depending on the experimental rig.

The projection based stereolithography method differs to the direct laser scan approach in that the laser light is uniformly exposed over the entire HIPE surface, as opposed to sequentially scanning the laser across the top surface. This means that the projection method can produce larger objects at a faster rate. In scanning stereolithography the fabrication time will be dictated by the amount of line passes to polymerise a set area.

The projection stereolithography set-up was used to produce PolyHIPE tubular structures. A violet laser (405 nm) was expanded and projected onto a digital micro mirror device (DMD). This digital mirror device has an array of micrometre-sized mirrors that each correlate to a pixel on the computer software, each of these micro-mirrors can tilt to selectively reflect the light to reflect any 2D image. Black and white images were drawn using Microsoft Paint with the pixels matched to the DMD (1024 by 768) and the images were saved as a monochrome bitmap to ensure only black and white pixels. A circle of violet light was selectively reflected and projected onto the top surface of a small glass vial of HIPE, with a flat metal stage positioned 500µm below the top surface of the HIPE to ensure the polymerised PolyHIPE adheres to the metal stage. A schematic of the experimental setup is shown in Figure 24. The stage

is slowly drawn in to the HIPE with its top surface constantly being exposed to the violet light. The polymerised PolyHIPE is drawn into the HIPE at a constant rate to produce the porous tubes shown in **Figure 25**. The water volume ratio of the initial HIPE was varied between 75-90% and the resulting structures are shown in **Figure 26**. The increase in the water volume also increased the viscosity of the HIPE which prevented the surrounding HIPE from filling in the polymerised tube, which created a 'well' like effect within the HIPE vial. This effect was also achieved by either increasing the laser power or lowering the speed of the stage, both of these methods polymerised the HIPE before it could fill the inner volume of the tube.

The overall shape of the tubes were adjusted by controlling the laser power and the speed of the stage. Typical speeds between 0.05 to 0.8 mm s^{-1} were used. Increasing the speed required us to increase the laser power to around 60-90mW in order to ensure sufficient polymerisation of the HIPE at these faster speeds. A range of nominal porosities were used for the polymerisation of the initial PolyHIPE tubes. These were 75, 80 and 90% water volumes as shown in **Figure 25** and **Figure 26**. The PolyHIPE tubes retained their typical PolyHIPE morphology as seen previously in the structures produce by direct laser write in **Figure 19**. The thickness of the tubes was dependent on the size of the reflected circle from the DMD, as well as the laser power; increasing the power increased the wall thickness of the PolyHIPE tube due to the light scattering outwards from its initial point of exposure.

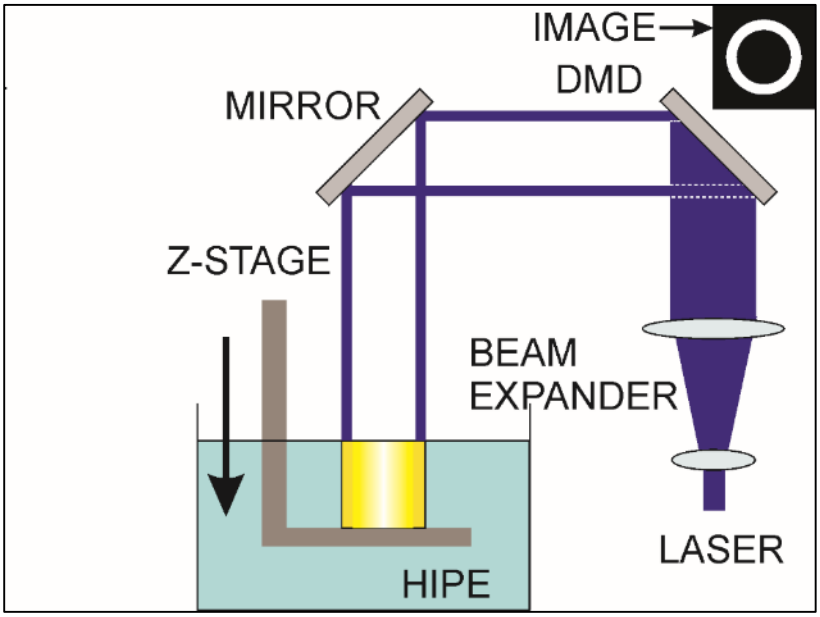

Figure 24: Schematic setup of the projection rig to produce the PolyHIPE tubes. The DMD stands for Digital micro mirror device. Image from [43]. The Laser is expanded and collimated before being reflected off the DMD. The reflected light, in this case a circle, is reflected down on top of a HIPE, where a copper stage 500 µm below the HIPE surface to ensure the initial exposure adheres to the stage so that it can be drawn into the HIPE during the polymerisation process.

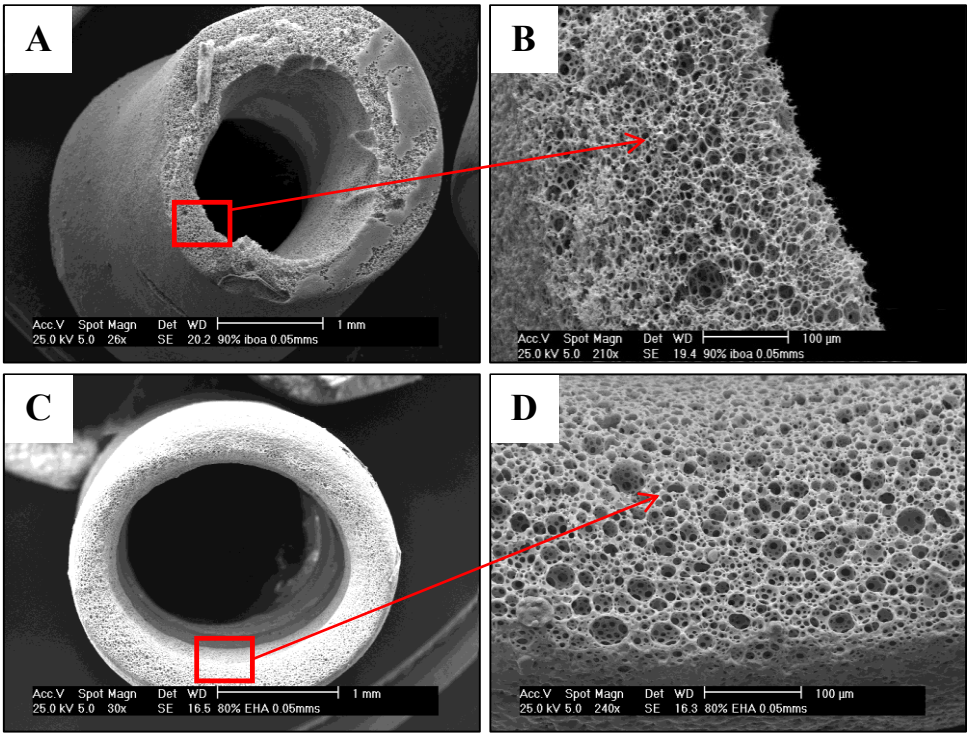

Figure 25: SEM images of PolyHIPE tubes. (**A** &**B**) 90% EHA overview and close up on porosity. (**C** & **D**) 80% EHA PolyHIPE, a surface skin can be seen around the outside of the tube in image **D**.

3.4 Effect of water content on the PolyHIPE tubes

The PolyHIPE structure is dictated by the pre-processing conditions of the initial High Internal Phase Emulsion, and this is especially the case or the water volume ratio. Increasing the water volume in the initial emulsion increases the porosity of the PolyHIPE, and this effect can be seen in Figure 26. The lowest water volume ratio used for the HIPE was 75%, and it can be observed that the porosity of the PolyHIPE increases in a similar amount as the water volume increase from 75 to 90% (Figure 26). Only the water volume ratio is being increased within these samples, with all the other parameters being kept the same. This is an expected observation as the same volume of the monomer phase will be stretched around an ever increased surface area of the higher water volumes. This will result in thinner walls between adjacent water droplets, these will be more prone to the effects of monomer contraction during the polymerisation process which will result in more interconnecting voids, this is effect is highlighted by the 90% PolyHIPE tubes having a porous structure, with very thin connecting polymer supports. Whereas the 75% PolyHIPE tubes have a less degree of porosity, and appear to have more polymer per unit area.

The viscosity of the HIPE proved problematic with both the direct laser write and projection polymerisation. The HIPE needs to be fluid enough to recoat the new layer for subsequent polymerisation, or to continuously fill the top surface of the polymerising structures from the projection based stereolithography. The increased viscosity of the HIPE due to the high 90% waver volume proved problematic.

In the literature this issue has been partially addressed, toluene has been used to reduce the viscosity of the HIPE in a layer-by-layer stereolithography fabrication of the PolyHIPE [25]. This approach can be adopted to reduce the viscosity of the HIPE which would improve the recoating of the new layers for more complex structures to be fabricated. Furthermore the addition of a porogen such as toluene to the emulsion should also increase the porosity of the PolyHIPE, which could be more advantageous for cell ingrowth.

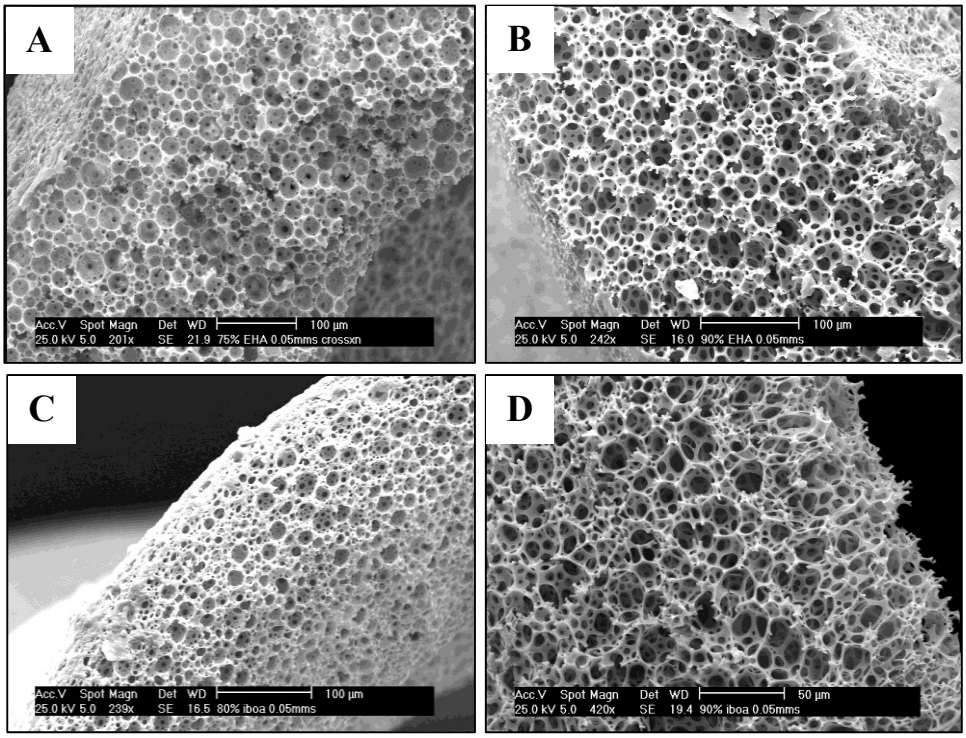

Figure 26: SEM images of the PolyHIPE tubes, (A) 75% EHA (0.6 mm/s speed and 75mW power. (B) 90% EHA (z speed 0.9mm/s power 90mW. (C) 80% EHA (0.8mm/s power 90mW. (D) 90% EHA (0.9mm/s, power 90mW at increased magnification.

3.5 Projection Polymerisation surface skin

The same surface skin effect was observed around the outer surface of the PolyHIPE tubes as seen previously in the direct laser written lines seen in **Figure 19** and Figure 23. The outer surface of the PolyHIPE tubes had closed morphology whereas the inner surface had an open one, this can be seen in image D in **Figure 25** and the surfaces can be seen in more detail in **Figure 27**. It was previously stated that the surface skin only occurs when there is a transition between the crosslinked PolyHIPE and the surrounding non-crosslinked HIPE. This same transition between the cured and non-cured polymer would exist around the outer boundary of the tubes, which could result in the surface skin effect. The more open pored inner surface on the other hand was achieve by matching the rate of polymerisation and stage speed to ensure the HIPE cures faster than it can fill the inner region of the tube. As a result a 'well' is formed in the middle of the tube, and the HIPE is cured against air and not uncured HIPE. Therefore a tentative explanation to the cause behind the surface skin at this stage suggests it is formed by the HIPE partially polymerizing adjacent to PolyHIPE.

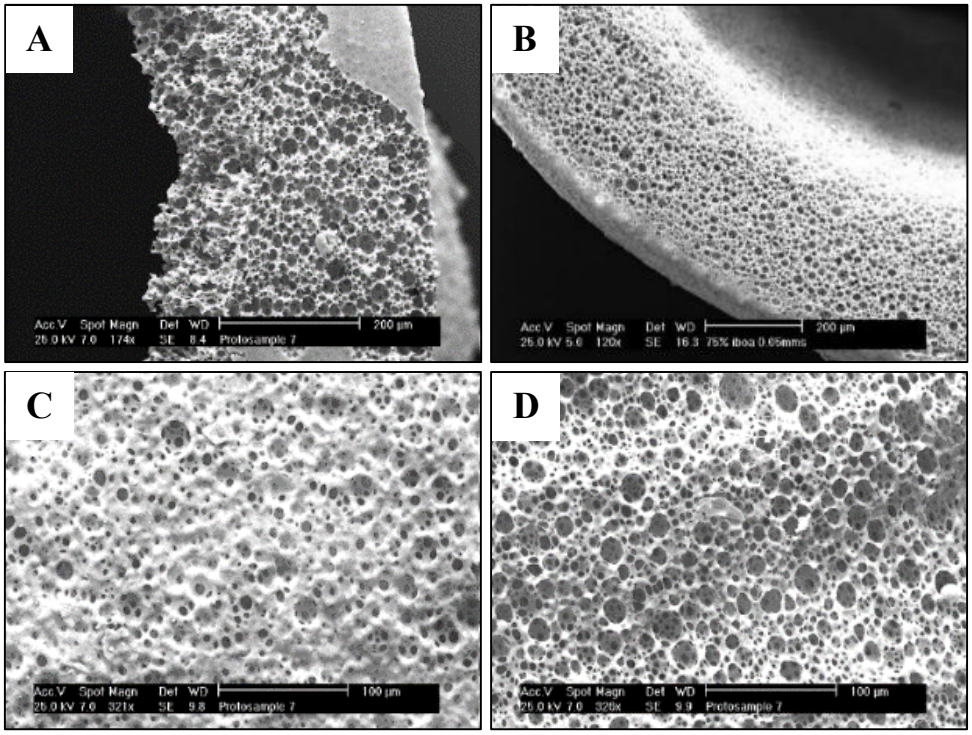

Figure 27: SEM images of PolyHIPE tubes. (**A**) Section of 75%IBOA PolyHIPE tube, (**B**) Top section of 75% IBOA tube showing top part of closed outer surface, (**C**) outside surface of 75% IBOA tube showing partial closed surface, **(D)** inside surface of 75% IBOA tube showing a more open porosity. IBOA 75 tube (z speed 0.6mm s^{-1}, power 75mW) bottom right

By varying the stage speed the PolyHIPE tubes can either be produced with an internal closed surface, or partially open one. This was achieved by altering the exposure conditions to control whether the surrounding HIPE could fill the inner region of the tube, or not. A more open internal porosity on the inner surface of the PolyHIPE tube was observed when it is polymerised against the air, and a closed one when there is a transition between the cured and non-cured material.

3.6 Porosity of projection stereolithography-based structures

The method of polymerising the PolyHIPE could potentially affect its porosity. Therefore a comparison of the pore sizes between the tubes produced by stereolithography (**Figure 26**) and the bulk polymerised PolyHIPE (**Figure 28**) was made. Both polymerisation methods were found to have similar pore sizes, although it should be taken into account a small degree of variances that could be artificially

introduced due to errors while manually measuring the pores. The average porosity was found to be similar between the different water volume ratios. Overall the average pore size of the different samples were found to be relatively similar despite the difference between the volumes of water used.

The differences between the 75% volume and 90% nominal porosities are determined by the volume ratio of water added to the initial emulsion. To calculate the porosity of the PolyHIPE from SEM images. 100 pores were measured using Image J, then the average pore measurement was multiplied by the statistical correction factor ($\frac{2}{\sqrt{3}}$) as defined in [48] [30]. This is used to give a more accurate prediction to the measured voids as the assumption is made that the cross section being imaged will not have intersected the spheres directly through their middle. So the initial measured values would be an underestimate of the actual values [14] [50].

3.7 Description of the SEM images of the PolyHIPE morphology.

All of the PolyHIPE samples had a morphology that is typical of the PolyHIPE structure; exhibiting large voids which have interconnecting windows between them. Analysing SEM images of the cross-section of the PolyHIPEs shown that the average void diameters were between 5-35 μm and that this increased slightly as the water volume ratio increased. The EHA/IBOA 90 had more interconnecting windows than their 75% counterparts. This was observed in both the projection stereolithography and the bulk cured samples, and the degree of interconnectivity followed this trend in relation to the water volume ratio 75<80<90, increasing the water volume increased the amount of interconnectivity.

The HIPE morphology was preserved by both the projection and the bulk polymerisation methods. This conservation of the porosity is important to ensure that

control over the pore size and interconnectivity is maintained during the stereolithography fabrication processes.

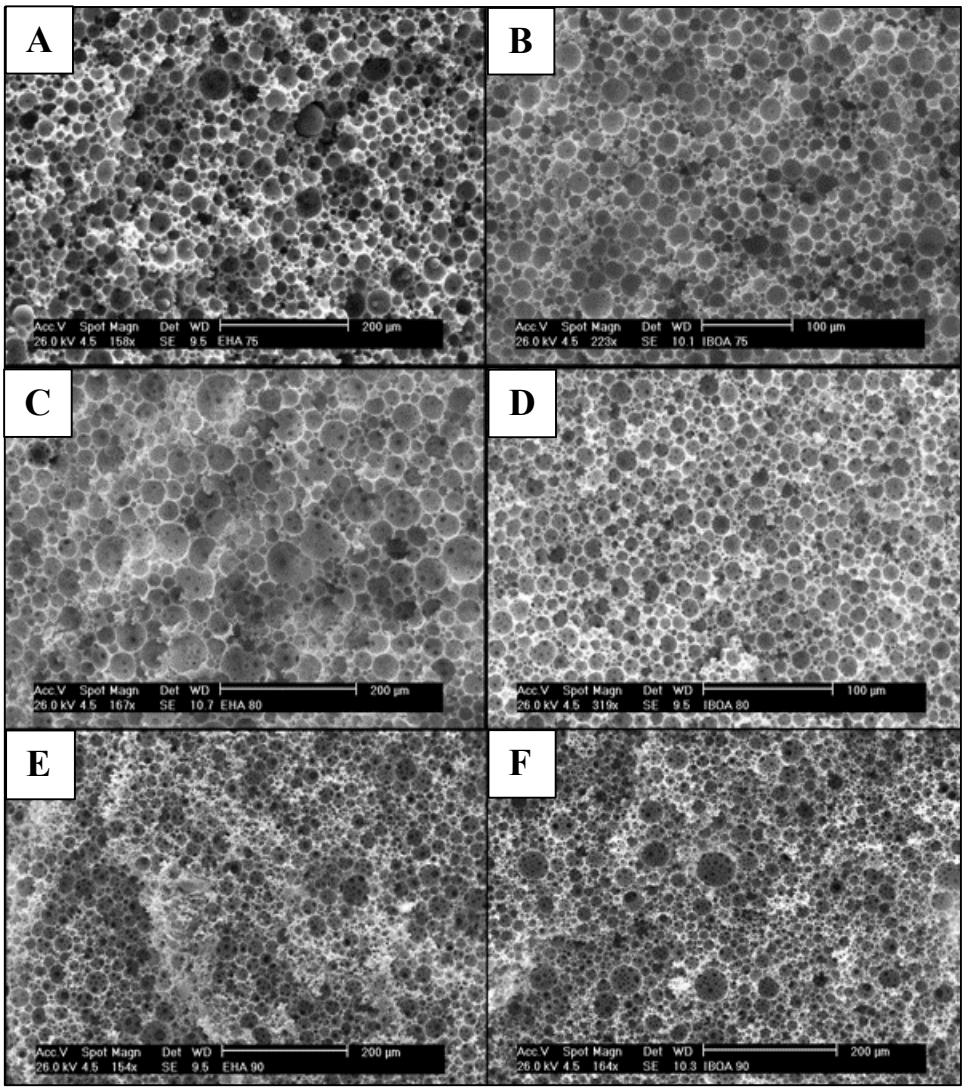

Figure 28: SEM images of bulk cured PolyHIPE: (**A**) EHA75; (**B**) IBOA75; (**C**) EHA80; (**D**) IBOA80; (**E**) EHA90; (**F**) IBOA90 [43].

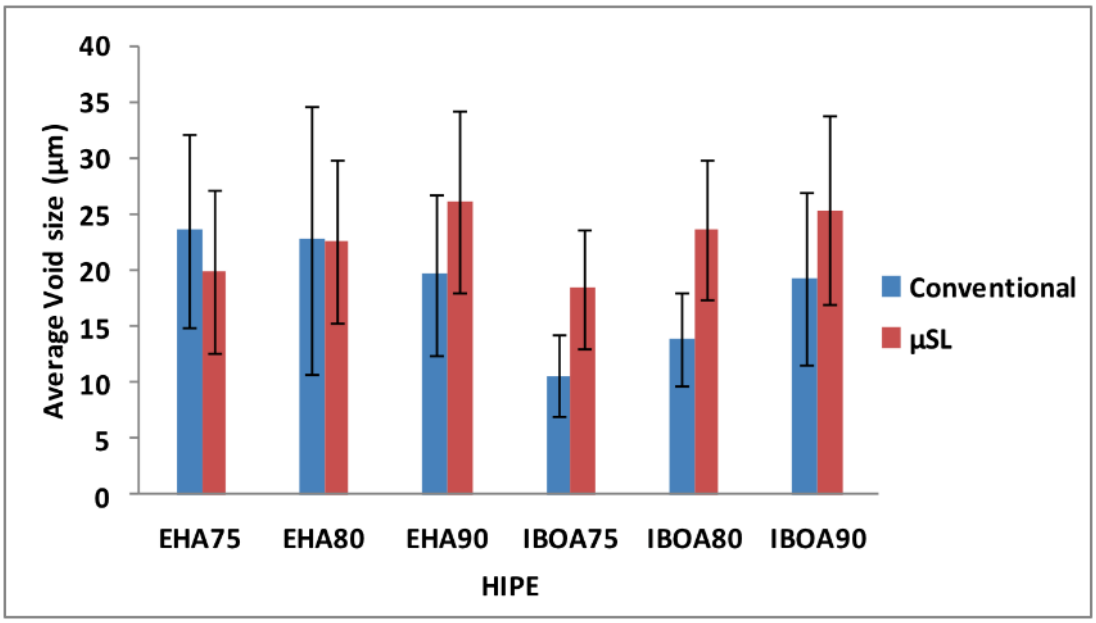

Figure 29: The average void diameters of the PolyHIPE produced from Bulk polymerisation by UV light and µSL. Measurements taken from SEM images Average void diameters of conventionally- and µSL-cured PolyHIPEs measured from SEM images [43].

3.8 Control over mechanical properties

An important advantage of using a monomer blend for the PolyHIPE formation is the control over the mechanical properties by altering the monomer ratios. By co-polymerisation of the rigid IBOA monomer and EHA elastomer the rigidity or elasticity of the PolyHIPE can be adjusted. The difference between these have been demonstrated by crushing the PolyHIPE tubes with a tweezer, and are shown in **Figure 30** and **Figure 31**. The high EHA ratio PolyHIPE tubes were very flexible and returned to their original shape after crushing, this can be seen in. The IBOA PolyHIPE tubes on the other hand were very rigid and cracked.

To determined the mecahnical properties of the PolyHIPE monomer blends two different approaches were made. Nanoindentation was used to determine the

mechanical properties of the polymer, and a tensometer to determine the bulk properties of the PolyHIPE.

3.9 Mechanical Properties of the EHA/IBOA PolyHIPE

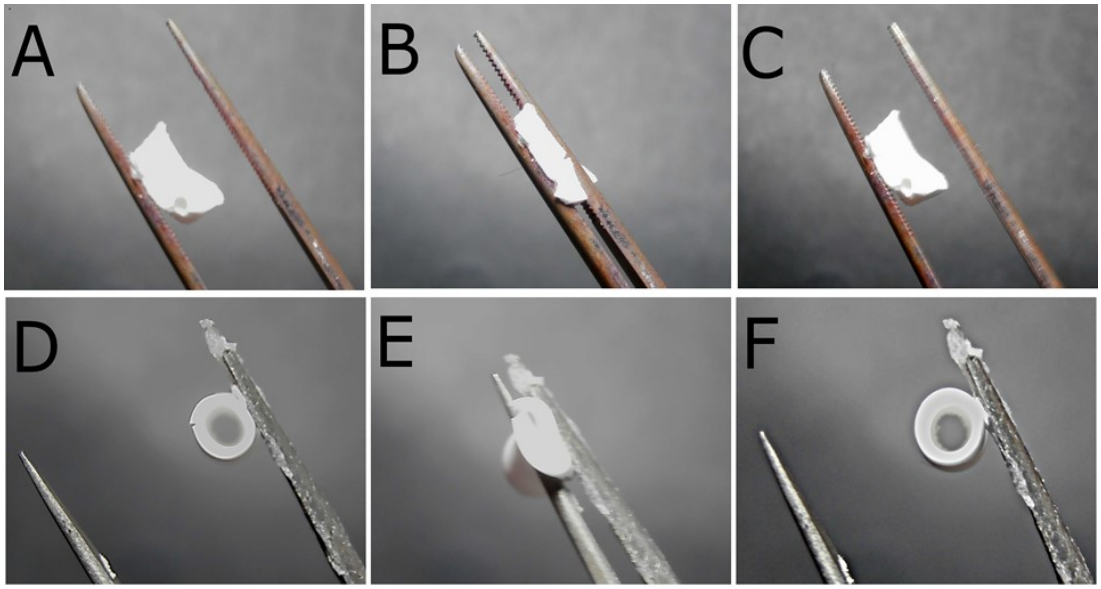

Figure 30 (**A**) EHA90 bulk cured; (**B**) EHA90 being compressed (**C**) EHA90 after compression of image **B**; (**D**) EHA90 PolyHIPE tube; (**E**) EHA90 being compressed; (**F**) EHA90 after compression of image **E.**

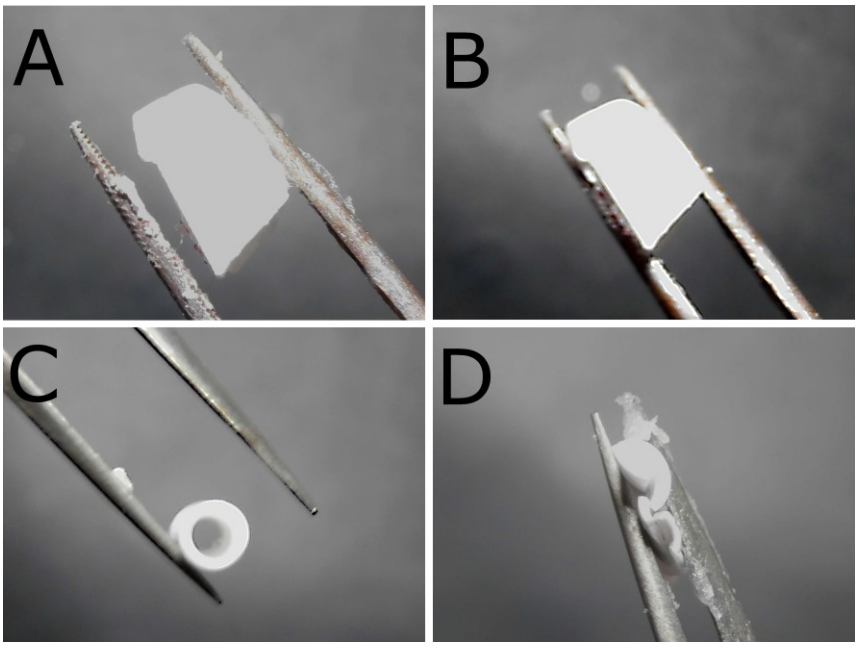

Figure 31 (**A**) Bulk polymerised IBOA90; (**B**) Bulk polymerised IBOA90 under load showing negligible sample deformation; (**C**) Projection polymerised IBOA90; (**D**) Projection polymerised IBOA90 under load, note the tube has been crushed.

3.9.1. Tensile testing of the PolyHIPE

To determine the mechanical properties of the PolyHIPE, dog bone shaped tensile samples were laser cut from bulk cured flat sheets. The maximum size of the sample for the extensometer is about 35mm therefore a scaled down version was drawn in in CorelDraw X5 and used, this is shown in **Figure 32.** 10 tensile testing dog bones were cut out for each sample for tensile testing.

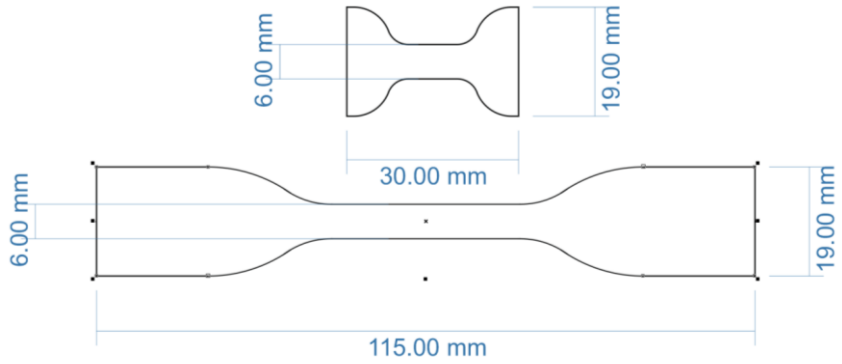

Figure 32: Top, the scaled down tensile specimen used for the extensometer testing. Bottom, original tensile specimen derived from American Society for Testing and Materials (ASTM) standard D638-10. The axial dimensions were kept the same to have the same cross sectional area.

Numerous PolyHIPE samples were created with different porosities and monomer blends to determine the effect of monomer composition and porosity on the mechanical properties. Flat sheets of the PolyHIPE polymerised via a UV belt curer and laser cut to the dimensions shown in **Figure 32**. An example of a typical stress strain plot from these experiments are shown **Figure 33.**

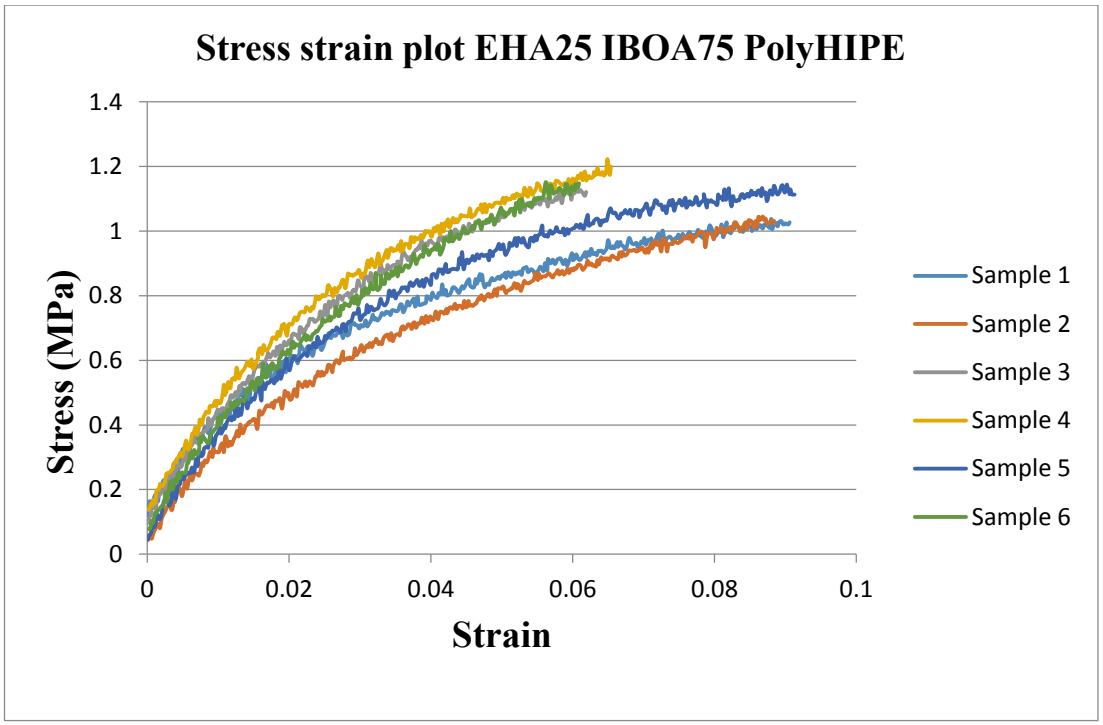

Figure 33*:* Stress strain plot for EHA25 IBOA75 PolyHIPE with 80% water volume ratio

To create the normalised load displacement, the original displacement reading was divided by the starting distance between the grips (10mm) and the load was divided by the cross sectional area (6mm) width multiplied by the thickness measured for each sample. This method was used to count for the variances in the thickness between all the samples produced.

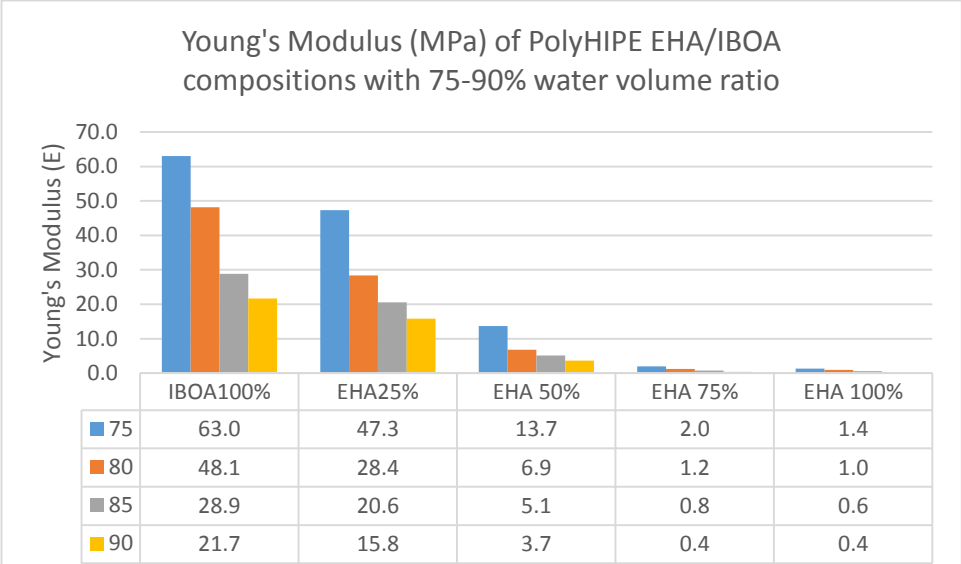

	IBOA100%	EHA25%	EHA 50%	EHA 75%	EHA 100%
75	63.0	47.3	13.7	2.0	1.4
80	48.1	28.4	6.9	1.2	1.0
85	28.9	20.6	5.1	0.8	0.6
90	21.7	15.8	3.7	0.4	0.4

Table 2: Young's Modulus of Elasticity relative to the different water porosities of the PolyHIPE and the ratio of the EHA to IBOA monomer. The table values are the Young's Modulus (E).

The Young's Modulus decreased with the increase in both the water content and ratio of the elastomer EHA. Increasing the droplet ratio from 75% to 90% with the same monomer volume, means that the finite amount of the monomer is being stretched over an ever increasing surface area of water, which will reduce the amount of polymer in the same comparative area to a lower water percentage PolyHIPE, which would result in a lower modulus values. The decrease in the E-moduli as the water porosity was increased from 75 to 80% has also been reported on in the literature, as well as [34].The EHA is added to polymers as an elastomer, it increases the elasticity of the polymer. It has been reported that increasing the IBOA increases stiffness and reduces swelling [8]. The predominately EHA based PolyHIPEs have been reported of as being a more elastomeric foam [16], and a similar trend was observed in ***Table 2***, increasing the EHA concentration decreased the modulus.

3.10 Laser cutting of the PolyHIPE: A subtractive manufacturing approach

Laser cutting is a subtractive manufacturing technique which offers some advantages over the additive manufacturing approach of the PolyHIPE material. From a bulk manufacturing perspective the main advantage is the speed of which the laser can cut and shape the PolyHIPE with a very high degree of accuracy, a wide range of materials can be cut or etched, as it is a very versatile technique [51]. Laser cutters have been reported to produce a finer finish than other conventional cutting techniques [52], the process is non-contact based and therefore will not damage the sample in the way the other cutting techniques will [52].

Laser cutting is a thermal process where a laser beam is focused onto a small focal spot. The high amount of IR radiation heats up the material in the focal spot causing it to both melt and vaporize as it absorbs the lasers energy [52], it can be described as a thermal ablation process, as the material is removed by its vaporization (or thermal decomposition) [53].

Large sheets of PolyHIPE can be readily fabricated and then post-processed using the laser cutter to produce a range of bespoke scaffolds by removing the material in a subtractive approach as opposed to adding it in a layer by layer one.

The PolyHIPE material has a very low density, therefore the thin polymer regions are highly susceptible to the heat generated by the laser cutting process. Any shape or structure can be etched within the PolyHIPE with well-defined open pored surfaces. The interface where the laser has ablated the PolyHIPE retains its open porosity, therefore this technique can be used as viable post processing method to introduce a user defined macro porosity within the PolyHIPE, while maintaining the micro porosity and interconnectivity.

3.11 Laser cutting of the PolyHIPE material

Flat sheets of PolyHIPE were created by passing sheets of HIPE under a UV belt curer. The HIPE was poured into a rectangle mould created by adhering a hollow rectangle of PDMS on top of a small sheet of glass (10×10cm). This was then passed under a UV conveyor belt several times while flipping the sample every consecutive pass to

evenly polymerise both sides. The UV lamp from the belt curer operated at a high temperature, only the speed of the conveyor belt could be altered to adjust the level of UV exposure. A faster conveyor belt speed with multiple passes was better than slower passes as the sample would become very hot. A conveyor belt speed of 10 m/minute was chosen as the benchmark speed.

A range of different lines were laser cut from a large sheet of PolyHIPE to determine both the optimum laser cutting parameters, and to find the suitable cutting parameters to prevent sample damage. A range of laser cutting parameters were used to determine whether a single laser pass at a higher power or multiple passes at a lower power produces a clean straight cut.

A 40 W CO_2 laser tube source (9-11 µm wavelength) was used within an Epilog Laser system. Cross sectional light microscope images were taken and used to assess the effect the laser has on the material cutting, and determine the lowest laser power to achieve a straight cut through the PolyHIPE material. The best cutting conditions found were a combination of low laser power and multiple passes, i.e. 8% power from a 40W CO_2 laser (3.2W) with 3 repeat passes as shown in **Figure 34**. The lower the laser scan speed the straighter the cut and the low laser power reduced sample damage.

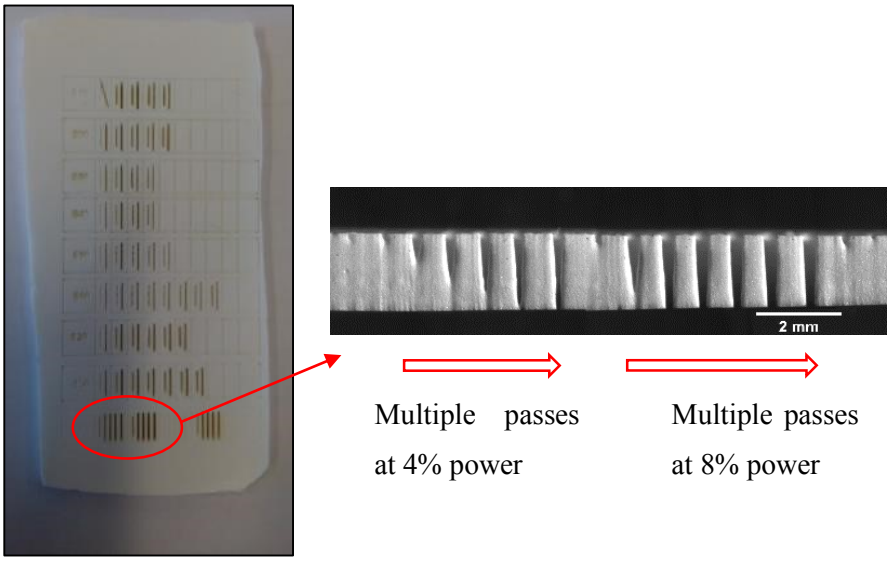

Figure 34: Left, PolyHIPE with multiple lines laser cut, each with a different power and speed. Right, Microscope images of the cross section of the highlighted region. The left part shows the gradual increase from 4-20watts with a 10% scanning speed. The right section shows 1-5 passes at 8% laser power e.g. 1 pass, 2 passes, 3 passes 4 passes and 5 passes until the laser has fully cut through the PolyHIPE.

The laser cutting parameters on the Epilog system were only given as a percentage, therefore the results shown are only comparable for the Epilog Laser cutter used for this experiment.

The array of lines produced in **Figure 34** were each ablated with a different laser power and scan speed and was used to determine the optimum laser cutting parameters for the PolyHIPE. The laser power is stated by the company as being 40 watts, therefore I can assume that as a guideline, 10% laser power will correspond to 4 watts. The left picture shows a sequence of rows with different lines all encased in a box that was lightly etched on the top surface to separate the different laser cut lines. Every row was produced using the same scanning speed, this ranged from 10 – 60% of the speed, and these were labelled S10-S60. From left to right in each of these rows the laser power was increased in 10% increments. The shorter line represents a single laser pass, and the longer one represents multiple laser passes over the same spot until the laser had cut all the way through the material. After each row the PolyHIPE was laser cut in half to create a flat surface to image the cross section of the laser cut lines.

The right image in **Figure 34** shows the gradual change in the level of PolyHIPE cutting as the laser is passed multiple times over the same spot. The multiple passes of the laser at 4% power gradually cut more of the PolyHIPE in each pass until it has fully cut the material after 5 laser passes. Whereas at 8% power the PolyHIPE was fully cut with only 2 passes. The multiple passes from the 8% laser power created a straight cut line through the PolyHIPE without the gradual narrowing effect that the single laser cut passes experienced. The same groove like laser etching has been shown by laser cutting PMMA [53].

When the laser gradually cut into the PolyHIPE the lines are thicker on the top surface and gradually get thinner as it goes into the PolyHIPE. This is caused by the increased absorption of the laser power as it penetrates and vaporises the material. The gradual increase in the laser cut region shows that different thicknesses of cut can be engraved into the PolyHIPE by simple altering the laser intensity or scanning speed. This effect was observed with all laser cutting speeds and powers.

The row S10, is shown in more detail in **Figure 35**. Disregard the diagonal line in the top image in **Figure 35** as this was an experimental error. This section was laser cut at

a stage speed of 10%, with the laser power increased in increments of 10% until it reached 40%, this is where the excess heat at this high powered slow scan speed has started to burn the material.

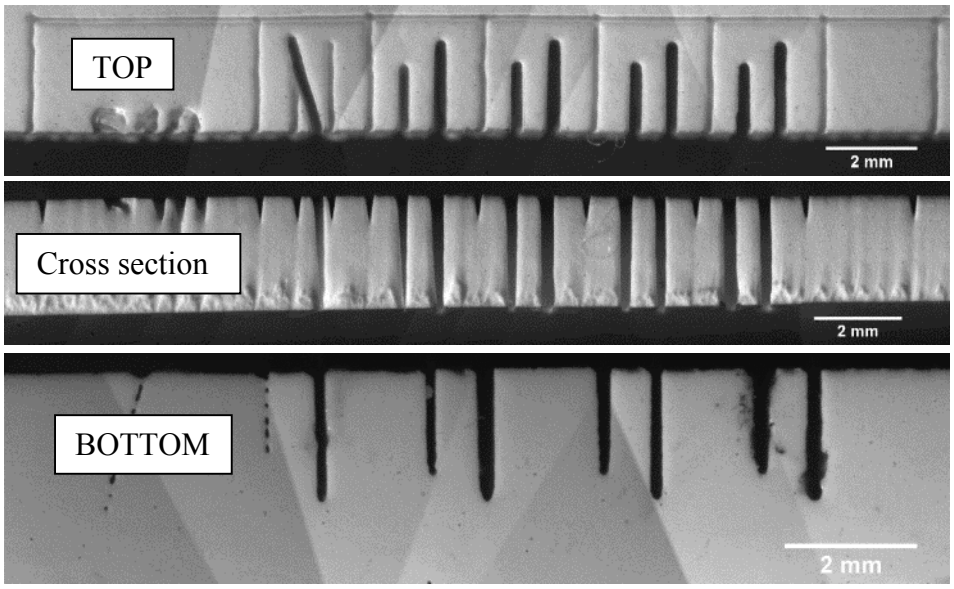

Figure 35: Top, cross section and bottom view of the top section in **Figure 34**. In this section the S10 refers to the use of 10% laser speed throughout all the lines in this row, the software does not specify an absolute value for speed. The laser power increased in increments of 10% to 40%. This should correlate to 4-16Watts laser power (increments of 4watts). The middle image has been laser cut to give a flat surface for imaging with the microscope. The bottom image shows where the sample has burned because of the high laser power. Disregard the diagonal line in the top image as this was an error.

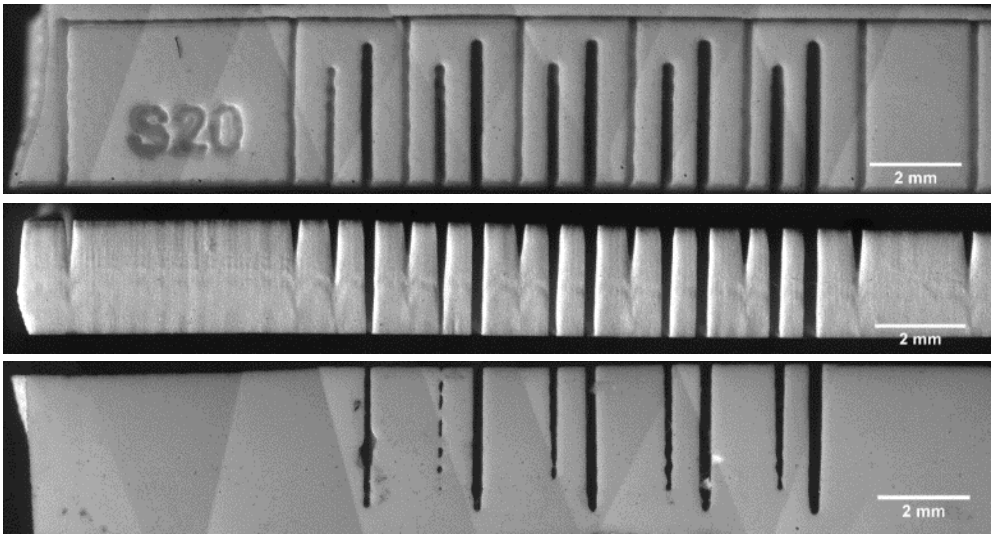

Figure 36: Top, middle and bottom section from the second section down from **Figure 34**. The difference between a single pass and multiple passes can be seen in the quality of the line straightness in the cross section image, and the difference between a single pass and multiple passes in the bottom image.

If a single pass of the laser cannot cut through the PolyHIPE it forms an upside-down triangle like cut into the material and tapers into a point. This triangle like shaped groove etched into the PolyHIPE is known as a kerf. It is the small section of material that the laser has burnt away as it cuts into the material. This can be seen in the cross section image in **Figure 35** and **Figure 36**. For the latter figure the scanning of the laser was set at a constant 20% speed, and the paired lines increase from 10 to 50% power. The single line passes had the smallest cut width. Increasing the laser power or the number of repeat passes increased the line width. This means that for any specific dimensional requirements, the variable thickness of the laser cut region has to be taken into account, otherwise the cut sample will be smaller than the original dimensions programmed into the software.

Increasing the scan speed created a laser cut wavy line. I am attributing this to the very fast movement of the stage during the 30% speed and above. This effect can be seen clearly in the figure below **Figure 37** where the top and side images of a 50% stage speed lines were cut. The side view also shows a distorted line caused by the uneven stage movement at these high speeds.

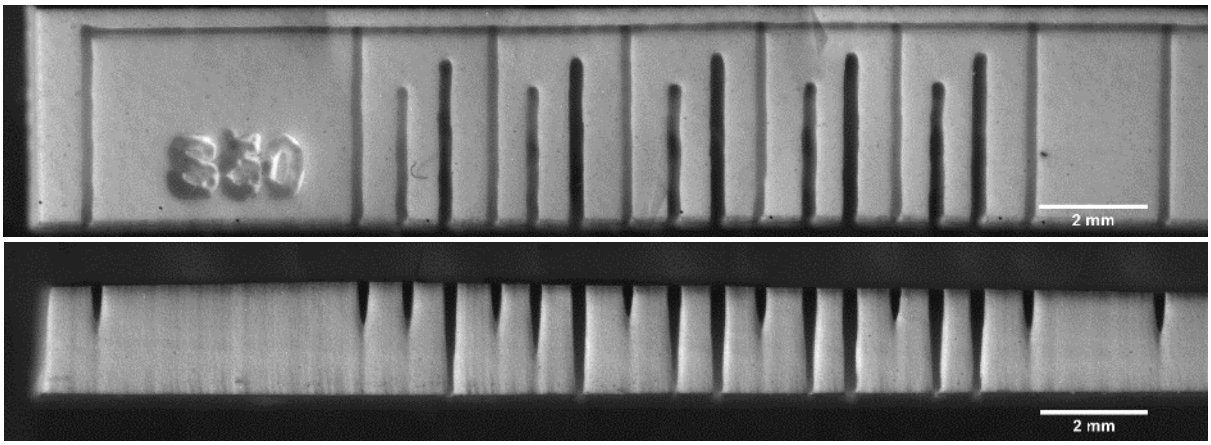

Figure 37: Top and cross section light microscope image of the laser cutting speed 50% and 10-50% laser power. A wavy line can be seen on the top surface, and an uneven cut through the PolyHIPE on the bottom image

The graphs in **Figure 38** and **Figure 39** shows the effect of the laser speed and cut depth within the PolyHIPE material. The higher powered laser scans at the low speed fully ablated a line through the PolyHIPE (2.5-3mm thick). A gradual increase in the laser ablation depth was observed as both the laser scan speed was decreased, or the laser power was increased.

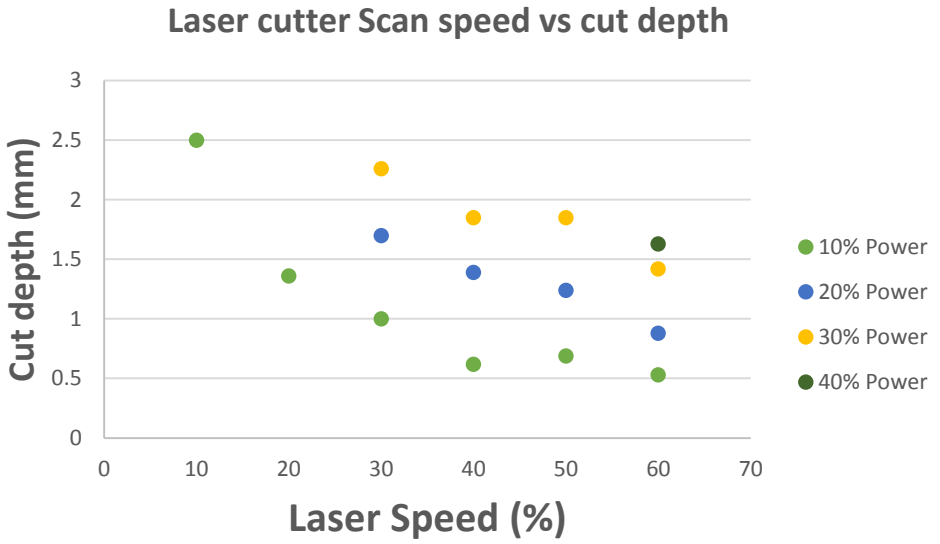

Figure 38: Scatter graph of the laser speed and the cut depth of the PolyHIPE ablated lines.

As the laser power increased the ablation depth increased for all parameters. This is because the amount of ablation will relate directly to the laser light absorption. There is a linear relationship between the laser speed and cut depth between 20-40% speeds

Figure 38. I expect the difference between the cut depths to gradually level off as the laser speed increases. For example; the increase in speed from 10 to 20% results in half the amount of light absorption, the difference between 20 to 30% is a third reduction in the light absorption, and so forth.

The lines ablated at 50% speed were wavy and uneven, also the ablation depth of the laser was non-uniform across the lines at this speed. This can be seen in the top image in **Figure 37**. Inside the ablated lines are faint patches where it is fully ablated through the PolyHIPE and other areas where it is only partially ablated the material.

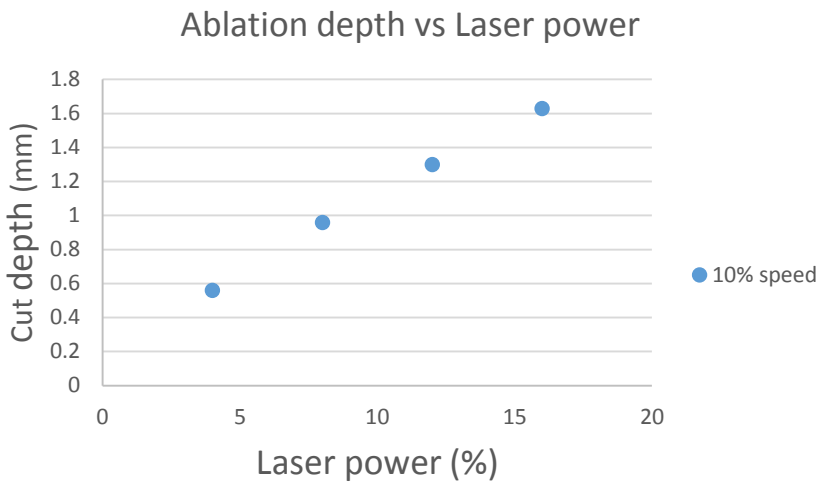

Figure 39: A scatter graph showing a gradual increase in the laser power at a low speed with the corresponding depth of the laser ablation.

Slow scan speeds and low laser power settings have the most accurate control over the PolyHIPE ablated regions. A linear relationship is shown between the laser power and the cut depth at these settings **Figure 39**, and the slow scanning speed has a smoother movement than the faster ones. Therefore the low speed and power means that a high amount of control is achievable both over the ablation depth and the ablated region.

3.11.1. Laser cut interface of PolyHIPE

The laser cut boundary produces a clean cut through the PolyHIPE material, whereas cutting using a scalpel blade or cracking the PolyHIPE produce a rough surface where the polymer has been fractured. In either case the porosity of the PolyHIPE is

maintained. It is unclear whether the large amount of heat generated at the laser cut interface has affected the properties of the surrounding polymer. On the laser cut interface there are no signs of the polymer being redeposited, which suggests that the polymer is being vaporized as opposed to being melted and then redeposited, or that there is simply a minimum amount of polymer melting taking place.

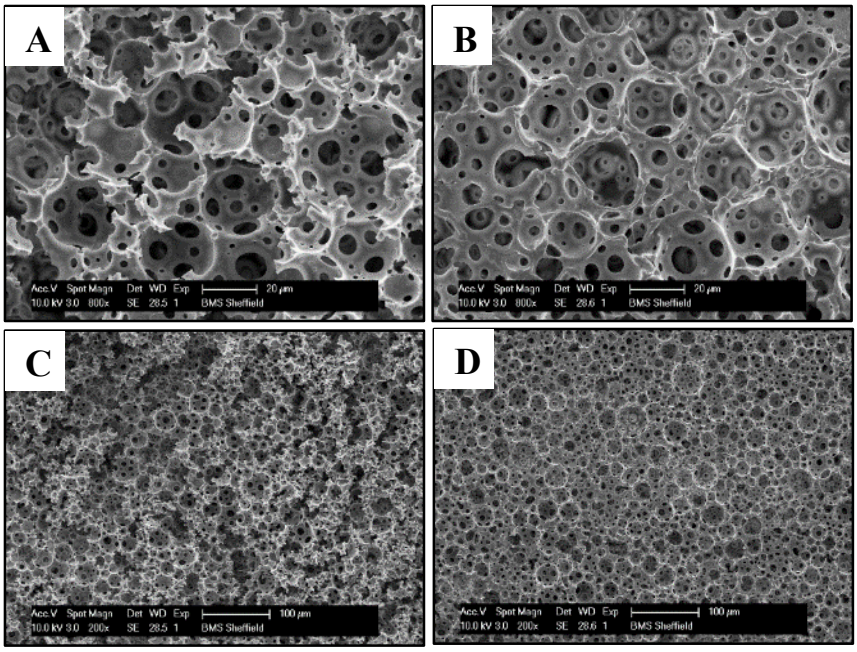

Figure 40: **A** & **C**, SEM image of the PolyHIPE interface that has been cut using a scalpel blade. **B** & **C,** Cross sectional SEM image of the laser cut interface.

The laser cutter can be used to etch away the material to create grooves within the PolyHIPE, without fully cutting through the material. This opens up this post processing method to create a secondary level of porosity within the PolyHIPE, as opposed to only having the porosity created by emulsion templating. This method has advantages over processing PolyHIPEs via stereolithography because both photocurable and thermally cured PolyHIPE sheets can be processed using this method. However this method cannot produce the same structural complexity is achievable with additive manufacturing. Laser cutting is ideal to produce topographical features into PolyHIPE monoliths with a high degree of control. For example, high aspect ratio structures can be built via etching grooved lines into the PolyHIPE (**Figure 40**).

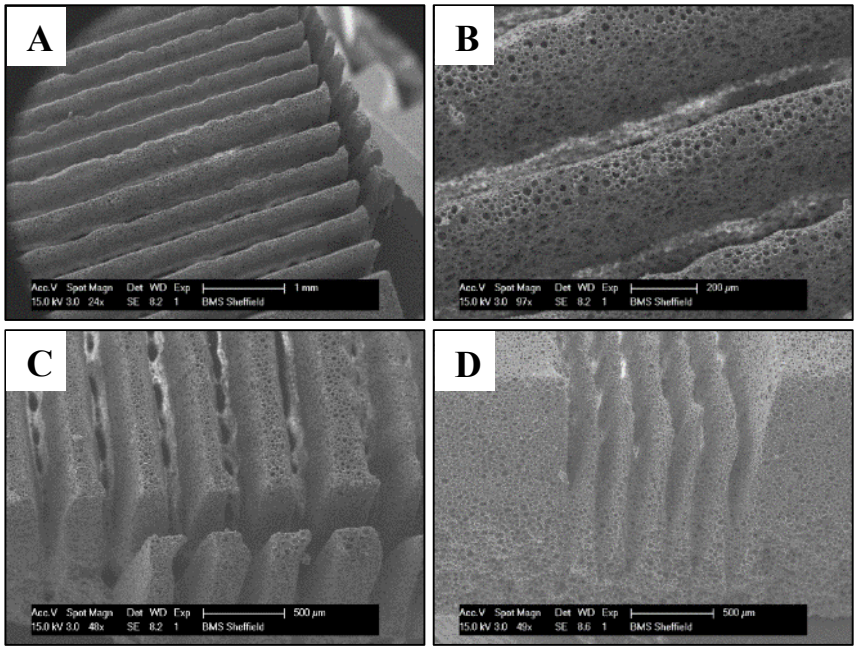

Figure 41. SEM images of the PolyHIPE that has been laser etched. **A**, overview of the top surface. **B,** the open pored nature can be seen from this angle. **C**, side view. **D**, multiple laser passes together with the cutting depth shown. An open porosity can be seen from all the images

Figure 41 above demonstrates one application of post processing subtractive manufacturing of the PolyHIPE with a laser cutter. Porous aligned channels were etched into the PolyHIPE. The SEM images show that the PolyHIPE has retained its porosity along the channels, and that deep grooved lines can be created using this process. This laser cutting method has the potential to produce bespoke scaffolds with the PolyHIPE that the current additive manufacturing direct laser write approach cannot currently achieve.

To improve the resolution and produce thinner etched lines it is better to have multiple passes over the same spot at a lower power, than one pass at a higher one. For multiple laser passes the laser energy is lower, therefore the sample will be exposed to less thermal energy. The first laser pass will etch the top flat surface of the PolyHIPE, whereas the second and third passes will be etching within the already formed triangle like groove, and will therefore only increase the depth of the groove and not the overall width from the top surface, this produces a thin etched line with, and its depth does not influence the thickness of the line. This effect has been used to produce micro channels with a better surface topography, and reduced bulging around the etched regions [53].

The polymer surrounding the initial laser etched may be affected by the heat generated during the cutting process and subsequent cooling, which may affect the mechanical properties of the polymer at the cut interface. There is a threshold that the thermal energy will have to supersede in order to vaporize the material, and this may have a subsequent effect on the cell/polymer interaction at the cut interface which will have to be determined for future experimentation.

3.12 Conclusion

The combination of stereolithography and HIPE templating is a new field in the literature. The use of photocurable materials for the PolyHIPE production is still in its infancy in comparison to the well-developed thermally cured PolyHIPEs.

The merging of HIPE templating and stereolithography were demonstrated to produce bespoke porous polymeric structures. The internal morphology was maintained and was found to be comparable to its bulk cured counterpart. This shows that despite the selective polymerisation of the PolyHIPE, its internal porosity can be maintained, and is similar to the bulk polymerisation of the HIPE. The pre-processing conditions to create and alter the pore sizes in the initial emulsion can therefore be controlled independently to the macro 'structured' porosity from the stereolithography approach. Scanning and projection stereolithography of the HIPE have been demonstrated, and porous lines, grids and tubes have been fabricated.

Glass surface functionalisation was successfully achieved to bind to the PolyHIPE structures to after polymerisation. This was required as the PolyHIPE structures could be damaged by the direct handling, the glass coverslips provided a support for them.

The laser parameters were found to have a high influence on the size of the polymerised region, and can be controlled to improve the achievable resolution of the grid lattice PolyHIPE structures. Undesired scattering of the UV light caused an increase in the polymerised regions.

The ratio between the water and oil were altered in the initial HIPE preparation. The water ratio was increased from 75 to 90% of the total liquid volume in the emulsion. The 75% water PolyHIPE appeared to have a more rounded pore geometry, and a low

amount of porosity and interconnectivity. The 90% PolyHIPE tubes had a highly branched and interconnected structure.

Viscosity of the HIPE proved problematic with both the direct laser write and projection polymerisation, as the HIPE needs to be fluid enough to recoat the new layer for subsequent polymerisation, or to continuously fill the top surface of the polymerising structures from the projection based stereolithography. This was the limiting factor when using the high (90% water volume) HIPEs, as the higher volume of water in the emulsion increased their respective viscosity.

Different monomer ratios were used to adjust the mechanical properties, rigid and elastic PolyHIPE tubes were produced with either flexible or rigid properties. The bulk mechanical properties were determined using an extensometer to produce the force/distance curves and the Young's Modulus calculated from them. The Young's Modulus ranged from 0.36 to 63.03MPa, and it was highly influenced by the porosity of the PolyHIPE, and the respective ratios between the monomers

A surface skin was found on the outer surface of all the PolyHIPE structures produced with stereolithography, regardless of laser power, or scanning speed. A tentative explanation is that is occurs when there is a transition between the polymerised and non-polymerised HIPE. Nevertheless however the internal morphology remained unaffected by this outer closed surface.

A subtractive manufacturing approach of PolyHIPE sheets was demonstrated using a commercial laser cutter. The laser power and scanning speed was shown to have an effect on the depth of the line cut into the PolyHIPE. These parameters could be controlled to either cut the PolyHIPE instantly or selectively ablate the top surface partially exposing the internal PolyHIPE morphology. Slower scan speeds with lower laser intensities produce the cleanest cuts, while the faster scan speeds produced a non-uniform etched line that had a slight wavy nature to it.

The cut interface of the laser ablated lines was flat and open pored with no evidence of cracking along the pores that is often seen with conventional cutting methods. This technique is a post processing method that can create a secondary level of macro porosity within the PolyHIPE, this porosity is independently controlled to the micro porosity from the HIPE templating. The cut interface does not have a surface skin, and remains open pored and interconnected. Furthermore the flat PolyHIPE sheets can be

prepared from a range of materials, therefore materials that are not suitable for the stereolithography technique, can have a secondary level of porosity from the surface etching method.

3.13 Summary

- Additive manufacturing and subtractive manufacturing have been used to alter the porosity of the PolyHIPE material independently from the initial emulsion conditions for the HIPE templating.
- A hybrid of HIPE templating and selective polymerisation by stereolithography has been demonstrated
- The porosity of the PolyHIPE is maintained despite the method of polymerisation
- A hatched grid network and porous tube have been created from the PolyHIPE highlighting the flexibility of this fabrication approach.
- A surface skin was reported on the outside of the stereolithography PolyHIPE structures
- Laser etching has been demonstrated as a subtractive manufacturing approach to create a secondary level of porosity within flat sheets of PolyHIPE

4. CHAPTER FOUR: Surface skin – Experimental determination

4.1 Aims and objectives

The aim of this chapter is to determine the cause behind the surface skin observed around the PolyHIPE, and investigate possible methods to eliminate it by:

1. Determining the stage during the polymerisation which the surface skin is created

2. Investigating the cause behind the surface skin in relation to the controllable polymerising parameters.

3. Investigate the effects of adding a light absorber on the surface skin

4.2 Introduction

With the recent work involving stereolithography of the PolyHIPE a surface skin has been observed around the polymerised material. The bulk of the structures are porous however the closed outer surface traps this porosity within the material, which limits the potential of this structuring technique. The surface skin surrounding the PolyHIPE has been reported on previously in the literature by Cameron. A poly(styrene/DVB) PolyHIPE was shown to have either an open or a closed surface morphology depending on the material it was thermally polymerised against [3]. The HIPE was placed into a vessel or mould and then heated to the polymerising temperature for a few hours. The material used for the mould can affect the open or closed surface porosity at the PolyHIPE/mould interface. Emulsion destabilisation occurred if it was in contact with Polyvinyl chloride (PVC), a closed outer surface if polymerised against a Polypropylene (PP) mould, and an open pored surface when polymerised against Polytetrafluoroethylene (PTFE) [3].

The surface skin is attributed to destabilisation of the emulsion at the material interface, and was subsequently covered by a thin layer of the monomeric material, which is possibly caused by a preferential wetting of the monomeric phase. The presence of the surface skin had no effect on the bulk morphology of the PolyHIPE,

and for large samples the outer surface skin is cut off. However with stereolithography of the PolyHIPE this is not an option, so an alternative solution is required.

4.3 Methods

4.3.1. Stereolithography of HIPE

A functionalised glass coverslip was placed in the centre of a glass slide and a 3mm thick PDMS cut into 2cm discs with an 11mm hole in the middle was affixed ontop of the glass coverslip. The HIPE was pipetted into the PDMS hole and remained in this temporary 'well' as the laser was either scanned or pulsed at different locations on the glass coverslip. The PolyHIPE structures attached to the glass coverslip were washed in acetone to remove the non-polymerised HIPE and left to air dry.

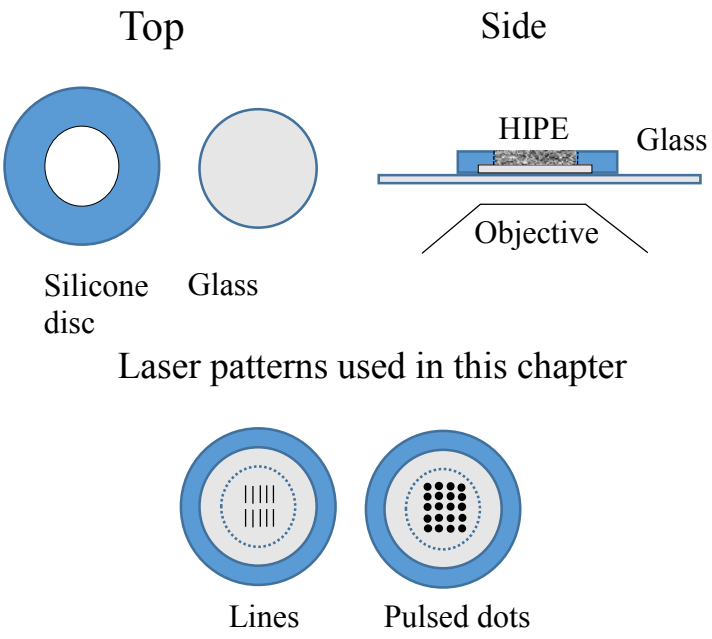

Figure 42: A schematic drawing of the circular sheet of PDMS and glass slide used to create a temporary 'well' to house the HIPE during the polymerisation stage. The laser patterns used in this chapter are shown on the bottom two drawings. These include the 2mm long lines and the pulsed grid array.

4.3.2. Hydrogen peroxide wash

PolyHIPE lines were soaked in a 30% Hydrogen Peroxide solution for 24 hours. Hydrogen peroxide was used as received with no alterations.

4.4 Results & Discussion

4.5 Effect of the polymerising speed on surface skin

The surface skin is always present on the laser produced PolyHIPE lines regardless of the polymerizing speed. This can be detrimental for given applications (e.g. filters) because it causes a closed pored outer surface that surrounds the internal porous PolyHIPE. As a result of this the inherent 3D interconnectivity and high surface area is trapped within the material as opposed to being open to the surrounding area. This is especially problematic for tissue engineering applications, as the cells will not be able to grow into the material and will be confined to the outer surface.

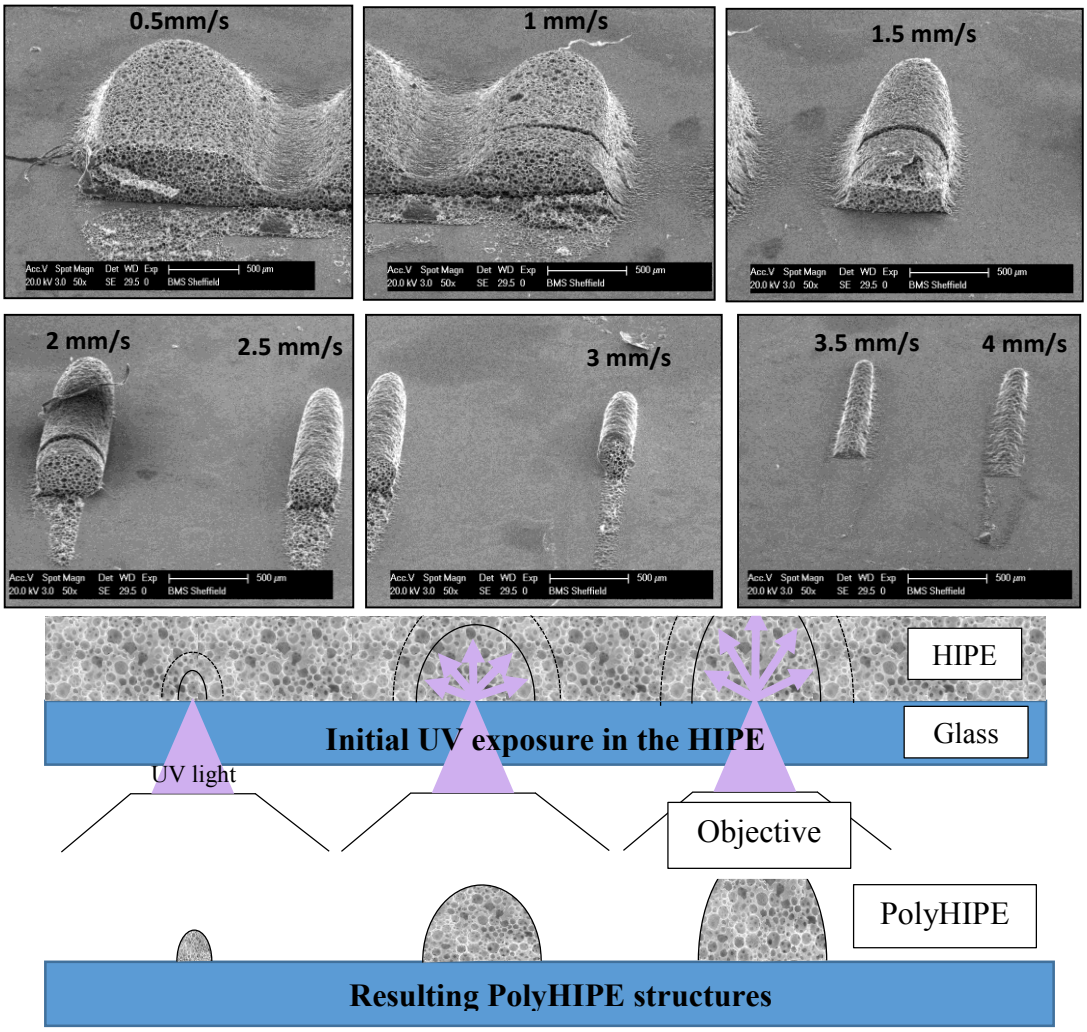

Figure 43: SEM images of 2mm lines of HIPE cured at a stage speeds of 0.5mm/s to 4mm/s to produce small lines of PolyHIPE. EHA 80, 1 mW power. The lines have been cut in half to expose the internal morphology, and to view the surface skin. A schematic drawing to illustrate the UV light scattering within the HIPE during the polymerisation stage. The solid lines in the top schematic shows the polymerised region, and the dotted region surrounding them is the partially activated region. The bottom schematic is the resulting PolyHIPE after the washing stage where the non-polymerised and partially activated regions have been washed away.

PolyHIPE lines were cured at different write speeds to determine the effect the laser speed has on the surface skin. Eight lines 2 mm long were polymerised using the elastic HIPE formulation (80%water), and the effects of the lasers scanning speed on the surface skin and morphology are shown in **Figure 43**. A closed surface skin is observed around the outside of all the PolyHIPE lines except the top of the slower written lines at speeds of 0.5 and 1 mm/s. The internal PolyHIPE morphology of the PolyHIPE lines was only maintained up 3 mm/s direct laser write speed at 1 mW UV

power; above this speed the lines had destabilized and did not retain their PolyHIPE like morphology.

Each of the 2 mm long polymerized PolyHIPE lines were thicker in the middle and tapered off to a rounded point at the edges. To create these PolyHIPE lines the UV light was reflected upwards through the glass surface into a well of HIPE, and moved sequentially in adjacent horizontal motions. Their rounded shape is created by the UV light scattering outwards from its initial focal spot. A drawing of this can be seen in the schematic in **Figure 43.** At the ends of the lines the UV light will gradually get absorbed by the surrounding monomer and its polymerising effect will decrease, creating a smaller rounded narrow point.

The surface skin is not present on the top of the slower written lines (0.5-1mm/s) but it is present on the side of them (**Figure 43**). This is because the polymerising region at this slow speed was sufficient enough to polymerise the entire height of the original HIPE well. Here the top surface of the PolyHIPE had been cured against air, which has resulted in a flat topped open pored surface. The difference between the open pored top surface and closed pore side surface indicates that the surface skin only occurs when a boundary between the cured and non-cured HIPE exists. A close-up of the transition between the open pored top surface, and the closed pored side one, can be seen more clearly in **Figure 44**.

The reason the flat topped surface of the slow 0.5-1mm/s PolyHIPE lines (**Figure 43**) are open pored, is because at this location the amount of polymerisation has been artificially stopped, there is simply no more material above this point to cure. The transition from the top surface to the side surface of the 0.5mm/s PolyHIPE lines shown in more detail in image **A** in **Figure 44**, here a gradual increase in the surface skin towards its side surface can be seen. The presence of this surface skin at the boundary between the cured and non-cured PolyHIPE/HIPE suggests that it could be related to a gradual transition of the monomer to polymer that exists at this boundary, but the precise moment it is created cannot be determined from these images.

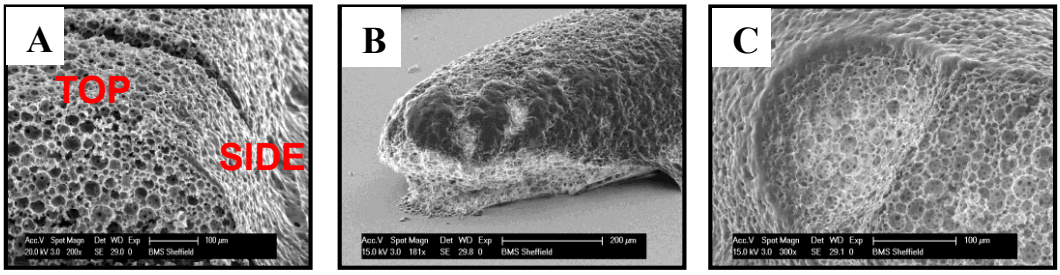

Figure 44: **A**, Close up of the Top and side of the 0.5mm/s PolyHIPE line shown in ***Figure 43.*** **B**, Surface skin shown around a PolyHIPE line that has partially detached from the glass surface. **C**, a close up of a defect in one of the PolyHIPE lines showing the internal and outer morphology.

Figure 44 shows a close up of the top and side of the 0.5 mm/s cured PolyHIPE line. Image A shows the transition from an open morphology on the top surface, to its gradual closure towards its side. Image **B** on the other hand is fully surrounded by a surface skin, except for the bottom region where it was attached to the glass surface. It appears that the PolyHIPE has been pulled off the surface at this point exposing its internal porosity. This has been caused by the PolyHIPE contracting during either the polymerising, or post processing stage. The base is firmly attached to the glass surface so the contraction would have ripped the PolyHIPE off the surface. Finally image **C** shows a defect in one of the PolyHIPE lines, a large droplet of water was at this location giving its slight concave appearance, the droplet would have been introduced as the HIPE was pipetted into the well. Nevertheless this defect shows the transition from the internal porous PolyHIPE towards the closed outer surface. The size of the pores appears to be gradually getting smaller towards the outer surface, which appears to have an uneven rippled texture. The smoothness of the polymer around the edge of this boundary suggests there has been a degree of destabilisation of the original HIPE and a few questions can be formulated: Has this surface destabilisation been caused during the point of polymerisation? And how does it relate to the excess cured region of PolyHIPE?

An understanding of the relationship between the surface skin, and the excess cured regions of the PolyHIPE, can be made by observing the cured regions between the 0.5 and 1 mm/s written PolyHIPE lines, and how these regions are different to the space between the 1 mm/s and 1.5 mm/s lines shown in **Figure 43**. In both this excess curing is outside the initial region of the UV light. The appearance of this extra polymerised

region suggests that the UV light has either scattered to such an extent with the slow write speed that it was able to polymerise the surrounding material. An alternative explanation is that there is another mechanism that only occurs between two cured regions. This would explain why the excess curing is isolated between two polymerised regions, and does not exist elsewhere around the lines.

The excess cured region shown in **Figure 43** is likely due to the overlapping partially activated regions surrounding the cured PolyHIPE. A drawn schematic is shown in **Figure 45** that shows this process in a simplified way. Here the overlapping dotted regions represents the overlapping of the partially cured monomer, and it is only here that excess curing can exist outside of the original polymerised PolyHIPE.

These overlapping regions dictates the minimum resolution that can be achieved using the direct laser write approach. If two polymerising regions are too close then excess curing will occur between them, lowering the achievable resolution that can be achieved using the scanning stereolithography.

During the photo-polymerisation reaction the monomers go through a gel point before they fully crosslink. This is the point at which the monomers connecting covalent bonds form a macromolecule with infinitely large molecular weight and viscosity [11]. The sub activated regions just outside of this threshold will have a higher molecular weight than their surrounding HIPE monomeric phase, this increase in molecular weight will decrease the flexibility and diffusion of the monomer in this region, and will cause it to remain localised to their respective PolyHIPE regions. When these regions overlap with the ones from the adjacent PolyHIPE excess curing will occur when these defined areas overlap.

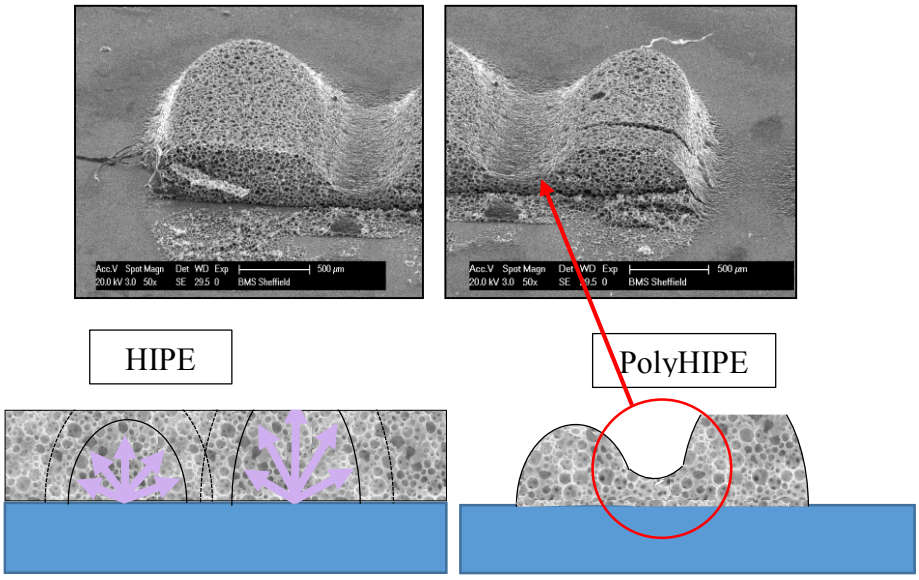

***Figure 45**:* SEM images from **Figure 43** and the corresponding drawings showing the formation of the excess polymerised regions between the PolyHIPE lines. These also correlate to the light microscope images in **Figure 47**. **Bottom Left**, a drawing the show the overlapping partially activated regions of the polymerised PolyHIPE within the HIPE. **Bottom Right**, The PolyHIPE and the excess cured region between two separate points that remain after the washing stages.

Upon close inspection between the lines written with a 1-1.5 mm/s speed in **Figure 43** there is a faint amount of cured polymer on the glass surface that is not observed elsewhere around the same lines. This observation is very important, as it has a similar appearance to the surface skin that surrounds the entire PolyHIPE, but here, this surface skin effect is present on the glass surface. Also a similar effect can be seen in the faster written lines between 3.5 mm/s upwards where there was insufficient polymerisation (due to the fast write speeds) to preserve the HIPE morphology, and the material has simple collapsed upon itself, and has created the same appearance of the surface skin seen surrounding the PolyHIPE lines.

If overlapping partially activated regions can polymerise, but elsewhere it does not, then the partial crosslinking of the polymer closest to the PolyHIPE has surpassed the gel point of the monomer to a polymer to a sufficient extent to be insoluble to the developer solution, but insufficiently enough to provide any mechanical strength to maintain its shape without collapsing. This is the same effect seen in the faster written lines with just a surface skin like appearance. Then the surface skin and excess

crosslinking regions have the same underlying mechanism. Both of these are caused by the transition between the monomer to polymer.

4.6 PolyHIPE morphology at the point of polymerisation

The next question to consider is the precise moment the surface skin is formed around the PolyHIPE. I have shown that the surface skin is created by the collapse in the outer surface of the PolyHIPE during the post processing washing stage, and not at the point of polymerisation within the bulk HIPE.

This was determined experimentally in **Figure 46**. Here four adjacent lines of HIPE were polymerised, then after a few minutes the entire HIPE well is bulk polymerised. This was then cut in half and the cross section imaged to determine if the collapse of the initial cured HIPE occurs at the point of polymerisation. If the pores collapsed during the point of curing, then I would expect to see a difference between the initial cured/non-cured regions.

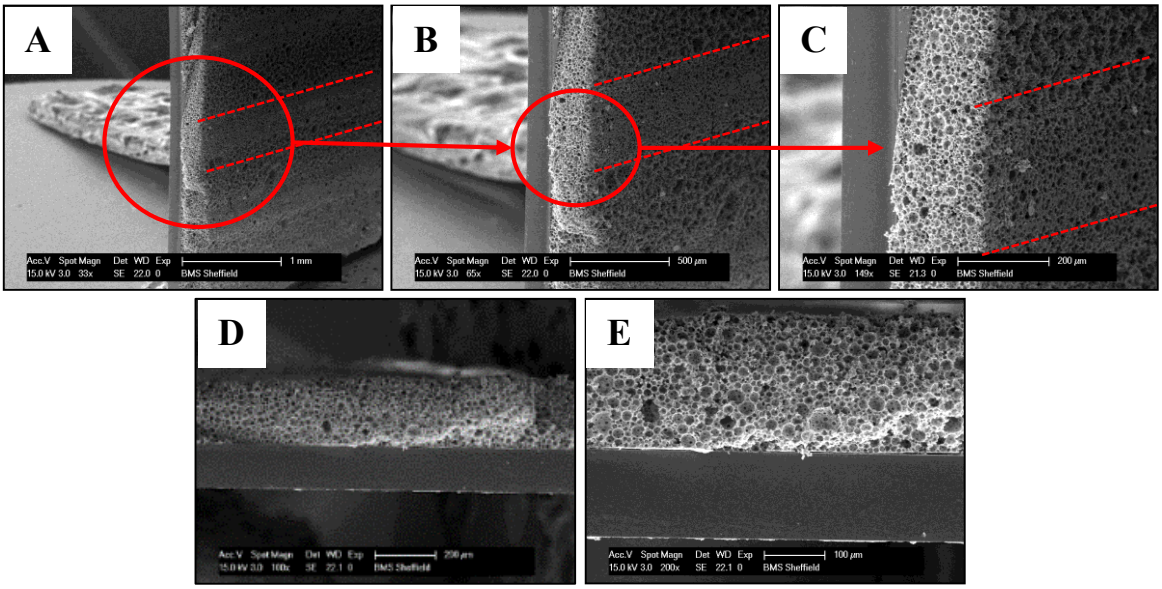

Figure 46: SEM images of the elastic EHA80 HIPE formulation. (**A-C**) overview and close-up of the PolyHIPE lines cured on top of a glass coverslip. (**D & E**) Side view of the line interface.

The sides of the PolyHIPE lines maintains an open porosity directly after its polymerisation. These cured lines can be seen in the middle regions of the flat sheet of the PolyHIPE, circled in red in image A-C in **Figure 46**. There is a continuous interface between these initially cured lines and the surrounding PolyHIPE cured via a UV lamp. SEM images of this interface were indistinguishable to the surrounding PolyHIPE, this suggests that the destabilization occurs during the post processing stages as opposed to the moment of polymerisation.

The top surface of the lines initially cured via a direct laser write has a slightly smaller pore size than the surrounding UV lamp cured PolyHIPE. This is understandable as the surrounding HIPE well is very thin, it consists of a 300 μm high layer in contact with a glass surface, with a selectively cured region adjacent to it. The liquid air boundary at the top surface would be more susceptible to the handling and movement of the stage and transfer to the UV lamp. This would cause destabilisation of the uncured HIPE as the water droplets merge together on the top surface creating larger pores.

4.7 PolyHIPE drying

It is believed that the surface skin s caused by the evaporation of the solvent during the washing stage. The capillary forces generated by the evaporating liquid pulls the mechanically weak polymer on the surface causing the pores to collapse upon themselves. This effect caused by the surface tension created by an evaporating liquid has been reported previously in the literature with the high resolution microfabrication using TPP, where the mechanically weak lines can be deformed by the developer solution [54].

Cured PolyHIPE lines were washed in acetone and then imaged over a few minutes as they dried to visualise the drying process in more detail. **Figure 47** shows the PolyHIPE surface turned from a glaze like appearance to its characteristic white appearance during the evaporation of the acetone solvent used in this case. The white appearance is due to the increased scattering of light as the PolyHIPE dries. The overall width of the PolyHIPE shrank as the solvent evaporated, which shows that acetone is a good swelling solvent for the PolyHIPE EHA 80 formulation.

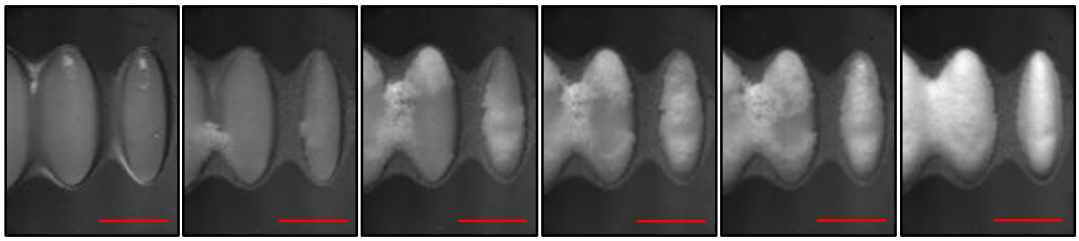

Figure 47: Time lapse light microscope images of the EHA80 PolyHIPE lines cured and washed in acetone and imaged every minute as it dried. Scale bar 500µm.

The PolyHIPE dries in small isolated patches which can be seen in the **Figure 47**. These randomly appeared around the PolyHIPE but when the PolyHIPE dries these islands appear very sudden, this fast appearance may be a contributing factor to the surface skin effect.

As previously suggested the excess cured areas between the separate lines of PolyHIPE are caused by overlapping partially cured regions that surround the cured ones. These regions can be seen quite clearly around the outside of the PolyHIPE lines in **Figure 47**. These excess cured regions only appear between previously cured parts, and not on the adjacent surrounding sides. The surrounding area is still partially cured but not to the extent to cause the monomer units to be crosslinked sufficiently for it to be insoluble to the developer solvent; therefore it is washed away. There is a gradual transition from the cured polymer outwards towards the uncured monomers as the material undergoes a gel phase transition during the monomer to polymer conversion. The bulk material manages to maintain its PolyHIPE morphology, as it is sufficiently crosslinked to be insoluble to the developer solution, whereas the weaker outer surface will be more susceptible to surface collapse as its degree of crosslinking decreases.

4.8 UV light partial activation within the PolyHIPE

There are no reports of the sub activated region with stereolithography of the PolyHIPE material. However it has been reported on other photopolymerisation techniques which use photocurable materials. My theory is that there is an overlapping similarity between the two processes, which will be discussed.

4.8.1. The accumulative effect of polymerisation

The accumulative polymerisation effect has been used to reduce the thermal cure time of an injectable biodegradable fumarate based PolyHIPE. The HIPE is thermally pre-treated to partially crosslink it to just below its gel point, and therefore it required less heat to fully crosslink the material when injected into a warm in vivo environment [26].

The sub-activated zone surrounding the small oval shapes produce by Two Photon Polymerisation (TPP) drawing shown in **Figure 48** are caused by the diffusion of free radicals outward from the initial polymerised region. The scale range of this is only a few microns. For the PolyHIPE structures the distance range of the partially activated monomer units is within a few hundred microns outside of the initial exposed region. Radical diffusion occurs over too small a scale for it to have an effect over this distance. However there are similarities between these two processes which can be used to understand the process, characterise it and eventually mitigate it

The experiments indicate that the PolyHIPEs partially activated regions are caused by the outward scattering and gradual decrease in the UV lights ability to break down the photoinitiator, this in turn will cause a gradual decrease in the amount of crosslinking between the monomer units, which in turn will cause a gradual decrease in their mechanical strength and will therefore be more susceptible to collapse during the post processing washing stages, which will result in the collapse of the outer PolyHIPE surface.

With the high precision TPP the connecting bridges formed between the micrometre sized structures from TPP are caused by the free radical diffusion outward from the initial exposed region. This radical distribution causes a partial change of state from the monomer to polymer, therefore directly after the polymerisation reaction there no clear cut boundary between the cured and non-cured polymer. The surrounding monomers have been partially crosslinked but are below a threshold for sufficient polymerisation. These regions have been called sub-activated, as overlapping of these regions will complete the polymerisation [55]. This transition is expressed more clearly in **Figure 48** from the paper [56]. This publication refers to the polymerising threshold within the sub-micrometer range.

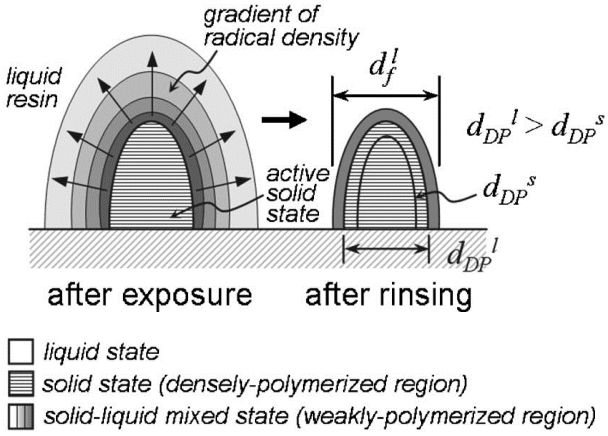

Figure 48: Schematic picture of the weakly polymerized region surrounding the densely polymerised one, the contours show the density gradient of the monomer radicals. Pre and post washing is shown where the weakly polymerized regions have been washed away [56].

4.8.2. Connecting bridges between PolyHIPE points

A better understanding of how the UV light scatters through the HIPE is needed to get a more detailed and quantifiable value of these partially cured outer regions of the PolyHIPE. For this, the following experiment was designed.

UV light was pulsed at different points across the EHA80 HIPE formulation. The laser power was maintained at 1 mW UV light and was focused into the HIPE at different points with a 10× objective focused on the glass interface. Only one variable was changed at any one time to determine its effect on the polymerised region, the resulting SEM images are shown in **Figure 49**.

The individually isolated PolyHIPE bulbs were found to have a surface skin over their top surface, they were small at the base where they were attached to the glass slide and gradually increased in circumference towards the top. This shape is attributed to the increased scattering of the UV light as it passes upwards through the HIPE. Increasing the UV exposure time increased the spot sizes until the point where the partially cured regions overlapped and bridges were formed between them. This effect has not been reported in the literature in the relation to the PolyHIPE material, as the stereolithography of the HIPE has only recently been reported up by our group [43].

In **Figure 49** the laser has been pulsed at the different points across the HIPE. The pulses were performed in sequence in a horizontal direction, and only at the edges does it move in the vertical direction to repeat of the next sequence of pulses. The pulsed duration was controlled by a shutter which opened and closed accordingly. The connecting bridges between adjacent PolyHIPE bulbs have not been formed by the UV passing between these points, it has formed by the overlapping of partially cured monomeric regions.

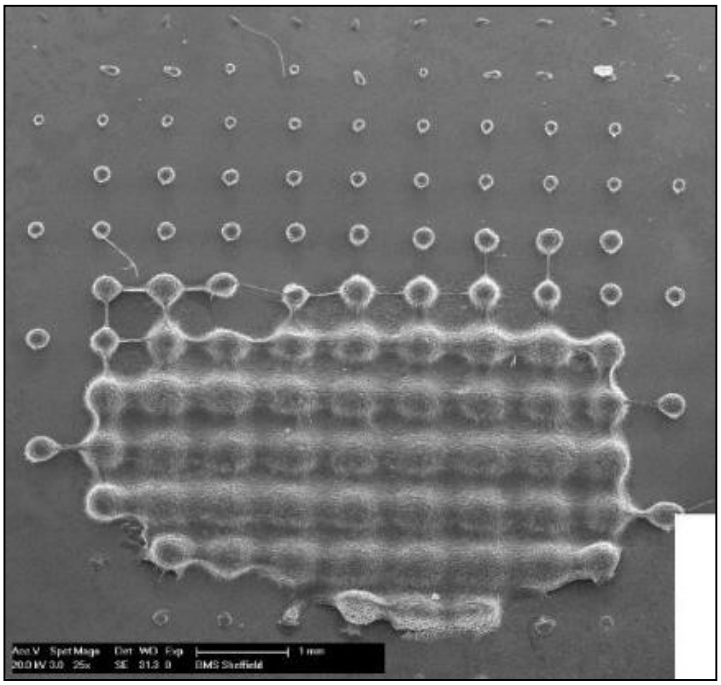

Figure 49: SEM image of a section of a 120 bulb array of the PolyHIPE on top of a glass coverslip. The laser was pulsed in 0.01second increments 120 times until the laser pulse was 1.2 seconds. Overcuring and bridges can be seen between the PolyHIPE spots. The bottom section was cut off by the laser passing over PDMS holding the HIPE well.

Figure 49 a 120 bulb array of the PolyHIPE that has been created by pulsing the laser 120 times with a constant spacing of 700 μm. The pulse duration increasing in 0.01 second increments from the top left towards a dwell time of 1.2 seconds for the bottom right position. The dwell time increased incrementally in horizontal rows left to right, then right to left in alternating scans. The top of the SEM image shows the polymerised polymer that has no structural strength and has only created small cured regions. As the pulse duration has increased the polymer starts to maintain the emulsion morphology to form the PolyHIPE dots (with an outer surface skin) and gradually the

PolyHIPE bulbs start to form bridges between them, these then merge together to form a completely overcured region.

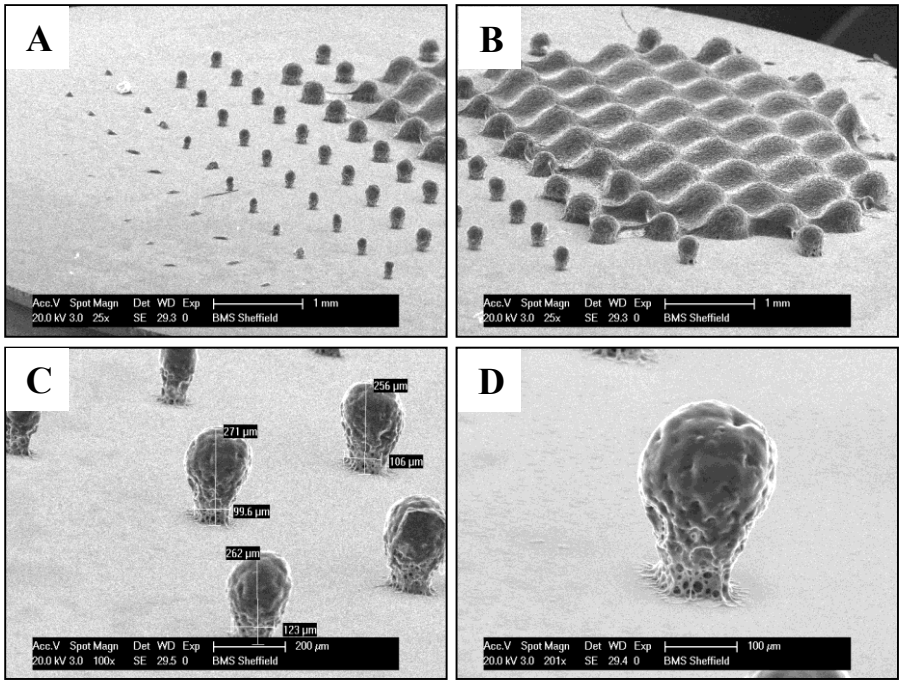

Figure 50: Side SEM images of the pulsed PolyHIPE dots seen in **Figure 49**. **A** and **B** shows the overall side view of the grid array. **C**, a few of the bulb like PolyHIPE dots. **D**, A close up of the surface skin surrounding the top part of the PolyHIPE bulbs, and some open porosity at the polymer glass interface.

The PolyHIPE bulbs can be seen in the above **Figure 50** and below in **Figure 51**. This shape supports the previous theory that the HIPE scatters the UV light [43]. The top surface has a closed surface caused by the surface skin, however the internal PolyHIPE morphology can be seen at the glass PolyHIPE interface. As the amount of UV light exposure has increased the gradual merging together of the dot array has created an egg box like structure.

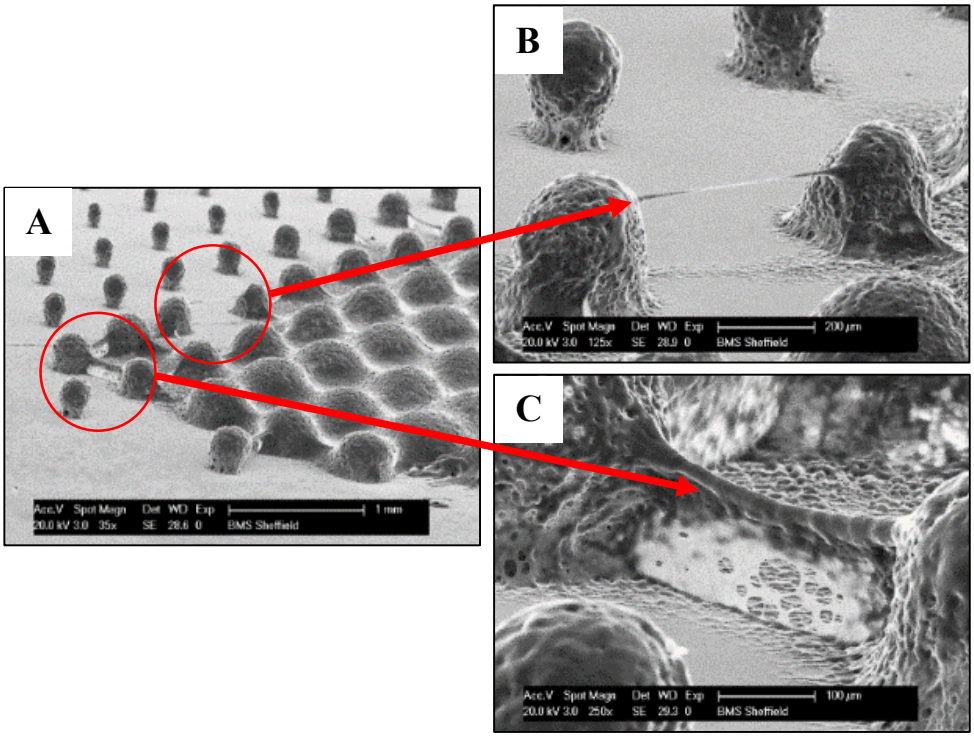

Figure 51: SEM images of the ribs that have formed between adjacent PolyHIPE spots. These bridges have been formed solely by the overlapping of the partially cured regions. **A** shows an overview of the sample**, B** shows a thin bridge that has joined two PolyHIPE bulbs, **C** shows a thicker bridge with a skin connecting it to the glass surface.

The above SEM image in **Figure 51** shows a close up of the polymer bridges that have formed between adjacent bulbs of PolyHIPE. The laser has not passed between these regions, it has only pulsed at the isolated points. The confinement of the polymerising region to small circular isolated spots within the HIPE, means that the sub activated region should form a uniform circle around the cured regions. The linking bridges form first at the shortest distance between these circular points, before gradually curing the excess region around the bulbs. This excess cured region first appears as a buildup of a polymer skin on the glass surface, this is where the polymer that has polymerised originally around the water droplets had insufficient strength to maintain the HIPE morphology, and has collapsed upon itself due to its very weak mechanical strength to form the skin.

The UV light passes through a circular pin hole prior to entering the objective which focuses it onto the HIPE surface. Therefore an uneven UV light distribution is not causing the connecting bridges. The connecting bridges are therefore forming as the

UV light scatters within the material. This scattering effect will be enhanced with the mismatch between the refractive index between the water and oil phases. This inherent scattering of light from the HIPE is also what causes its white colour.

In the SEM image **A** in **Figure 52** does not have any cured polymer on the glass surface on the left side of the PolyHIPE bulbs. At this location there is no overlap of the partially cured regions so this monomer is washed away during the developing stage. The surface skin on the glass does appear in-between the cured bulbs of the PolyHIPE seen in images **B** and **C**.

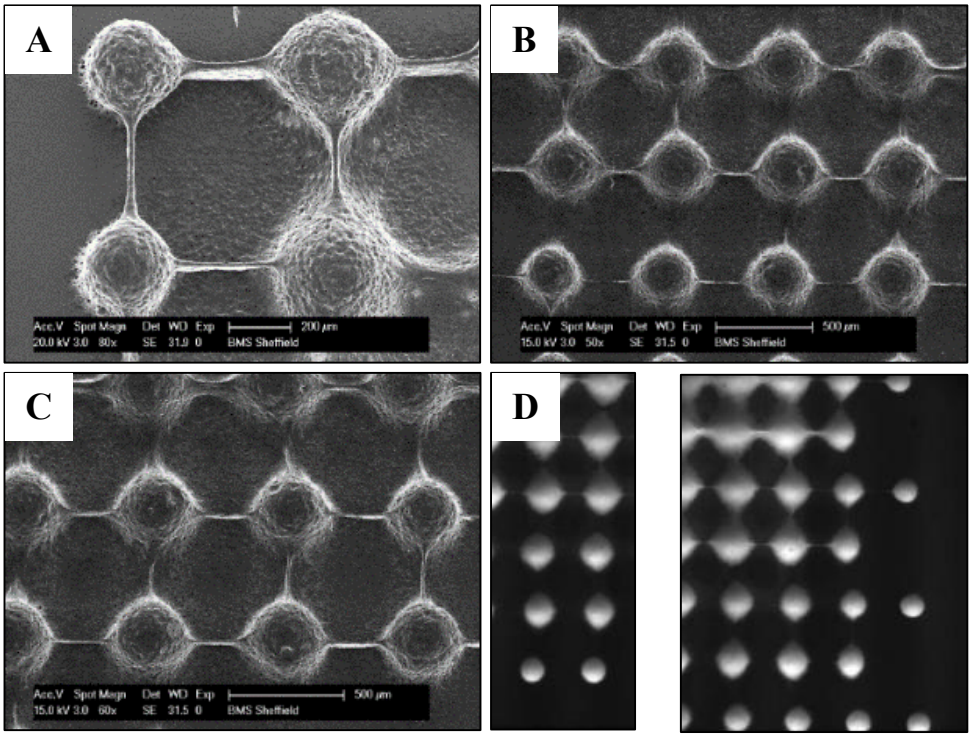

Figure 52: SEM and light microscope images of the EHA80 HIPE formulation. **A**, close up of the bridges seen in **Figure 49**. **B** & **C**, SEM images of a repeated grid array of PolyHIPE with connecting bridges, here the UV pulse duration was kept constant and the spacing was gradually decreased between the different exposed regions. **D**, light microscope image of the Pulsed PolyHIPE with connecting bridges

The connecting bridges of polymer have been repeated in **Figure 52**. Here the laser pulse duration was constant, and the spacing between the exposed regions was gradually decreased. The gradual shift from the isolated rounded PolyHIPE bulbs to more diamond like shape is observed, with the edges of this 'diamond' gradually

forming bridges between the adjacent regions. A simplified drawing of the observed effect is shown in **Figure 53**.

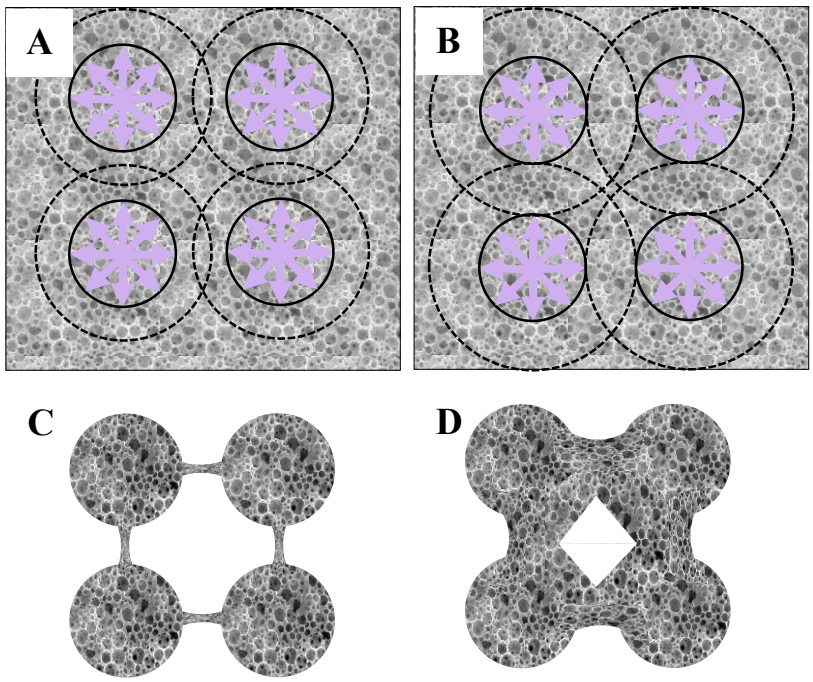

Figure 53: Schematic of the sub activated regions around the PolyHIPE, the arrows represent the UV light scattering from their initial point of exposure, the solid line is the polymerised PolyHIPE and the dotted line represents the outer region of the sub activated polymer. **A** & **C**, UV exposed region in the HIPE with partial overlapping of the partially cured regions and resulting polymer bridges formed between them. **B** & **D**, Large amount of overlapping between the partially activated regions with a large amount of excess crosslinking between them.

Figure 53 shows a simplified aerial view of the overlapping polymerised and partially activated regions. Image **A** and **C** show the point at which the connecting bridges are beginning to form as the sub activated regions overlap at the closest distance between them. Image **B** and **D** show the effect of increasing the crossover between the overlapping sub activated regions, either by increasing the UV exposure of decreasing the distance between them, in both cases this results in a higher degree of polymerising and connection between the originally PolyHIPE spots, and elongation of the original spherical cured region towards its neighboring PolyHIPE spots.

A spherical partially cured region is assumed to be surrounding the cured PolyHIPE. This is supported by both the original circular polymerised regions, as well as the unaffected diamond shaped region in the middle of the four polymerised bulbs. If the

partially cured regions are circular then the resulting overlapping shape would have a diamond like as shown in **Figure 53** and demonstrated experimentally in **Figure 52**. This also explains the egg box structure seen previously in **Figure 50**, the central region between four overlapping cured points will have the least amount of free radical generation, and therefore will result in a smaller crosslinked area causing the dipped sections in the egg box structure.

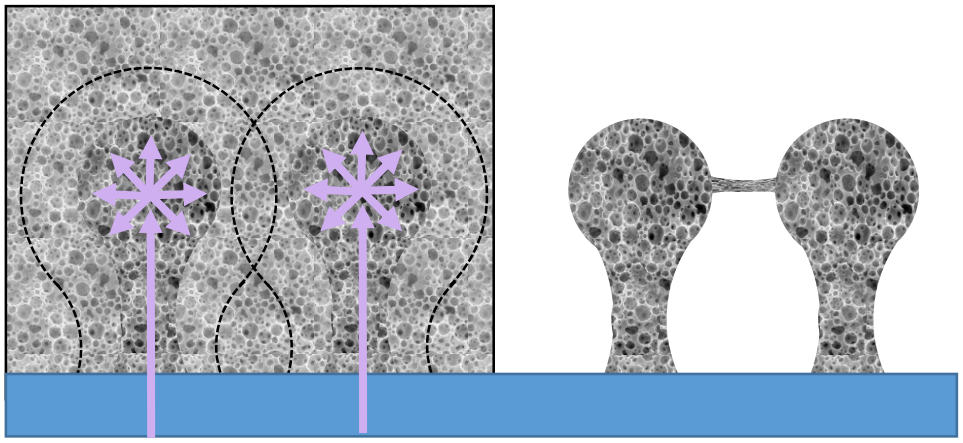

Figure 54: **Left,** side schematic of the original polymerised PolyHIPE bulbs within the HIPE, arrows shows the UV light scattering and the dotted line shows the sub activated region within the HIPE. **Right**, the resulting PolyHIPE bulbs with the excess crosslinked polymer bridge formed between them. The blue base is the glass coverslip which the PolyHIPE bulbs are attached to.

Figure 54 shows a side drawn schematic demonstrating the partially cured region surrounding the initial PolyHIPE bulbs, and the respective bridges that form between them. This is a simplified visual demonstration to the experimental SEM image shown in **Figure 51**. The drawing highlights the closest distance between the two cured PolyHIPE bulbs is the top section, it is here that the overlapping partially cured regions allow for polymerisation between the two bulbs. This also explains the beginning of the polymer bridge initially connecting the PolyHIPE bulbs in **Figure 51,** as well as the thick connecting bridge in the bottom right image with the thin film connecting this bridge to the glass surface. I cannot tell if the internal structure of the connecting bridge is porous, however the surface skin is evidently present in these images.

4.9 Post processing to remove surface skin

In the patent literature the surface skin around spherical PolyHIPE spheres has been dissolved using an oxidizing agent [57]. Therefore EHA80 PolyHIPE lines were soaked in a 30% Hydrogen Peroxide solution at pH 9 for over 24 hours. This had no effect on the surface skin. Varying the solvent used to remove the uncured HIPE had no effect on the surface skin. Acetone, ethanol and isopropanol were used but had no effect.

An alternative method that has been suggested in the literature would be to use supercritical CO_2 drying of the PolyHIPE samples [9]. This technique has been used to preserve very delicate, high aspect ratio structures, which collapse due to the surface tensions associated during the drying phase after washing the structures [58]. This technique does not address the resolution issues that direct laser write structuring with the PolyHIPE encounters. The surface skin and the achievable resolution are linked by the same mechanism of the partially crosslinked monomeric material surrounding the polymerised PolyHIPE. A viable technique would be to control the generation of the surface skin and achievable resolution during the fabrication stage, as opposed to post processing the sample.

4.10 Light absorbers

The surface skin surrounding the polymerised PolyHIPE is undesirable and reduces the local porosity. The addition of light absorbers into the oil phase of the initial HIPE should absorb UV light outside of the initial polymerised region, and therefore help to reduce the partial polymerisation surrounding the polymerising polymer which is what collapses upon itself causing the surface skin.

The UV light emitted from the Nd:YAG laser has a wavelength of 355nm. A range of light absorbers were tested with a broad absorption range within 355nm to determine their effect on both the surface skin and achievable resolution. The commercial UV light absorber Tinuvin® 234 (2-(2H-Benzotriazol-2-yl)-4,6-bis(1-methyl-1-phenylethyl)phenol) has been used previously in the literature to improve the resolution of polymeric structures produced via stereolithography [59], as well as the stereolithography of PolyHIPE [25]. This publication improved the achievable

resolution of the structured PolyHIPE structures by reducing the photoinitiator concentration as well as adding 0.1wt% Tinuvin respective to the organic phase of the HIPE to limit the lights penetration depth and improve the resolution of the structures [25].

Tinuvin is assumed to be toxic and therefore may not be suitable for tissue engineering based applications of this material. The EHA/IBOA PolyHIPE is non-degradable, therefore the leaching out of any residue Tinuvin may not be an issue. Tinuvin 234 has been used in the literature for the production of a three-dimensional scaffold for tissue engineering [60]. No toxicity was reported on their material. Nevertheless the potential cytotoxicity will need to be determined if it is to be incorporated into a tissue engineering scaffold. Both flat sheets of PolyHIPE containing 1wt% Tinuvin have been fabricated by members of our group, and it was found that as long as the samples have an extensive Soxhlet extraction wash then no toxic effects were observed with the growth of the MLOA5 and hES-MP cell line on the PolyHIPE (Data generated by R.E. Owen).

4.10.1. Effect of light absorber on stereolithography

The addition of a UV light absorber has been reported to increase the achievable resolution with other sterolithographical techniques [59]. The polymerising mechanism for the PolyHIPE is a photochemical reaction that relies on UV light as the initiating source. 1wt% Tinuvin® 234 (2-(2H-Benzotriazol-2-yl)-4,6-bis (1-methyl-1-phenylethyl) phenol) was added to the oil phase of the HIPE prior to the addition of water. Tinuvin is very hydrophobic and does not mix with water therefore it could only be added to the oil phase. Therefore the Tinuvin should not affect the UV light from scattering within the spherical droplets of water.

4.10.2. Stereolithography of PolyHIPE: improving the resolution

To quantify the effect the light absorber has on the achievable resolution I repeated the pulsed PolyHIPE experiment while varying either the laser exposure, or the spacing between the polymerised PolyHIPE bulbs. In each experiment the laser exposure time was different, it ranged from 0.1 to 1 second for 10 separate pulses. The

laser was pulsed in a line with a gradual decrease in the spacing between the exposed regions. This created an array of PolyHIPE dots that gradually got closer together until the dots started to merge into a solid line, an example of this is shown in **Figure 55**. The minimum achievable resolution was determined by measuring the distance between the cured spots when there was excess curing visible between them. This was determined by the appearance of either the connecting bridges, or in the absence of this, when the PolyHIPE spots started to touch.

As the pulsed PolyHIPE bulbs gradually got closer together their size and shape started to be affected. These bulbs gradually increased in overall size and elongated towards each other. This is caused by the gradual overlapping of the partially cured regions. **Figure 55** shows an array of PolyHIPE dots, each dot on both image was exposed to a pulse duration of 0.8 seconds. The starting distance between each spot was 1.5mm for the normal HIPE, and 0.5mm for the HIPE with 1wt% Tinuvin. The dots were brought closer together in increments of 10µm until they started to merge together.

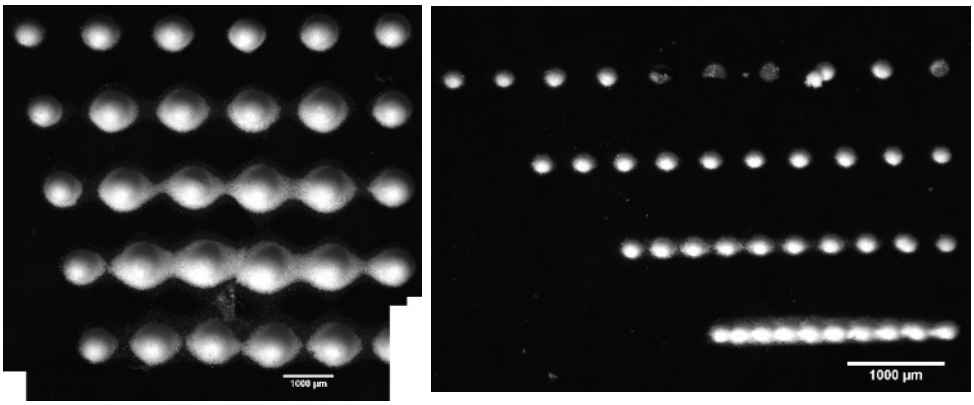

Figure 55: Two light microscope images showing the effect of adding 1wt% Tinuvin to the HIPE. **Left**: an array of PolyHIPE bulbs produced with a 0.85 second dwell time. The distance between pulses was reduced by 10 µm after each pulse. **Right**, 1wt% Tinuvin added to the emulsion, 0.8 second pulse duration with a decrease in the spacing by 10 µm after each pulse.

The experiment shown above in **Figure 55** was repeated 10 times from a 0.1 to 1 second dwell time in increments of 0.1 seconds. This set of experiments was designed to give a quantitate measurement of the improvement in the achievable resolution that the addition of Tinuvin has on the stereolithographic of the HIPE. These readings are shown in **Figure 56**.

The addition of 1wt% Tinuvin to the HIPE significantly increases the achievable resolution. With 1wt% Tinuvin and a high 0.8 second laser dwell time the PolyHIPEs only start to merge when the spots are 360µm apart. When no light absorbers are used the PolyHIPE spot starts to merge when they are 1.4mm apart.

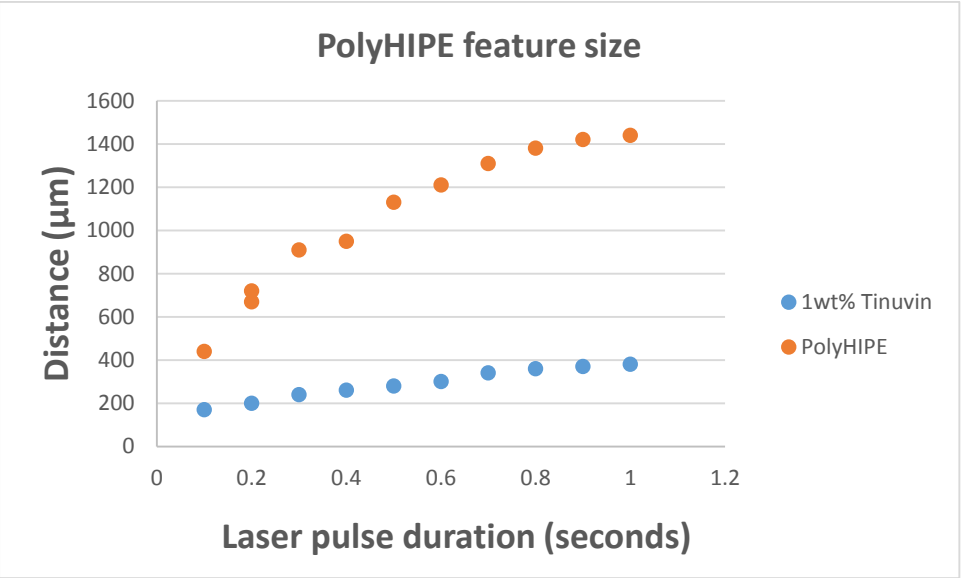

Figure 56: Scatter graph of the distance between PolyHIPE spots before they started to touch. Normal PolyHIPE vs PolyHIPE with 1wt% Tinuvin added to the oil phase.

4.10.3. Stereolithography of PolyHIPE: quantitative representation of the connecting bridges

The second experiment purely focused on the minimum distance the connecting bridges started to form. This experiment is shown in **Figure 57** where the difference between the normal EHA80 HIPE formulation and the same formulation with the addition of 1wt% Tinuvin are compared

For every PolyHIPE spot the laser pulsed with a 0.5 second exposure, and a 3 × 3 spot array was created. For every repeat 3 × 3 spot array the spacing between the 9 spots were uniformly decreased. This was repeated until the individual PolyHIPE spots started to form bridges between each other.

The central PolyHIPE spot gradually formed connecting bridges between the vertical and horizontal PolyHIPE spots. It never formed a connecting bridge between the

corner ones. This is because the overlap between the surrounding partially polymerised regions only form at the closest distance between adjacent PolyHIPE spots. As the Spots are circular, this overlapping region will be a large circle surrounding the cured PolyHIPE. The corner ones are too far away for the overlap to occur, while the horizontal and vertical ones are close enough.

The connecting bridges between the cured PolyHIPE did not occur with the HIPE with 1wt% Tinuvin. The Tinuvin is quenching the excess UV light that is scattering outwards from the cured PolyHIPE, and is therefore creating a highly confined barrier between the cured and non-cured HIPE, and therefore significantly preventing the formation of the partially cured region that normally surrounds the Polymerised PolyHIPE.

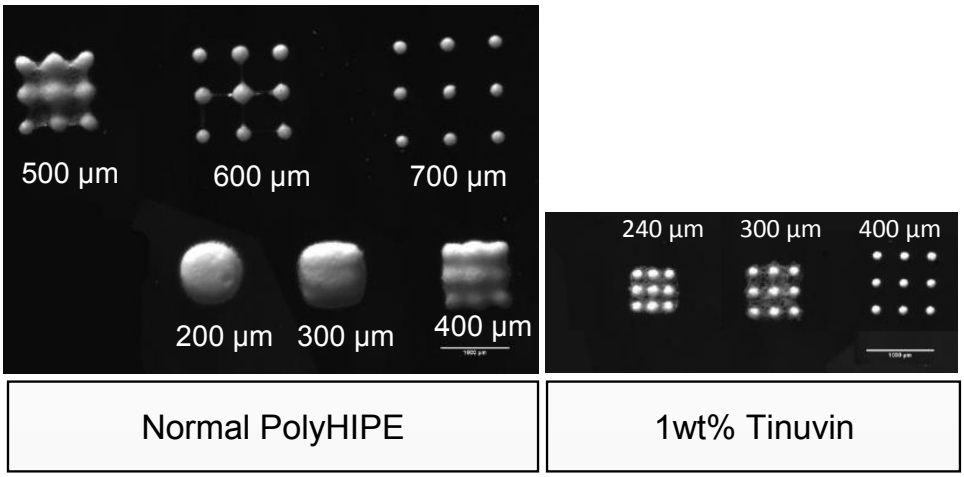

Figure 57: Light microscope image of the pulsed PolyHIPE dots. **Left** image EHA80 PolyHIPE. **Right,** image with 1wt% light absorber added. Both samples had a pulse duration of 0.2 seconds, at 1mW laser power

Figure 57 shows a 3×3 array of the PolyHIPE bulbs with a gradual decrease in the distance between them as the PolyHIPE bulbs go from being spatially isolated to connected ones. The minimal spacing achieved before the PolyHIPE started to merge was 600 µm. It was at this point that the central PolyHIPE bulb started to form connecting bridges between its vertical and horizontal neighbour. Its shape also went from being circular to a diamond like shape. This is because its degree of polymerisation is being affected by the surrounding polymerised PolyHIPE bulbs. The corners are the last to be affected because they only have two other cured regions

which can affect their shape, which can slightly affect its shape but not to the same extent.

4.11 Elimination of surface skin

The addition of the light absorber Tinuvin had a significant effect on the presence of the surface skin. This can be seen experimentally in **Figure 58.** For the normal HIPE formulation when polymerised formed a smooth lightly textured surface skin around the outside, this can be seen in the SEM images **A** and **B**. Here the surface Polymer has completely collapsed and encased the internal PolyHIPE structure. Image **A** shows the excess cured region between two PolyHIPE regions which also have this surface skin. The outer surface of the PolyHIPE SEM images in **C** and **D** on the other hand have a significantly more open pored surface. This was achieved by the addition of 2wt% Tinuvin to the monomeric phase of the HIPE prior to polymerisation.

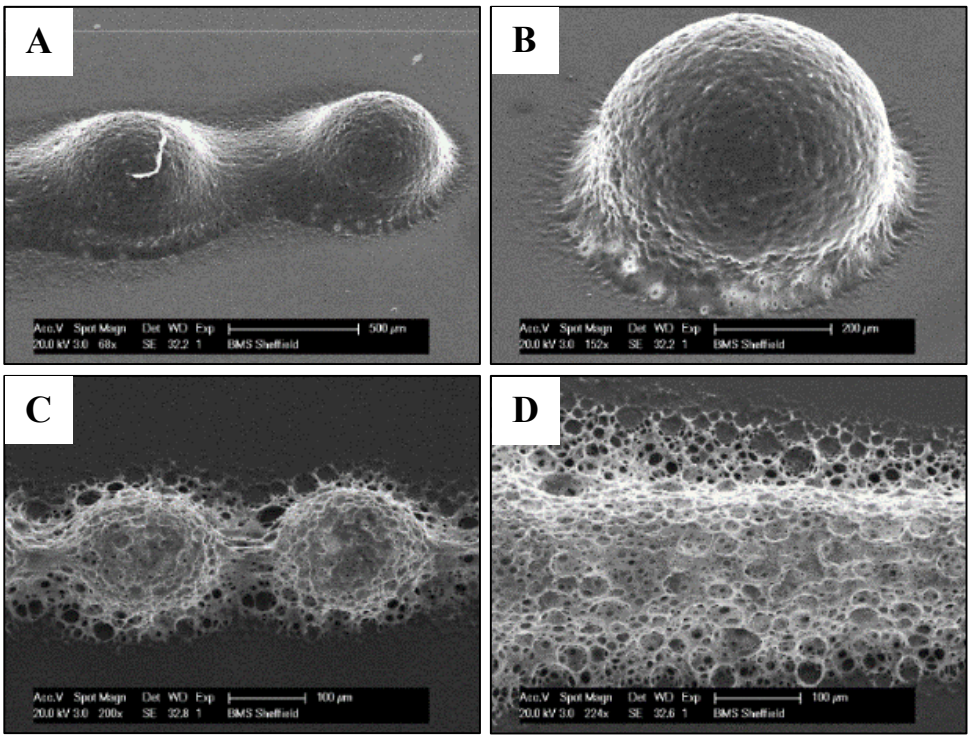

Figure 58: SEM images of PolyHIPE with surface and without surface skin. (**A**) Two PolyHIPE dots with excess crosslinking between them and a surface skin, (**B**) single PolyHIPE point with surface skin, (**C**) Two PolyHIPE spots with increased open pored surface from the addition of 2wt% Tinuvin, (**D**) PolyHIPE line with an open pored surface.

Tinuvin strongly quenches the scattered UV light. It reduces the polymerising region significantly enough so that the transition from the liquid monomer to solid polymer is confined. There is not a large surrounding area of partially crosslinked polymer which can collapse upon itself during the post processing stage. The highly defined region between the cured and non-cured polymer also means that the PolyHIPE can be cured very close to each other without the neighboring cured regions affecting each other. The increase confinement of the polymerising region has therefore both increased the achievable resolution and eliminated most of the surface skin that surrounds the outer regions of the cured PolyHIPE.

4.12 Conclusion

My main findings in this chapter was that the surface skin surrounding the PolyHIPE was caused by the collapse of the partially polymerised polymer during the post processing washing stages. The underlying cause behind the surface skin also contributed to connecting polymer bridges between adjacent PolyHIPE bulbs. The addition of a light absorber reduced the surface skin effect and increased the achievable resolution when structuring with the PolyHIPE

There are currently only two publications in the literature on the stereolithography of PolyHIPEs [25, 43]. Neither of these publications explore the achievable resolution, nor provide an explanation, or solution behind the surface skin effect.

One method to address the issue that has been suggested in the literature is to use Supercritical CO_2 drying to preserve the fragile outer surface of the PolyHIPE [9]. However this does not address the resolution aspect of the PolyHIPE structuring, or the underlying process that leads to the formation of the fragile outer surface, that is susceptible to collapse.

The surface skin surrounding the polymerised PolyHIPE was determined to be caused by collapse of the outer PolyHIPE surface. The collapse was isolated to the post processing washing stages, and the initial attempts to eliminate the surface skin with different solvents and drying steps were unsuccessful.

The UV light was pulsed in a grid array with an ever increasing pulse duration to get an indication on the UV light scattering with respect to the level of exposure. Bulb

like PolyHIPE structures were formed which indicated that the UV light scattered outwards as it traveled through the HIPE from its initial point of exposure. The formation of connecting bridges between the PolyHIPE bulbs and the gradual increase in a surface skin layer covering the close spaced bulbs indicated that there is an interplay between the surface skin and excess polymerisation between two separate PolyHIPE bulbs, and that both were caused by the scattering of UV light.

The connecting bridges between the PolyHIPE bulbs originally formed between the closest point between the bulbs, this indicated that there was a limited region surrounding the polymerised section in which the excess curing could take place.

The connecting bridges have a similar appearance to ones previously reported upon in the literature for TPP [55] [56], and I have seen the same effect with the TPP of rod like structures in my previous work. Although the radical diffusion with the TPP and the UV light scattering with the HIPE are caused by different mechanisms, there is an underlying similarity between the two.

To quantify the UV scattering, the laser was pulsed at different points until they merged together. The distances between each PolyHIPE bulb was measured until they started form bridges between them. This gave a controllable method to characterise the amount of light scattering.

The addition of a light absorber became the logical method to prevent the scattering of the UV light. The light absorber will quench any UV light that escapes outside of the initial exposed region [59]. This created a highly confined polymerised boundary which significantly improved the achievable resolution. As theorised earlier there was an interplay between the surface skin and UV scattering. The reduction in one caused a reduction in the other and a more open outer pored PolyHIPE was produced. The light absorber currently used may not be suitable for a degradable material, potential biocompatible light absorbers that could be used include Riboflavin or Vitamin B12.

4.13 Summary

- The surface skin around the outside of the PolyHIPE structures polymerised by stereolithography was found to be caused by the collapse of the outer region during the washing stages
- The collapse of the outer surface was attributed to the decrease in the mechanical properties of the PolyHIPE as it is only partially crosslinked.
- The internal morphology of the PolyHIPE was maintained irrespective to the presence of the surface skin.
- The presence of a surface skin reduced the achievable resolution of the stereolithography of the PolyHIPE
- Connecting polymer bridges formed between pulsed PolyHIPE spots, these were caused by overlapping partially cured regions surrounding the polymerised PolyHIPE.
- The addition of the light absorber Tinuvin increased the achievable resolution of the structured PolyHIPE, eliminated the connecting polymer bridges and reduced the surface skin surrounding the PolyHIPE. This was attributed to the light absorbers creating a tighter cut off boundary between the cured and the non-cured polymer.

5. CHAPTER FIVE: PolyHIPE woodpile structure

5.1 Aims and Objectives

The aim of this chapter is to determine the logistics and feasibility behind the layer by layer stereolithography approach to produce complex structures using the HIPE material, as well as determining its suitability for a porous scaffold for the support of human dermal fibroblast cells. This is done by:

1. Scanning the laser in consecutive horizontal and lateral lines on top of the HIPE surface to produce the woodpile structure.
2. Determining the resolution limits and effect of the surface skin on the woodpile structures.
3. Curing flat sheets of PolyHIPE for toxicity testing using a 'wetting' and a dry sterilisation technique to determine its effect on the cell growth of human dermal fibroblast cells.
4. Determining the suitability of the PolyHIPE woodpile structures with the osteosarcoma cell line MG-63 and the effect of an acrylic coating on the cell attachment.

5.2 Introduction

The direct laser write of the HIPE can be used to produce large porous structures in a layer by layer process. The PolyHIPE is an inherently porous material, and the degree of interconnectivity and pore size distribution can be controlled by both the emulsion components, and degree of mechanical agitation. The larger polymerised regions are controlled by the selective direct laser write in both the X and Y directions, as well as the vertical Z direction which will be explored more in this chapter to produce large 3D porous structures, as opposed to the predominately single layer features polymerised on the glass surface explored previously [43].

Selective polymerisation in a layer by layer approach can be used to produce a 'macro' porosity can be controlled in three dimensional space as well as having control over the inherent 3D micro porosity. By the word 'macro' I will be referring to the large

gaps between the polymerised PolyHIPE lines, and 'micro' to the pore size distribution in the PolyHIPE.

The transition from a single layer to a larger macro multi-layered three dimensional structure requires an understanding on how the HIPE polymerises in the vertical direction as well as the horizontal and longitudinal directions explored previously. This is especially important to ensure adequate attachment to the previously cured PolyHIPE while maintaining acceptable resolution in all directions.

The woodpile design is the simplest structure that can only be achieved via additive manufacturing, and has been used with other microfabrication devices as the initial scaffold design to study the effect the 3D environment has on cell growth and migration [61].

5.3 Methods

5.3.1. PolyHIPE woodpile fabrication

A functionalised glass coverslip was placed in the centre of a glass slide and a 3mm thick PDMS cut into 2.6 cm discs with a 15mm hole in the middle was affixed around the glass coverslip on top of the glass slide. The HIPE was pipetted into the PDMS hole and remained in this temporary 'well' as the laser was scanned in a lateral direction to polymerise the HIPE. To produce the woodpile the HIPE was pipetted into a silicone well (13 mm) on top of a functionalized glass coverslip. The initial layer had 60 µl of HIPE to compensate for the extra space around the coverslip, for each subsequent layer 50 µl of HIPE was dispensed into the HIPE well and the laser scan was alternated between a horizontal and lateral direction. The z-height was increased by 50µm for each layer to compensate for the increased height of the HIPE. This was repeated four times to create a woodpile structure with four layers. A schematic of this setup can be seen in **Figure 59**.

The larger well size was used to ensure the coverslip had a flat even coating of HIPE, because at the edge of the PDMS where the HIPE was in contact with it produced a slight lip. The lines were polymerised by focusing the UV light at the top surface of the HIPE, and the stage holding the sample was translated in the linear horizontal and

lateral directions. The PDMS well was 15 mm wide to surround the 13 mm glass coverslip.

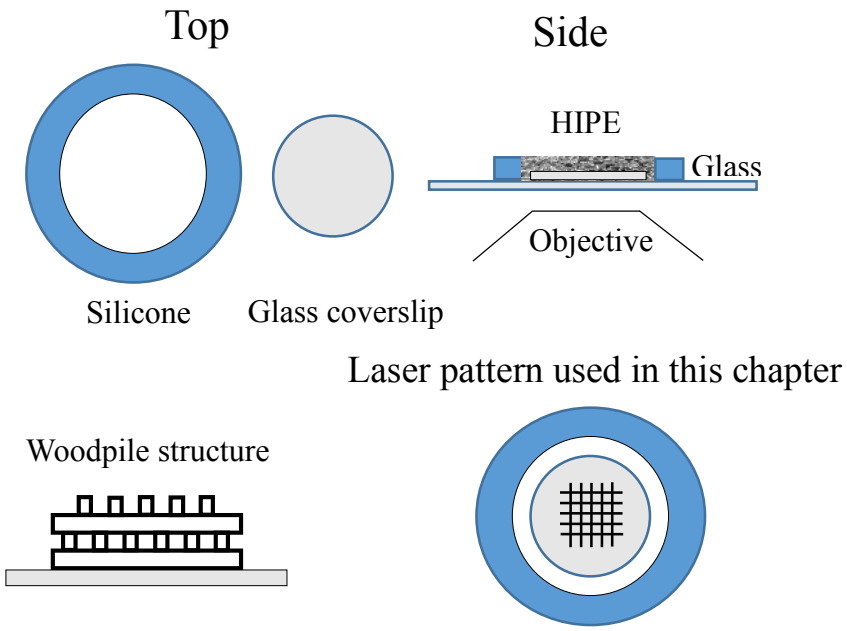

Figure 59: Schematic of the temporary HIPE 'well' created to house the HIPE during the polymerisation stage. The laser is scanned in horizontal and lateral directions to produce the PolyHIPE lines that make up the woodpile structure. The position of the woodpile structure on the glass coverslip is shown.

5.3.2. Ethanol sterilisation for cell culture

To sterilize the PolyHIPE discs they were submerged in a 70% ethanol solution for 24 hours in a non-sterile 24 well plate. Afterwards the samples were transferred to a sterile well plate in a culture hood. The samples were washed with sterile PBS 3 times with a minimum 10 minute wait duration between the removal and addition of fresh PBS.

5.3.3. Ultraviolet Light sterilisation

To sterilize the PolyHIPE discs they were exposed to UV light from a 100 Watt mercury arc lamp (Lumen Dynamics) For 20 minutes in a non-sterile 24 well plate. The lid to the container was kept on during the duration of the UV exposure. The well plate was transferred to a culture hood where the samples were transferred to a sterile well plate for cell seeding.

5.3.4. Acrylic acid plasma deposition

PolyHIPE samples were plasma coated with acrylic acid in an in-house built system. The samples are placed on a foil plate in the centre of a cylindrical borosilicate chamber with stainless steel plates either end. The chamber is put under vacuum and the acrylic acid flow rate is controlled using a needle valve to 2.4 cm^3 min^{-1}, and the pressure was adjusted to at $3.0x10^{-2}$ mbar with the acrylic acid valve open. The Chamber pressure is detected using an active Pirani gauge. An electromagnetic field is generated using an electromagnetic radiofrequency generator set at 15W power through wires wrapped around the chamber. This generated a plasma within the chamber which coated the surface of the PolyHIPE with acrylic acid.

5.4 Results & Discussion

For tissue culture applications a greater porosity is advantageous for cell ingrowth into the PolyHIPE, however the viscosity of the HIPE that had a nominal water porosities above 80% were too high, which caused problems creating an even layer as well as the pipetting volume accuracy. Therefore an 80% HIPE was used as it could accurately be pipetted into the temporary wells, and was fluid enough to settle as a flat surface for the polymerization of the subsequent layers. The viscosity of the resins used for stereolithography is a common factor to consider [41], as the liquid has to be fluid enough to recoat each layer quickly and uniformly.

Figure 60 is a computer generated image of the stereolithography based fabrication technique used to polymerise different alternating layers of a polymer. The UV light is polymerising through the top surface, and the previously cured lines are submerged in the pre-polymer solution which is housed in a temporary well. The previously cured woodpile structure can be seen in this image. A light microscope image of the produce woodpile structures are shown in **Figure 61**.

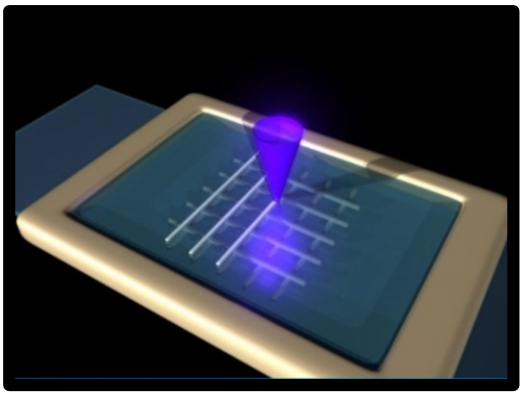

Figure 60: Computer generated image of the laser scanning over a photocurable liquid. The previously cured layers can be seen. A woodpile structure can be seen submerged in the uncured monomer solution, and the laser only polymerises the top surface by sequential scanning.

The design used is called a woodpile structure as it resembles the alternative stacking of wood on top of each other. The woodpile structure was produced by curing alternating parallel lines slightly offset and on top of each other in a layer by layer fashion with repeating line arrays every 4 layers. This is the first example of the woodpile structure being produced from a PolyHIPE, and it enables user design over the macro porosity in all directions.

5.4.1. Woodpile shrinkage

It is known that during the polymerisation of the HIPE the continuous phase will shrink as the monomers are converted into a polymer network, and this shrinkage is what forms the interconnecting windows between adjacent pores [12]. The shrinkage of the monomer to polymer during the polymerisation process is caused by the polymer has a closer packing arrangement than the monomers, which results in a smaller volume [62]. The bulk structure will also shrink as it goes from a wet state to a dry one, although this is a reversible process and will re-expand when wetted, and the shrinkage can be reduced to less than 5% if the PolyHIPE is freeze dried [8].

The EHA/IBOA woodpile structures shrank during the drying process after the structures were washed in acetone to remove the non-polymerised material. The shrinkage exerted the same force uniformly over the entire structure. Although the base layer remained firmly attached to the glass coverslip, which caused a deformation

of the overall woodpile structure. To reduce this effect the woodpile lines were made thicker to compensate for the shrinkage, also using a greater ratio of the more rigid IBOA monomer reduced the shrinkage and swelling.

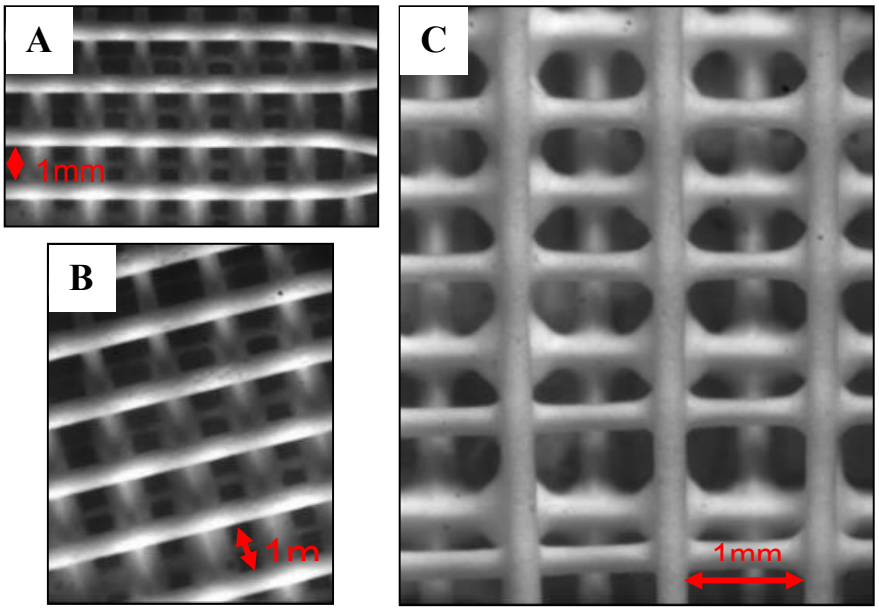

Figure 61: Light microscope image of the woodpile structure patterned using elastic PolyHIPE EHA80 formulation. In images A & B the top PolyHIPE lines have only attached to the previous layer at its base. Image C shows a higher amount of over curing at the interface between the horizontal and vertical PolyHIPE lines. This is a similar effect seen previously in **Figure 22**.

The above light microscope images in **Figure 61** shows a typical woodpile structure produced from the PolyHIPE. Only the top 3 lines can be clearly seen as the base layer is both too dark and out of focus. The PolyHIPE lines in images **A** and **B** are separate from the underlying ones, however in image **C** there is a small degree of merging between these alternating lines where they overlap each other. This can be seen by the diamond shaped PolyHIPE being present at the joints between them. This is caused by overexposing the top layer sufficiently enough for it to cure on and around the previous layer underneath. I suspect the partial activation of the surrounding HIPE around the previously cured PolyHIPE may also be a contribution factor as well. A

similar effect was observed with the single layer PolyHIPE grid lattice shown in **Figure 22**.

It is difficult to visualise the four different layers of the woodpile structure using a light microscope. Therefore 4 images were taken of the same location with different light exposures. These are shown in **Figure 62**.

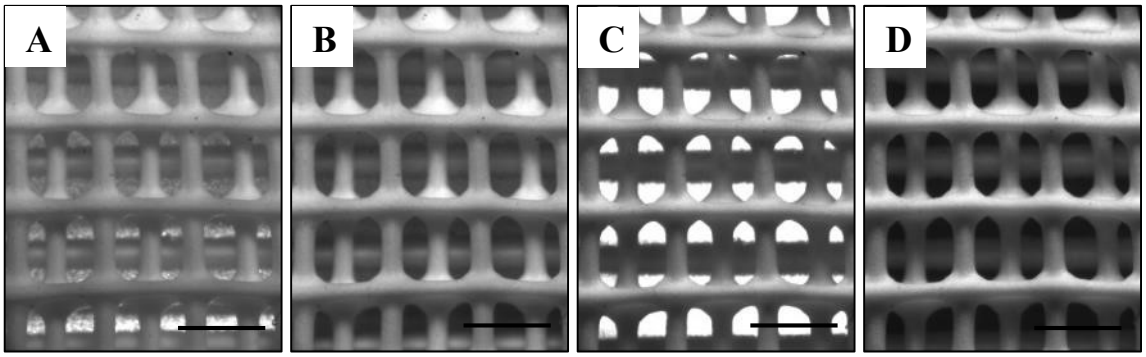

Figure 62: Four light microscope images of the same woodpile structure (PolyHIPE EHA80). The objective was focused at different heights with different light exposures to highlight the depth of the structure. (**A**) Underside lighting at an angle, (**B)** Top illumination at an angle, (**C**) Underside light, (**D**) Top only light. Scale bar is 1mm.

The above 4 light microscope images (**Figure 62**) shows a woodpile structure that has been photographed with different light exposures alternative from underneath the sample to the top surface only. The PolyHIPE white appearance can clearly be seen with all the images. Excess polymer can be seen on the glass surface in image A, and an overlapping excess cured region between the line interfaces. This same effect on the glass surface can be seen in the below SEM images in **Figure 63** image B.

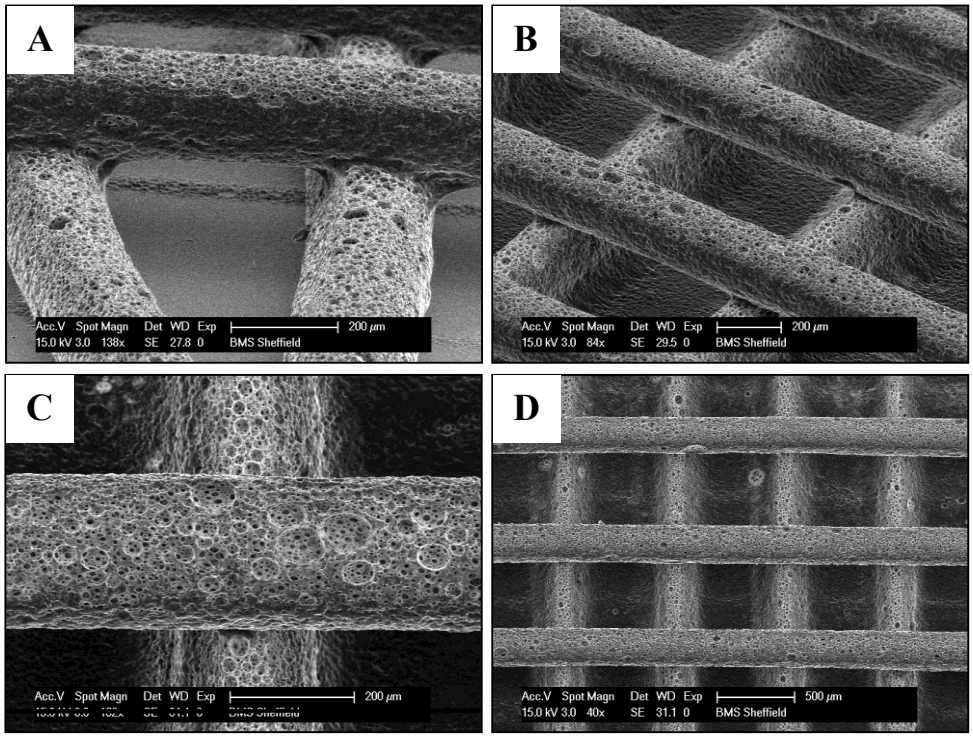

Figure 63: SEM images of a PolyHIPE EHA80 2 layer woodpile structure. **A**, a surface skin can be seen on the side of the PolyHIPE lines. **B**, The base layer has a high amount of excess polymer that has cured against it. **C**, close up of the open porosity on the top of the lines. **D**, An overview of the sample.

The cure depth is dictated by the Beer-Lambert law which relates to the decay of the lights intensity as it passes through an absorbing medium [41]. By increasing or decreasing the thickness of the HIPE the thickness of the PolyHIPE lines can be controlled. If the HIPE layer is too thin the two lines will over cure and produce a diamond like shape between the previous and top layer. This effect can be seen in image **A** in **Figure 64**.

The PolyHIPE woodpile structure maintains an open porosity at the top surface of the lines, however as reported previously with the polymerised lines and tubes, where there is a cured/non-cured boundary a surface skin will form around the PolyHIPE. A closed pore surface skin can be seen in on the side of the PolyHIPE lines in **Figure 63** images **A** and **B**. There is no significant overcuring between the base and top lines because the degree of UV exposure was sufficiently controlled to prevent any overcuring below the top HIPE layer.

5.4.2. PolyHIPE woodpile: achievable resolution

The achievable macro resolution was controlled by altering the scanning speed and laser power as well as using a pinhole to reduce the amount of UV light passing through the objective prior to exposing the HIPE. Using a pinhole prior to the objective created a more uniform circular UV beam, as well as artificially creating a smaller spot of UV which was used to polymerise a smaller area. The scanning speed has a very high influence on the polymerized region, and finally the amount of HIPE pipetted onto each layer will affect the amount of UV exposure required to only polymerise the top surface, and not the previously cured region. As well as the previously mentioned factors that affect the achievable resolution, it is also dictated by the overlapping sub activated regions surrounding the cured lines as shown previously in **Figure 43**. If these regions overlap then the separate lines will start to merge together. Typically a laser current of 2.2 A, with a pin hole of 3.1 mm was used, which resulted in a UV power of 4mW. The maximum resolution that could be achieved between adjacent PolyHIPE lines in the woodpile structure was about 500 µm spacing before they started to merge together. These woodpile structures were produced before the PolyHIPE spot experiment and the effects of the light absorber Tinuvin were unavailable at the time.

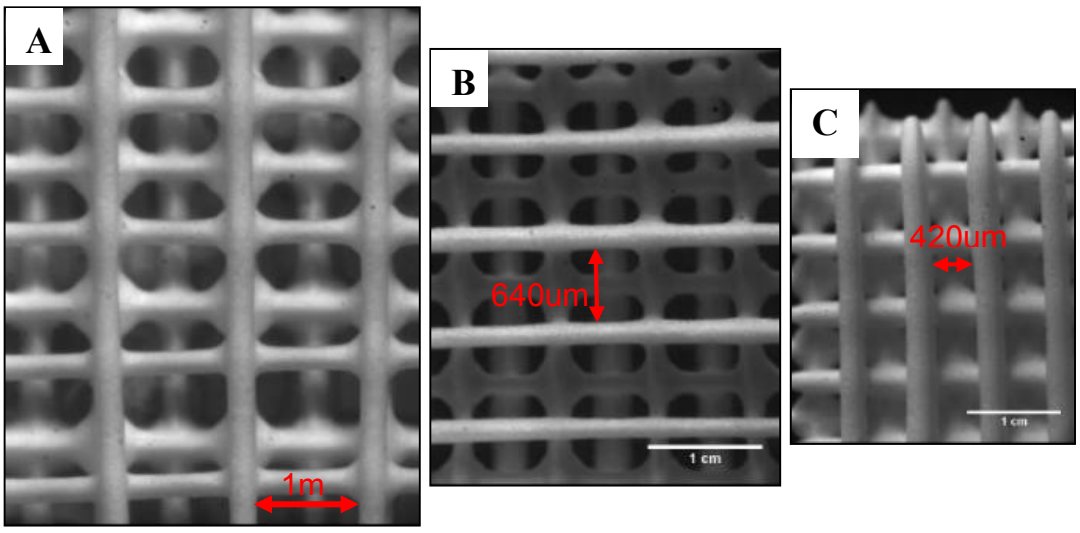

Figure 64: Light microscope image of three woodpile structures with an ever decreasing space between the lines. **A**, 1mm spacing. **B**, 640µm spacing. **C**, 420µm spacing. In image **C** the PolyHIPE lines have increased in size and the central regions of the scaffold have been extensively over cured.

The effect of the spacing is shown in more detail above in **Figure 64**. As the PolyHIPE lines get closer together, they start to get wider until they eventually over cure completely. The maximum achievable resolution achieved in the initial woodpile structures was between the 400-500µm. The resolution was defined visually by the minimum distance between the PolyHIPE lines before there was excess crosslinking between them. In image C **Figure *64*** a line spacing of 400µm resulted in a solid block of PolyHIPE, whereas a spacing of 420µm produced very thick PolyHIPE lines.

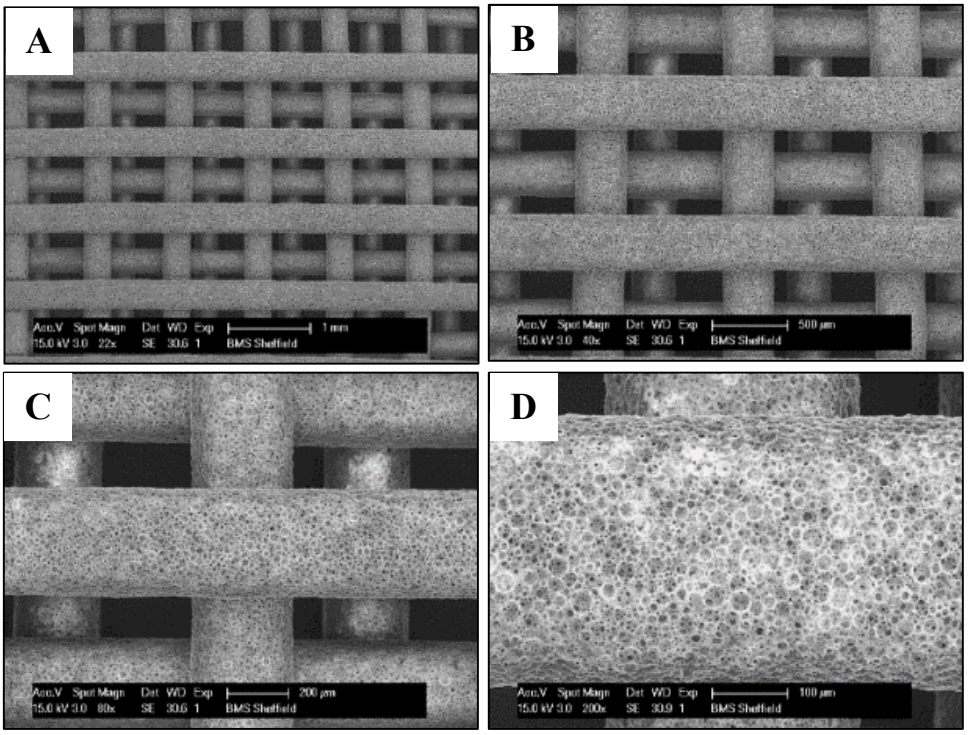

Figure 65: SEM images of a refined Woodpile structure EHA80 formulation. **A**-**D** gradual zooming in on the PolyHIPE lines [63].

The following factors that affected the size of the PolyHIPE lines were optimized: Pinhole diameter, laser power, scan speed, volume of HIPE pipetted into the 'well' and the distance between each PolyHIPE line. The pin hole and laser power had a big effect on the thickness of the PolyHIPE line and therefore were kept as a constant. The optimum parameters for the base layer were found to be 60µl of HIPE, a scan speed of 1.75mm/s and 4mW laser power. This was determined by changing each parameter separately to produce horizontal lines that were well defined and had no excess crosslinking between them.

Different volumes of HIPE were pipetted on the top surface, and the lateral lines were polymerised on top of the horizontal ones. The optimum volume of HIPE to add to the 'well' was found to be 50µl, and the z-stage was raised by 50 µm to compensate for the increased height of the HIPE 'well. This allowed a PolyHIPE woodpile structure with no overcuring and define layers to be produced (**Figure 65**).

5.4.3. Woodpile contraction

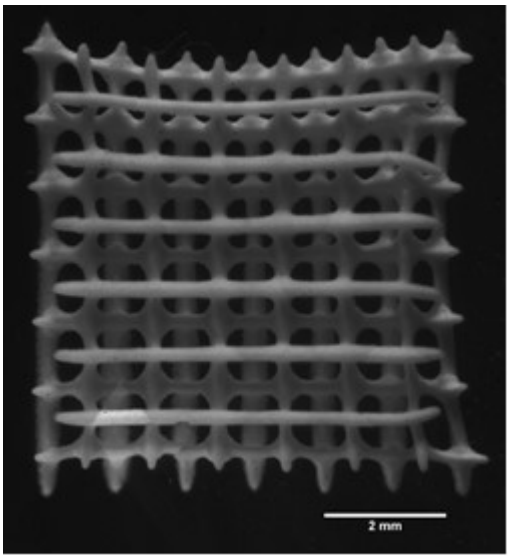

Figure 66: A PolyHIPE woodpile structure after it had been washed in acetone and air dried. The overall structure has contracted from its original square shape. The top surface has been pulled inward caused by the vertical lines contracting during the drying stages. The base layer has had minimal contraction because it is adhered to the glass surface. This can be seen on the far left hand side.

The thin lines of the woodpile structure are mechanically weak, and the bulk structure has poor mechanical strength because of its inherent porous nature. The alternating PolyHIPE lines have a limited amount of attachment to the tops of the previous ones and therefore are more prone to the effects of contraction during the drying stages. This especially evident when a swelling solvent such as acetone is used. The contraction only effected the outer regions of the woodpile structure, while the middle ones retained their uniformity. This contraction effect can be seen in **Figure 66.**

To counteract the contraction the best methods were found to quickly dry the fibers, include an outer region around the bottom set of lines to provide additional support. The easiest method is to structure thicker lines which will be more robust, however this does not address the issue if smaller woodpile structures are required, and are achievable with the addition of a light absorber into the HIPE.

5.5 Cell culture on the PolyHIPE material

The porous and interconnected nature of the PolyHIPE scaffold is appealing for the growth of cells. A polystyrene based PolyHIPE scaffold is currently on the market as a scaffold for the 3D culture of cells, it is under the trade name alvetex. The porous PolyHIPE material offers cellular support in a 3D fashion which gives the cell numerous contact points between adjacent cells and the scaffold.

In this chapter the EHA/IBOA based PolyHIPE has been tested as a support scaffold for tissue engineering. Different types of sterilization methods were used to determine their respective effect on the cell growth. Due to the nature of the PolyHIPE preparation using a water in oil emulsion the monomers and resulting polymer is hydrophobic; this may affect the washing stages and cell growth of the PolyHIPE.

Both ethanol and UV light was used to sterilize PolyHIPE samples prior to cell culture. Both of these sterilisation techniques were used to determine the optimum method for the EHA/IBOA PolyHIPE material. The use of ethanol has been reported to increase the wettability of the PolyHIPE. UV was chosen as it will provide a 'dry sterilization' method for comparison to determine the effect of an untreated PolyHIPE sample on the growth of human dermal fibroblast cells. This is because the EHA/IBOA PolyHIPE material is inherently hydrophobic to form the initial water in oil emulsion.

The EHA/IBOA blend PolyHIPE are a non-degradable that are insoluble in aqueous environments, a PolyHIPE scaffold with a controlled degradation time period would be better suited for tissue engineering materials. Nevertheless this material can be used for the 3D culture of cells. This will provide also a benchmark for future work towards a more clinically relevant porous PolyHIPE biomaterial.

For the initial experiments human dermal fibroblast were used. These experiments should give an indication to the cell responses towards the PolyHIPE disks using the photocurable monomers.

5.5.1. PolyHIPE sample fabrication for cell culture

For the cell culture flat PolyHIPE disks were polymerised on top of functionalized coverslips which act as both a weight to ensure the discs are fully submersion in cell media, and also to allow for ease of handling without damaging the structures. If the PolyHIPE is cured on a normal coverslip, then it will detach during the washing stages.

To create uniform PolyHIPE disks on the coverslips, a thin layer of PDMS with 10 mm diameter holes within it was adhered to the functionalised coverslips. The partially tacky nature of the silicone makes it ideal to lightly adhere to the glass. The HIPE emulsion (40 µl) was pipetted in to the well and subsequently cured under UV irradiation. The silicone wells adhered sufficiently to the glass coverslip to prevent the HIPE from leaking out of the sides. PDMS was chosen over adhesive tape for the temporary wells as the cured PolyHIPE stuck to the sides and would partially break off when peeling the tape away. This step by step process is shown in **Figure 67**.

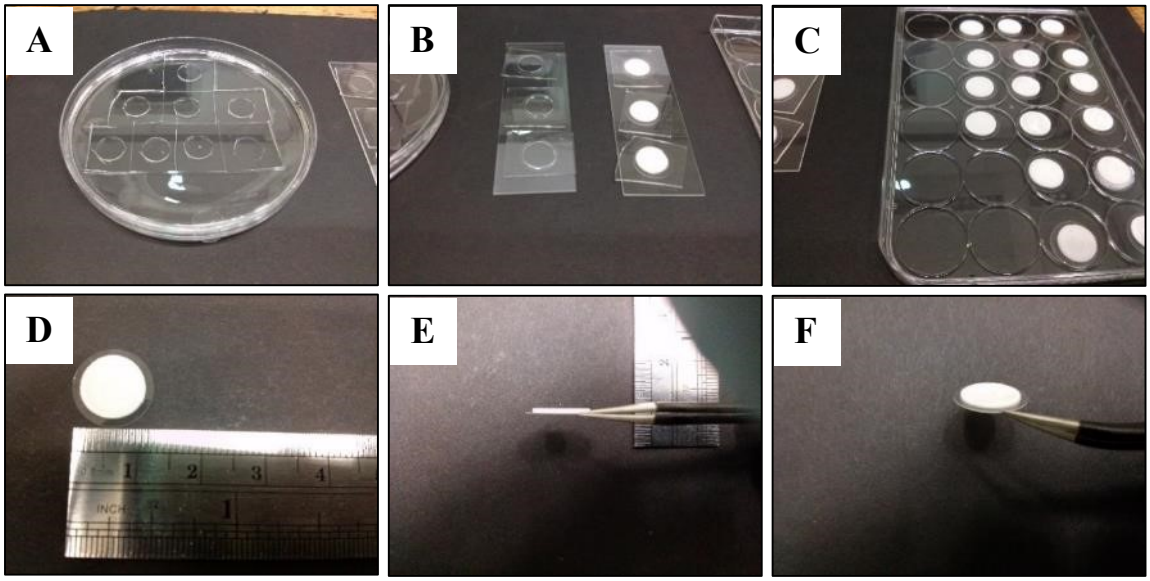

Figure 67: PolyHIPE disk fabrication for cell culture using EHA80 formulation, (**A**) silicone sheet with wells cut out, (**B**) Silicone attached to 13mm glass coverslip on top of a glass slide and 40µl of HIPE pipetted into the well, (**C**) Polymerised PolyHIPE discs on top of glass coverslips, (**D-F**) Polymerised PolyHIPE on glass at different angles to show size and thickness.

5.5.2. Human dermal fibroblast cell culture

18 PolyHIPE disks were split into 2 x 9 experiments for a day 1, 5 and day 7 culture of fibroblast cells using two different sterilization methods, soaking in 70% ethanol or by UV sterilization. All samples were washed in PBS prior to adding the fibroblast cells. Cell culture media DMEM + GlutaMAX with the addition of 0.01% penicillin streptomycin, 0.0025% amphotericin B and 10% FCS (fetal calf serum) was used.

30,000 fibroblast cells were added onto each of the 18 PolyHIPE samples, and 18 TC (Tissue Culture) wells were used as a control. 1,440,000 cells were required in total. The cells were suspended in 40 µl for each sample, therefore 48×40 µl = 1920 µl of media with the total cell number was required. The original cell suspension had 750,000 cells per ml, this equated to 750 cells per µl. So 30,000/750 = 40 µl to get the number of required cells. 1920 µl from the total cell suspension was removed and put into a small aliquot. This was then used to dispense out 40 µl onto each sample. This dispensing technique was used because for such a small volume of liquid, it is easier to ensure an even cell suspension than trying to suspend a few ml every time using the 40 µl micro pipette. The 40 µl droplet was left for about an hour in the incubation hood to allow for the cells to attach to the scaffolds. 1ml of media was then added to every well, and a MTT assay was used to assess cell viability on the scaffolds on days 1, 5 and 7.

5.5.3. MTT assay of Fibroblasts on PolyHIPE disks

An MTT assays was performed on days 1, 5 and 7. Samples were washed in sterile PBS and placed in to clean well plates. 1ml of the MTT reagent was added to the culture plate for 40 minutes for each sample. The reagent was removed and 600 µl of 0.125% acidified isopropanol was added to lyse the cells for 30 minutes. 3× 200 µl was taken from each well for the MTT reading on the plate reader.

The MTT assay is an indirect method to measure the mitochondrial activity of the cells and therefore can give a quantitative value on the cell viability on the PolyHIPE material [50]. This is achieved by measuring the conversion of the soluble (3-(4, 5-dimethylthiazol-2-yl)-2, 5-diphenyltetrazolium bromide) (MTT) into the insoluble formazan by the cells mitochondrial succinic dehydrogenase (SDH). Formazan is a

purple colour and gradually builds up in the metabolically active cells. After an hour the formazan is removed from the cells by lysing them with acidified isopropanol. This dissolves the cellular membrane, killing the cells. The formazin is soluble in the acidified isopropanol and its amount can be quantified by a spectrophometer. The absorbance of this purple solution was measured at 570nm.

A comparison between the light absorption between the fibroblast cells growth on the PolyHIPE samples over one, five and seven days was performed. An increase in the amount of formazan indicates that there are more cells growing on the scaffold.

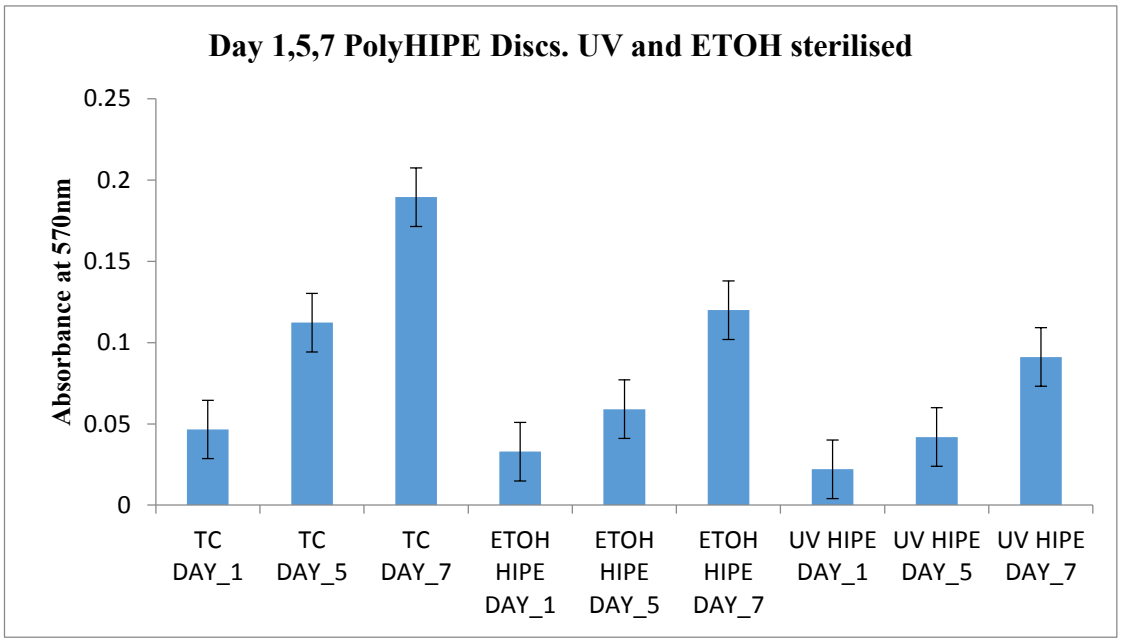

Figure 68: MTT assay of fibroblasts grown on the PolyHIPE discs at days 1, 5 and 7, 70% etoh and UV sterilised samples. The absorbance can be seen to increase over the course of 7 days on all the samples and tissue culture plastic.

Initial observations during cell seeding indicated that the ethanol sterilized PolyHIPE disks had a greater wettability than their UV sterilized counterparts. The 40µl of cell suspended media spread out evenly across the entire sample that as pre-sterilized with ethanol, whereas with the UV sterilized samples the droplet retained its spherical shape on the top surface. This was problematic as the cell suspended droplet could easily slide off the PolyHIPE if it was knocked which happened for one of the day 5 ETOH samples, this resulted in a significant reduction in cell count compared to the others due to this so it was omitted from the data. For days 5 and 7 there was a

significantly increased cell growth on the tissue culture plastic, and the only significant difference between the ethanol and UV sterilized PolyHIPE samples were observed on day 7. I suspect this is due to the more even spread and distribution of the cells at the initial seeding stage on the ethanol sterilized PolyHIPE.

The increased wettability of the ethanol sterilized PolyHIPE samples may account for the increase in cell numbers over the first seven days when compared to the UV sterilized PolyHIPE. Firstly ethanol is a non-swelling water miscible solvent, it can be used to dissolve any uncured monomers and is a popular choice for sterilization of samples for cell culture. The ethanol is unaffected by the hydrophobicity of the polymer, it can penetrated into the material and displace any trapped air, and then can be displaced by PBS in the subsequent washing stage to remove the trapped ethanol. PBS washing on the other hand, on its own will be affected by the hydrophobicity of the polymer, and will not penetrate the PolyHIPE, therefore trapped air may remain in the PolyHIPE during cell culture which will prevent cell ingrowth.

The increased hydrophobicity of the PolyHIPE in comparison to the tissue culture plastic could account for the difference between the spectrometer absorbance readings. The PolyHIPE discs also remained purple after the acidified isopropanol wash which could indicate that there was trapped formazan within the PolyHIPE which hasn't gone into the surrounding solution for analysis, this would lower the absorbance readings.

The MTT assay doesn't give any indication on the cell morphology. One method used in the literature involves imaging the cells via SEM has been used to give a qualitative representation of shape on the PolyHIPE surface [64].

5.6 Cell culture on a woodpile scaffold: introduction

The woodpile structure is an attractive 3D environment for the study of 3D cell culture, the PolyHIPE structure is inherently 3D, however the introduction to two tier porosity, i.e. the macro porosity, provides another level of openness that cannot be produced by bulk polymerisation alone. The woodpile design is a common 3D scaffold that has been produced using other microfabrication techniques such as TPP [61]. In this study the maximum spacing between the beams was 110 μm, significantly larger than the

size of a fibroblast cell. The cells were confined to the beams within the woodpile structure. This study also found that the cells migrated within the smaller 12 μm gaps, this is promising as this indicates that the cells have the capability to potentially migrate through the small interconnecting voids within the PolyHIPE scaffold.

In this chapter the PolyHIPE woodpile structure was made from a non-degradable polymeric material. Therefore the cells will not be able to degrade the scaffold or be able to modify its shape.

5.6.1. MG63 osteosarcoma cell line

The culture of the osteosarcoma cell line MG63 on a polymeric PolyHIPE has previously been reported in the literature [50] . In this study the elastomer EHA component was used within a thermally cured PolyHIPE and reported the osteoblast like cells to have proliferate on and adhered to the PolyHIPE samples, and to have spread over the porous material. This study used a high water volume of 90% and an elevated temperature to destabilise the emulsion for larger pore size distribution for increased cell in growth.

The HIPE water volume ratio was limited to a nominal porosity of 80% due to the increased viscosity of the HIPE when a higher water volume ratio is used. This limits the amount of interconnectivity within the PolyHIPE, however for the woodpile structures the direct laser write was used to control the macro porosity of the scaffold.

This work was done in collaboration with a colleague for the cell culture of the MG63 osteosarcoma cell line on the PolyHIPE woodpile structures. This data is presented to show the potential of the PolyHIPE woodpile structures for 3D culture applications. The cell culture, acrylic acid plasma deposition and imaging was done by Atra Malayeri. Confocal images of the MG63 cells are shown in **Figure 69.** She also demonstrated the cell viability using an MTT assay up to 7 days (data not shown).

For tissue engineering applications the hydrophobic PolyHIPE material can post-modified to increase the hydrophilicity acrylic acid plasma deposition. This has been shown to increase the cell attachment to the PolyHIPE material for 3D cell culture [6].

Plasma deposition of was used to increase the cell attachment on the woodpile structures. Cell attachment was visually shown to increase in comparison to the non-coated PolyHIPE woodpile structures.

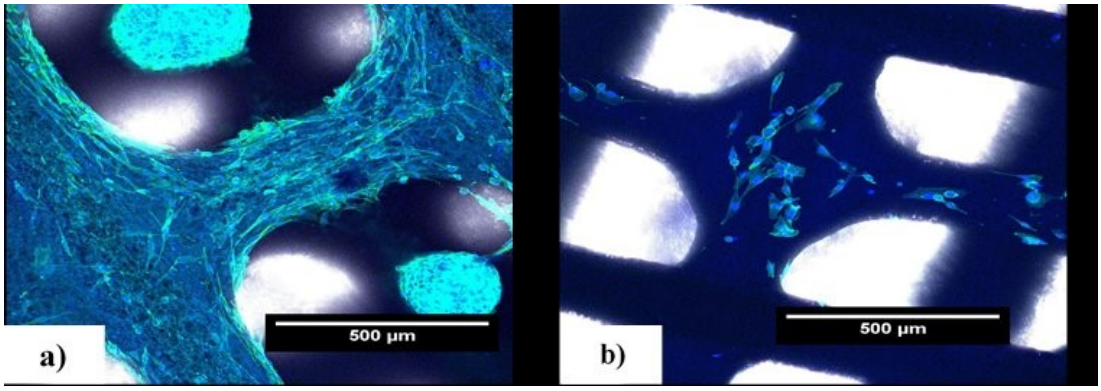

Figure 69: Immunofluorescence micrographs of PolyHIPE woodpile scaffolds. The MG63 cells were stained with DAPI and Phalloidin-FITC **a)** Acrylic-acid coated woodpile scaffold with a greater amount of cell attachment **b**) non-coated woodpile scaffold with a few cells attached to the surface.

5.7 Layering of PolyHIPE with different mechanical properties.

Different HIPE monomer compositions EHA 80 and IBOA80 formulations were cured together in subsequent layers to determine the feasibility of both layering the PolyHIPE material; which is a requirement for more complex stereolithography based manufacturing, and to explore the use of the use of two different monomer formulations to alter the mechanical properties of select layers within the PolyHIPE. A similar approach has been demonstrated in the literature recently [65].

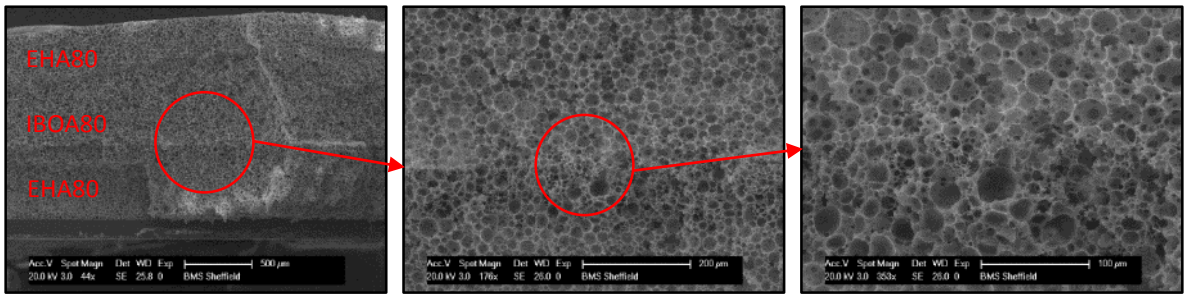

Figure 70: SEM images of EHA80/IBOA80/EHA80 PolyHIPE layers that were each cured separately. The boundary between the layers can be seen in all images.

Figure 70 shows different magnifications of a layer by layer bulk cured PolyHIPE. A uniform transition of the porosity can be seen between the two PolyHIPE formulations, despite them being cured a minute apart, and consisting of a different initial HIPE. This could be due to the water droplets 'filling in' the hollow voids on the top surface prior to the next HIPE being cured on top, as the top surface retains its open porosity.

5.8 Conclusion

The layer by layer direct laser write of the HIPE was used to create a woodpile structure. From an additive manufacturing perspective the woodpile structure is a very simple structure to create. The stage programming only involved linear translation commands for the horizontal and lateral directions, and for tissue engineering applications the woodpile structure has been reported on previously [61].

The PolyHIPE woodpile structure is a simple demonstration of the 3D structuring capabilities emulsion templating and stereolithography techniques to produce a more complex PolyHIPE structure. This process enabled separate control over the macro porosity from the selective polymerisation, and micro porosity from the emulsion templating. The alternating lines within the woodpile structure were found to adhere to each other if there was sufficient overlap between them. If the UV exposure was too high then these joining regions over cured to produce a diamond like shaped PolyHIPE region.

As previously reported, the polymerised lines in the woodpile structure maintained their internal porosity, however there was a surface skin on the side of the lines that was present on all the samples. The top regions of the PolyHIPE lines were open pored because they were polymerised adjacent to the surrounding air, and there was no transition between the cured and non-cured emulsion.

The PolyHIPE lines on the woodpile structure were prone to contraction and warping during the drying stages as the material contracts. The volume shrinkage of the PolyHIPE is caused by the conversion of the monomers into a more tightly packed polymer network which takes up a smaller volume [62]. Also the warping can be

caused by the thin lines which become very flexible in their expanded state during the washing stages, this can be seen in **Figure 66**.

The minimum resolution of the polymerised PolyHIPE lines were found to be between the 400-500μm depending on the laser parameters used. When the spacing between the lines was below this distance then excess curing of the PolyHIPE would start to appear between the two lines. This is due to the partially polymerised region that would surround the outer perimeter of the PolyHIPE, overlapping of these regions will initiate polymerisation of the monomer.

For improved resolution the light absorber Tinuvin could be added to the HIPE. This has been explored with a colleague (Rob Owen), and he has managed to achieve 300μm spacing distance between adjacent lines (data not shown).

The osteosarcoma cell line was grown on to the woodpile structures by a work colleague, and I have presented an image of her work **Figure 69**. Her experiments shown that there were more cells attached to the PolyHIPE woodpile scaffold that had been plasma treated with acrylic acid than the non-coated structures. Therefore the surface chemistry of the PolyHIPE can be controlled independently to the mechanical properties to allow potential tailoring of the material for specific applications, such as bone regeneration [63]. The PolyHIPE woodpile structure has also recently been demonstrated within the group to support the growth of human embryonic stem-cell derived mesenchymal progenitor cells (hES-MPs)[63].

Flat sheets of PolyHIPE supported the growth of human dermal fibroblast cells for up to 7 days, and their viability was shown by the MTT assay. The ethanol sterilisation method was found to be the best as it increased the wettability of the PolyHIPE prior to cell culture, which meant that during the cell seeding, the cells were spread out over a larger area, and were therefore more spread out able to proliferate and grow more freely.

5.9 Summary

- Scanning stereolithography was used to produce a woodpile structure in a layer by layer fabrication method.
- There was a side skin on around the woodpile lines, which was caused by the collapse of the PolyHIPE during the post processing stages.

- The woodpile structure warped during the washing stages if a swelling solvent was used. This is a reversible process and rapid drying preserves the structure
- The PolyHIPE woodpile maintained its internal porosity, and had an open pored top surface of the PolyHIPE lines
- The acrylic acid coated PolyHIPE woodpile structure supported the attachment and growth of more MG63 osteosarcoma cells than the non-coated structure, as demonstrated by work colleagues.
- Initial data on the layering of different HIPE formulations was shown, this opens up the potential for alternating woodpile structures with tailored mechanical strength on way, and flexibility the other.

6. CHAPTER SIX: Development of a Biodegradable PolyHIPE for tissue engineering applications

6.1 Aims and Objectives

This aim of this chapter is to develop a PolyHIPE based on the biodegradable monomers thiolene and PCL. As well as determining its potential suitability as a porous support structure with an electrospun barrier layer for the co-culture of cells. This is achieved by:

1. Reproducing the thiolene PolyHIPE based on the literature.
2. Developing a PCL/thiolene blended PolyHIPE using the thiolene PolyHIPE as a baseline.
3. Determining the suitability of the PCL/Thiolene PolyHIPE for the growth of human dermal fibroblast cells.
4. Exploring the potential of a PCL/thiolene PolyHIPE with an electrospun barrier layer to prevent cell crossover for the development of a trilayer scaffold for the co-culture of cells.

6.2 Introduction

For a scaffold to be implantable into the body it needs to be degradable/resorbable, and the material should not elicit any inflammatory responses and it should degrade into non-toxic compounds [41]. The main purpose of the scaffold is to provide a temporary support structure for the cells to grow and proliferate onto, and the growing tissue will eventually replace the scaffold completely over time. Therefore there is a requirement for a high level of control over the scaffold's architecture and additive manufacturing based approaches are finding ever more applications, especially in the field of tissue engineering [41]. The development of new materials that can be 3D printed opens up a wide range of new possibilities for the field of tissue engineering that would otherwise not be available [66].

The level of interconnectivity, as an open pored structure is particularly important for tissue engineered scaffold applications where high interconnectivity facilitates cell infiltration and sufficient nutrient transport and removal of metabolic waste within the

bulk material [47] [67]. Advantages of a synthetic material for the scaffold production include their reproducibility in regards to the purity and tunability of the mechanical properties [47].

The micro architecture of PolyHIPEs makes them a strong candidate for tissue engineering applications, as their inherent 3D porous and interconnected nature can provide cellular support [6], have tuneable pore size, interconnectivity of the pores and mechanical variability [14]. These factors make them an appealing candidate for tissue engineering applications [1].

The porosity of these scaffolds plays an important role, smaller pores will limit the migration of cells into the scaffold, therefore constraining them to the outer surface of the PolyHIPE while larger pores the cells are able to penetrate the porous structure [48]. PolyHIPE-based scaffolds have been shown to support the growth of an osteoblast like cell line for 35 days, smaller pores between 10-40 micron did not shown any significant difference in the cell morphology, however it was shown that larger pores (100 μm) had the most cell penetration (up to 1.4 mm) [68]. Hydroxyapatite was incorporated onto the surface of these non-degradable styrene based PolyHIPE materials by adding it to the aqueous phase by dissolving it in 15% phosphoric acid, and then post treating the PolyHIPE in 1M of NaOH to introduce the hydroxyl groups onto the hydroxyapatite, this coating was reported to increase the osteoblast cell penetration into the scaffold [68].

Strict control over all the pre-processing parameters are paramount in order to increase the reproducibility of the PolyHIPE scaffolds. PolyHIPE scaffolds have been shown to be a good candidate for the 3D growth of cells *in vitro* [50]. For example the porosity can be controlled by adding an organic additive such as a solvent that can partition between the two water phases, or by increasing the temperature of the aqueous phase to increase the pore diameter [14]. The elevated temperature produces larger droplets as the emulsion is not as stable against the effects of coalescence. Also for example, 1% of the water miscible solvent THF can be added to the droplet phase, which facilitates water transport through the monomer film resulting in a larger pore size with the PolyHIPE [3].

Polystyrene based PolyHIPEs are being used as a commercial available 3D support structure for the three dimensional (3D) cell culture under the name Alvetex®

produced by Reinnervate, and have been ability to be used for routine three dimensional cell culture shown [69], and have been used as a point of comparison within other PolyHIPE publications [21]. Recently degradable injectable PolyHIPEs based on a fumarate material have been developed [26] and were further developed to exhibit a short cure time of less than 15 minutes [70].

Many of the crosslinked polymeric materials used in PolyHIPE production are not cytotoxic, however, any residues that may be trapped within or around the material may be, for example; any unreacted monomers or photoinitiator residues that could be trapped within the polymer will need to be removed prior to implantation [41]. Therefore it is imperative that the PolyHIPE structures are sufficiently washed after polymerisation to remove any contaminants, non-cured monomers and any surfactant residue, a Soxhlet apparatus can be used to remove any residue components or surfactant on the PolyHIPE [19].

6.3 Degradable PolyHIPE scaffolds for Tissue Engineering applications

There is a limited range of materials that can be used to create a PolyHIPE because the material has to be either hydrophobic or hydrophilic enough to be able to be used to create a stable emulsion. For a W/O emulsion the range of potential materials is decreased, and the choice of materials is further decreased for biodegradable photocurable materials that are hydrophobic enough to create a stable emulsion. The surface of the PolyHIPE can be treated for specific cell type attachment if required, for example a non-degradable styrene based PolyHIPE can be coated with bioactive molecules to increase the attachment of neuronal cells by the coating of poly-d-lysine and laminin by submersion into an aqueous liquid of these proteins for 24 hours [71].

The study and growth of cells *in-vitro* allows to study the development and proliferation of cells in a controlled environment [72]. It is important to mimic the conditions that the cell would experience in its native environment, and research towards the usability of 3D scaffolds produced with PolyHIPEs is a step towards this direction. A drive for the development of 3D scaffolds for tissue engineering comes from the shortage of organ and tissue donation availability. For in vivo applications

degradation of the implanted material is required to allow for the cells to eventually replace the scaffold.

A range of synthetic polymers can be processed into different foam like structures, they can be prepared using a variety of different techniques, and their properties such as degradation rate and mechanical properties can be varied by the use of monomer blends and the addition of porogens [73].

The following review sections will cover a range of biodegradable materials that have been used to create the PolyHIPE structure, and I will focus on the use of Poly ε-caprolactone (PCL).

6.3.1. Poly (propylene fumarate) (PPF) based PolyHIPE scaffolds

A biodegradable PolyHIPE from poly(propylene fumarate) (PPF) with the cross-linker propylene fumarate diacrylate (PFDA) has been reported [4]. PPF is an unsaturated polyester which can degrade by hydrolysis of its ester linkages into the biocompatible fumaric acid and propylene glycol [4]. In this paper the authors produced a PolyHIPE with large macropores >500 μm, however for the majority of the pores that were greater than 50 μm were closed pored. This was attributed to the thick continuous layer being more resistant to the contraction process during the polymerisation process, which creates the interconnecting windows between adjacent pores [12]. The smaller droplet suspension of around 50 μm would result in a greater surface area which the continuous phase is stretched around, and therefore cause it to be a thinner film, which would be more prone to the contraction process during the polymerisation reaction. The solvent toluene was varied between 40 to 60wt% which resulted in 2-fold decrease in the viscosity and allow for the formation of the fumarate-based PolyHIPE, although the upper limit of 60% toluene started to destabilise the emulsion. The addition of a solvent affected the interfacial tension between the two phases and therefore the emulsion stability, and can be altered as another factor to control the porosity.

Injectable porous scaffolds based on an emulsion templating of biodegradable propylene fumarate dimethacrylate (PFDMA PolyHIPEs that crosslink at the body temperature (37°C) have been developed and reported in two publications in 2014. The group characterised the injectable PolyHIPE and addressed the formulation

parameters in an initial publication [26]. This was followed up by an improved formulation with a reduction in the cure time to be comparable to bone cement, the study also addressed the long term storage effect on the HIPE [70].

6.3.2. Thiolene

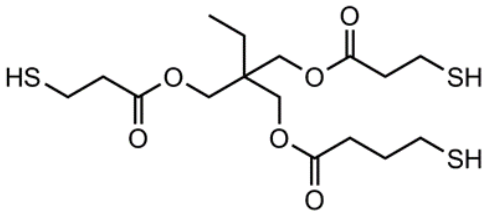

Trithiol

Figure 71: Chemical structure of the Trithiol

Biodegradable PolyHIPEs have been created using Thiol-ene chemistry in 2011 [74] and 2012 [21]. The thiol-ene-based polymer was formulated with ester functionalities in the thiolene backbone which are susceptible to hydrolytic cleavage, therefore creating a biodegradable PolyHIPE. 19% mass loss was shown over 15 weeks in cell culture medium [21]. Larger Voids and interconnecting windows were created by destabilising the HIPE emulsion by using a high (80°C) water droplet temperature, it was reported that larger voids are more beneficial for cell proliferation into the material, the material was shown to support the growth of keratinocyte cells (HaCaTs) for up to 11 days [21].

6.3.3. Polylactic acid (PLA) containing PolyHIPE

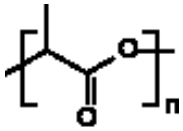

Figure 72: Chemical structure of Polylactic acid (PLA)

A publication in 2002 reported on a thermally cured PolyHIPE containing either PLA-diol or PCL with both a blend with styrene, and also demonstrated the use of the non-

reactive diluent toluene to reduce the viscosity. An emulsion with as much as 60% PLA was produced, however the PolyHIPE shrank by up to 50% upon drying. PLA is a more hydrophilic polymer in comparison to PCL, this is due to the smaller aliphatic carbon chain in its backbone [75]. A large amount of the surfactant Span 80 was used to stabilise the emulsion and the study highlighted that the interfacial tension and the viscosity are important parameters for emulsion stability [75].

6.3.4. Poly (ε-caprolactone) (PCL)

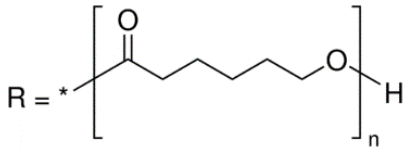

Figure 73: Chemical structure of Poly (ε-caprolactone) (PCL)

Poly (ε-caprolactone) (PCL) is a semi crystalline polyester that is degradable [48], it has excellent biocompatibility and has been used to create scaffolds for tissue engineering [76]. In 2007 Silverstein published a paper where PCL was thermally copolymerised with a vinyl-terminated PCL (PCL-VL) to produce a biodegradable PolyHIPE [77]. The authors reported that the addition of the PCL, due to its relative hydrophilicity, is the cause behind the destabilisation of the initial emulsion. Nevertheless this study mentions that this destabilisation is advantageous for tissue engineering, as the typical PolyHIPE porosity is between 5-30 microns, while for tissue engineering applications a large porosity size can be more suitable [77]. In 2008 a thermally cured biodegradable PolyHIPE was created by Silverstein *et al* by blending up to 50% of a biodegradable component consisting of an oligomeric PCL diol (PCL-OL) with the organic phase monomers Styrene or 2-ethylhexyl acrylate [17]. The PolyHIPE was thermally cured using the surfactant Span 80, and the incorporation of PCL was reported to destabilise the emulsion, this was partially attributed to it decreasing the hydrophobicity of the organic phase. The PCL/EHA PolyHIPE was reported to as undergoing degradation, and this was attributed to the PCL promoting disintegration of the macromolecular structure, this is because the

PCL will undergo a hydrolytically degradation by cleavage of its ester links however the authors mentioned the production of fragments afterwards which were under investigation, as a control the EHA/DVB PolyHIPE did not degrade [17]. In 2009 the same group also published another paper [48] with 50 wt% PCL incorporated into the PolyHIPE. This study reported on the large interconnecting pores created by the destabilisation of the emulsion by the addition of the PCL allowing for an enhanced suitability for tissue engineering applications, with increased cell adhesion and ingrowth, and the complete disintegration of the PolyHIPE.

The aliphatic polyester PCL is insoluble in water, so it can be used as part of a hydrophobic monomer blend for the PolyHIPE synthesis. However PCL will degrade under aqueous conditions by hydrolysis of its backbone. This occurs though cleavage of its ester linkages by water molecules, this produces the by-products carboxylic acid and hydroxyl chain ends, which if these groups are left in contact with the PCL they can act as a catalyst, accelerating the rate of degradation [48].

The surfactant Span 80 has been used for the PCL based HIPE as it is used as a stabilizer in foods, and therefore was raised to 40 wt% to help increase the stability of the PCL based emulsion [48]. One of the main limitations that has been reported on with the addition of PCL into the emulsion is that it increases the viscosity of the emulsion, this will prevent efficient mixing of the oil and water phases and can lead to droplet coalescence as a result. The ester groups can affect the solubility of the water in the oil phase, which would increase the rate of Ostwald ripening. The ester groups on the PCL could increase the solubility of water that can go into the continuous phase, which in turn would lead to Ostwald ripening [48].

A biodegradable PCL based scaffold that has been fabricated using a high resolution two photon polymerization process has been reported within our group [45] nevertheless the slow fabrication speed of 50 μm/s is prohibitive for large mm sized structures, whereas the templating process used to create the PolyHIPE has been structured within the mm range [43]. PCL porous foams can be produced by emulsion freeze-drying, and, for example growth of human bladder stromal cells has been demonstrated on these scaffolds. An increased rate of cell growth was attributed to the storage modulus of the PCL being close to the cells native environment [78]. PCL has been used for bone growth by the incorporation of hydroxyapatite into the porous

scaffold to improve the osteoconductivity, the relatively high hydrophobicity and slow degradation rate of the PCL makes it an appealing material for bone formation [79].

Recently in 2015 a publication by Cameron *et al* produced a PolyHIPE from a blend between a poly ε-caprolactone and a thiol-acrylate, which was reported on as being a fully biodegradable polymer scaffold and supported the growth of fibroblast cells for up to 7 days [80]. The significance of the monomer phase viscosity was highlighted and the solvent 1, 2-dicholoroethane (DCE) was used to reduce it to enable a stable emulsion. The PolyHIPE samples collapsed under drying and therefore were used in their wet state for cell culture.

PCL is a slow degrading polyester and can have a long degradation time of up to 4 years depending on conditions. PCL degrades by hydrolysis, and the rate and mechanism is dependent on factors such as the molecular weight and its degree of crystallinity, as the degradation by hydrolysis relates to the accessibility of water molecules to its ester linkages [81]. High crystalline regions which are more protected against hydrolysis due to their ordered structure, while the amorphous regions with their lack of a clearly defined shape which will be more susceptible to degradation [82]. PCL is a semi crystalline polymer and its degree of crystallinity will decrease with an increase in the molecular weight [83]. The hydrophobic nature of PCL can be modified by exposing it to a 5 M solution of NaOH for 3 days[82] to make the surface of the material more hydrophilic and rough.

PCL can degrade via bulk or surface degradation depending on the external conditions. Artificial degradation studies will generally result in surface degradation, which results from a gradual thinning of the external surface [82]. As the bonds are cleaved it will lead to shorter oligomers of lower molecular weight by-products. The ester bond cleavage produces carboxylic acid, which itself, is a catalyst for further hydrolysis if it does not diffuse away. This can become problematic in the centre of the scaffolds as well as the tissue because the pH of the surrounding material can drop. The rate of degradation can be controlled by blending it with different polymers [73].

A long term degradation study of a tube of poly (ε-caprolactone) (PCL) in a rat over 3 years has been reported [84]. This study shown that the PCL gradually broke into smaller molecular pieces causing its molecular weight Mw to decrease over time. The PCL remained intact for 2 years and had broken up into fragments after 30 months.

By using a radioactive tracer the study confirmed the degradation by products of the PCL did not remain in the tissue and was being excreted by the mouse [84].

6.3.5. Addition of non-polymerising agents

The main factors that affect the stability of the emulsion are the surfactant, oil phase and relative water volume; and to a lesser extent the composition of the oil phase, as long as it is sufficiently hydrophobic enough [9]. Therefore apart of the oil phase can be replaced by a solvent i.e. a porogen. The better this porogen is at holding on to the monomer up until the final stages of polymerisation, delaying the polymer from being leached out of the solvent, then the better that porogen is at increasing the porosity of the polymer and PolyHIPE [9], as well as introducing a secondary level of porosity within the polymer itself [1].

The addition of non-polymerisable additives to the initial HIPE affect the surface area and density of the PolyHIPE material [30], and overall increases the PolyHIPE wall porosity [18], and is used as an extra component to control and tune the morphology of the PolyHIPE [85] [14]. Overall it has a substantial effect on the morphology and porosity of the PolyHIPE [86].

Depending on the choice of solvent, and its ability to adsorb at the barrier film interface, it can affect the porosity by either preventing or encouraging Ostwald ripening [30]. For example if the solvent is partially soluble in both phases it can facilitate the transport of water through this continuous film, which will result in larger pores through Ostwald ripening [30] [14].

Typically the PolyHIPE material has been shown to have a surface area between 3–20 m^2 g^{-1} but can be significantly increased to 457 m^2 g^{-1} by incorporating a non-polymerising agent such as an organic porogen into the continuous monomeric phase [3]. The diluted monomer units in the solvent will have a greater degree of freedom of movement, and the functional groups will be easily accessible by the initiating/polymerising radicals. For tissue engineering applications, the rate of Ostwald ripening for styrene based HIPEs can be encouraged by the addition of 1% (v/v) of tetrahydrofuran to the droplet phase, Large voids were created by this water

miscible organic solvent aiding the transport of water through the continuous phase which resulted in large pores between 50-100 μm range being created [71].

Phase separation will eventually occur between the monomer/solvent during the polymerisation process, and this results in a highly porous structure, however increasing the porosity in this manner compromises the mechanical properties of the PolyHIPE. The effectiveness of the porogen in this sense depends on whether it is a 'good' solvent or a 'bad' one for the monomer. A good solvent will have a similar solubility parameter to the monomer, and therefore the monomer will be very soluble in the solvent [87]. The solubility parameter relates to the molecules strength of attraction between each other within a material. A good solvent will cause the monomer units to be fully solvated even during the later stages of its polymerisation to a polymer, so the phase separation between the solvent/polymer will be delayed. The stages of the growing polymers chain will first result in microgelation of the small particles, then finally the macrogelation of the smaller particles joining together to eventually form an extended network, the solvent's solvating ability is continuously decreasing as the monomer is crosslinked into a polymer unit the solvent can no longer solvate the high molecular weight polymer, then the polymer precipitates out of the solution [88].

A good solvent precipitates out at these later stages producing a very high surface area, although the pore size is within the sub-micron range [85]. A poor swelling solvent will precipitate out earlier and result in a lower surface area in comparison.

When a solvent is present during the polymerisation process, it will not affect the degree of crosslinking, such as the amount of unreacted double bonds. This remains about the same (35% regardless). However, it will affect the gelation point of the monomer to polymer polymerisation, which in turn, will dictate the final porosity of the polymer [88]. Polymers polymerised with the presence of a porogenic solvent, will have an increased permanent porosity in the dry state [87].

6.3.6. Swelling of PolyHIPEs in solvents

The PolyHIPE can be characterised by swelling studies that give an indication to the degree of porosity and interconnectivity of the material [64]. In this process pre-

weighed samples are submerged into various solvents of different hydrophobicity for 24 hours and weighed again afterwards. The degree of swelling is an important factor to consider for tissue engineering based applications, as it can give useful information to how much the cell culture medium can permeate the scaffold.

The solvent choice for washing the PolyHIPE is an important factor to consider, as solvents that can swell the polymer may be useful to adequately remove residual monomer and surfactant that may be trapped within the PolyHIPE walls. The effectiveness of Soxhlet extraction on the PolyHIPE is partially due to the monomer and surfactant used as well as extraction duration, which can result in an increased secondary porosity due to the removal of residual materials from the PolyHIPE wall [36].

The interaction strength between the organic solvent and the polymer will relate to how well the solvent can solvate the polymer, and an appropriate solvent can be used depending on the required effect. This can result in the polymer going from a solid material to a more soft plastic like one and hence will swell the polymer, if the crosslinking agent is increase then the swellability of the polymer network will be reduced as the crosslinking limits the expansion [87].

It has been shown for 4-Vinylbenzyl Chloride Based PolyHIPE [86], that if the sample is dried from different solvents, one that swells the polymer and one that does not, will have an effect on the porosity and morphology of the PolyHIPE. Although the swelling solvent opened up additional porosity within the wet PolyHIPE upon drying the pores collapsed more and this was attributed to the capillary forces generated during this drying process. It was reported that the morphology was preserved more when dried from a non-swelling solvent, as the polymer had more resistance during the during the drying process [86].

The same publication [86] also reported on a more granular morphology at the sub-micrometer range if the monomer within the PolyHIPE was polymerised while it was dissolved in the presences of a solvent than the polymer that was polymerised within any solvent. The increased level of porosity is caused by the phase separation during the monomer to polymer conversion during the polymerising stage.

6.3.7. Single and mixed porogenic solvents

A porogen that resides in the continuous phase may be acting like a co-surfactant by affecting the arrangement of the surfactant at the oil-water interface. This will influence the interfacial tension, and as a result could create a more stable emulsion. The influence of the solvent blend will be in-between the influence of the pure solvents [85].

6.3.8. Tissue engineering applications for PolyHIPE

Important requirements for a biocompatible scaffolds is that it is porous and has sufficient sites for cell attachment, cells such as osteoblasts require surface attachment because they are anchorage dependent [68]. A styrene based PolyHIPE scaffold has been shown to support the growth of osteoblasts over 35 days, which resulted in the formation of a bone-like matrix.

For *in-vitro* cell experimentation the growth of cells on a flat surface is different to the complex 3D architectural environment that the cells experience in their natural in vivo environment, both in the difference in the cell to cell surface area of contact, the flat surface area altering the cells morphology [67], although the use of 2D cell culture has provided fundamental knowledge of cells it does not truly represent the cells natural environment. A 3D scaffold can be used as a bridge to extend the current knowledge to a more 3D environment, as well as there is a need to develop and validate 3D models for cell culture and can be a stepping stone towards a more complex *in-vitro* models.

Increased complexity analysing and imaging cell grown in a 3D environment over a 2D one. A 2D cell can be imaged using a basic microscope, while in a 3D environment more complex stacking imaging technique is required to determine the cell morphology. Therefore more complex imaging tools and techniques are also required.

Polystyrene PolyHIPEs based on thermally polymerised styrene (STY), EHA and the cross linker divinylbenzene (DVB) with span 80 as the surfactant have been used for the 3D *in-vitro* cell culture of the MG63 osteoblast cell line [50]. Three methods were used to increase porosity and its controllability: the aqueous temperature as increased to controllably destabilise the emulsion for increased coalescence, a high 90% aqueous volume was used reduced variation between samples through a controlled addition of

the aqueous phase. A combination of these factors resulted in a highly porous 3D cell culture construct [50].

6.3.9. Porous Particles

From a scaffold perspective porous spheroidal beads can be used to create a two tiered layer of porosity for tissue engineering applications. In a similar approach as reported previously [43], the porosity of the PolyHIPE can be independently controlled to the selective laser polymerisation, this allows user control over both the micro and macro porosity of the scaffold. An alternative method to produce a scaffold with a microporosity is to use PolyHIPE beads, where the microporosity of the beads can be controlled independently to the macro porosity of the spacing between the beads can be controlled separately. Porous PolyHIPE beads produced via photocuring have been reported on in the literature previously [89]

Porous particles have been used as an injectable cell carrier as they can be injected to the target location with a minimal invasive procedure and do not have the same vascularisation issues as a larger scaffold [90]. The beads were seeded with primary culture aortic smooth muscle rat cells, and their small structure allowed media diffusion as well as cell migration into their core.

The porosity of the beads can be tailored for cell ingrowth, and the larger macro porosity of the space between the particles can be controlled by altering the particle size distribution, and hence the packing arrangement which could be beneficial for less material resistance for angiogenesis. Furthermore the PolyHIPE beads can be injected into the target location in vivo and will fill the void, while a direct laser write stereolithography approach will require more processing steps to prepare the scaffold, as well as a larger surgical procedure in comparison to insert into the body. Porous alginate beads have been shown to allow cell invasion of macrophages and fibroblasts after two weeks of implantation [91]. The pores were large enough for vascularization within the polymer.

PCL based porous particles have been fabricated using a melt moulding particle leaching method to create 400-550 μm sized particles [92]. As well as a thermally induced phase separation technique and porogen leaching to create particles in the size

range of 150-250 μm [93], their aim was to create a porous degradable microparticle for both cell and drug delivery for tissue engineering applications.

From a scaffold perspective; the use of a bulk porous scaffold can be limited in the amount of oxygen and nutrients that can be transported into the bulk of the material to support cellular growth, as well as sufficient waste removal from this location. With porous beads the cell medium can freely flow around the large gaps between adjacent particles, and porous particles have been shown to have an increased cell density and growth rate than non-porous ones in comparative conditions [92].

6.4 Materials and Methods

6.4.1. Thiolene PolyHIPE: Materials

The thiolene (trithiol) (trimethylolpropane tris (3-mercaptopropionate), crosslinking agent trimethylolpropane triacrylate (TMPTA), photoinitiator (a 50:50 blend of diphenyl (2,4,6-trimethylbenzoyl) phosphine oxide/2-hydroxy-2-methylpropiophenone) were bought from Sigma Aldrich. Chloroform was purchased from Fisher Scientific. Hypermer B246 was used as the surfactant, it is a triblock copolymer of polyhydroxystearic acid and was given free of charge from Croda. All items described were used as supplied.

6.4.2. Thiolene PolyHIPE preparation

Thiolene (trithiol) and the crosslinking agent TMPTA were mixed with the surfactant Hypermer B246 and heated to 40°C to dissolve the surfactant. The mixture was cooled and the chloroform, toluene and photoinitiator were added. The monomer/solvent (oil phase) was mixed using an overhead stirrer (Pro40, SciQuip) at 350 rpm in a 50 ml glass beaker (Fisher Scientific). The water was added dropwise and then the emulsion was left to mix for a further 5 minutes. The HIPE was transferred to either a small glass petri dish, or a square silicone mould on top of a glass sheet, and then the container was exposed to UV light from either an Omnicure spot curer or a UV conveyor belt for polymerisation. In the conveyor belt the PolyHIPE was turned upside-down to ensure a full polymerisation of the sample. In both cases the polymerising container was temporarily sealed to limit the evaporation of the solvents during the polymerisation process. The resulting was either washed in acetone for 24 hours or washed in a Soxhlet extractor for 24 hours with ethanol as the solvent.

6.4.3. PCL methacrylation: Materials

Photocurable PCL was created by methacrylating a commercially available PCL thiol monomer (M_n 900 g/mol) from Sigma Aldrich. Triethylamine (TEA, Sigma-Aldrich, >99%) and methacrylic anhydride (MAA, Sigma-Aldrich, 94%) with

dichloromethane (DCM, Sigma-Aldrich, anhydrous, >99.8%) as the solvent. Methanol (Fisher Scientific) was used for the polymer precipitation.

6.4.4. PCL methacrylation

The PCL (M_n 900 g/mol, 1 molar equivalent, Sigma Aldrich) was dissolved in an excess of DCM. Trimethylamine (6 molar equivalent) was dissolved in 50ml DCM was added to the solution. The mixture was cooled by submerging in a salted ice bath for 30 minutes. Methacrylic anhydride (6 molar equivalent) dissolved in 50ml DCM was added dropwise using an addition funnel. After the methacrylic anhydride was added the solution was allowed to warm up slowly to room temperature and was left to react for 24 hours while covered in foil.

6.4.5. PCL purification

After methacrylation the PCL and remaining reactants and solvent were poured into a rotary flask and the remaining solvent and TEA was removed by evaporation. The round bottom flask was wrapped in foil to prevent premature polymerisation as the solvent evaporated. The remaining yellow liquid was then purified by dissolving in an excess of methanol and placed in -20°C freezer inside a glass container wrapped in foil, a normal freezer can be used but the methanol solution will take longer to cool. The PCL and contaminants remained dissolved in the methanol, however as the temperature is decreased the PCL's solubility in methanol decreases and it starts to precipitate out, whereas the contaminants remain in the methanol. After 2 hours the glass container was removed from the freezer. The PCL is a solid at the base of the glass and the yellow solution of methanol containing the contaminants is poured off. An excess of methanol was added to the PCL and allowed to warm up and re-dissolve it, and then the cycle is repeated until the methanol was clear. Generally this took about 3-4 cycles. Final PCL is separated from the methanol by rotary evaporation. The remaining PCL has a viscous honey like consistency. The PCL was stored in the freezer in a glass container wrapped in foil to prevent any light polymerising the polymer.

To test the photocurability of the PCL a drop was mixed with the photoinitiator and placed on top of a glass slide under UV light. If the droplet solidifies under then the methacrylation process has worked.

6.4.6. PCL/Thiol PolyHIPE preparation

The PCL/Thiol HIPE was prepared in a similar manner to the thiolene PolyHIPE preparation stated earlier. Smaller monomer volumes were used due to the limited availability of PCL and therefore the monomers were prepared in smaller glass vials using magnetic stirrers to emulsify the liquids. The thiolene (trithiol), crosslinking agent TMPTA, PCL and surfactant (Hypermer B246) are added to the glass vial and heated to 40°C to dissolve the surfactant. The mixture was cooled and the chloroform, toluene and photoinitiator were added. The monomer/solvent (oil phase) was mixed using a magnetic stirrer at 350 rpm, and the water was added dropwise and then the emulsion was left to mix for a further 5 minutes. The PCL/thiolene HIPE was polymerised in the same manner as the thiolene HIPE.

6.4.7. PCL PolyHIPE preparation

The same protocol was used for the preparation of the PCL HIPE as the PCL/Thiolene one. However a reduced temperature was used by lowering the water bath temperature to 35°C

6.4.8. Preparation of PCL-Thiolene for cell culture

PCL-Thiol PolyHIPE samples were washed in a Soxhlet extractor for 24 hours with ethanol. For cell culture the samples were transferred to a 70% ethanol and distilled water solution for 30 minutes. The samples were transferred to sterile PBS and washed three times to remove traces of ethanol. To remove all trapped air from the discs the samples were kept in sterile PBS container, a lid affixed with a 0.2 µm pore syringe filter was used to seal the container which was then put into a vacuum oven and cycled from being under vacuum to normal atmospheric pressure to draw the trapped air out and pop the bubbles that escaped. This was repeated 3 times until all the sample

remained submerged in normal atmospheric pressure. The samples were cut in half using a scalpel blade. The use of a blade to section the PolyHIPE has been reported on in the literature [21].

6.4.9. PCL PolyHIPE beads: microfluidic rig

Small tips with different internal diameters (0.15 – 0.5 mm, Nordson EFD) were used at the end of a 20 ml syringe to inject the PolyHIPE into a 6 mm silicone tube (Advanced Fluid Solutions). Deionized water was pumped continuously through the tube by a peristaltic pump (Masterflex L/S tubing pump, Cole-Palmer) with both ends of the tube at the base of a plastic container housed within a UV light box, and was irradiated using UV light from a mercury lamp (Omnicure S1000), guided through a light guide to just above the water level. A syringe pump (GeniePlus, Kent Scientific) was used to have a controlled flow of HIPE into the water. The polymerised PolyHIPE beads were collected by passing the water and particles though a 40 μm cell sieve (BD Falcon).

6.4.10. Human Dermal fibroblast cell culture

Human dermal fibroblast cells were isolated from split thickness skin grafts were obtained from the Hallamshire hospital, the patients gave consent for their removed skin to be used for research. The tissue collected was used under the requirements stipulated by the Research Tissue Bank Licence 12179 and fibroblast cells were isolated by the lab technician staff. The cells were grown in a T-flask in an incubator at 37°C with 5% CO_2 gas and cultured in Dulbecco's modified Eagles media (DMEM).

6.4.11. Cell culture medium

A 500 ml flask of Dulbecco's modified Eagle's medium was used, 61.25 ml of medium was remove and the following components added. 50 ml (10%) of Foetal Calf Serum (FCS), 0.01% L-Glutamine, 0.01% penicillin-streptomycin and 0.0025% amphotericin B. The medium was stored in a fridge at 4°C when not being used, and it was heated up in a water bath 20 minutes prior to cell culture.

6.4.12. Cell passaging

Human dermal fibroblast cells were culture in a T75 flask and passaged when they were 80% confluent. The cell culture medium was removed, and the cells were washed in phosphate buffered saline (PBS) to remove any excess culture medium. 5 ml of trypsin was added to the T75 flask and then placed into the incubator for 5 minutes to detach the cells. Afterwards the cells were viewed under the microscope to confirm detachment. If the cells remained attached the flask was gently tapped to detach the cells, if this did not detach the cells the flask was placed back into the incubator for a further 3 minutes. Following this 10 ml of the culture medium was added to the cells as the FCS inhibits any further action from the trypsin. The detached cell suspension was transferred to a centrifuge and centrifuged for 5 minutes at 1000 rpm to create a cell pellet. The excess supernatant was removed and the cell pellet was re-suspended in 1 ml of culture media. The cells were counted in a known volume of medium with a cell haemocytometer. A known volume of medium containing 250,000 cells was added to a sterile T75 flask with 10 ml of culture medium.

6.4.13. Confocal Imaging

The fibroblast cells were imaged on the PCL/thiolene PolyHIPE using a Zeiss LSM Meta upright confocal microscope. To do this, the cells were stained with fluorescent markers. First the cells were fixed on the scaffold by submerging them in a 3.7% solution of paraformaldehyde for 20 minutes. The samples were washed and stored in PBS afterwards at 4°C in the fridge for no longer than 24 hours at most. The samples were submerged in a 1% BSA, 0.1% Triton-X100 solution for 20 minutes to permeabilize them. Afterwards the cells were washed with PBS 3 times. To image the fibroblast actin filaments the cells were stained with a TRITC-labelled phalloidin from a 0.1% stock solution containing 0.5 mg/ml in dimethyl sulfoxide (DMSO), and left for 30 minutes in a foil container as the fluorophore is light sensitive. Following this the samples were washed three times with PBS before the fibroblast nucleus was imaged by staining with 4',6-diamidino-2-phenylindole (DAPI). The samples were submerged in a 1ml of a solution containing 10 μg/ml, and left in a foil container for 20 minutes. The sample was washed and stored in PBS in a foil wrapped container

prior to confocal imaging as the fluorescent markers are light sensitive. The light source was from a Chameleon Ti:sapphire multiphoton laser (Coherent, CA, USA). The DAPI was imaged at a wavelength range between λ_{ex} = 365 nm and λ_{em} = 461 nm (blue). TRITC was imaged using λ_{ex} = 545 nm and λ_{em} = 573 nm.

6.4.14. Pico green assay:

For the PicoGreen DNA quantification assay, the scaffolds are washed, then treated with TE buffer (10 mM Tris-HCl, 1 mM EDTA, pH 7.5) which is supplied by the PicoGreen kit. The samples were subjected to three freeze-thaw cycles to breakdown of the cells as the freeze/thaw cycles causes cell lysis, a volume of 100 µl of supernatant was taken from the samples and added into 100 µl of PicoGreen reagent (diluted 1:200 in TE buffer). Fluorescent readings were taken at the excitation and emission wavelengths of 485 nm and 520 nm using a spectrometer.

6.4.15. Gold coating vs Carbon coating of PCL PolyHIPE

Gold coating of PolyHIPE samples prior to SEM imaging is used to make them more electrically conductive at the surface and to protect the samples from becoming charged during the imaging process as the process uses an electron beam to illuminate the sample. The gold coating creates a conformal layer of 20 nm thick [94]. It has been reported that for this type of high resolution carbon coating can be used to preserve the resolution at this level, this is especially evident in preserving the details with SEM images of human blood fibrin [94]. Carbon coatings were used as an alternative to gold coating for the PCL PolyHIPE samples. This gave a similar image quality with increased contrast.

6.4.16. Live Dead cell staining

Live/Dead staining was used to determine if the cells viewed under the microscope are alive or dead. The staining involves two nucleic acid stains. The green fluorescent Syto® 9 stains cells that are alive and dead while the red fluorescent propidium iodide stain only goes into cells that have a damaged membrane. When the stains are used

together the red stain masks the green one. Both dyes were diluted in DMEM in the ratio 1:3000 in sterile conditions. This was added to the cell culture medium in a 1:1 ratio and incubated at 37°C at 5% CO_2 for 20 minutes. The culture medium was removed and fresh medium added before imaging by confocal microscopy. Green stain λ_{ex}= 495nm and λ_{em}= 515nm. Red stain λ_{ex}= 528nm and λ_{em}= 617nm

6.4.17. Tri layer PCL/thiolene PolyHIPE and electrospun PHBV mat

To create a PolyHIPE version of the electrospun trilayer scaffold two silicone elastomer 4 mm thick sheets were cut into round disks with a smaller hole in the middle. A sheet of PHBV sheet was cut into a larger circle and sandwiched between the inner and outer silicone circles. The PCL/Thiol HIPE was poured on the top, spread evenly and then cured Under the UV lamp. The sample was flipped over and the process repeated to coat both sides of the PHBV with the PolyHIPE.

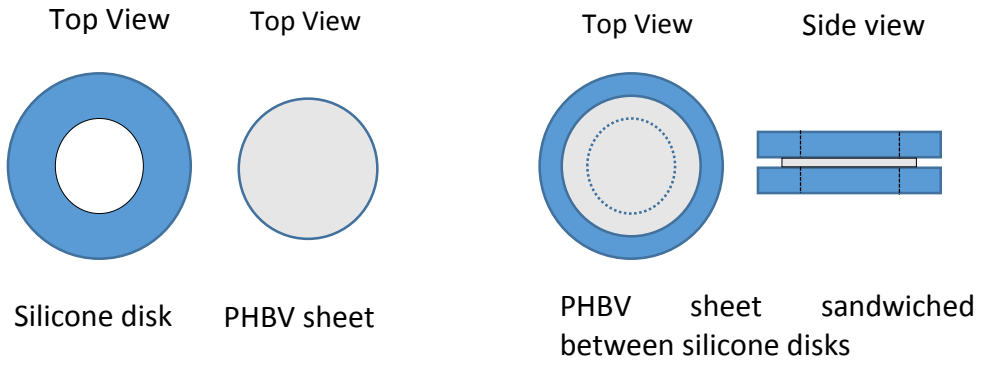

Figure 74: PHBV PCL-thiol PolyHIPE sample preparation. The silicone is represented as blue, and the PHBV sheet as grey. The PDMS disc was larger than the electrospun one so that it temporarily adheres together to create a 'seal' between them, this enabled the PDMS to effectively house the HIPE within the well before it was polymerised.

The PCL-thiol HIPE was mixed at 60°C and after the water addition it was further mixed for 5 minutes to create a viscous paste before pipetting it onto the PHBV. Pre-wetting the PHBV with either ethanol or water prevented PolyHIPE attachment after polymerisation, causing the PolyHIPE to peel away from the PHBV layer. To prevent this the PHBV was not pre-treated or pre-wetted before the HIPE was pipetted onto the sample.

6.4.18. CellTracker™ fluorescent marker

Cell tracker Red is a fluorescent dye that can freely pass through the cell membrane enabling the cells to be stained, this allows for their movement to be visually monitored and tracked. A 250 µM solution was made by diluting the original lyophilized product in 20µL DMSO to create a 1mM (1000X) solution. This was then diluted by a further 1:750 to create the working concentration.

To stain the fibroblast cells on the scaffold the medium was removed and the samples washed in PBS to remove excess medium. The CellTracker™ Red CMTPX dye was added to the cells and incubated for 30 minutes in the culture hood. The cells were imaged using the Zeiss LSM Meta upright confocal microscope at λ_{ex}= 577nm and λ_{em}= 602nm

6.5 Results and Discussion

Blends of PCL and other monomers such as EHA have been reported on in the literature [17]. Recently the Cameron group reported on a degradable emulsion based from thiolene photopolymerisation [21]. This previously reported degradable PolyHIPE was used to blend it with PCL towards creating a pure PCL based PolyHIPE. During the time of my project the Cameron group did, unfortunately, report a follow on paper where also a blend of photocurable PCL with the thiolene monomer was used [80].

6.5.1. Thiolene PolyHIPE initial work

Blends of PCL and other monomers such as EHA have been reported in the literature [17], however the use of non-degradable materials for the preparation of a biodegradable PolyHIPE is undesirable. The PCL used in this chapter is a higher molecular weight triol PCL (Mn=900 g/mol) than ones used previously in the literature. Silverstein *et al* for example in 2009 used a monomer blend of PCL diol (Mn=530 g/mol) with styrene, EHA and DVB [48]. Recently a thiolene monomer (trithiol) has been structured into a PolyHIPE and its suitability for a biodegradable 3D cell support scaffold has been demonstrated [21], and its mechanical properties

can be altered by controlling the degree of crosslinking. The initial publication used a 1:1 ratio of monomer to solvent. The initial experimentations were designed to both reproduce this work, and use it as the groundwork to produce both a PCL/Thiolene PolyHIPE as well as a PCL PolyHIPE. The publication used the same surfactant, initiator and chloroform as the diluting solvent that is used in this chapter [21].

During this end stages of this work a publication was published by Cameron *et al*. on the blend of the thiolene monomer and PCL [80]. This group used the same monomers and commercially available PCL and surfactant that I have been using. However the techniques I developed for the emulsion are different. The study used the solvent 1,2-dicholoroethane (DCE) to control the viscosity of the continuous phase, while chloroform is used in this chapter. The authors also reported on significant PolyHIPE collapse during the drying stages of the PolyHIPE while the samples presented in this chapter had more structural strength upon drying. In the publication the authors prevented the collapse of the PolyHIPE during drying by leaving the samples in a wet state, and by freeze drying the PolyHIPE to prevent its collapse. The auto fluorescent nature of the PolyHIPE was exploited as another imaging method, and a pore size of up to 82 μm was reported upon by this fluorescent microscope imaging technique. The work presented in this chapter will be related to theirs as the chapter progresses.

6.5.2. Thiolene PolyHIPE: effect of solvent volume

The optimum monomer to solvent ratio for the thiolene PolyHIPE was determined to be a 1:1 ratio. The effect of the solvent on the PolyHIPE is shown in **Figure 75**. The 1:1 ratio produced a viscous (mayonnaise-like) emulsion, visually it had a white appearance that is characteristic of a stable emulsion. Increasing the solvent to a 1:2 ratio produced an emulsion, however it took significantly longer to polymerise and significantly cracked upon drying. A W/O emulsion would not form in the absence of a solvent, spherical particles of the Thiolene were instantly produced upon the addition of water.

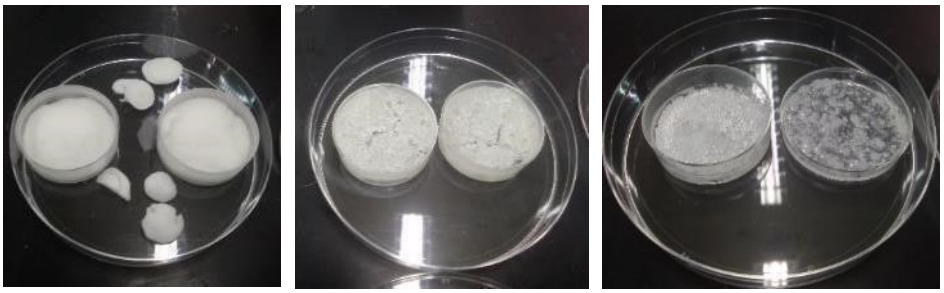

Figure 75: Ratio of monomer to chloroform for the thiolene PolyHIPE preparation. The 1:1 ratio produced the most stable emulsion. 1:2 ratio produced an emulsion however it cracked significantly upon drying. When using no solvent the thiolene instantly separated into spherical droplets suspended in the water phase. A 1:4 ratio between the oil and water was used i.e. 80%

6.5.3. PCL/Thiolene emulsion templating: initial work

When the emulsion started to separate out initially more solvent was added to increase the stability of the emulsion. However this meant that the emulsion had a low volume of water in comparison to the oil phase. Initial work only involved the addition of the single solvent chloroform as the solvent and the resulting emulsion formulation that was created from the experimentation is shown in **Table 3**.

Table 3: PCL thiolene emulsion formulation

Sample	reference	PCL (g)	Thiolene (g)	X-Linker (g)	$CHCl_3$ (g)	Solvent to polymer ratio	Surfactant Hypermer B246 (g)	Photoinitiator (g)	H_2O (ml)
1	M17_S1&2	0.9	1	0.6	4.5	2.5: 1	0.8	0.13	4

A stock solution of PCL thiol and the cross-linker was prepared with the initiator. Different ratios of the Chloroform were used, with different amounts of the surfactant to determine the effect of the solvent and surfactant amount on the emulsion.

Figure 76 shows the initial PCL/Thiolene material from the corresponding monomer ratios can be seen in **Table 3**. The material was very flexible, and from initial SEM images the material appears to have a porous morphology. A small amount of interconnectivity can be seen however for the most part the material is closed pored. This may be due to the low amount of water initially used in the emulsion preparation as well as the shrinkage of the material during the drying stages. High amounts of

solvent were originally required as the PCL was very viscous and this prevented the emulsion from forming.

The gold coating of the material reduced the level of light scattering when viewed under a dissection microscope. This meant that light microscope images of the porosity could be taken and used to visualise the larger macrospores as an inexpensive alternative to SEM imaging when high resolution images are not required.

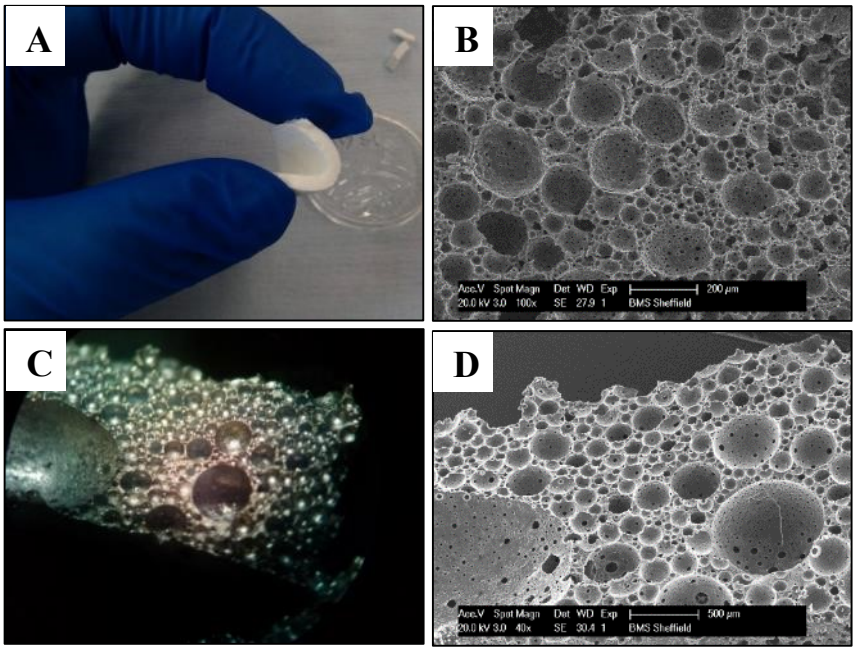

Figure 76: PCL/Thiolene PolyHIPE samples. **A**, Picture showing the flexibility of the material. **B**, SEM image of the PolyHIPEs morphology. **C**, light microscope image after gold coating, **D**, SEM image of **C**. A&B are sample M17_S1, C&D are sample M17__S3

The initial PCL/Thiolene material underwent significant shrinkage after the washing stage. This is shown in **Figure 77** and is caused by the high surfactant concentration and solvent that was originally used to stabilise the emulsion. Interestingly also is that the original wet sample was very fragile, and it became very flexible after it had shrunk. One it had shrank the material was very flexible and stretchy.

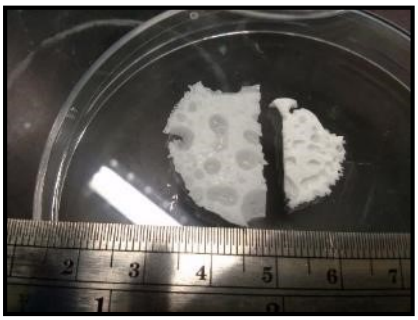

Figure 77: wet and dry PCL/Thiolene PolyHIPE showing the level of shrinkage caused during the drying stages m17 S1 with the addition of 0.8 g surfactant.

Due to the high instability of the initial emulsion, it would separate out very quickly during the polymerisation process. The original UV conveyor belt had a high amount of air flow, this disrupted the top surface and caused further destabilisation. However after a few passes the PCL/Thiolene would polymerise and trap the emulsion. A partially destabilised material is shown in Figure 78. Very large voids are seen on the top surface, these are created by large droplets of water as the emulsion destabilised by the air flow. A high degree of porosity was observed when viewing the sample under the microscope. However this destabilisation is detrimental to the emulsion and indicates that the formulation is unstable.

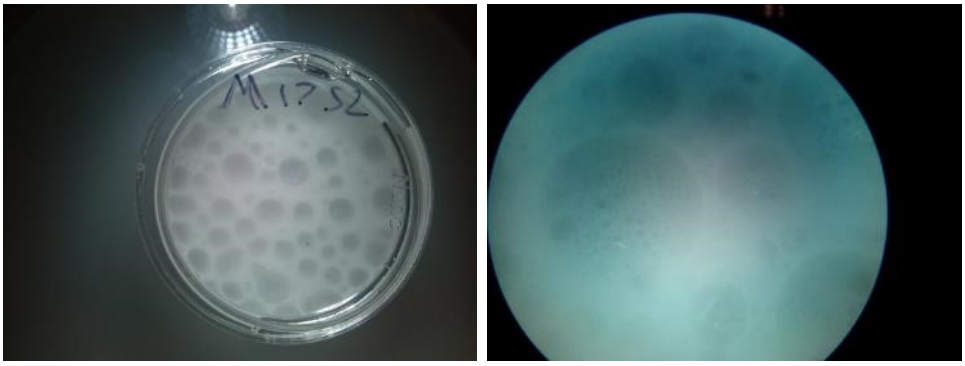

Figure 78: Light microscope image of the PCL/Thiol PolyHIPE with separation on the top surface. The large voids were caused by the emulsion separating as it was being photo-polymerised. This had the same formulation as M17_S1

6.5.4. PCL/Thiolene emulsion templating: the steps to create a stable emulsion

The initial formulations presented here are tentatively stable. Eventually the determining factors to have the most effect on the emulsion stability were (i) having an efficient mixing of the two phases, (ii) a solvent blend incorporating a low amount of toluene, as well as (iii) a slow addition of water. During this process subtle changes in the emulsion appearance were observed over the course of the mixing, to pinpoint when the emulsion is about to invert. Variations occurred between different samples, perhaps due to human error, nevertheless numerous repeats, and blend formulations created the groundwork for a more stable emulsion.

A solvent blend was used instead of using a pure solvent, the cross-linker, surfactant amount and the water volume ratio were all altered. The ratio of PCL to the thiolene and cross-linker were kept at a constant 0.9:1:0.3 (all in grams). The solvent was first kept at a 1:1 ratio with the respective ratio between the chloroform and toluene varied to determine their individual effect on the emulsion stability, and each variable had different surfactant concentrations and water volume ratios to determine the point of emulsion inversion.

Increasing the toluene concentration caused the emulsion to separate out into a particle suspension, while chloroform appeared to stabilise the emulsion, and could be added to the particle suspension to create a W/O emulsion again (sometimes this required an increase in temperature at the same time). The significance of the low ratio between the solvent blend was eventually determined after testing a range of possible variations of solvent/surfactant and water. The formulations that created a 'stable' emulsion is shown in **Table 4**. Here a stock solution was made and split into 4 glass vials and each one had a different variation to fine tune the stability of the emulsion.

Table 4: Refined monomer to solvent variations for the PCL/Thiolene emulsion

reference	PCL (g)	Thiolene (g)	X-Linker (g)	$CHCl_3$ (g)	Toluene (g)	Solvent to polymer ratio	Surfactant Hypermer B246 (g)	Photo initiator (g)	Water (ml)	Temp (^oC)
STOCK	0.9	1	0.6	2		2.5: 1	0.8	0.15	-	-
M19_S1	Used 1g of stock			+0.5	+0.15	-	-		5	60
M19_S2	Used 1g of stock			-	-	-	-		4	60
M19_S4	Used 1g of stock			+1	+0.15	-	-		5	RT

When the oil to water ratio is increased from 1:4 to 1:5 the emulsion becomes very unstable, however the addition of 0.15 g of toluene and a further 0.5 g chloroform stabilised the emulsion with higher water volumes, but at a cost to the mechanical integrity of the resulting material. Later on the temperature was decreased and toluene added at the initial stages of the emulsion preparation. Initially the emulsion separated into monomer droplets at room temperature, however increasing the chloroform concentration enabled a stable emulsion to form at high rpm. The sample M19_S2 was chosen as the formulation to take forward for cell culture.

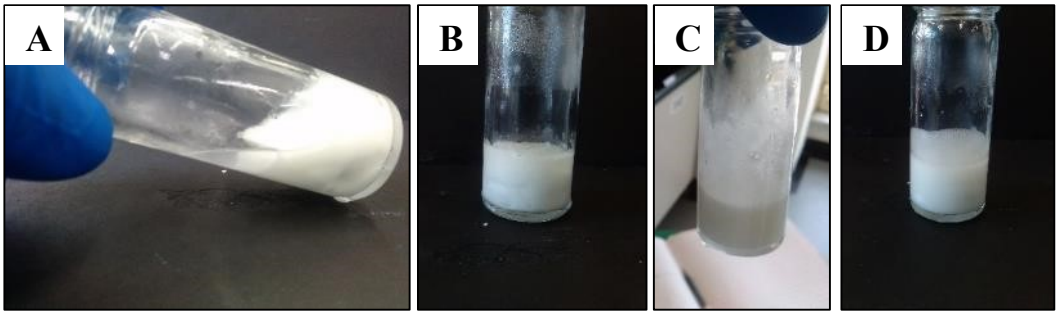

Figure 79: 1: An example of the PCL/thiolene emulsion (with chloroform as the diluting solvent). **A**, the addition of 4ml water with some separation. **B**, the emulsion starting to separate out after agitation was stopped. A layer of water can be seen around the inside of the glass. **C**, the same emulsion with the addition of 0.35g toluene and more mixing. **D**, the emulsion after the addition of a total of 8 ml of water.

Figure 79 shows the effect of adding toluene to the unstable PCL/thiolene emulsion (with chloroform already added to improve stability). The initial emulsion has a thin layer of water on the top surface caused by the phase separation, and it is gradually destabilising. Image **C** is of the same emulsion but the addition of toluene to stabilise it, this also increased the amount of water than can be added to the emulsion.

6.5.5. Imaging methods the PCL/Thiolene PolyHIPE

Three different imaging techniques were used to view the PCL/Thiolene PolyHIPE. The samples auto fluoresced under UV light enabling fluorescent microscope images to be taken without any post-processing. Confocal microscope images were taken to give both a visual indication of the porosity of the PolyHIPE samples. Furthermore the Z-stack ability of a confocal microscope can be used to create a 3D view of the top

morphology which can be rotated to give both a more representative view of the depth of the pores on the imaged surface, or converted into a stereo image.

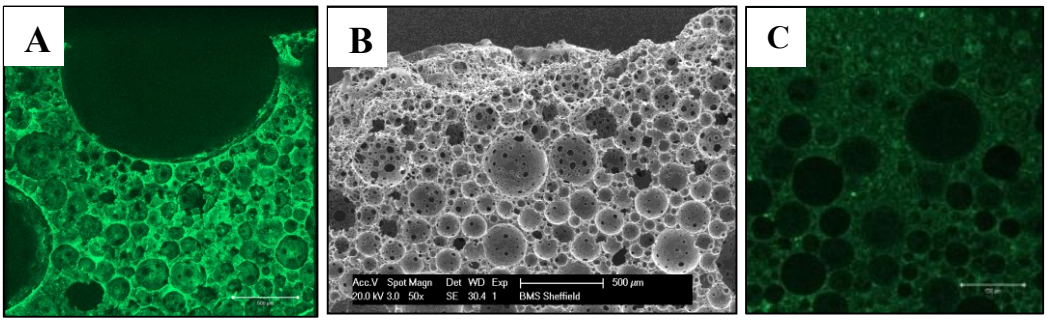

Figure 80: Different images of the PCL/Thiolene PolyHIPE with corresponding formulation shown in M19_S2 in **Table 4**. **A**, Z-stack confocal image of the side surface of the PolyHIPE, multiple scans were taken and compiled to give a 3D view of the surface. **B**, SEM image of a cross-section of the PolyHIPE. **C,** confocal image of a thin section of the PolyHIPE to give an indication of the pore sizes.

Light microscope images give a good overview of the macro pore distribution within the emulsion templated samples. Large voids can be seen spread through the PCL/Thiolene material when the light is shone from below in **Figure 81**. The gold coating and SEM images were taken of the same section to give a comparison between the levels of detail that they both pick up. Comparing images B & C with the SEM images E & F shows. The light microscope is good to give an overall impression on the larger pore distribution and the light scatter within the material gives an indication of the interconnectivity within the material that is only shown in the SEM images as black regions.

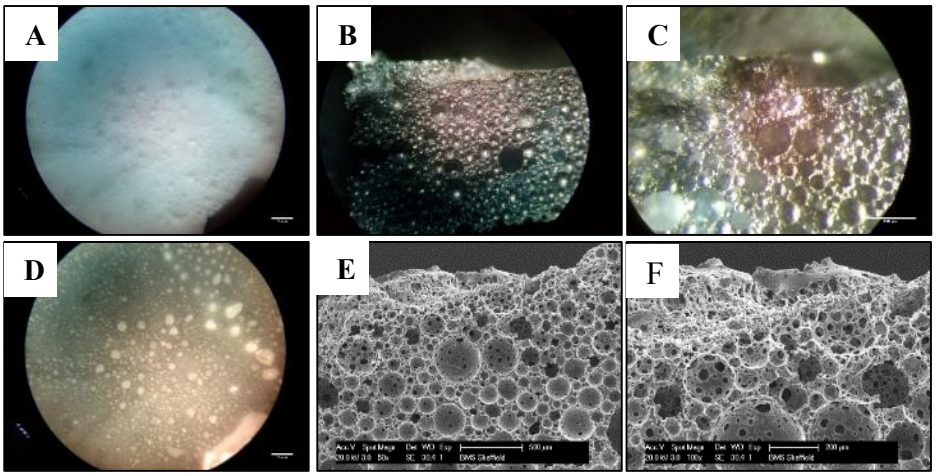

Figure 81: PCL/Thiol PolyHIPE blend (M19_S4) imaged with light microscope and Scanning electron microscope. **A**, Light microscope image top surface. **B & C,** gold coated light microscope image. **D,** light microscope image under light. **E&F** SEM images of the PolyHIPE showing the same regions as the images **B & C.**

6.5.6. Soxhlet wash

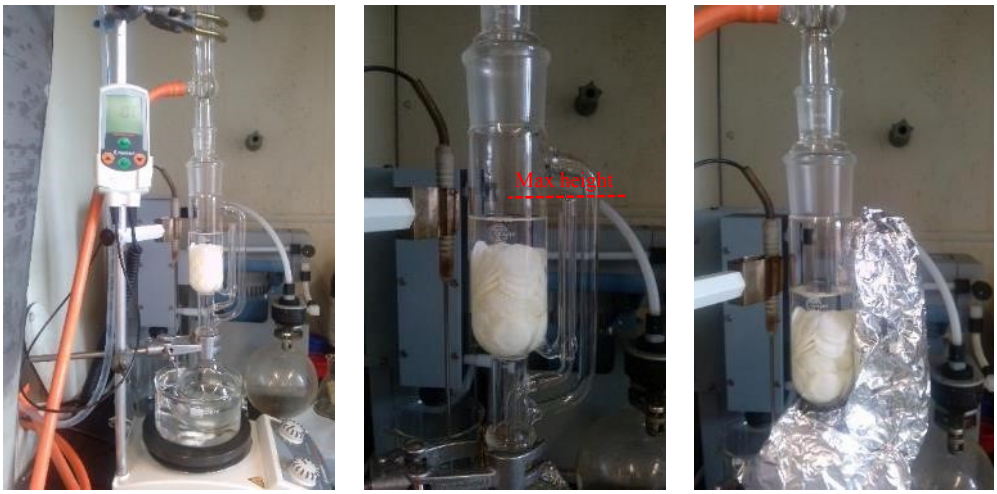

Figure 82: The Soxhlet extractor with the PCL/Thiolene PolyHIPE being washed in ethanol. The soxhlet had to be wrapped in foil to prevent the ethanol condensing in the glass tubes before it reached the main chamber. When a finite amount of ethanol fills the main chamber itself empties into the round bottom flask attached below to repeat the process.

Chloroform and the same surfactant Hypermer B246 have been used as a diluent for the degradable thiolene PolyHIPE [21]. The use of a solvent as a diluent and residue surfactant on the PolyHIPE could have an adverse effect on the cell toxicity. Therefore the PolyHIPE samples were washed in either acetone or in a soxhlet extractor with

ethanol as the solvent **Figure 82**. The toxic components and residue surfactant do not bind covalently to the crosslinking polymer, and therefore should be removed during a sufficient post processing washing stage. The soxhlet apparatus was used with ethanol as the solvent for 24h to remove any residue surfactant or solvent that may reside within the PolyHIPE [19]. The original authors washed the PCL/thiolene PolyHIPE in acetone and dried them under vacuum prior to cell culture, and reported on no cell toxicity, which indicates that a solvent wash is sufficient to remove any toxic residue material.

The Soxhlet extractor heats the ethanol to above its boiling point (78.37°C). The evaporated ethanol travels up the outer glass tubes into the main chamber were the samples are housed. Above this chamber a condenser with cold water flowing through it causes the water to condense and fill the main chamber. Once the ethanol has reached a certain height, it self-empties itself back in to the main round conical flask that is submerged in a hot oil bath to repeat the cycle. The samples are constantly being rinsed in pure ethanol, while all the contaminants removed remain in the round flask. The PCL/Thiol samples were vacuum dried after 24 hours in the Soxhlet extractor until dry.

After 24 hours the ethanol in the round flask had a cloudy appearance which indicated that contaminants had been removed from the PCL/Thiol PolyHIPE samples. This prolonged Soxhlet wash may have a detrimental effect on the mechanical properties of the samples [36]. However this will be dependent on the materials used for the PolyHIPE preparation, furthermore a more prolonged wash will be required to remove any residue surfactant that may be present due to the high amount of surfactant used in the PCL/PolyHIPE preparation.

6.5.7. MTT reduction on PCL/Thiolene PolyHIPE

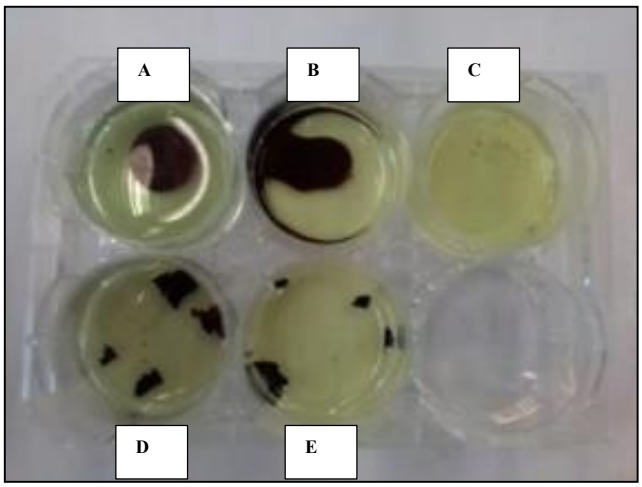

Figure 83: Different components of the PCL thiolene PolyHIPE in a MTT assay. **A**: Thiolene and the crosslinker TMPTA was photocured directly into the 6-well plate**. B**: PCL-Thiol blend. **C**: PCL only. **D**; PCL thiol blend PolyHIPE. **E:** PCL-thiol PolyHIPE after 24 hours wash cycle.

It was observed that the MTT assay on the control PCL/thiolene PolyHIPE sample gave a false reading. The Thiolene polymer was found to reduce the MTT assay to the insoluble purple formazan dye. The polymerised PCL and crosslinker with surfactant did not reduce the MTT assay. The purple formazan can be seen in **Figure 83**. Long term washing of the PolyHIPE was attempted by soaking the samples in either methanol, acetone or PBS for up to a month. However this did not have any effect on the thiolene reducing the MTT assay. This effect was not noticed in the literature on the initial thiolene PolyHIPE paper. A MTT assay was used in this publication to determine the cell viability [21]. The study showed an increase in the production of the purple formazan dye over the course of 11 days in relation to the cell culture. A follow-up publication of the same group on the thiol-acrylate (PCL) based PolyHIPEs [80] also used an MTT assay to show the cell viability on the material. It is unsure from these publications whether the thiolene polymer gave a false reading.

6.5.8. Cell viability on the PCL/Thiolene PolyHIPE

To qualitatively determine fibroblast cell viability on the PCL/thiolene material flat sheets of the monomer were polymerised on top of glass slides and cultured for 3 days before imaging under the confocal microscope. The images shown in **Figure 84** produced indicated that the cells had a high confluence over the top surface which

gave an initial indication that the cells were growing on the material. To get a quantitatively value a PicoGreen assay was then performed on the PCL/thiolene polymer.

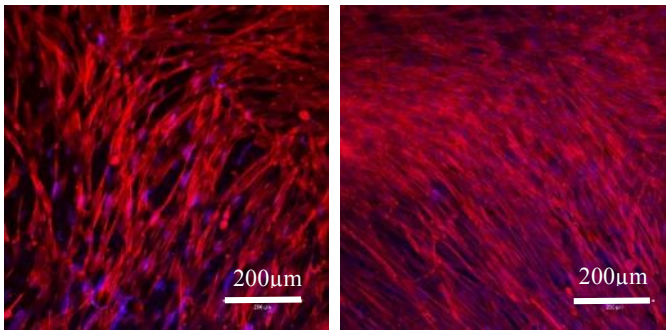

Figure 84: Confocal image of fibroblast cells growing on PCL-Thiol. Nucleus is shown as Blue with the stain DAPI (only faint blue dots were seen). The red shows the cells f-actin from the phalloidin-tritc stain. Both samples were from 1 week in culture.

PicoGreen is a DNA quantification assay and was used to determine the amount of cell growth on the surface by measuring the amount of DNA that was produced. A PicoGreen assay was performed on the human dermal fibroblast cells grown over 5 days on flat sheets of the PCL-Thiol PolyHIPE **Figure 85**. An increase in the amount of DNA produced indicated that the cells were proliferating over the surface of the PCL/thiolene.

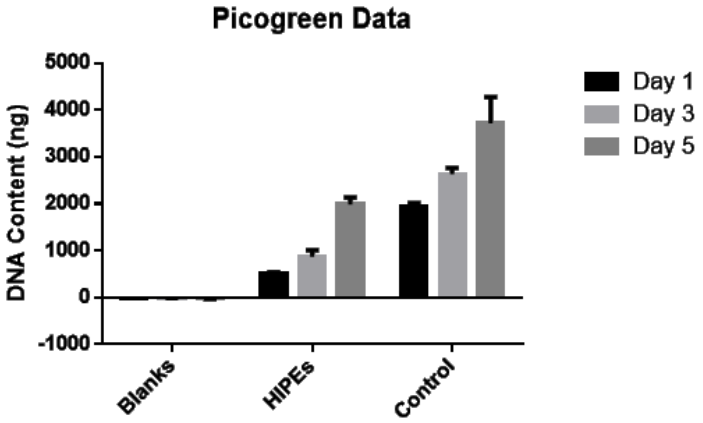

Figure 85: PicoGreen assay of the human dermal fibroblast cells on the PCL/thiolene PolyHIPE up to 5 days. The blank control used was tissue culture plastic with no cells. The HIPEs is the PCL/thiolene material and the control was tissue culture plastic with fibroblast cells. Work done in collaboration with Lindsey Dew.

6.5.9. Cell culture on the PCL/Thiolene PolyHIPE

PCL/Thiolene PolyHIPE samples were prepared (shown in the Soxhlet extractor in **Figure 82**) and sample images of the same blend of the M19_S2 formulation shown in **Table 4**, and representative SEM images shown below in **Figure 86**. This formulation was chosen due to its relative stability over the previous PCL blended ones. Human dermal fibroblast cells were grown on the PCL/Thiolene PolyHIPE up to 7 days, and confocal z-stack image of the cells growing on the material as well as a live/dead stain were used to image the cells **Figure 87**.The live/dead stain shows that the fibroblast cells have grouped together with 3 anchorage points across 800µm distance within one of the larger pores. The centre of the cell mass was red, indicating that these centre cells are dead, possibly due to lack of oxygen. The PCL/thiolene PolyHIPE auto fluoresced during the confocal imaging, this was advantageous as the pore morphology could be seen as well as the cells. Due to the large pore sizes the cells lined the outer edges of the pores. They had a flat spread out morphology and bridged over the smaller interconnecting windows connecting adjacent pores. This can be seen in image A **Figure 87**.

The growth and support of fibroblast cells on the PCL/thiolene PolyHIPE suggested that this material has the ability to support the growth and cell proliferation of cells up to seven days.

6.5.10. Floating PolyHIPE

For cell culture studies the PCL-Thiol PolyHIPE samples often floated to the top of the culture medium. The floating of the PolyHIPE samples were a common issue with the cell culture on the PolyHIPE discs, this has been addressed in numerous ways in the literature. Discs of PolyHIPE have been adhered to the base of a 6-well plate using sterilized silicon-based high temperature vacuum grease[68], and weighed down using glass and an inert adhesive [71].

The PCL-Thiol PolyHIPE samples remained submerged during the sterilisation washing stage in 75% ethanol solution however they floated when washed in PBS solution. This was attributed to trapped air that could have been present in the PolyHIPE during the transfer stages between containers. The presence of trapped air

within the PolyHIPE during cell culture will prevent the migration of cells within the bulk material, and the cell migration studies could therefore be an underestimate of the cell proliferation within the scaffolds. The bubbles will act as a barrier to cell migration. To remove the trapped air the PolyHIPE was were placed into a sterile PBS container with a lid that had a 0.2 μm filter placed on top to prevent bacterial from contaminating the scaffolds when the container was outside the culture hood, and allowed for the free movement of air into and out of the container. The container was then placed in a vacuum oven to draw out the trapped air. Under vacuum the samples floated to the top surface of the liquid as the trapped air expanded in size. After a few cycles of being under vacuum then returning to normal atmosphere pressure the samples eventually remained submerged in the PBS.

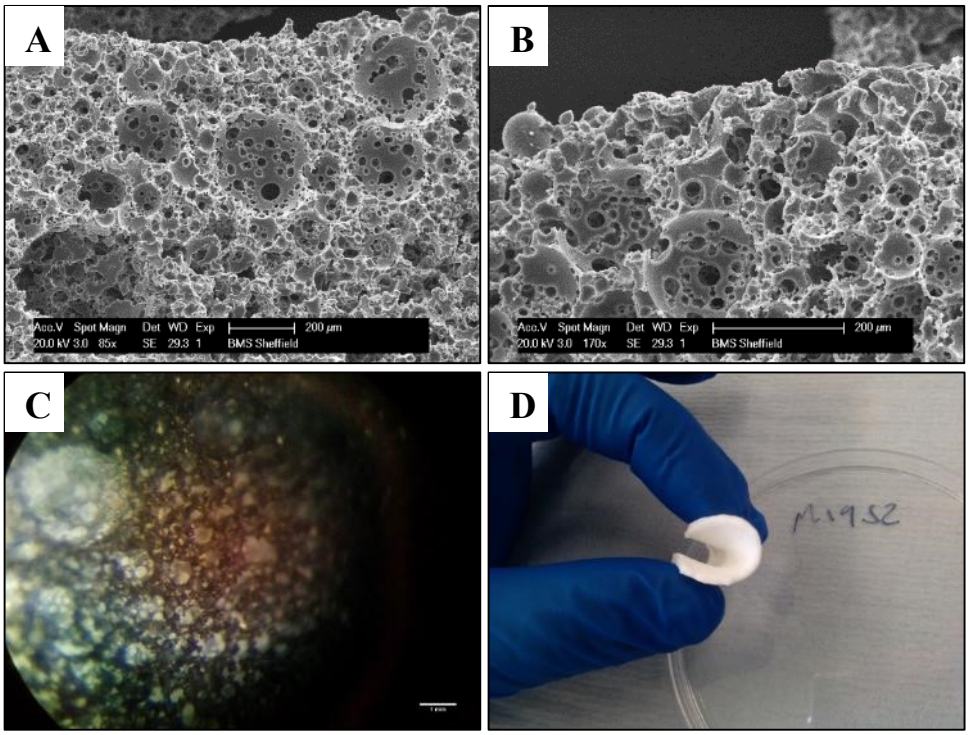

Figure 86: SEM and light microscope image of the PCL/thiolene PolyHIPE used for cell culture (sample M19_S2) **A & B**, SEM images of different sections of the PCL/Thiolene PolyHIPE, the material shrank during the drying process. **C**, Light microscope image of the material with a light shining on its side to highlight the porosity. **D,** image showing the flexibility of the material.

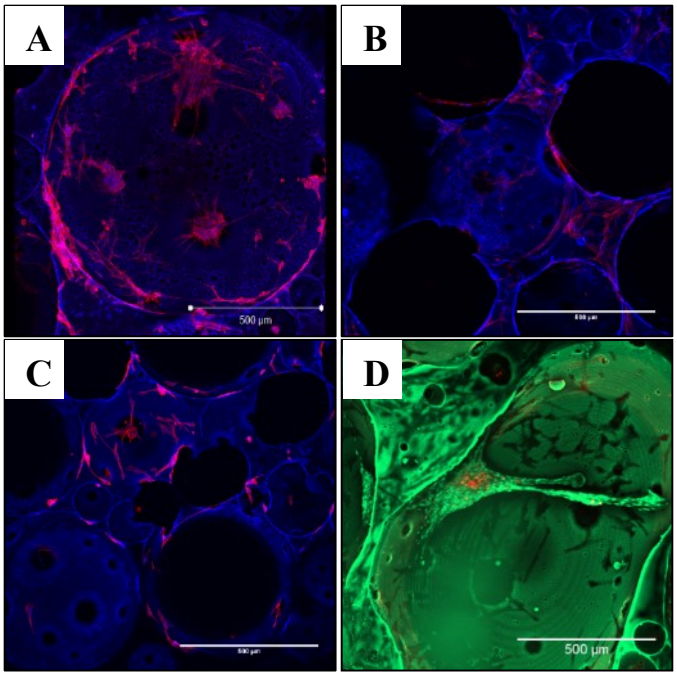

Figure 87: Fluorescent confocal images of human dermal fibroblast cells growing on the PCL/Thiol PolyHIPE. **A-C**. Cells were stained with Phalloidin (TRITC) (Red F-actin) and DAPI (Blue Nucleus), the scaffold has a slight blue fluorescence. **D**, A live/dead stain of human dermal fibroblast cells within one of the large voids on an auto fluorescent background.

The degradable PCL/Thiol PolyHIPE was photocured either side of an electrospun PHBV (polyhydroxybutyrate-co-hydroxyvalerate) nanofibrous scaffold to act as a barrier to prevent cell migration through the PolyHIPE. The PHBV electrospun mat was produced by my co-worker Lindsey Dew. This opens up the possibility for a co-culture on the PolyHIPE material. A nanofibrous electrospun layer in the middle in a trilayer electrospun scaffold has been used previously [95]. In the paper by Bye *et al.* a nanofibrous layer acted as a barrier for the culture of two types of skin cells; keratinocytes and fibroblasts, within an electrospun scaffold.

The study investigated the integration of these 2 technologies to make a hybrid PolyHIPE-based scaffold incorporating a barrier layer. This opens the opportunity to combine the advantages of PolyHIPEs, e.g. building of complex 3D structures, with the advantages of electrospun scaffolds, e.g. incorporating of nano porosity in the scaffolds. The combination of electrospun scaffolds and PolyHIPEs has yet to be explored in this manner and this will present the initial work for a cell barrier layer within the PolyHIPE scaffolds. The corresponding SEM images are shown in **Figure 88**.

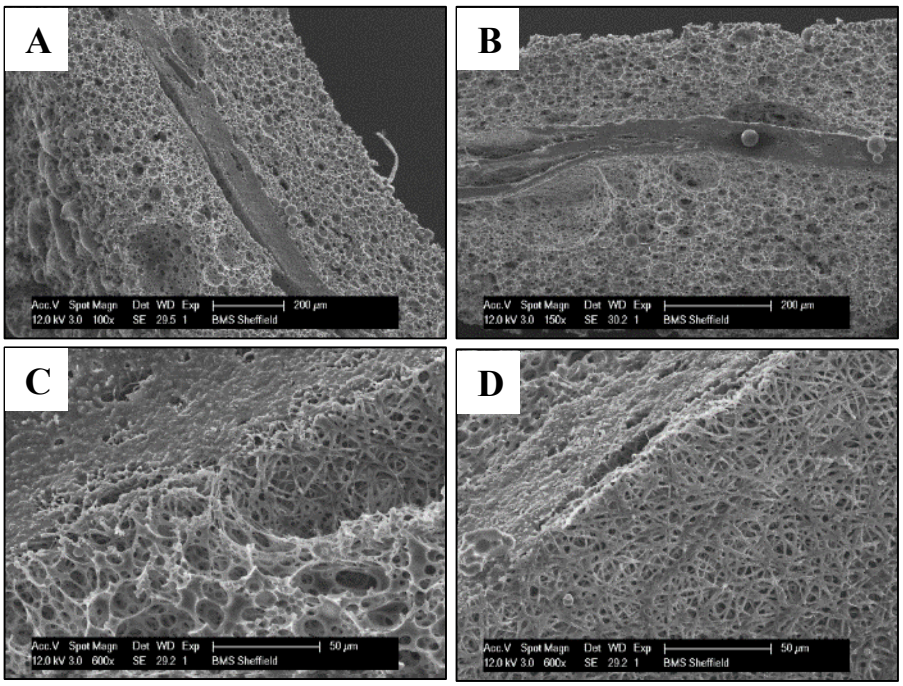

Figure 88: SEM images of the PCL/Thiol PolyHIPE with a PHBV fibrous layer in the middle. (**A** & **B)**, side images of the scaffold. **B**, the attachment of the PolyHIPE to the PHBV. (**C** & **D**) The underside of the PHBV with only one side with the attached PolyHIPE.

The PCL/thiolene PolyHIPE maintained its PolyHIPE morphology either side of the PHBV barrier layer as shown in **Figure 88**. Image **C** shows the interface between the PolyHIPE and the PHBV where the porosity and interconnectivity of the PolyHIPE is maintained up to the point where it binds to the PHBV. No detachment was observed between the two materials during handling and the cell culture.

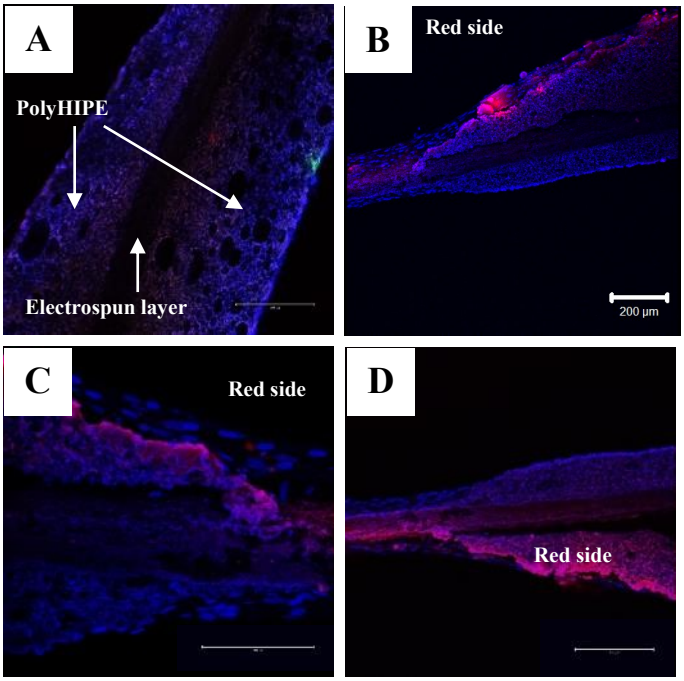

Figure 89: Confocal images with fibroblast cells growing on both sides of the PCL-Thiol PolyHIPE for 5 days. Cells on one side have been labelled with CellTracker™ Red to track the fibroblast cells to see if they passed through the PHBV barrier layer. **A**, cross-sectional image of the scaffold with the PolyHIPE and electrospun layers highlighted **B**, fibroblast nuclei can be seen surrounding both side of the tri layer. **C** and **D** shows the side regions around the outer edge of the scaffold to show the red stained fibroblast cells had not passed through the barrier layer. The red layer has been labelled in the images B, C and D.

Fibroblast cells with CellTracker™ Red was cultured on one side of the PCL/thiolene PolyHIPE tri layer scaffold, and unlabelled fibroblast cells were seeded on the PolyHIPE on the other side of the electrospun barrier layer. After 5 days the samples were fixed in 3.7% solution of formaldehyde and stained with DAPI to stain the nucleus. The samples were sectioned using a scalpel blade to image their cross section under confocal microscope to determine if the cells have passed through the PHBV barrier layer. The images are shown in **Figure 89**. One side of the samples was red in comparison to the other. In image **D** the red colour can be seen on the underside of the cross-section with a few red cells, although they are very faint and may just be part of the PolyHIPE material, which appears to have been stained red also. The red does not appear to have crossed over the PHBV barrier layer indicating that the cells remained on one side of the scaffold.

Primarily the edge of the tri layer scaffolds were imaged because at these regions the scaffold was thin enough to allow both sides of the tri layer to be captured in one

image. A small amount of ingrowth into the scaffolds can be seen in image A **Figure 89**, although the DAPI stain is very faint against the auto fluorescent nature of the material.

6.6 Conclusion

The Thiolene PolyHIPE method and formulation was successfully reproduced from the publication [21], and the ratio of a 1:1 monomer to solvent confirmed as being a suitable ratio for both the stable emulsion and PolyHIPE preparation. This publication was used as the ground work to produce a PCL/Thiolene PolyHIPE by using a modified version of the solvent and protocol. The methacrylation of the PCL was successfully achieved from an adapted version of a protocol that has been published previously [46], and the PCL incorporated into the PolyHIPE.

The addition of non-photocurable solvents was found to increase the stability of the emulsion prior to the formation of the PolyHIPE. The use of the solvents made the oil phase less viscous and overall hydrophobic enough to have a 'stable' emulsion, this is because the hydrophobicity of the oil phase is more so important than its composition for the formation of a stable emulsion [9]. A blend of the solvents was found to significantly increase the stability of the emulsion, and the blend influenced the emulsion in-between two extremes if these were used on their own [85].

Initial work shown that the material had significant destabilisation, this resulted in the formation of large pores indicated by both SEM and light microscope images. If too much surfactant was shown to cause shrinkage in the PolyHIPE. Gold coating of the light microscope images was also used as an alternative to visualise the macro pore distribution within the material.

The Soxhlet wash removed a lot of waste material, the ethanol waste and afterwards the ethanol was very cloudy, as the Soxhlet should remove any surfactant residue and trapped monomer within the material [36].

The reduction of MTT assay by the thiolene component meant that the use of this quantifications method could not be reliably used, although it has been used before in the literature for the thiolene PolyHIPEs [21]. A PicoGreen assay was used instead to shown that the material supported the growth of fibroblast cells up to 5 days.

To address the floating issue with the PCL/thiolene PolyHIPE samples during cell culture, a vacuum was used to removed trapped air from within the material, and the material did not require any weighting down that has been used previously for the culture of cells on the PolyHIPE such as using sterilized vacuum grease [68] or weighing it down with glass and an adhesive [71].

The PCL/Thiolene PolyHIPE was cured either side of electrospun fibers as an alternative to an electrospun trilayer [95].

6.6.1. Summary

- PCL/thiolene PolyHIPE was successfully created.
- The significant factors that determined the emulsions stability was found to be a blend of two solvents that incorporated a low amount of toluene respective to the chloroform.
- The Soxhlet extraction removed excess contaminants that would be detrimental to the cell growth, and the material was found to support the growth of human dermal fibroblast cells up to 5 days.
- There were variations between different emulsions prepared, which can be due to a wide range of variables that affect emulsion stability, such as; insufficient mixing stages, temperature variation and human error.

7. CHAPTER SEVEN: The systematic development of a PCL PolyHIPE

7.1 Aims and Objectives

The aim of this chapter is to develop a PCL PolyHIPE and characterise the processing parameters that affect the emulsion stability, and the resulting PolyHIPE structure. This chapter will present the systematic experimental procedure used to create an emulsion from a new material that has only been used as polymer blends in the literature. Furthermore the fabrication of porous PCL PolyHIPE beads will be presented. This is achieved by the following:

1. Determine the optimum solvent dilution and surfactant to create a PCL based emulsion
2. Fine tune the emulsion parameters to create a stable PCL based HIPE
3. Characterise the porosity of the PCL PolyHIPE with respect to the processing parameters
4. Fabrication of PCL PolyHIPE beads using a water-in-oil emulsion (W/O).

7.2 Introduction

This chapter follows the experimental route to create the stable high internal phase emulsion from the monomer PCL. The addition of PCL in the literature has been reported on as destabilising the emulsion, and has been only used in blends to create a degradable PolyHIPE [80] which was published in 2015.

From the literature the surfactant often used for the emulsion of a PCL blended PolyHIPE has been Span 80 so this was used as the starting surfactant. During the initial evaporation stages to purify the PCL from the methanol washes some methanol was kept in the PCL to prevent premature polymerisation, these batches of PCL were found to form an emulsion with more water addition than just using chloroform alone, and therefore were used as part of the chloroform/methanol blend to create the initial emulsions. A solvent was always required to dilute the PCL as on its own it is a very viscous liquid. Eventually through the experimental procedures detailed below the

methanol was replaced with toluene and the critical parameters that affect the emulsion stability were identified.

If the single solvent to dilute the PCL was toluene the only emulsion formed was O/W, this is droplets of PCL suspended in the water phase. Whereas with only the solvent chloroform the emulsion was stable but only up to a limited amount of water addition. It was determined that chloroform had to be the dominant solvent and the small addition of other solvents were required to form a stable HIPE. Careful observation of the emulsion throughout the mixing stages with respect to different parameters enabled this conclusion, and gradual incremental steps were made to determine which factors had the most significant effect on the emulsion. this was an important finding as the choice of diluent is important to create a stable emulsion [85]. This will be presented in the following section.

The experimental approach presented on within this chapter is similar to the methodology used in reference [9]. To create a 99% water volume PolyHIPE. The authors of this study found the upper point of the water addition with the emulsion, then to increase the achievable emulsions first the mixing efficiency was addressed. The next milestone for them was the addition of a solvent and finally the use of a different surfactant to stabilise the emulsion. I addressed the mixing efficiency by using two magnetic stirrers in a small volume emulsion preparation, this was because of a limited amount of material available. I condensed the emulsion fabrication into 1 ml samples of oil, and then mixed this small volume with the water (3 ml-8 ml addition).

Cameron *et al* [85] originally used single porogenic solvents to adjust the surface area of the PolyHIPE, however this study found that the PolyHIPE had a very high surface area but very weak mechanical properties when using one solvent. Therefore this study used a mixture of two porogens to have a balance between a high surface area and acceptable mechanical properties. They found that the mixed porogen produced better results than the solvents used on their own, which is the same approach that I eventually used for increased emulsion stability.

7.3 Methods

7.3.1. PCL PolyHIPE Protocol:

The following protocol is developed in this chapter:

0.3 g of the surfactant Hypermer B246 is added to 3 g of PCL in a 50ml beaker. The beaker is heated on a hot plate at 40^{o}C until the Hypermer has dissolved. The PCL is allowed to cool down before a 1:1 ratio of chloroform is added (3 g). Toluene is added at 15-20% in relation to the chloroform (0.45 - 0.6 g). Take 1g of this stock solution and add to a glass vial submerged in a clean water batch at 35^{o}C. Mix the solution using either a magnetic bar or overhead stirrer at 350rpm. For an 80% water volume ratio use a 1:4 ratio of the total amount of oil to the water amount to be added. Gradually add 4ml of warm water at 35°C to the solution over 5 minute. If the emulsion is on the verge of separating or a water layer can be seen on the top surface, add toluene and record the amount added. Once the emulsion has been prepared allow a minimum of 5 minutes for efficient mixing and to increase the viscosity of the emulsion. Pour the HIPE into a flat mould and repeatedly pass it under UV light on both sides to ensure sufficient polymerisation. Wash the PCL in acetone to remove the bulk contaminants and excess solvent and water. Use a soxhlet extractor for 24 hours using ethanol as the solvent to remove any residue surfactant or solvent. Vacuum dry afterwards.

7.3.2. PCL PolyHIPE: Initial work

The methacrylated PCL on its own is too viscous to prepare an emulsion therefore its viscosity had to be reduced. The two main parameters that are used to reduce the viscosity are temperature and the use of a diluent, although a lower molecular weight PCL can be used. This option will be explored in future work.

Increasing the PCL's temperature will reduce its viscosity, but and at the same time too high a temperature will destabilise the emulsion. Dissolving the PCL in a solvent will also decrease the viscosity, however as with the temperature, a fine balanced between the PCL, solvent type and volume will be required, the usable range of solvent dilution will need to be determined both in terms of emulsion stability and PolyHIPE morphology.

The surfactant choice is very significant for the emulsion stability. Initially I used Span 80 for the PCL HIPE emulsion. This surfactant has been used previously in the literature and has been reported on as being a suitable surfactant for the emulsion of a PCL blend HIPE [64]. Methanol was present in the initial samples as it was used during the PCL purification and it was determined that the addition of methanol as opposed to pure chloroform provided a greater emulsion stability. Therefore the initial work involved testing different solvent blends for emulsion stability.

Table 5. Initial PCL HIPE experiment with chloroform and methanol solvent mixes as a diluent for the PCL. The photoinitiator was kept at 0.05wt% relative to the total monomer phase.

	reference	$CHCl_3$	MeOH	Solvent to PCL ratio	Temperature °C	PCL (g)	Surfactant (Span 80)	water	Emulsion stability
1	Aug5_S5	1	-	1:1	50	1	0.1	1-2	Y
2	Aug5_S1	0.8	0.2	1:1	50	1	0.1	3	Y
3	Aug5_S2	0.6	0.4	1:1	50	1	0.1	2	N
4	Aug5_S3	0.4	0.6	1:1	50	1	0.1	2	N
5	Aug5_S7	0.4	0.1	0.5:1	50	1	0.1	3	N
6	Aug5_S9	1.87	0.8	2.67:1	46	1	0.2	2	Y
7	Aug5_S10	3.4	0.8	4.2:1	60	1	0.3	2	Y

The maximum water volume ratio that could be achieved with the blend of chloroform and methanol was a 1:3 ratio of oil to water, increasing the water content above the stated values in Table 5 caused the emulsion to invert. This is understandable as the increase in the methanol volume may facilitate the transfer of the water through the continuous film as it is soluble in both phases. In small volumes the methanol may be transferring predominately into the water phase and therefore will have a low impact on the emulsion stability.

In the literature regarding polystyrene-based HIPEs, the addition of methanol in small quantities has a minor effect on the morphology of the PolyHIPE, and high amounts are required for it to have a significant effect [14]. Methanol has a minor effect on the rate of Ostwald ripening, and it was speculated that the methanol may be playing a

small role in the depletion of some surfactant at the interface, although this will be countered at high surfactant volumes.

Only O/W emulsions formed at low temperatures, therefore the initial oil and water temperatures were increased to 50°C to create an emulsion. All the produced emulsions separated out within a short amount of time after the initial mixing was stopped, which was due to both the high temperature as well as a relatively unstable emulsion formulation.

Early experimental results indicated that a small amount of methanol in respect to the chloroform caused an increase in the stability of the emulsion. Increasing the solvent to polymer ratio above 1:1 gradually increased the time required to polymerisation time, and the resulting PolyHIPE had both poor mechanical properties and contracted during the drying process. The emulsion could be prepared at an elevated temperature, although this aided with the emulsion process, it also caused the emulsion to destabilised quicker after the mixing was stopped.

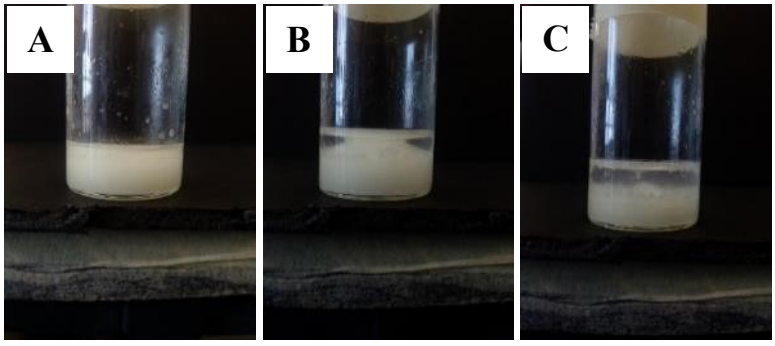

Figure 90: A PCL based emulsion gradually separating out into two phases over the course of a minute. **A**, the initial emulsion after mixing. **B**, the emulsion can be seen to separate out, spherical emulsion beads can be seen in this image. **C** Fully separated out into two phases. Emulsion formulation, sample 2 from **Table 5**.

The effects of an unstable emulsion can be seen in **Figure 90**. In this figure the emulsion is gradually separating out into two phases. The white appearance that is commonly seen with a HIPE is not seen in these emulsions. This white appearance that I am referring to is shown in image **A** in **Figure 91**. This effect is due to the scattering of the light from the high density of spherical droplets of water in the more stable emulsion.

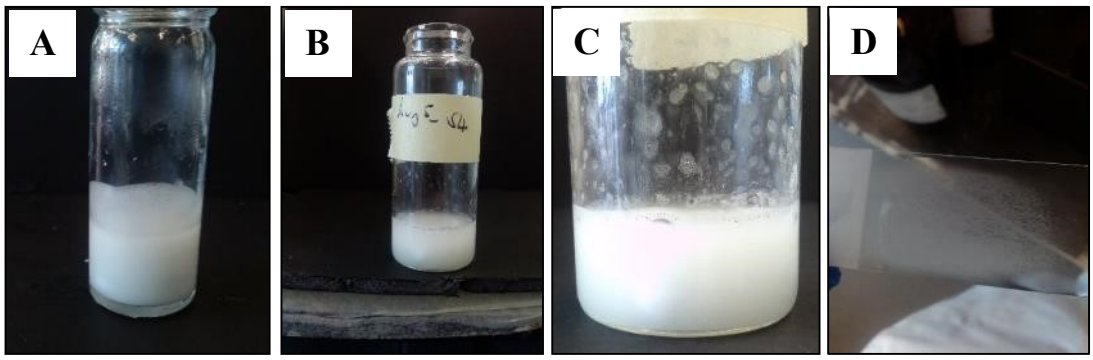

Figure 91: An example of a stable W/O emulsion and an inverted O/W one. **A**, A stable W/O emulsion. **B &C** show an O/W emulsion. **D**, the polymerised particles from the O/W emulsion on a glass slide. The W/O emulsion was very viscous while the O/W emulsion was very runny.

Figure 91 shows the difference between a stable emulsion and the emulsion that has inverted. The inversion of the emulsion can be caused by an instability between the two phases, as well as by the addition of too much water. The once continuous oil phase with a suspension of water droplets becomes the droplet phase suspended in a continuously connected water phase. For the emulsion stability it is important to know when the phase is on the verge of inverting, as it is here that the effect of additives or different external conditions have the most significant effect on the emulsions stability.

The use of a photocurable oil phase in the emulsion means that the emulsion morphology can be preserved rapidly by UV irradiation **Figure 92**. However despite this, if the emulsion is not stable it can still separate out during repeat passes under UV light, the rate of separation is further increased by the repeated moving of the emulsion as well as the air flow of the UV conveyer belt. In **Figure 93** the resulting photocured samples were not interconnected and had a few large pores. Small spherical polymer particles can be seen distributed throughout the voids from where the emulsion has inverted and has started to form an O/W emulsion.

Table 6: Initial emulsion with the chloroform and methanol blend, Y/N indicates an emulsion that quickly started to separate out

Sample	$CHCl_3$	MeOH	Solvent to PCL ratio	Temp (°C)	PCL (g)	Surfactant (Span 80)	Photoinitiator (g)	Water (ml)	Emulsion stability
Aug5_S9	1.87	0.8	2.67:1	46	1	0.2	0.86	2ml	Y/N
Aug5_S10	3.4	0.8	4.2:1	60	1	0.3	0.8	2	Y/N
AUG7_S1	0.8	0.2	1:1	70	1	0.1	0.05	4	Y/N

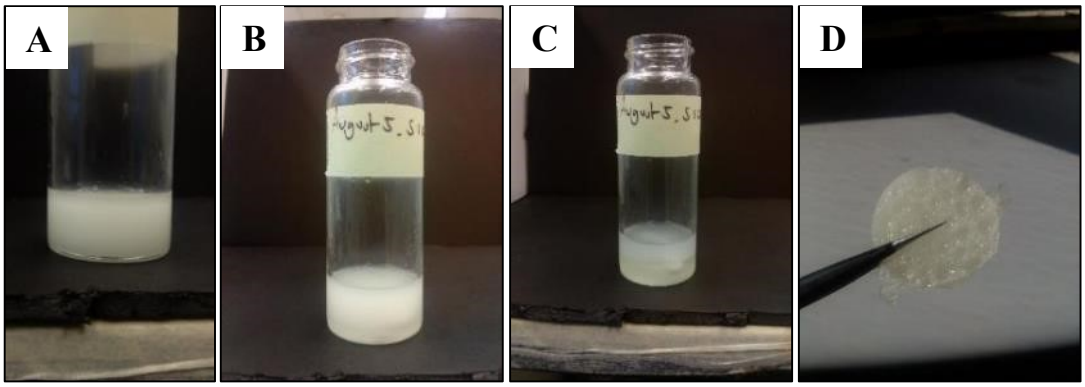

Figure 92: The sample (Aug5_S10), **A-C,** gradual separation of the oil and water phases over a minute. **D**, The polymerised scaffold after remixing.

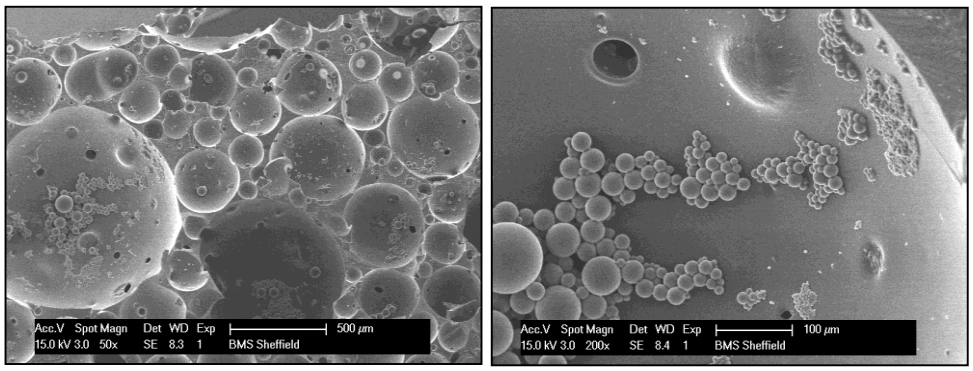

Figure 93: This is the photocured material from **Figure 92**. The sample name is AUG7_S1. A very small degree of interconnectivity can be seen, and there are a few spherical non-porous beads present in the pores.

Different solvent blends between the water immiscible toluene and chloroform were tested with the surfactant Hypermer B246. This blend was chosen based upon the recent success with the PCL/Thiolene PolyHIPE work that was worked on in parallel to the current PCL emulsion work. A set of images demonstrating the effect of toluene on the stability of the emulsion when used with chloroform are shown in **Figure 79**. The formulations of the more stable emulsions are shown in **Table 7.**

Table 7: PCL emulsion formulations with chloroform and toluene as the diluting solvent

Sample	$CHCl_3$ (g)	Toluene (g)	Solvent to PCL ratio	Temp (°C)	PCL (g)	Surfactant Hypermer B246 (g)	Photoinitiator (g)	Water (ml)	Emulsion stability
Aug21_S4	2	0.35	2.35:1	56	1	0.4	0.02	8	Y
Aug21_S6	1.24	0.35	1.35:1	60	1	0.4	0.094	5	Y
AUG21_S7	1	0.35	1.35:1	60	1	0.4	0.02	8	Y

Increasing the solvent to monomer ratio increased the emulsion if it was on the verge of phase inverting, however this also caused the resulting PolyHIPE to collapse if insufficiently polymerised afterwards. This collapse was evident in the sample Aug21_S4. If the emulsion was insufficiently polymerised then the material collapsed in on itself as shown in **Figure 94**. The increase in solvent concentration, increased the required amount of UV exposure to fully polymerise the material, and insufficient exposure caused both sample collapse and an uncured middle region. The collapsed material has a similar morphology has been observed in the literature when using a blend of PCL in the HIPE [64].

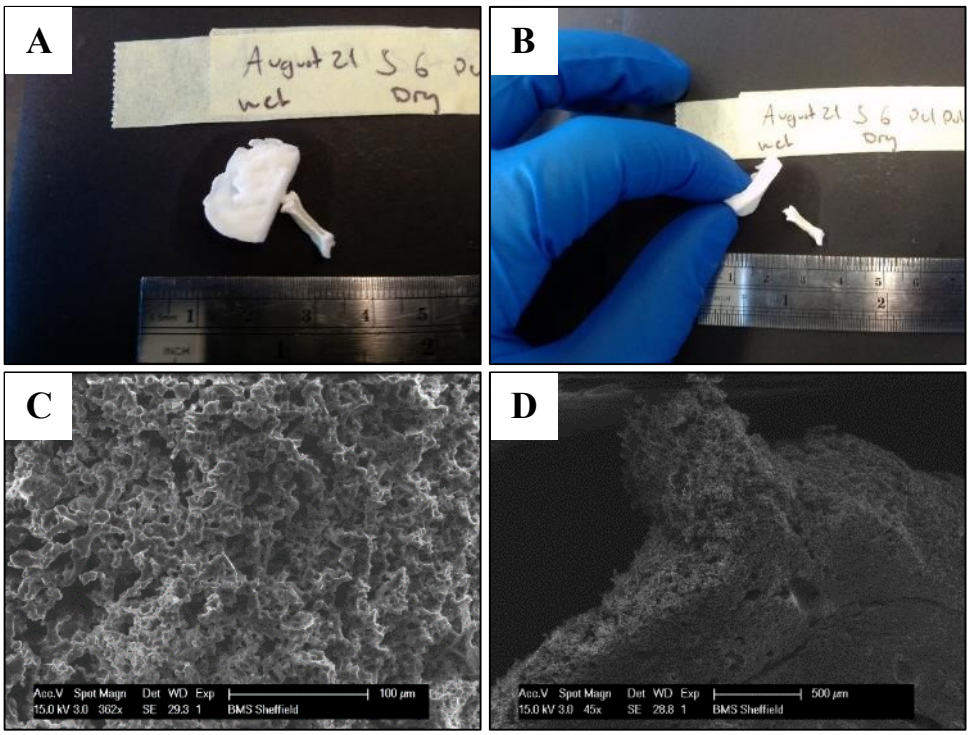

Figure 94: Images of the PCL PolyHIPE before and after drying when insufficiently exposed to UV light. **A** and **B**, pictures of the PolyHIPE before and after drying. The middle region has a yellow like appearance caused by the collapse and solidification of the emulsion, this inner surface is rigid to the touch. **C**, SEM image of the collapsed region. **D**, An overall SEM image of the material.

To stabilise the emulsion and determine the optimum amount of solvent blend to add, the emulsion was mixed with water and more solvent was added when the emulsion started to destabilise. I found that adding an excess of Toluene create droplets of PCL whilst adding an excess of chloroform brings the emulsion section together more, but prevents the addition of more water. If too much is added and will also lead to emulsion destabilisation. Occasionally if the emulsion inverted a high rpm and increase in temperature can sometimes invert the emulsion by bringing the droplets together. Increasing the amount of UV exposure on the sample AUG21_S7 as shown in **Figure 94** and in **Figure 95** leads to a polymerised PolyHIPE that does not collapse to the same extent as the non-sufficiently polymerised one.

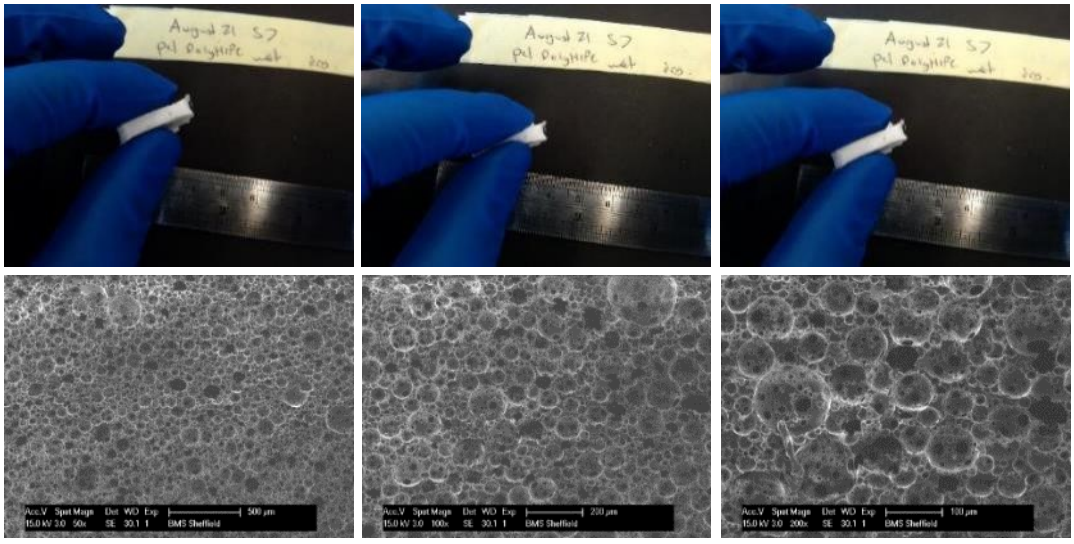

Figure 95. The sample formulation Aug21_S7, PCL PolyHIPE after several UV passes on either side of the material. **Top**, The elastic nature of the material is being demonstrated by crushing the sample and it returning back to its original shape. **Bottom**, SEM images of the corresponding PCL PolyHIPE.

7.4 PCL emulsion refinement

Different emulsion formulations and emulsion parameters were tested to determine the effect of temperature, surfactant, solvent ratio and surfactant amount on the stability of the PCL based PolyHIPE. Increasing the amount of mixing was shown to increase the stability of the emulsion as it went from a runny like liquid with the initial addition of water, to a white viscous mayonnaise like paste after sufficient mixing. The PCL PolyHIPE was found to be highly influenced by the blend of two organic solvents Chloroform (polar) and Toluene (non-polar) that are used to dissolve it and reduce its viscosity and maintain a stable emulsion. The solvents are non polymerisable and will leach out as the PCL polymerises. In the following experiments the remaining HIPE was allowed to cool before polymerisation. If the emulsion remained stable at room temperature it was polymerised and imaged afterwards to determine the effect the cooling has on the morphology. A table of the formulations are shown in **Table 9**. The two parameters that were varied were the temperature and surfactant percentage, and their effect on both the emulsion stability and resulting PolyHIPE were determined. The minimum amount of toluene that was used to stabilise a 1:1 ratio of PCL to chloroform was 15 wt% of the chloroform.

Table 8: The boiling points, density, volume and respective mass of the solvents and PCL used. Both 0.35g and 0.2g of toluene were used and their respective volumes are given.

Oil Phase	Boiling point	Density	Volume	Respective mass
Chloroform	61.2°C	1.483 g/cm3	0.674308833	1
Toluene	111 °C	0.87 g/mL	0.229885057	0.2
Toluene	111 °C	0.87 g/mL	0.402298851	0.35
PCL		1.08g/cm3	0.925925926	1

For the emulsion preparation the solvent ratios in respect to the PCL were all measured by weight. However for the emulsion the respective ratios between the oil and water are normally done by volume. Therefore the conversion between the weights and volume of chloroform, toluene and PCL are given in

. The boiling point of chloroform is 62.1^{o}C. The emulsion when the PCL/chloroform/toluene blend was heated to 60^{o}C which is just below this value.

The density of PCL M_n 900 g/mol is 1.08 g/mL. The volume of PCL used for every single batch of PCL PolyHIPE is 0.93 ml. 1g of chloroform and 0.35 g toluene has a volume of 1.08 ml. The ratio of monomer to solvent is 1:1.02. For the later formulations a reduced amount of toluene is used with the solvent blend consisting of 1 g of chloroform and 0.15 g of toluene with a total combined volume of about 0.9 ml. These volume ratios is just shy of a 1:1 ratio between the PCL and solvent. For the emulsion preparation a stock solution was first created, and then 1 g of the respective solution was used for each emulsion experiment.

PCL PolyHIPE formulations

Name	SURF %	Surfactant	PCL (g)	CHCL3 (g	Toluene (g)	Temperature	Oil phase	Water volume m	Water phase %	Initiator	Stock	RPM	Emulsion
SEP10_S1	10wt%	0.1	1	0.9	1.37		1	8		0.1	1g taken	500	
SEP10_STOCK	**10wt%**	**0.3**	**3**	**3**						**0.27**			
SEP10_S2	-				0.35	60	1	4	80		1g taken	450	Yes
SEP10_S3	-				0.35	60	1	6	85.7		1g taken	450	Yes
SEP10_S4	-				0.35	60	1	8	88.8		1g taken	450	Some separation
SEP10_S5	-				0.35	50		4	80		1g taken	450/500	
SEP10_S6	-				0.35	50	1	6	85.7		1g taken	450	Yes
SEP10_S7	10wt%	0.1	1	1	0.35	50	1	8	88.8	0.08	1g taken	450	yes
SEP11_STOCK	20wt%	**0.6**	**3**	**3**						**0.24**			
SEP11_S1	-				0.35	60	1	4	80		1g taken	450	Yes
SEP11_S2	-				0.35	60	1	6	85.7		1g taken	450	Yes
SEP11_S3	-				0.35	60	1	8	88.8		1g taken	450	Yes
SEP11_S4	-				0.35	50	1	4	80		1g taken	350/450	Yes
SEP11_S5	-				0.35	50	1	6	85.7		1g taken	450	Yes
SEP11_S6_STOCK	20wt%	0.2	1	1	-	-	-	-	-	0.08	-	-	-
SEP11_S6	-				0.35	50	1	8	88.8		1g taken	450	Some separation
SEP12_STOCK	**30wt%**	**0.9**	**3**	**3**						**0.24**			
SEP12_S1	-				0.35	60	1	4	80		1g taken	450	Yes
SEP12_S2	-				35	60	1	6	85.7		1g taken	450	Yes
SEP15_S1	-				0.35	60	1	8	88.8		1g taken	450	Yes
SEP15_S2	-				0.35	50	1	4	80		1g taken	450	Yes
SEP15_S3	-				0.35	50	1	6	85.7		1g taken	450	Yes
SEP15_S4	-				0.35	50	1	8	88.8		1g taken	450	Yes
SEP15_S5	-				0.35	50	1	6	85.7		1g taken	450	Yes
SEP16_STOCK	**5wt%**	**0.15**	**3**	**3**						**0.24**			
SEP16_S1	-				-	60	1	4	80		1g taken	450	No
SEP16_S2	-				0.35	60	1	4	80		1g taken	450	Yes
SEP16_S3	-				0.35	60	1	6	85.7		1g taken	450	No
SEP16_S4	-				0.275	60	1	6	85.7		1g taken	450	No

Table 9: PCL PolyHIPE formulations

7.4.1. PCL PolyHIPE

The initial work presented here demonstrates the characterising of the appropriate emulsion preparation parameters to create a PCL based HIPE. The effect of temperature was shown to have a high influence on the porosity of the PCL PolyHIPE material, and was found not to cause premature polymerisation during the mixing stages. The high temperatures used in the emulsion preparation did not crosslink the PCL. A limited range of surfactant is identified for emulsion stability. Despite the limited amount of photocurable PCL, a range of potential different processing parameters and a tentative explanation of their effect on the porosity will be presented.

A mixing rate of 450 – 500 rpm was used for all emulsions in an attempt to isolate the porosity changes in respect to the temperature, water volume ratio and surfactant concentration. As any variances in the amount of agitation will affect the pore sizes of the emulsion as it directly relates to the amount of kinetic energy put into breaking up the droplet suspension. Visually the pore size distribution is very similar due to the same degree of mixing used for all the samples presented.

For the SEM image analysis all the samples were prepared using 1g of the corresponding stock solution shown in **Table 9**. Either 4, 6 or 8 ml was added to this initial 1g of the organic phase. Therefore for the sample comparison I will refer to the wt% of surfactant, its corresponding temperature and either the 4, 6 or 8ml of water.

7.4.2. PCL PolyHIPE SEM image analysis

The low (5 wt %) surfactant formed an unstable emulsion and rapidly destabilised after the initial mixing was stopped. The emulsions were only stable during the mixing at the higher temperature used (60°C). The low water volume (4 ml) was more stable than the 6 ml emulsion, and produced smaller pores in comparison. The SEM images of the 4 ml and 6 ml 5wt% surfactant PCL PolyHIPEs are shown in **Figure 96**. The very large pores in the 6 ml PolyHIPE are caused by the droplet coalescence, as this low surfactant is insufficient to stabilise the emulsion against destabilisation at higher water volumes.

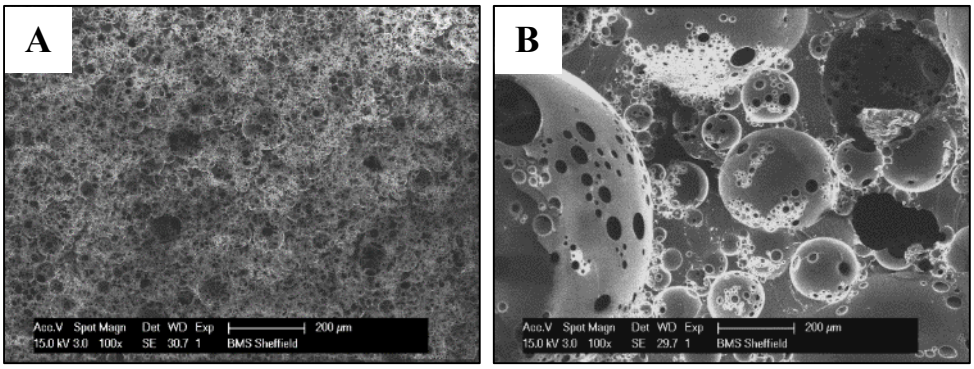

Figure 96: 5wt% surfactant 60°C PCL PolyHIPE. **A,** 4ml water. **B**, 6ml water. The emulsion rapidly destabilised after the mixing was stopped and during the polymerisation stage in image B.

The PCL PolyHIPE with 10wt% surfactant produced at 50 and 60°C are shown in **Figure 97**, 20wt% surfactant in **Figure 98** and 30wt% surfactant in **Figure 99**. These 18 SEM images show the PCL PolyHIPE each made with different processing conditions. The images are organised in to paired groups of 3 horizontal images. From left to right the water volume ratio is increases from 4 ml to 8 ml corresponding to a water volume fraction ratio increase from 80% to 88.9%. These 3 images are grouped together into two rows each corresponding to the emulsion preparation temperature 50°C or a 60°C, and each grouped section of 6 SEM images was produced using different surfactant ratios. This image array allows for the similarities and differences between the separate parameters to be compared, and their effects on the emulsion stability and PolyHIPE morphology determined.

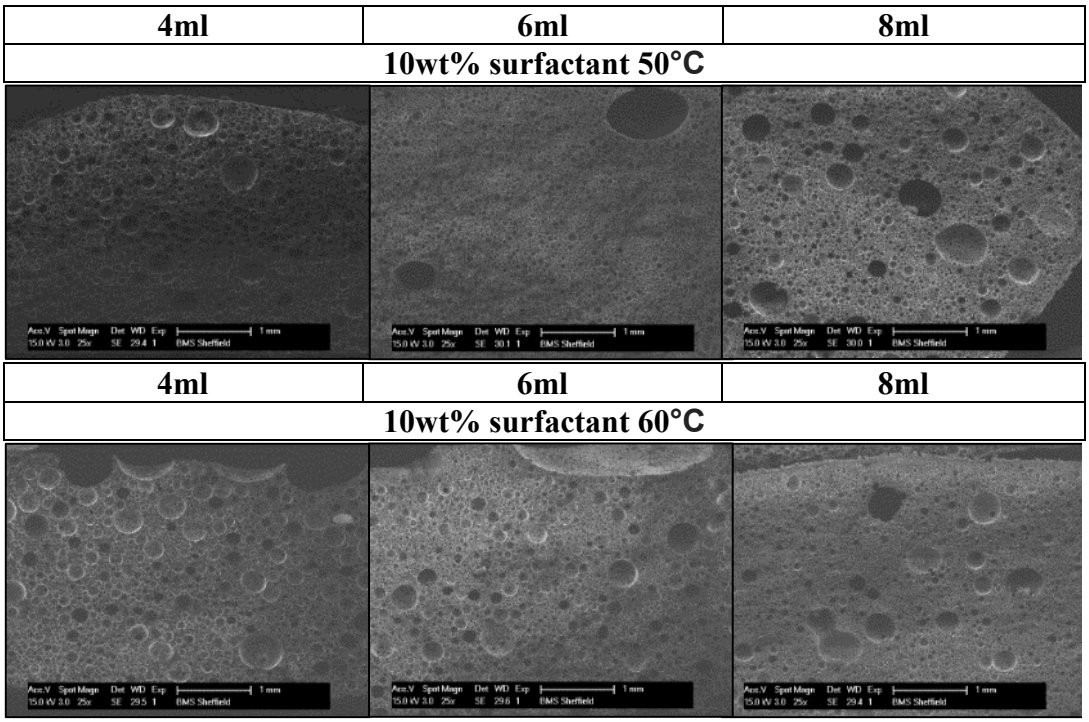

Figure 97: Two rows of SEM images (25X) of the PCL PolyHIPE with 10wt% surfactant mixed at 50 and 60°C. From left to right the water volume added increased from four to eight ml.

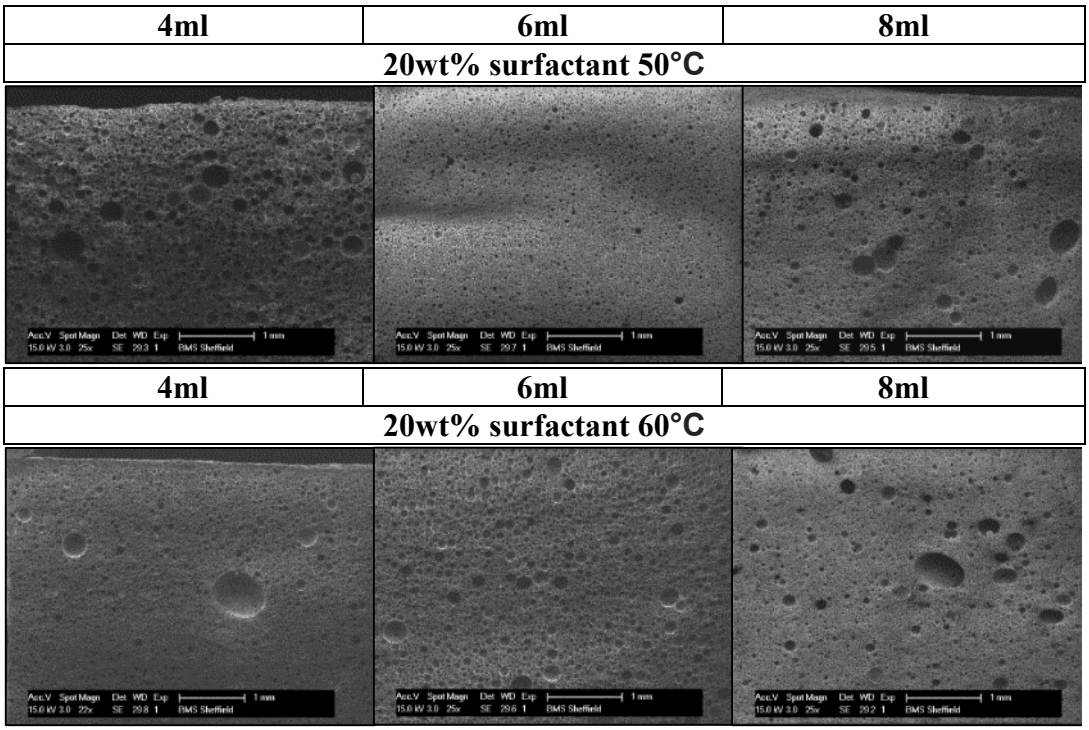

Figure 98: Two rows of SEM images (25X) of the PCL PolyHIPE with 20wt% surfactant mixed at 50 and 60°C. From left to right the water volume added increased from four to eight ml.

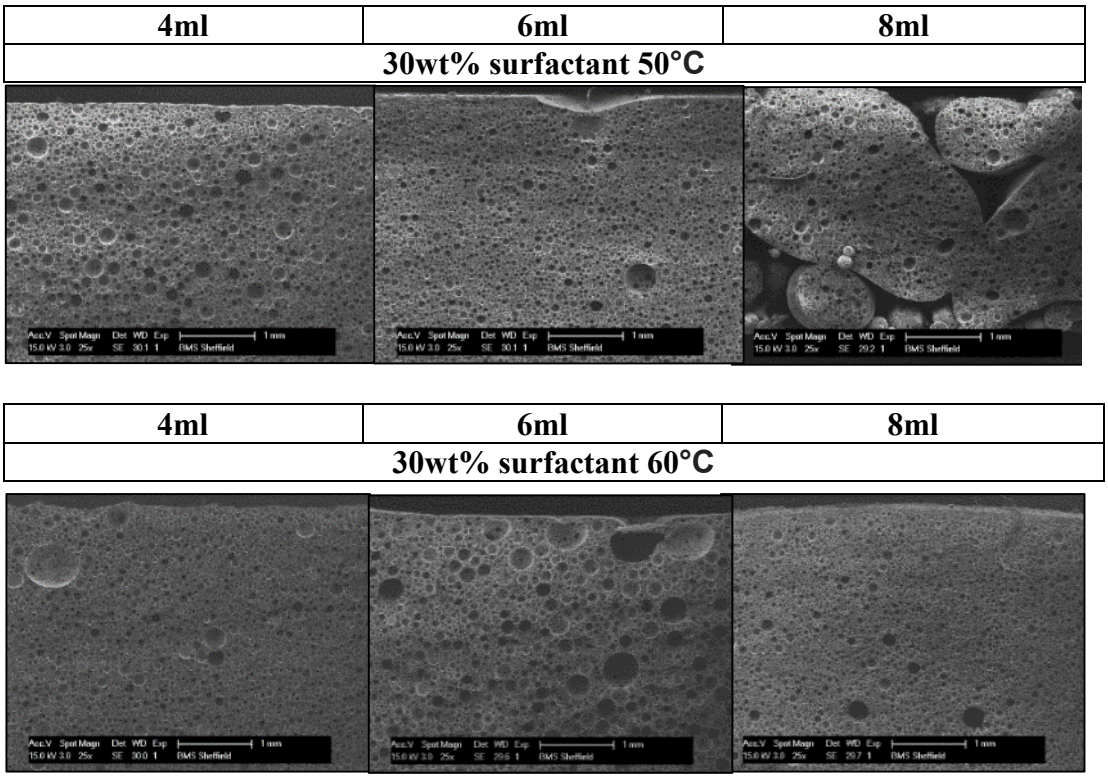

Figure 99: Two rows of SEM images (25X) of the PCL PolyHIPE with 20wt% surfactant mixed at 50 and 60°C. From left to right the water volume added increased from four to eight ml.

7.5 PCL PolyHIPE SEM image analysis: Effect of temperature

Within each surfactant concentration group increasing the temperature increases the amount of the larger macro pores (over 300 μm size) that are distributed through the material. This is especially evident in the low surfactant low water volume samples such as the 10wt% surfactant 4-6 ml water PolyHIPEs, although it is not case with the high surfactant (30wt %) samples.

It is expected that increasing the temperature will cause an increase in the average pore size. The increase in the emulsions temperature for a polystyrene based PolyHIPE from 50-60-80°C has been reported to cause an increase in the pore size distribution. This is attributed to the temperature causing an instability in the emulsion, which results in an increased rate of coalescence [14]. I expected to see similar results caused by the temperature increase. The higher surfactant concentration (30wt %) did not show this effect. In all cases the increase in the temperature increased the stability of this emulsion. The increase in temperature from 50 to 60°C prevented a three phase emulsion (W/O/W) from occurring. This can be seen in the differences between the 8

ml water addition in this group. At 50°C the oil phase may have been too viscous PolyHIPE formed a W/O/W emulsion where the oil phase would no longer stretch around the increased water surface area. Whereas at the higher temperature (60°C) a continuous emulsion was formed. This can be seen more clearly below in **Figure 100**.

The temperature has a very high influence on the PolyHIPE morphology, it has been used in the literature to controllably destabilise the emulsion to produce larger pore sizes. For example, a high water phase temperature of 80°C has been used to increase the pore size for improved cell ingrowth into the PolyHIPE [21]. The effect of the aqueous phase temperature from 50°C, 60°C and 80°C has been shown to increase the size of the pores [14].

Some of the emulsions as the temperature is increased a smaller distribution of the larger pores are seen. The high water volumes (8 ml) at the 10wt% surfactant samples, the low water volumes (4 ml) with 20wt% surfactant samples as well as the low 4-6 ml 30wt% samples. This could be due to an inefficient mixing method caused by the magnetic stirrers, differences in the rate of water addition from the manual pipetting of the water, as well as the time frame between the emulsion preparation and polymerisation. Over time the UV conveyor belt became very hot, which in turn caused the samples to warm up after a few passes under the UV light. This may have contributed to the variances between samples. The 60°C formulations were produced before the 50°C temperatures ones, therefore the lower temperature emulsions would be exposed to more heat during the polymerisation stage.

A limited range of samples were made at this stage due to the limited availability of the photocurable PCL. For a more accurate indication on these processing times multiple different formulations will need to be produced and subsequently characterised.

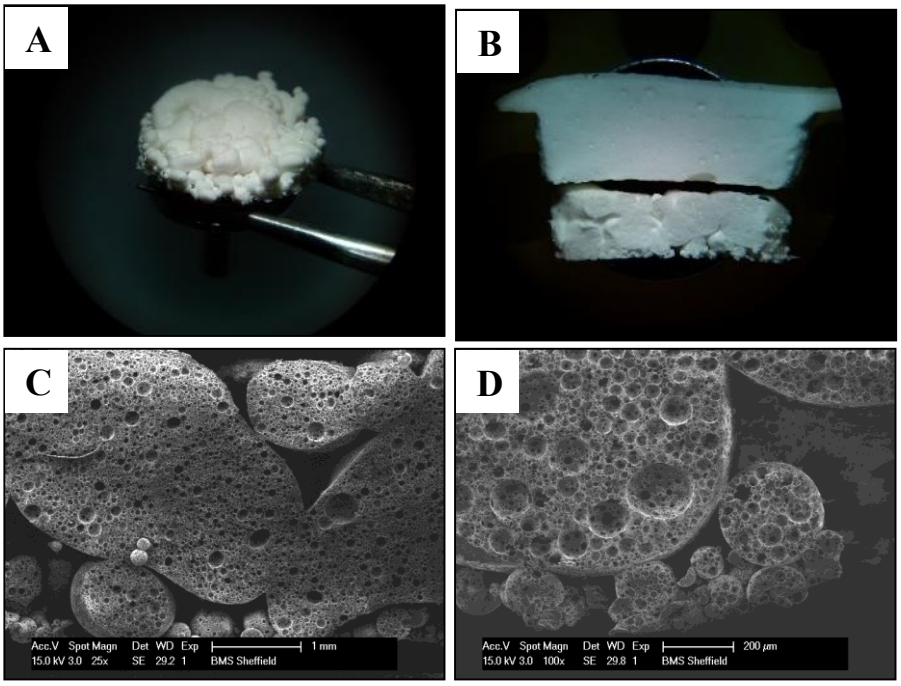

Figure 100: PCL PolyHIPE showing the difference between different water volume ratios with 30wt% surfactant at different water volume ratios. A: 1:8 water volume ratio with the corresponding SEM images in C & D, the emulsion formed a W/O/W emulsion, and the addition of more water no longer resulted in a continuous emulsion. B shows the 1:6 oil to water ratio on top and the 1:8 ratio oil to water on the bottom.

Water cannot be added to the emulsion indefinitely, as there is a critical point were the addition of more water is not incorporated into the emulsion but forms a separate third phase around the existing emulsion in a system known as W/O/W emulsion. This effect can be seen in **Figure 100**. Image B shows the difference between the emulsions with a 1:6 and a 1:8 oil to water ratio. With the higher 1:8 oil to water ratio the water is no longer mixed into the HIPE and it remains around the outside, and eventually causes the HIPE to separate into larger isolated sections. These separated spherical like beads of PolyHIPE are interconnected between each other where they have been in contact. Adding more water led to catastrophic phase inversion. This is where the emulsion swaps its internal phase, so it goes from a W/O to an O/W emulsion [97], and results in a sudden reduction in the viscosity of the emulsion from a viscous mayonnaise-like substance, to a runny white liquid.

4ml	6ml	8ml
10wt% surfactant 50°C		

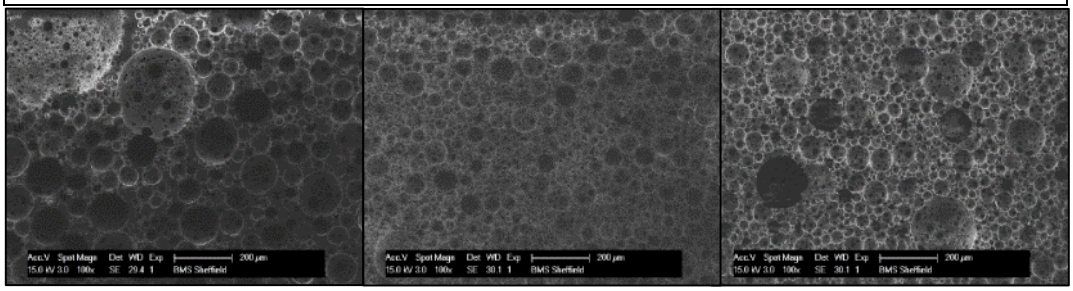

4ml	6ml	8ml
10wt% surfactant 60°C		

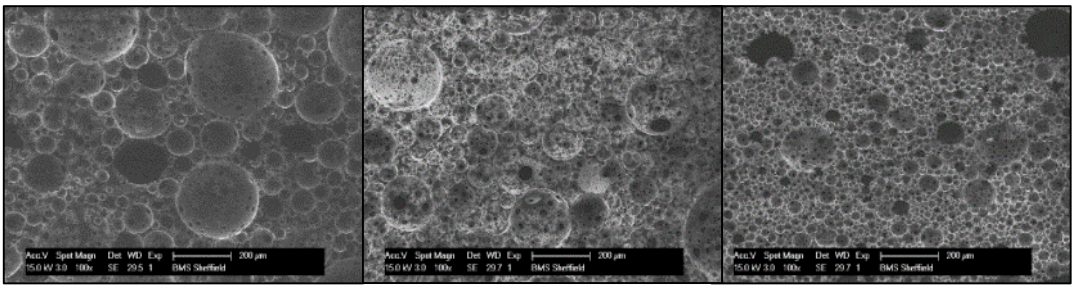

Figure 101: Two rows of SEM images (100X) of the PCL PolyHIPE with 10wt% surfactant mixed at 50 and 60°C. From left to right the water volume added increased from four to eight ml.

4ml	6ml	8ml
20wt% surfactant 50°C		

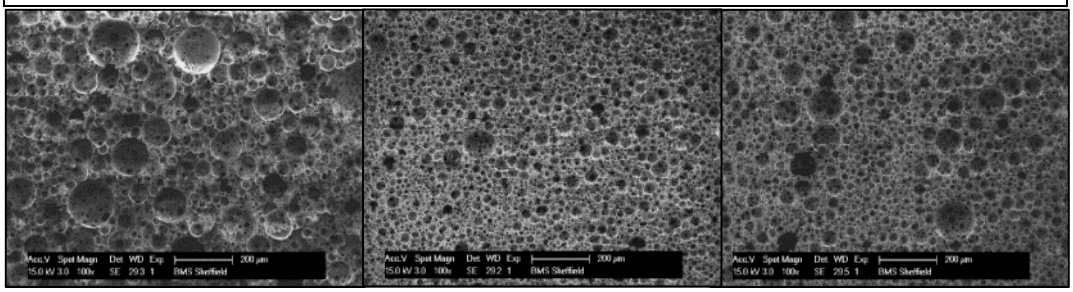

4ml	6ml	8ml
20wt% surfactant 60°C		

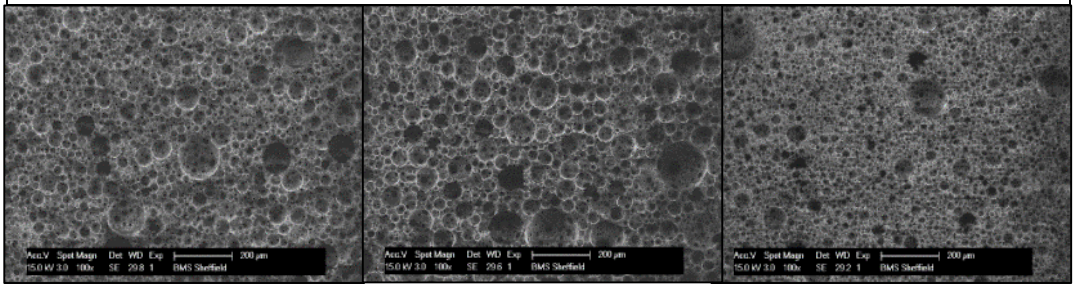

Figure 102: Two rows of SEM images (100X) of the PCL PolyHIPE with 20wt% surfactant mixed at 50 and 60°C. From left to right the water volume added increased from four to eight ml

4ml	6ml	8ml
30wt% surfactant 50°C		
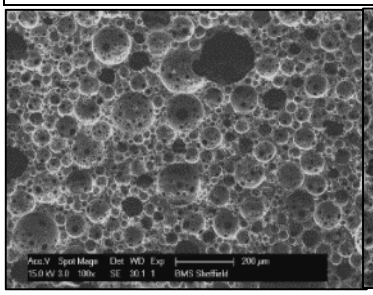	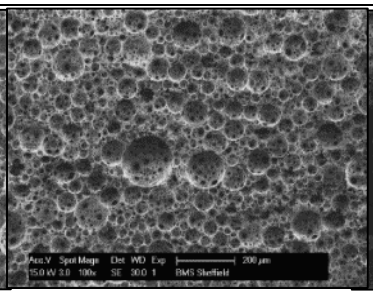	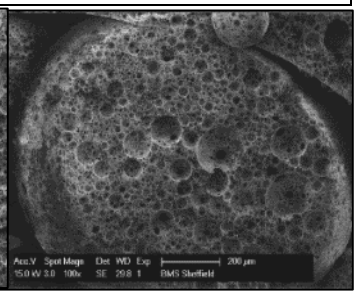

4ml	6ml	8ml
30wt% surfactant 60°C		
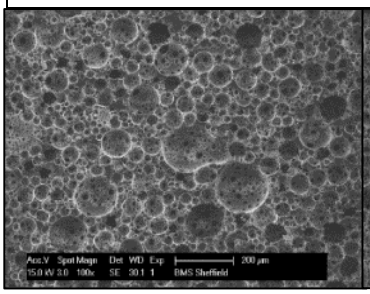	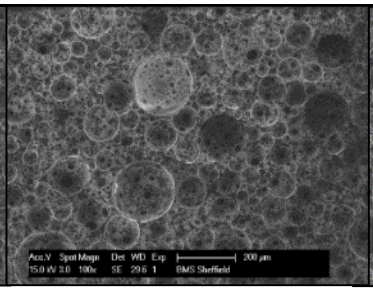	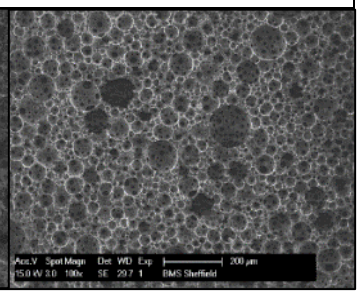

Figure 103: Two rows of SEM images (100X) of the PCL PolyHIPE with 20wt% surfactant mixed at 50 and 60°C. From left to right the water volume added increased from four to eight ml

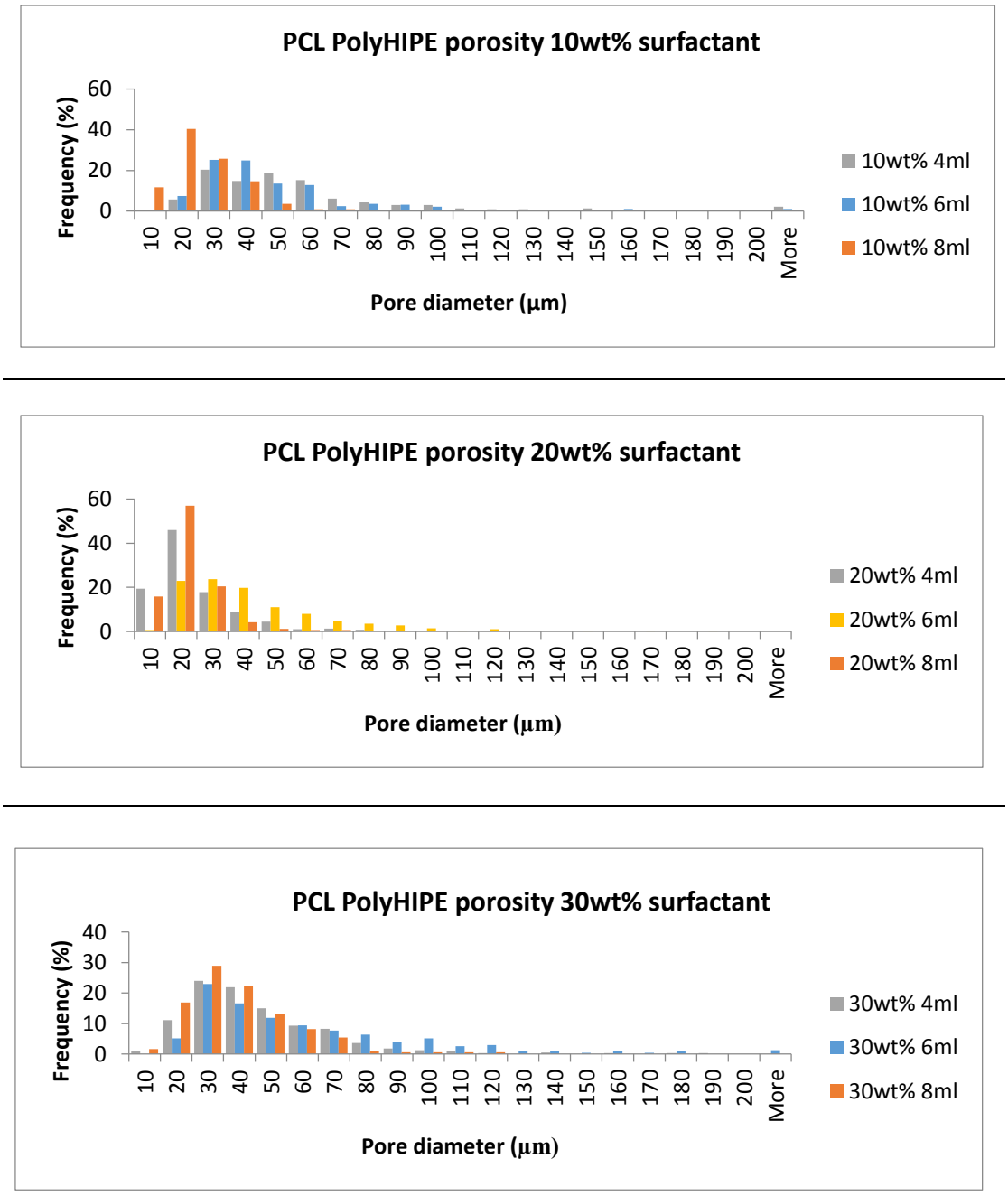

Figure 104: Histogram showing the pore size against its frequency for the 60°C PCL PolyHIPE with the increase in water volume for different surfactant concentrations 10wt%, 20wt% and 30wt%.

7.6 PCL PolyHIPE: Water volume ratio and Surfactant

The ratio between the oil phase and the water phase was increased from 1:4 to 1:8 for all PCL based PolyHIPE formulations. A 1:4 ratio correlates to an 80% nominal volume ratio, a 1:6 to 85.7% and a 1:8 to 88.9. For each PolyHIPE 1 g of the monomer phase taken from the initial stock solutions for each formulation, and then the water is added dropwise under agitation. The surfactant amount was not taken into account when measuring when calculating the ratio between the oil and the water phases.

7.7 Effect of water volume ratio

Increasing the water volume ratio increased the level of interconnectivity and decreased the pore size distribution. This effect can be seen in the lower surfactant (10 wt %) SEM images in **Figure 105** and the histology diagrams in **Figure 104**. The increase in water from the SEM images from left to right shows a gradual decrease in the pore size for the PCL based PolyHIPE. The large pores with the 4 ml PolyHIPE sample has thick regions of polymer between adjacent pores, whereas the 8 ml water PolyHIPE, in comparison, has a thinner more interconnected morphology.

From the histogram analysis; increasing the water volume ratio from 4 to 8 ml decreased the pore size distribution. 4ml had a larger spread of pore sizes ranging from 20- over 200µm, increasing the water volume ratio decreased the range of pore sizes with 8ml water volume ratio having a narrower range of pore sizes between the range of 10-60 µm. This is shown in the gradual grouping of the pore size frequency towards the 20-60µm size range seen in **Figure 104**.

For the 20wt% the pore size distribution from 4ml to 6ml water volume ratio increases the pore size distribution from 10-80 µm to 10-190 µm. Increasing the water volume ratio from 6ml to 8ml decreases the pore size distribution to 10-70 µm (**Figure 104**). The 6ml water volume ratio has destabilised during the preparation and polymerisation stage to cause the larger pore size distribution. This could be due to human error or the excess heat generated by the UV conveyor belt.

Finally for the 30 wt% surfactant concentration there is a broad distribution of pore sizes for all the water volume ratios, however a similar trend is seen to the 20 wt%

concentrations. The pore size distribution decreases from 6 – 8ml water addition **Figure 104**.

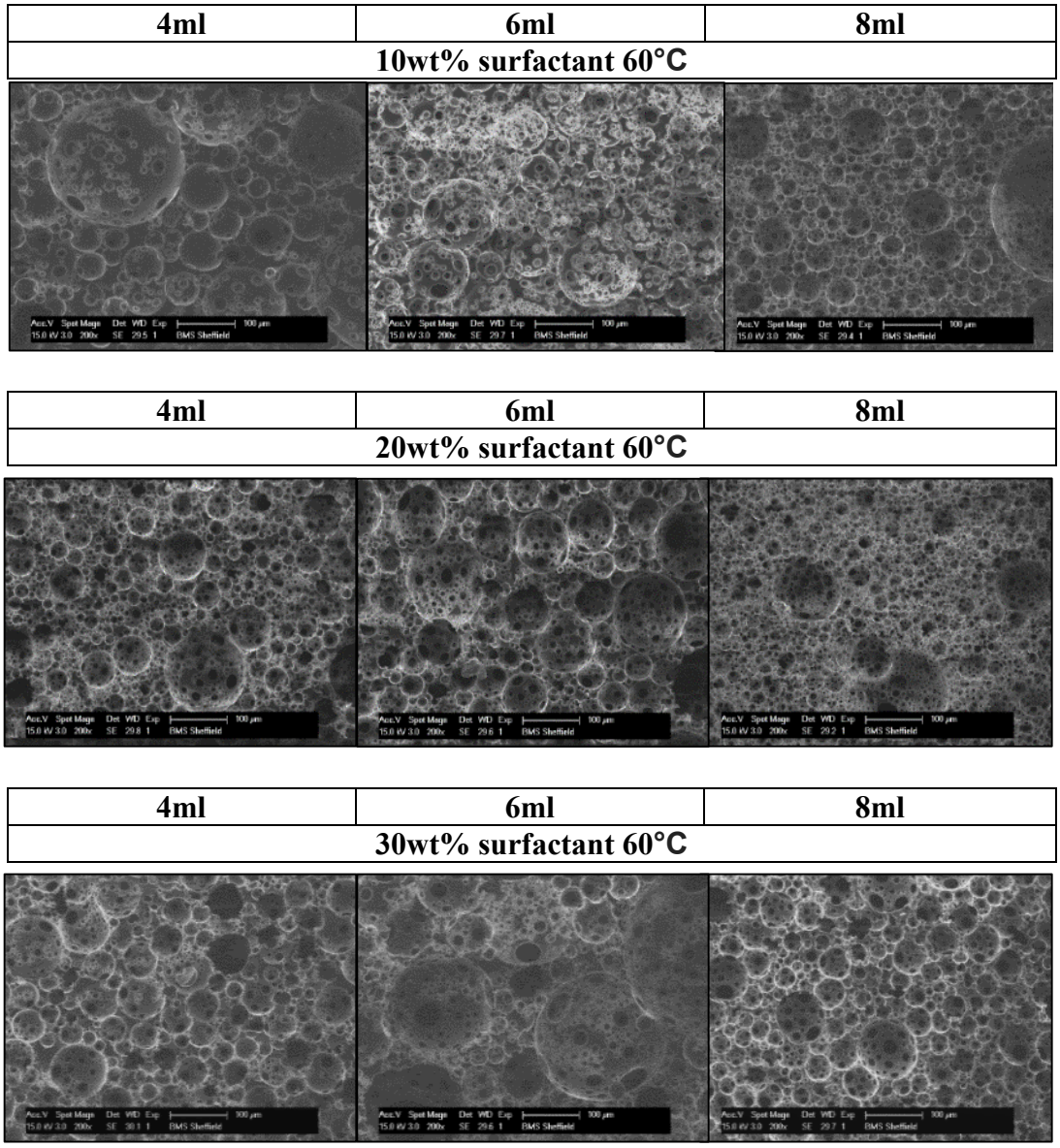

Figure 105: 9 SEM images showing the effects of increasing the surfactant concentration from 10-30wt% with the PCL PolyHIPEs prepared at 60°C.

In all cases the pore size distribution has decreased by comparing the difference between the 4ml and 8ml water volume ratios, and only the 10wt% concentrations was there a consistent decrease in the pore size distribution as the water volume ratio was increased as shown in **Figure 104.**

Two outliers with the water volume ratio increase are with the 30wt% surfactant water increase from 4-6 ml, and the 20wt% 4-6 ml samples. In both cases the 8 ml samples have a very smaller pore distribution, however the transition from 4 to 6 ml water volume does not show the same effect. I suspect this is due to experimental differences that may have occurred during the day of polymerisation. The PolyHIPE morphology could have been altered due to a prolonged or insufficient amount of mixing. Although the high temperature and the temperature the emulsion may have been subjected to during the UV conveyor belt curing could have caused these discrepancies. Furthermore from an observational standpoint during the polymerisation process. The UV lamp appeared to decrease its curing ability as it was left on for long periods, and gradually more repeat passes were required to polymerise the material and often it was turned off and allowed to cool. This was a part of the experimental equipment and may have had a contribution to the porosity discrepancies.

7.8 Effect of Surfactant concentrations on the PCL PolyHIPE

Increasing the surfactant volume increased the interconnectivity and decreased the pore size for the PCL based emulsions between 4-8 ml of nominal water volumes for the 10-20wt% surfactant samples. This can be seen in the differences shown in the 4 ml (water volume) PCL PolyHIPE SEM images where the surfactant has been increased from 10-30wt% in **Figure 106**. The increase in the surfactant from 20 to 30wt% on the other hand did show a small increase in the pore size distribution. Each emulsion was mixed at the same rpm therefore the amount of kinetic energy put into the emulsion to break up the water droplets is very similar for every emulsion, the pore sizes is expected to be similar because of this, the increased addition of surfactant should increase the interconnectivity as it should allow for a thinner more stable emulsion to form, this would have a thinner barrier film around the water droplets which are more susceptible to the material contraction during the polymerisation process, resulting in more interconnecting windows [34]. The SEM images of the 4 ml water PCL PolyHIPE samples in **Figure 106** show that the increase in the surfactant concentration causes a decrease in the pore size distribution from 10-20wt%, however visually there is not much difference between the 20-30wt% surfactant.

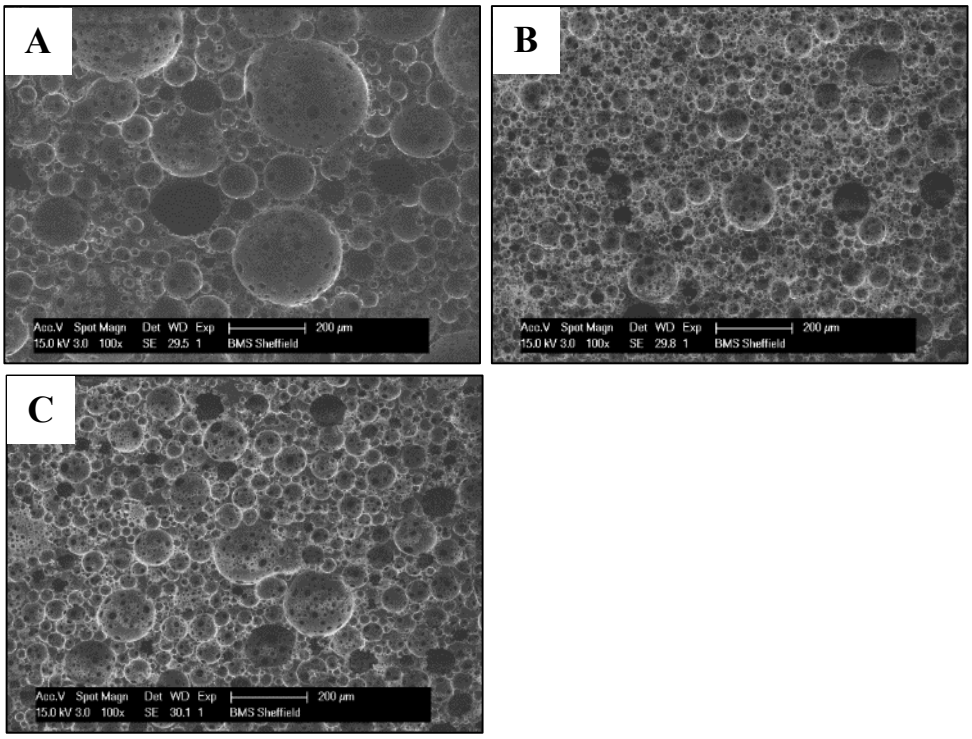

Figure 106. 4 ml water PCL PolyHIPE with different ratios of surfactant. **A**, 10wt%. **B**, 20wt%. **C,** 30wt% at 60°C. An increase in the interconnectivity and decrease in the pore sizes can be seen from the 10wt% surfactant PolyHIPE.

In **Figure 106** an increase in the surfactant from 10wt% in image A, to 20wt% in image B causes a reduction in the pore size. The temperature, water volume and mixing speed were kept constant so the change is most likely to be caused by the difference in the surfactant concentration. However the increase from 20 wt% to 30 wt% surfactant appears to have had less of an effect, if anything a larger pore size distribution can be seen. The same discrepancy between the pore size distributions can be seen in **Figure 109**. The higher water volume ratios (8 ml) PolyHIPEs with 30wt% surfactant have a larger pore size distribution than the 20wt% surfactant PolyHIPEs when both emulsions were prepared at 50°C. The pore size increased from 20 to 30wt% surfactant, however in theory the pore size distribution should either decrease or remain the same with an increase in the surfactant concentration, but an increase in the pore size is shown in **Figure 109** between images **B** and **C**. The two main factors to consider is the effect of the high temperature, as well as the effect this will have on the surfactant. Increasing the temperature and surfactant may be causing the surfactant

to become more miscible in the water phase, which will cause a destabilisation of the emulsion resulting in larger pores.

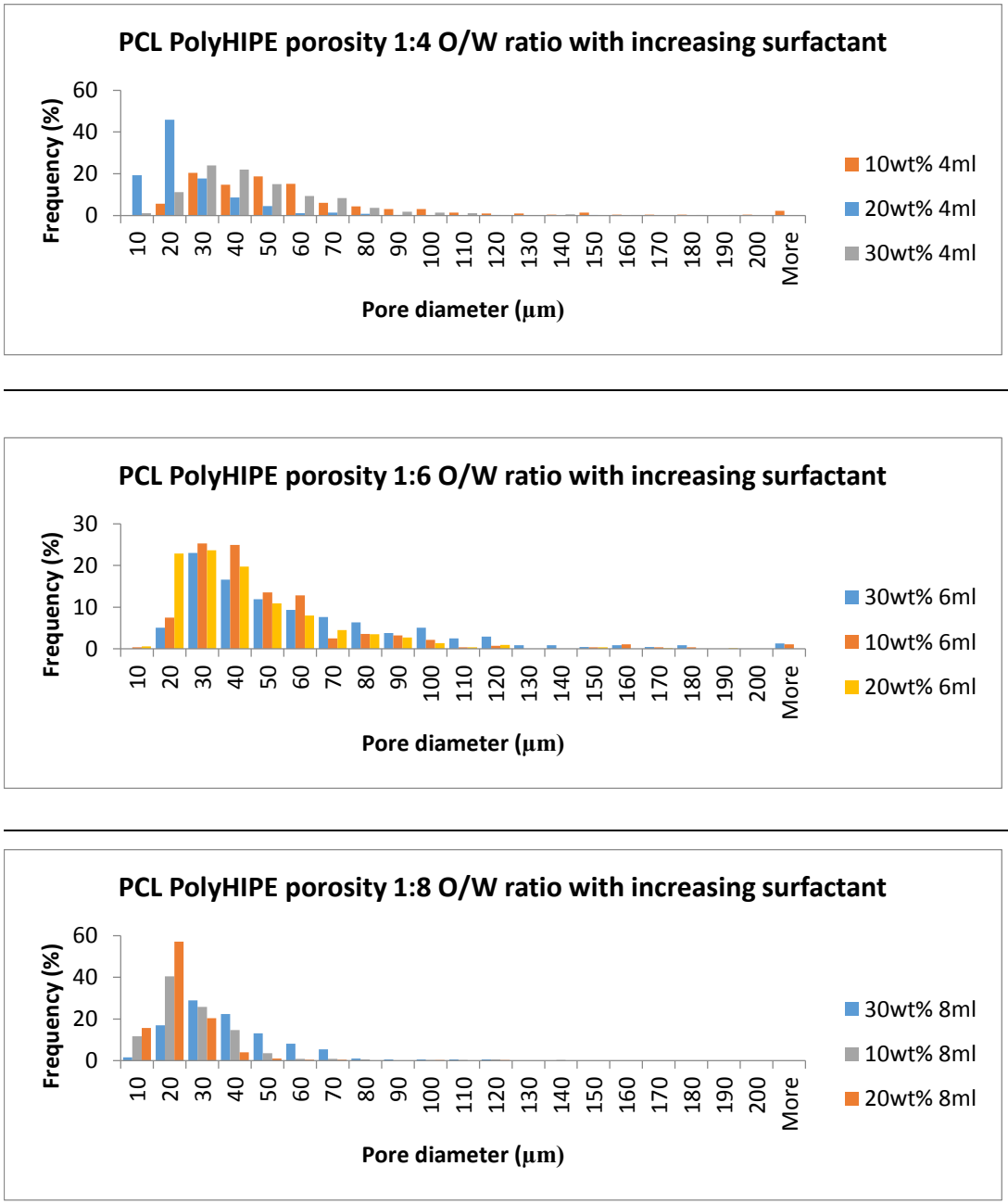

Figure 107: Histogram diagram showing the pore size against its frequency for the 60°C PCL PolyHIPE from increasing the surfactant concentration within each water volume ratio

With 4ml water volume ratio increasing the surfactant from 10 – 30 wt% caused a decrease in the pore size distribution, with 6ml having the most narrow distribution (10-80 µm) in comparison to the 10 wt% and 30 wt% of water (20-200+ µm) and (10

– 190 μm) **Figure 107**. This suggests that the increase in the surfactant has caused an increase in the stability of the low water volume PCL emulsion.

For the 6 ml PCL PolyHIPE increasing the surfactant concentration from 10-30 wt% caused a gradual broadening of the pore size distribution (**Figure 107)**. No direct trend can be seen. This is understandable as the 6 ml water volume ratio PCL PolyHIPE samples did not follow the intermediate trend between the 4 ml and 8 ml volume ratio samples as seen previously in **Figure 106.**

For the 8ml water volume ratio samples there is a gradual decrease in the pore size distribution from increasing the surfactant from 10-30 wt% (20-200+ μm) to (10-120 μm), the pore size distribution decreases sharply from the 10 to 20 wt% (10-70 μm), and increases from 20-30 wt%. Sample SEM images of the 60°C PCL PolyHIPE with 8ml water volume ratio are given in **Figure 109**.

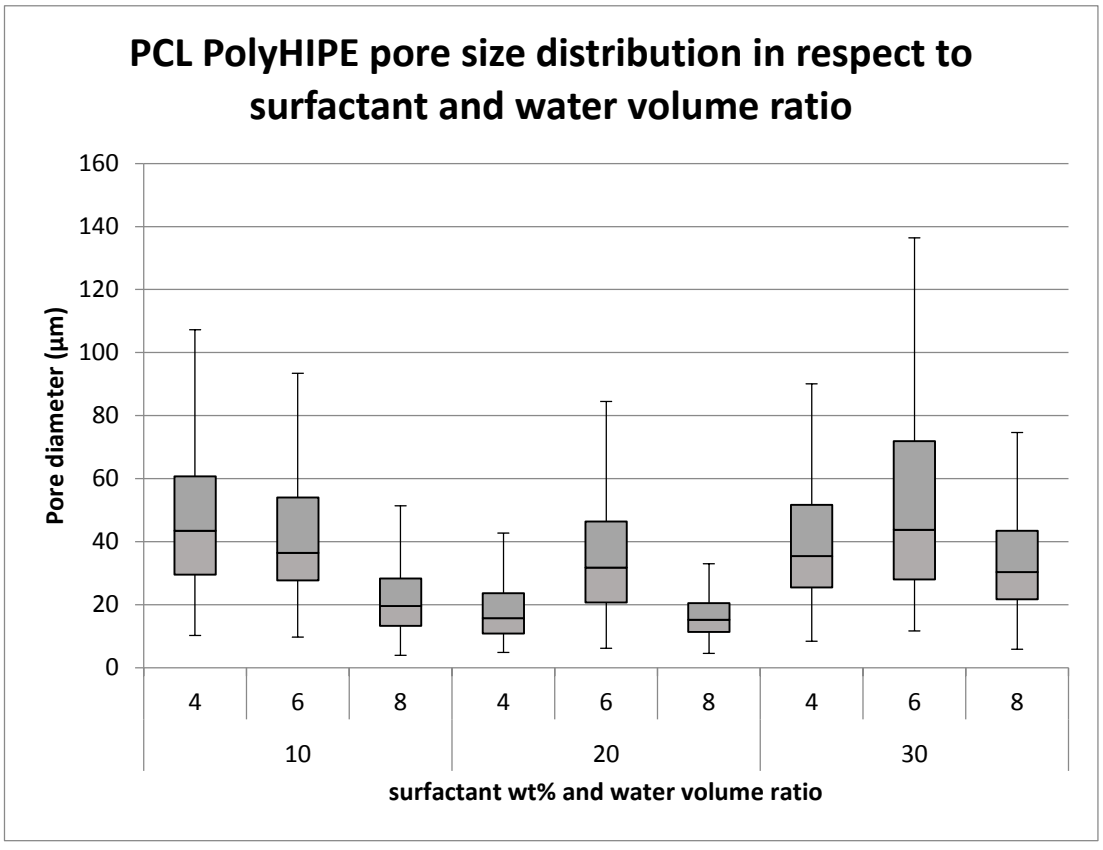

Figure 108: Box and whisker diagram showing the pore diameter and the variability above and below the upper and lower quartiles with respect to the surfactant concentration (10, 20 and 30wt %) and the respective water volume ratios within each surfactant concentration, 4, 6 and 8ml.

The box plot diagram in **Figure 108** shows the overall variation within the pore size distribution for the different surfactant concentrations and water volume ratios. A decrease in the overall pore diameter occurs between all the 4ml and 8ml water volume ratio samples, with the 20 wt% surfactant showing the lowest pore diameter distribution in comparison to the other plots. The 6ml water additions all have a large range of measured pore sizes which correlates to the previous findings that there is not a reliable trend between the 6 ml water volume ratios for the 20 and 30 wt% surfactant PCL PolyHIPE samples.

7.8.1. Effect of temperature on the emulsion stability: 8 ml water volume ratio

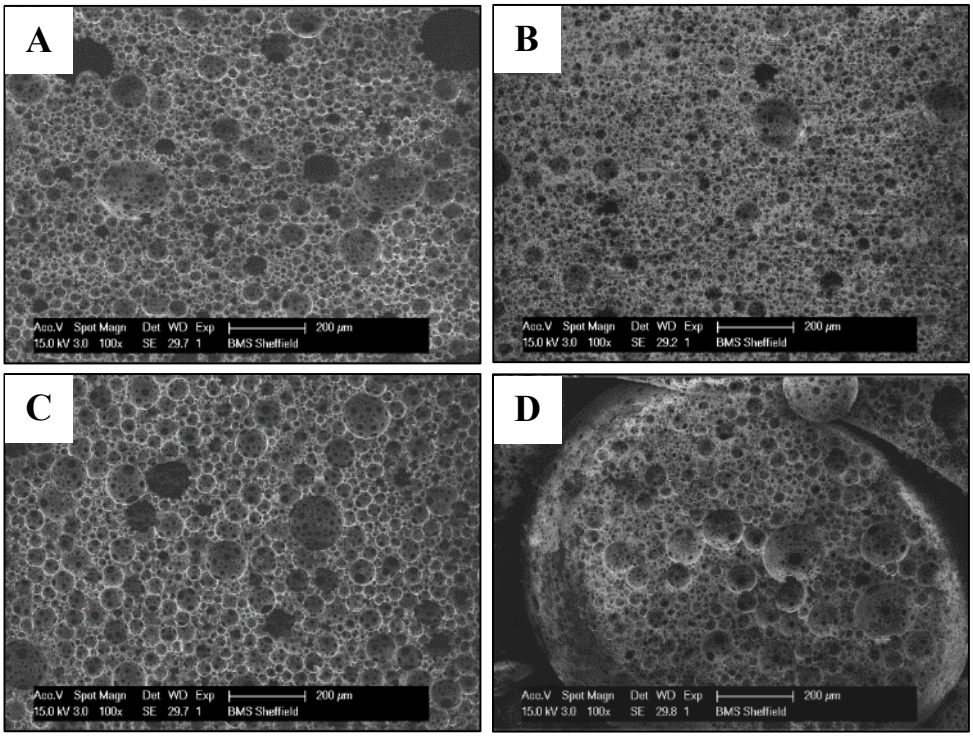

Figure 109: PCL based PolyHIPE with increasing surfactant concentration from 10-20wt% using, 8ml water, **A-C** were mixed at 60°C. **A**, 10wt%. **B,** 20wt%. **C**,30wt%. **D**,30wt% at 50°C. The surfactant causs a decrease in pore volume from 10-20wt%, however the 20-30wt% has an incrase in pore volume. The same formulation at 50 °C has a more intermitent pore size. This suggests that temperature is having a significant effect on the pore volume as well as the surfactant concentration.

The most significant effect of the relationship between the temperature and surfactant is shown in **Figure 109**. It was only at the higher temperature of 60°C that the high amount of surfactant (30wt %) in the emulsion, that it was able to incorporate the high

water volume (8 ml). While at 50°C a W/O/W emulsion was formed with the other parameters kept the same, these resulted in the large bulbs of PolyHIPE joining together in **Figure 100.**

The lower surfactant PCL PolyHIPEs were able to stabilise the emulsion with 8 ml water addition without the same difficulties as the higher (30wt %) surfactant concentrations. This suggests that there is a strong interplay between the temperature, surfactant and emulsion stability, and the high surfactant concentration of 30wt% is no longer increasing the stability of the emulsion, and if anything it could be having a detrimental effect at these elevated temperatures. The emulsion stability depends on the surfactants adsorption at the water/oil interface, and any factors that affect the surfactant will also have an effect on the stability of the emulsion. At the elevated temperatures the surfactant will become more miscible in the aqueous phase of the emulsion, which would increase the likelihood of it facilitating the transfer of water molecules through the barrier film. This will be further increased when combined with the reduction in oil phase viscosity, and increased kinetic energy of the water molecules. Using the same Hypermer B246 surfactant the increase in temperature to 80^{o}C has been used to increase the average pore size distribution through a controlled destabilisation brought on by the high temperature [21].

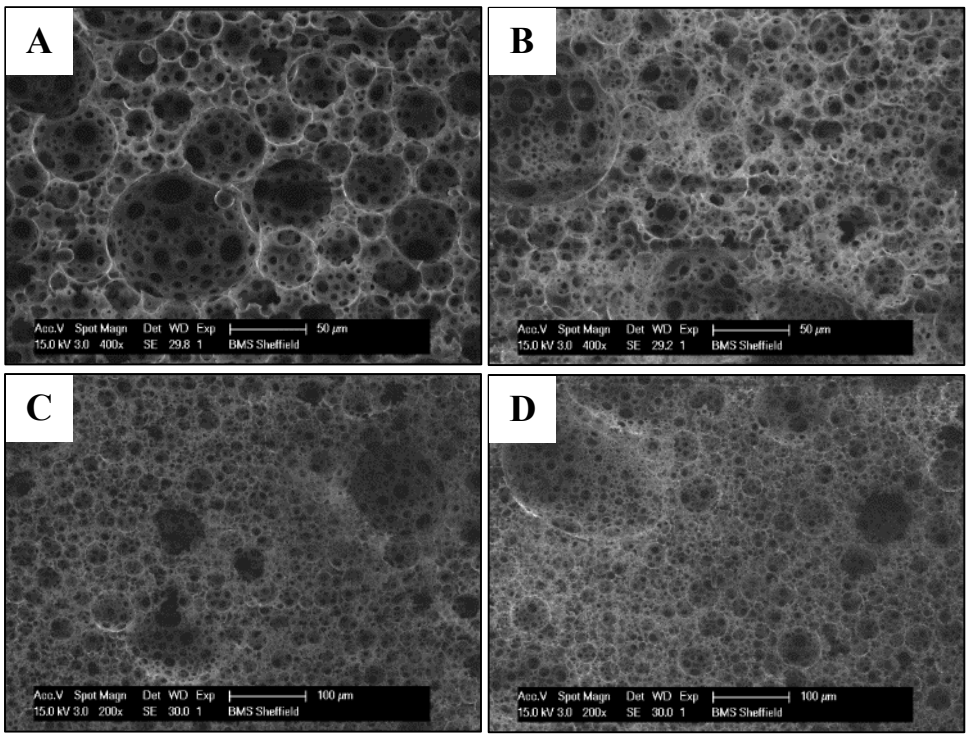

Figure 110. SEM images of the chosen PolyHIPE formulation that will take forward for future work. **A** 20wt% surf 8ml 50°C**. B**, 20wt% 8ml, 60°C. **C** and **D** 20wt% surfactant 8 ml 60°°C at 200x magnification

7.8.2. HIPE preparation at room temperature

The next question to consider is how to further improve the stability of the emulsion, as increasing the surfactant concentration is not increasing the stability of the emulsion with the 50-60°C temperatures. The temperature needs to be reduced while maintain the emulsion stability.

A more stable emulsion will enable its use within a direct laser write approach and for the production of porous particles, both techniques rely on a stable emulsion over the course of a 10's of minutes and up to an hour with the porous particle synthesis. Both techniques and other post processing methods of the emulsion require it to be stable and have a good degree of handleability.

Most of the HIPE formulations in **Table 9** separated out as they cooled down to room temperature. However some of the formulations remained stable afterwards. These were polymerised and the resulting SEM images are shown in **Figure 111**.

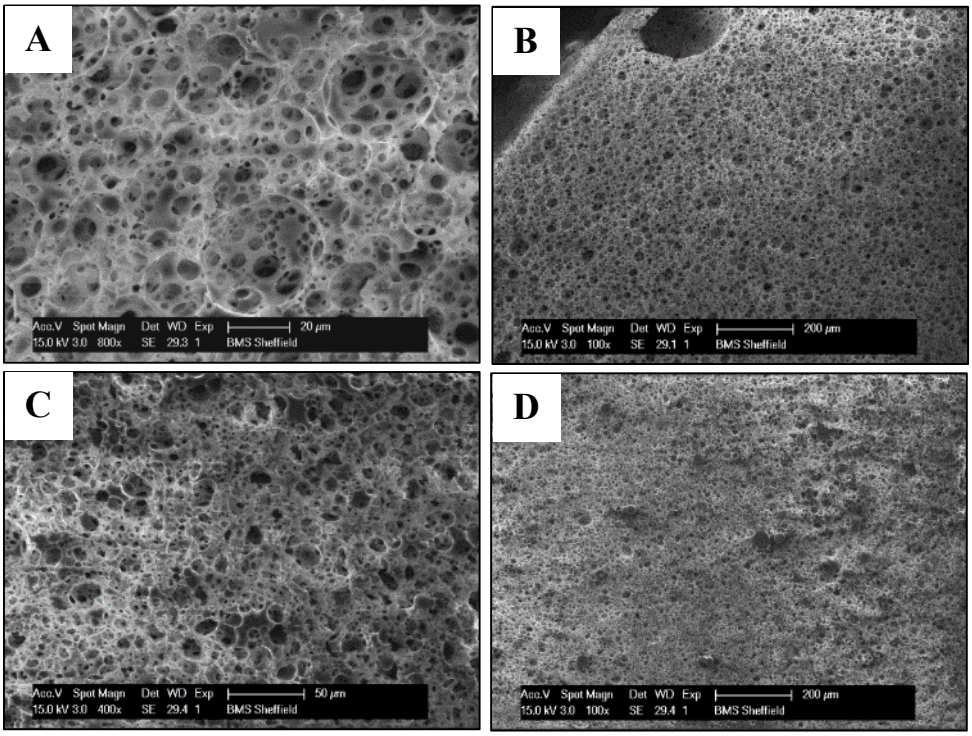

Figure 111:.**A** and **B**, 30wt%surf 6 ml water, 50°C cold. **C** and **D** 20wt% 4ml 50 °C cold.

The stability of the cold emulsions show that the emulsion can be prepared at an elevated temperature, and then slowly cooled to create an emulsion that is stable at room temperature. The SEM images in **Figure 111** show PolyHIPEs prepared from the cold emulsions consisting of 20 and 30 wt% surfactant. Visually the PolyHIPE shrank during the drying process which may explain the smaller pore sizes than the previously higher temperature PolyHIPEs.

A two fold decrease in the viscosity of the emulsion has been demonstrated with a Fumarate-based PolyHIPE by adding 40-60% of the porogenic solvent toluene [4], therefore I focused on adjusting the solvent blend as well as increasing the water phase volume ratio of the PCL emulsion to increase the viscosity of the HIPE as a means to stabilise it more. It is already known that by increasing the water volume ratio of an emulsion causes the droplets to deform into a more polyhedral shape, this contributes to the increase in the emulsion viscosity [40], also the emulsion viscosity has an inverse relationship with the average droplet size [98], so as the emulsion degrades its viscosity will decrease. Furthermore the solvent blend and volume used is vital because it has to be tailored to find the minimum amount of dilution that can be used

to create a stable emulsion, while maintaining the PolyHIPE integrity, as there is a finite range where the solvent can be beneficial to the emulsion stability [4].

To increase the stability of the emulsion a lower toluene was used. 0.15 – 0.2 g of toluene was used for every 1 g chloroform. The emulsion stability was increased by both leaving the emulsion to mix for longer at a temperature of 30-35°C. Occasionally the emulsion is pipetted up and down using a glass pipette to increase the degree of mixing when a layer of water started to form on the top surface, a more efficient mixing tool will not require this extra step. The emulsion had a gradual transition from having a slight yellow tint to a 'white appearance' that was characteristic of a HIPE. If the emulsion turned white straight away this indicated that the emulsion had inverted and there was a suspension of droplets of PCL within the water.

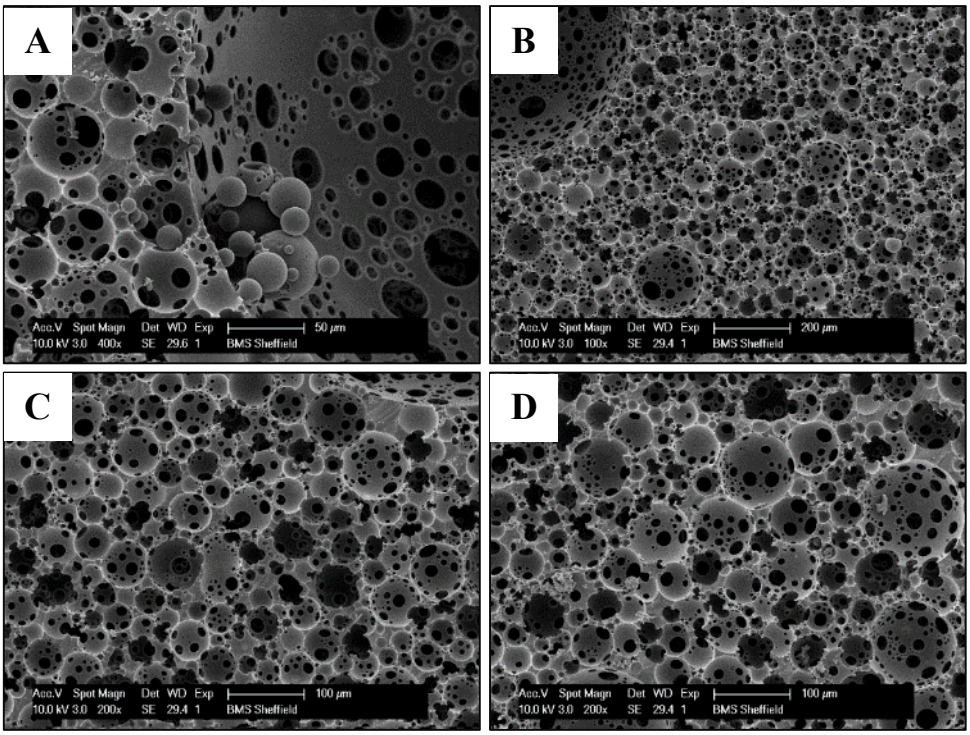

Figure 112: SEM images of the PCL PolyHIPE produced at 35°C in a bulk batch, 10wt% surfactant, with 80% water volume was used. The HIPE was prepared using 3g of PCL, 3g $CHCl_3$ and 1.8 g toluene. PolyHIPE samples were carbon coated prior to imaging. Image **A** shows some PCL particles that have formed within one of the larger pores. **B** – **D** show the PolyHIPE at different magnifications.

An overhead stirrer was used with an increased amount of the oil phase consisting of a total of 7.8 g, requiring the addition of 31.2 ml of water all at 35°C. The decrease in the emulsion temperature to 35°C meant that the emulsion remained stable after the mixing had stopped. The PCL based PolyHIPE shown in **Figure 112** and **Figure 113**

were prepared using a new batch of PCL. A tentative explanation to the increase instability may also be due to the methacrylation stage and post process purification stages of the PCL. These may have an effect on the hydrophobicity and viscosity of the PCL.

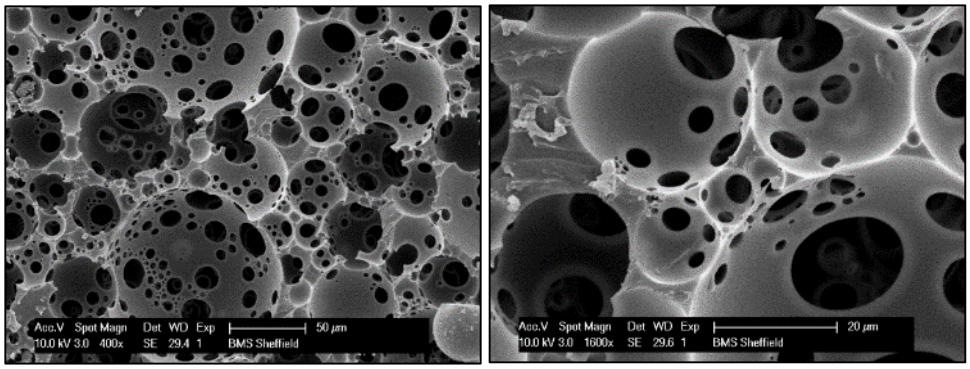

Figure 113: PCL PolyHIPE with 0.15g toluene, bulk cured at 35°C

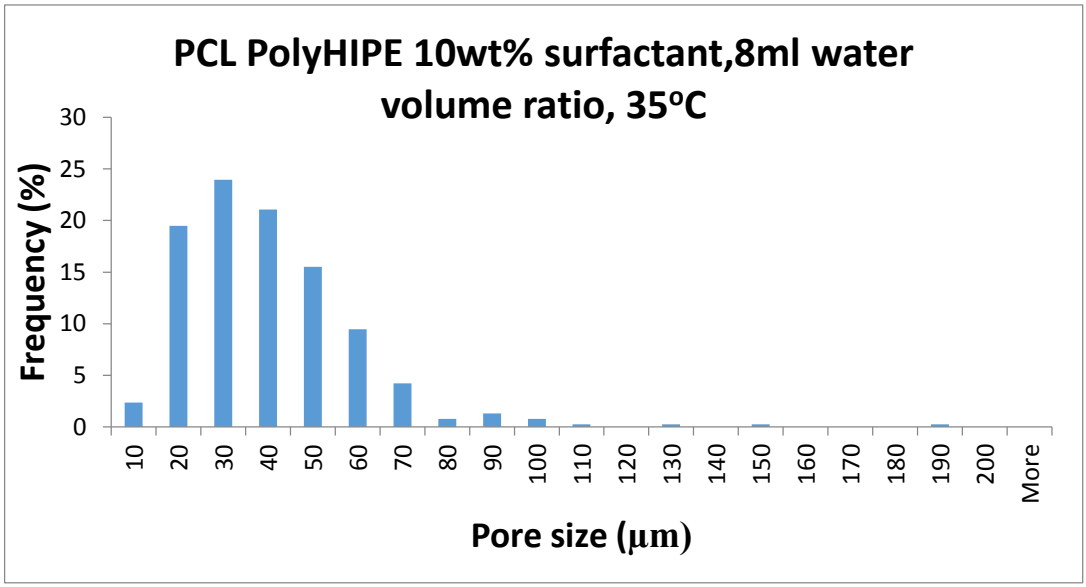

Figure 114: Histogram diagram for the pore size distribution of the 35 ℃ prepared PCL PolyHIPE shown in **Figure 112**

The PCL PolyHIPE prepared at 35°C has a pore size distribution ranging from 10-100 µm with a few pores measured at 150 and 190 µm. This is a similar range that was achieved using 10 wt% surfactant with 8 ml of water at 65°C. A tentative statement at

this stage is that the lower temperature more stable HIPE produces a similar porosity distribution as the higher temperature one with the same surfactant and water volume ratio. This also highlights that the lower surfactant volumes appear to have the most stability than the higher 20 and 30 wt% ones.

7.9 PCL PolyHIPE Beads

Porous beads made from PCL PolyHIPE have the potential to offer a two-tied layer of porosity. The micro porosity of the beads can be controlled by the emulsion conditions, while the 'macro porosity' of the spaces between adjacent particles can be controlled by tailoring the size of the beads. For example a monodisperse distribution of spheres will have a lower packing density than a polydisperse one [1]. The PCL based PolyHIPE remained stable for an hour while being housed in a syringe and injected into flowing water inside a silicone tube. The hydrophobic nature of the monomeric solution used in the HIPE preparation caused the emulsion to form spherical beads in the water due to the surface tension created by the hydrophobic material interacting with the water.

The slow injection of the PolyHIPE into the flowing water in the tube caused it to bud off into smaller beads forming a water in oil in water emulsion (W/O/W), which is then transported to a large water beaker in a light box that had a constant high UV light exposure. The water was recirculated to ensure the sufficient polymerisation of the PCL PolyHIPE beads. This method was chosen as the HIPE was insufficiently polymerised when the silicone tube was coiled inside the UV enclosure, and the particles collapsed afterwards due to insufficient crosslinking.

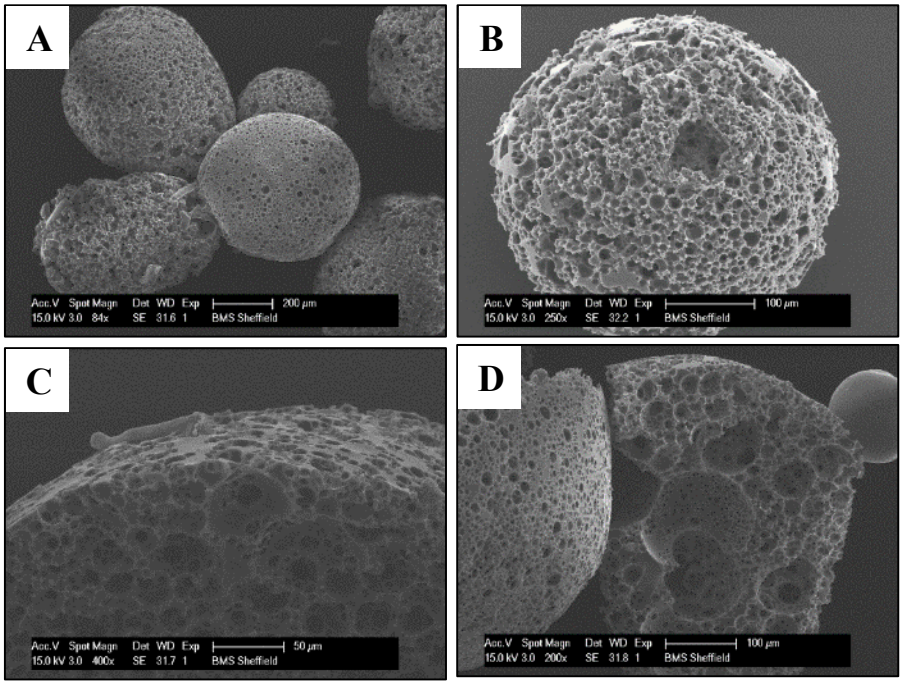

Figure 115: SEM images of the Porous PCL PolyHIPE beads. **A-D** PCL PolyHIPE beads produced by injecting the emulsion into a flowing tube of water. **A**, a few beads with a small degree of openness on the outer surface. **B,** a single bead. **C,** side section of one of the beads. **D**, Porous bead that has been cut in half. A high degree of porosity can be seen within the material.

Porous PCL PolyHIPE particles were fabricated and the corresponding SEM images are shown in **Figure 115** and **Figure 116**. The PolyHIPE has maintained its internal porosity during this fabrication technique and the outer surface of the beads have an open pored nature.

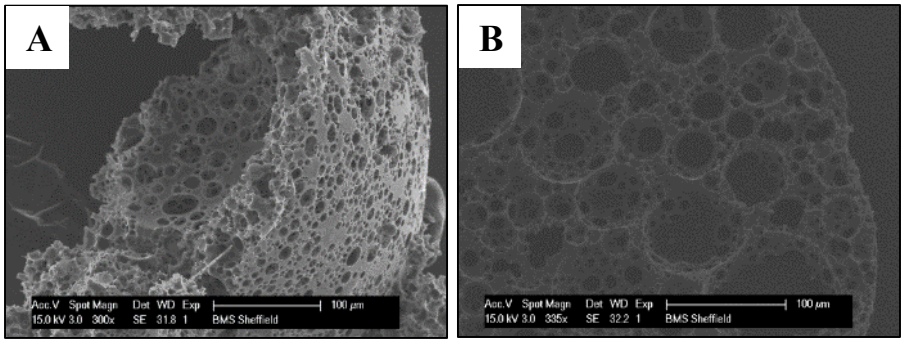

Figure 116: SEM images of PCL porous beads. A, a fractured PCL bead showing the internal porosity. B, a sectioned PCL PolyHIPE bead (70µm slice) to show the internal porosity.

7.10 Summary

To illustrate the experimental procedures described in this chapter to formulate a stable PCL PolyHIPE the methodology has been shortened here below. The key parameters for emulsion stability, and their discovery thereof are highlighted. The experimental procedures were done at the same time with the PCL/Thiol emulsion work as the two experiments complimented each other. Different parameters were always altered in isolation to determine their effect, and to increase the amount of parameters that could be altered from a limited supply of photocurable PCL the minimum volume for the emulsion rig was used, which was 1 ml.

Visual monitoring of the emulsion is vital, and the influence of each parameter needs to be noted. The efficiency of the mixing is important, occasionally the water needed to be pipetted into the emulsion directly as opposed to dropping it on the top surface to determine if it was the mixing efficiency or other factors that was preventing the large volume of water being added to the emulsion.

1. The use of the hydrophobic polar solvent chloroform was chosen as it was demonstrated previously for the preparation of a thiolene based emulsion [21].
2. Blended emulsions with the thiolene and PCL were unstable at first when substituting 50% of the thiolene for PCL. However the addition of methanol allowed for a slight increase in the amount of water that could be added before emulsion inversion.
3. Experimenting with different chloroform/methanol blends was unsuccessful for high volumes of water.
4. Increasing the surfactant concentration failed to increase the stability of the emulsion.
5. Therefore temperature was chosen to reduce the viscosity of the liquids. This resulted in a slight increase in the volume of water being successfully added to the emulsion without inverting.
6. The emulsion was prepared to the point just before inversion, increasing the chloroform at this point created a more stable emulsion, however it did not allow for the extra addition of water.
7. The surfactant was changed from the Hypermer B246 to Span 80 as it has a lower HLB value (4.2 from 5.6) to increase the emulsion stability. This

surfactant has been used previously in the literature for a PCL blended PolyHIPE [64].

8. Initial experiments with Span 80 and different concentrations was unsuccessful for adding high volumes of water.
9. The surfactant was changed back to Hypermer B246 and the solvent type and ratio was altered instead.
10. The addition of toluene caused the emulsion to invert into droplets straight away.
11. I noted that the excess chloroform held the emulsion together more, and excess water only ever pooled on the top surface, therefore I decided to add toluene to this emulsion as it should encourage the emulsion separation enough to allow the extra water volume to be added.
12. Different chloroform to toluene ratios were tested at the elevated temperature.
13. Emulsion stability was increased at room temperature. The emulsion was originally prepared with only chloroform and toluene was added when it would no longer mix with the water. Fine adjustment of the volumes created a stable emulsion.
14. For increased stability a longer duration (minimum of 5 minutes) of mixing was used to increase the viscosity of the emulsion, as well as adding a high amount of water to further increase the emulsion viscosity aided the emulsion stability after agitation.
15. There were slight variations between different methacrylated batches of PCL, which could have accounted to slight variances in the emulsion preparation.

7.11 Conclusions

An emulsion between a blend of PCL and thiolene was successfully created and polymerised to produce a PCL/Thiolene PolyHIPE. This material supported the growth and attachment of human dermal fibroblast cells for 5 days. A blend of the two solvents chloroform and toluene were essential for a stable emulsion.

PCL PolyHIPEs were created and the complex interplay between the temperature, surfactant, solvent amount and type as well as the resulting porosity and its effect on the PolyHIPE morphology was demonstrated.

The solvent blend between chloroform and toluene were essential for the preparation of a PCL HIPE. There was a narrow window between the ratios of these two solvents to produce a stable emulsion.

A high temperature in the original emulsion resulted in a high amount of destabilisation which caused the formation of larger pores. Increasing the surfactant above 20wt% seemed to cause an increase in the destabilisation of the emulsion at the higher temperatures. The positive gain from temperature in terms of emulsion preparation has been counterbalanced by the increased destabilisation after the mixing was stopped.

The mixing efficiency was vital for the emulsion preparation, at lower water volumes the small batches were mixed sufficiently, whereas at higher water volume ratios (1:8) the mixing may have been inefficient to create a homogeneous emulsion.

PCL based PolyHIPE was eventually prepared at 35^{o}C which was stable over an hour without any visual significant destabilisation. This lower temperature more stable PCL HIPE has a significant advantage in its stability for the use in other more complex stereolithography based applications.

8. CHAPTER NINE: FUTURE WORK

The initial HIPE structuring at the beginning of this thesis covers the ground for the potential development of the material for tissue engineering applications. The different pre-processing parameters of the emulsion its subsequent effect on the final PolyHIPE morphology after fabrication by stereolithography have been demonstrated. The PolyHIPE retains its internal morphology and the two structuring techniques; projection and scanning stereolithography were used to produce a range of novel structures. Further work is required to develop these materials for specific applications. The micro architecture, material and chemical properties will need to be tailored towards a specific cell type to produce a porous scaffold that mimics the cells native environment. The use of a photocurable monomeric material means that these properties can be fine tunes reproducibly for different applications. This has been demonstrated to a preliminary level. The potential for future work is to fine tune the porosity, morphology and mechanical properties towards cell specific applications.

The surface skin effect is currently reduced by using a toxic light absorber Tinuvin. This is not an issue with the non-degradable PolyHIPEs, and sufficient washing of the sample removes any toxic residue, however alternative light absorbers which are more biocompatible will need to be used, especially for the stereolithography of a biodegradable PolyHIPE.

The PCL PolyHIPE protocol I have developed offers a good starting position for its comprehensive characterisation in regards to its long term cell viability, degradation and stereolithography structuring potential. The reproducibility of the PCL methacrylation needs to be improved for increased control over the PCL PolyHIPE material, and the degradation characterised in respect to the PolyHIPE morphology.

The blended PCL/thiolene PolyHIPE can be successfully polymerised around a PHBC electrospun scaffold. The next stages of this will be to incorporate the PolyHIPE around a vascularised perfusable network which has been developed previously in the group using a combination of robocasting and electrospinning with PHBV [96].

The subtractive manufacturing approach to remove PolyHIPE material to create bespoke structures with tailored porosity has the potential to be used in a high throughput mass produced process. Flat sheets of any PolyHIPE formulation can readily be created and post processed to create a secondary porosity without the need for any expensive stereolithography equipment. This technique does not have the same surface skin effect, and the etched interface retains its open porosity. The process is fully automated, reproducible and is built upon a widely used industrial method which means it can be readily adapted for mass production of bespoke scaffolds. Future research should take this technique forward with a comprehensive characterisation and surface analysis to determine if the etched interface has any effect on the growth of cells.

The initial work involving the PCL PolyHIPE particles was presented. This was in collaboration with Hossein Bahmaee and Tom Paterson. The future work on this requires a more extensive characterisation on the fabrication parameters and the cell culture.

9. APPENDIX

9.1.1. Stereo image of the PolyHIPE structure

The morphology of the PolyHIPE structure can be determined from SEM images, and the interconnectivity and porosity calculated from these images. However they are still a two dimensional image of a three dimensional structure, and cannot fully portray the nature of the 3D porosity of the PolyHIPE.

Stereo images provide extra information on the topographical surface and enable the viewer to have a better understanding of the spatial relationship between different features by allowing them to view the surface in 3D. The uneven fractured surface will stands out and the stereo image gives a good degree of depth perception. This imaging process has been used previously to image the fine topographical details on a metallic surface [99], and to image the PolyHIPE morphology [29]. The PolyHIPEs interconnectivity is within a spherical 3D environment, stereo images can be beneficial by enabling the easy identification of the topographical features that are often not apparent in the 2D image.

Stereo images can be taken of the PolyHIPE which when viewed correctly give an extra degree of visual information about the 3D nature of the material, subtle details that may be missed with the conventional SEM images stand out more in the stereo ones, such as the interconnecting window distribution within the large voids relative to each other. An example of a stereo image is shown in **Figure *117***.

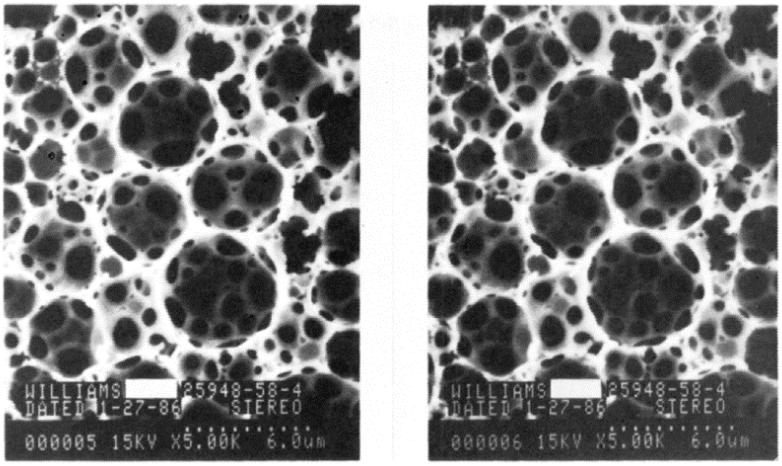

Figure 117: SEM Stereo image pair of a PolyHIPE containing 4.7% styrene/divinylbenzene (50/50) and 2.1% sorbitan monooleate. Image taken from [29]

To view the stereo image the easiest method is to cross your eyes (converge them). If the user crosses their eyes while looking at the two images, gradually as the images separate from each other a third image will become present in the middle of them. If the user relaxes his eyes to an extent so that the image overlaps in the middle then the 3D image will 'jump out', the easiest method is to try and overlap a specific point between the two images to make the overlapping easier. Essentially the left eye is now looking at the right image, and the right eye at the left one.

One way to cross your eyes is to focus on the tip of your nose, and you will observe that everything in your vision becomes doubled. If you then keep this double vision and then gradually bring your vision towards the pair of images you will see the images being widely separated in their respective pairs (you will see two sets of pairs). Gradually relax your eyes until the images start to come together and the middle images overlap to produce the 3D effect.

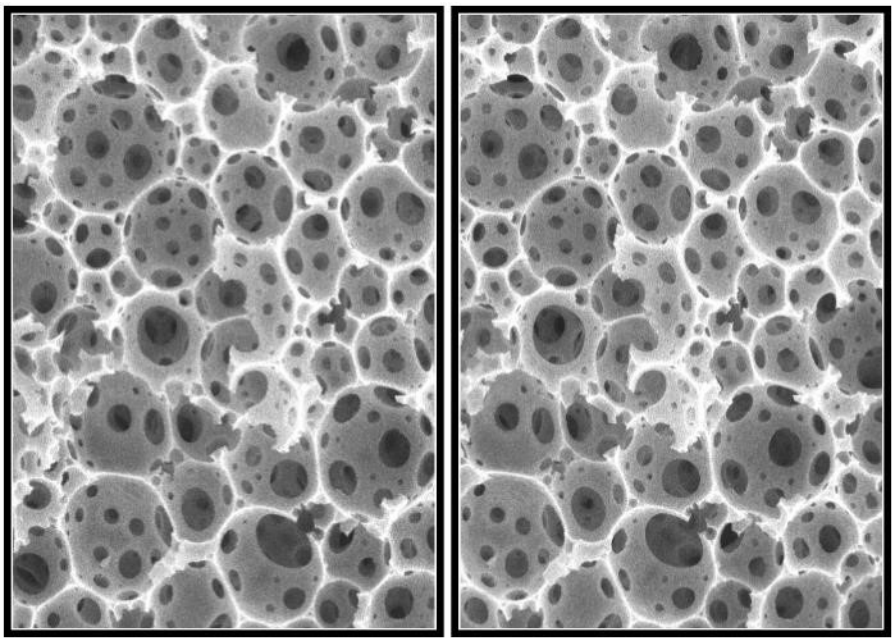

Figure 118: Pair of SEM stereo images of the EHA 75% PolyHIPE with 5wt% surfactant. Both images were taken at a different angle with the SEM to give a different perspective of the same region. The depth of the large pore and size of the pore behind it can be seen very clearly when viewed as a stereo image, this perspective is not shown when it is only viewed as a single SEM image. Stereo image created using StereoPhoto Maker *(http://www.stereo.jpn.org/eng/stphmkr)*

The stereo images can be overlaid in quick succession on a computer as a .gif file to give the illusion of a 3D effect, and has been used in presentations to illustrate that the PolyHIPE is a 3D porous material. The stereo images shown above and below in **Figure 118** and **Figure 119** give a sense of depth within the pores, which doesn't stand out when viewed as a single SEM image.

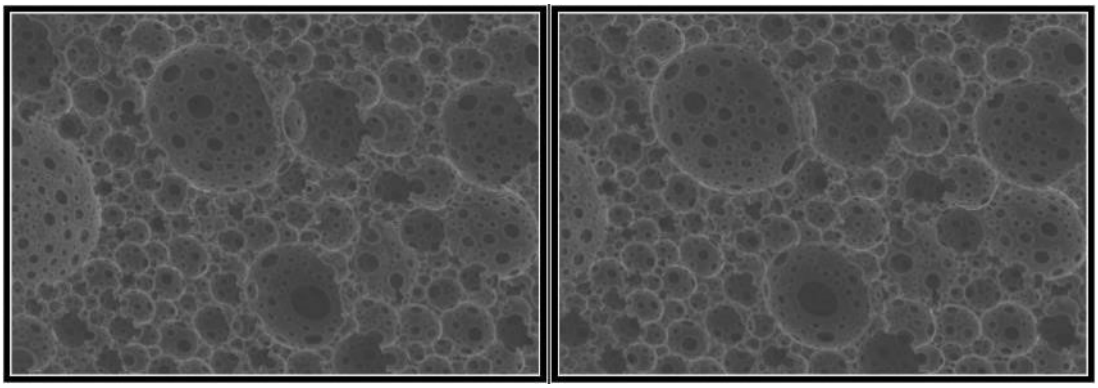

Figure 119: Pair of SEM stereo images of the PCL PolyHIPE cross section. These images are darker than the previous ones because the filament needed to be replaced, and the samples were carbon coated instead of being gold coated.

In **Figure 119** the SEM images don't fully represent the depth of the large pore seen in the central/left region of the image. However if view as a stereo image, the pore can be seen to be very deep, and also that overall the right hand side of the SEM image is raised more than the rest of the cross section. Either way this imaging technique only requires a few extra minutes to produce and provides extra information that may be missed otherwise.

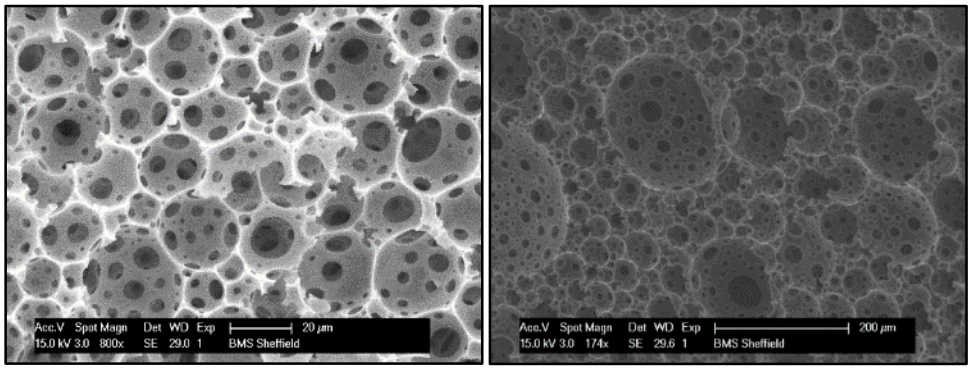

Figure 120: SEM images showing the scale bar for the SEM images in **Figure 118** and **Figure 119**.

Taking stereo images provide depth within the images, which is caused by the two images being taken at a different angles of the same region, each eye is used to viewing the world at different angles, and the difference in images which the brain receives gives us depth perception, both in real life and the stereo images.

10. References

[1] M.S. Silverstein, Emulsion-templated porous polymers: A retrospective perspective, Polymer 55(1) (2014) 304-320.
[2] I. Pulko, P. Krajnc, High internal phase emulsion templating–a path to hierarchically porous functional polymers, Macromolecular rapid communications 33(20) (2012) 1731-1746.
[3] N.R. Cameron, High internal phase emulsion templating as a route to well-defined porous polymers, Polymer 46(5) (2005) 1439-1449.
[4] E.M. Christenson, W. Soofi, J.L. Holm, N.R. Cameron, A.G. Mikos, Biodegradable fumarate-based polyHIPEs as tissue engineering scaffolds, Biomacromolecules 8(12) (2007) 3806-3814.
[5] T.F. Tadros, Emulsion formation and stability, John Wiley & Sons2013.
[6] A.S. Hayward, N. Sano, S.A. Przyborski, N.R. Cameron, Acrylic-Acid-Functionalized PolyHIPE Scaffolds for Use in 3D Cell Culture, Macromolecular rapid communications 34(23-24) (2013) 1844-1849.
[7] T.H.M. Lau, L.L.C. Wong, K.-Y. Lee, A. Bismarck, Tailored for simplicity: creating high porosity, high performance bio-based macroporous polymers from foam templates, Green Chemistry 16(4) (2014) 1931-1940.
[8] S.J. Pierre, J.C. Thies, A. Dureault, N.R. Cameron, J.C.M. van Hest, N. Carette, T. Michon, R. Weberskirch, Covalent enzyme immobilization onto photopolymerized highly porous monoliths, Advanced Materials 18(14) (2006) 1822-1826.
[9] A. Richez, H. Deleuze, P. Vedrenne, R. Collier, Preparation of ultra-low-density microcellular materials, Journal of applied polymer science 96(6) (2005) 2053-2063.
[10] L.C. Wong, Hierarchical Macroporous Polymers: Synthesis and Characterisation, (2013).
[11] R. Foudazi, P. Gokun, D.L. Feke, S.J. Rowan, I. Manas-Zloczower, Chemorheology of Poly (high internal phase emulsions), Macromolecules 46(13) (2013) 5393-5396.
[12] N.R. Cameron, D.C. Sherrington, L. Albiston, D.P. Gregory, Study of the formation of the open-cellular morphology of poly (styrene/divinylbenzene) polyHIPE materials by cryo-SEM, Colloid and Polymer Science 274(6) (1996) 592-595.
[13] N.R. Cameron, D.C. Sherrington, High internal phase emulsions (HIPEs)—structure, properties and use in polymer preparation, Biopolymers liquid crystalline polymers phase emulsion, Springer1996, pp. 163-214.
[14] R.J. Carnachan, M. Bokhari, S.A. Przyborski, N.R. Cameron, Tailoring the morphology of emulsion-templated porous polymers, Soft Matter 2(7) (2006) 608-616.
[15] T. Gitli, M.S. Silverstein, Bicontinuous hydrogel–hydrophobic polymer systems through emulsion templated simultaneous polymerizations, Soft Matter 4(12) (2008) 2475-2485.
[16] M.R. Moghbeli, M. Shahabi, Morphology and mechanical properties of an elastomeric poly (HIPE) nanocomposite foam prepared via an emulsion template, Iranian Polymer Journal 20(5) (2011) 343-355.
[17] Y. Lumelsky, M.S. Silverstein, Biodegradable porous polymers through emulsion templating, Macromolecules 42(5) (2009) 1627-1633.

[18] I. Gurevitch, M.S. Silverstein, Polymerized pickering HIPEs: effects of synthesis parameters on porous structure, Journal of Polymer Science Part A: Polymer Chemistry 48(7) (2010) 1516-1525.
[19] S.D. Kimmins, P. Wyman, N.R. Cameron, Photopolymerised methacrylate-based emulsion-templated porous polymers, Reactive and Functional Polymers 72(12) (2012) 947-954.
[20] D. Cummins, P. Wyman, C.J. Duxbury, J. Thies, C.E. Koning, A. Heise, Synthesis of functional photopolymerized macroporous polyHIPEs by atom transfer radical polymerization surface grafting, Chemistry of Materials 19(22) (2007) 5285-5292.
[21] S. Caldwell, D.W. Johnson, M.P. Didsbury, B.A. Murray, J.J. Wu, S.A. Przyborski, N.R. Cameron, Degradable emulsion-templated scaffolds for tissue engineering from thiol–ene photopolymerisation, Soft Matter 8(40) (2012) 10344-10351.
[22] S. Jerenec, M. Šimić, A. Savnik, A. Podgornik, M. Kolar, M. Turnšek, P. Krajnc, Glycidyl methacrylate and ethylhexyl acrylate based polyHIPE monoliths: Morphological, mechanical and chromatographic properties, Reactive and Functional Polymers 78 (2014) 32-37.
[23] M.T. Gokmen, W. Van Camp, P.J. Colver, S.A.F. Bon, F.E. Du Prez, Fabrication of porous "clickable" polymer beads and rods through generation of high internal phase emulsion (HIPE) droplets in a simple microfluidic device, Macromolecules 42(23) (2009) 9289-9294.
[24] S.D. Kimmins, N.R. Cameron, Functional porous polymers by emulsion templating: recent advances, Advanced Functional Materials 21(2) (2011) 211-225.
[25] M. Sušec, S.C. Ligon, J. Stampfl, R. Liska, P. Krajnc, Hierarchically Porous Materials from Layer-by-Layer Photopolymerization of High Internal Phase Emulsions, Macromolecular rapid communications (2013): 938-943.
[26] J.L. Robinson, R.S. Moglia, M.C. Stuebben, M.A.P. McEnery, E. Cosgriff-Hernandez, Achieving interconnected pore architecture in injectable polyHIPEs for bone tissue engineering, Tissue Engineering Part A 20(5-6) (2014) 1103-1112.
[27] A. Menner, A. Bismarck, New evidence for the mechanism of the pore formation in polymerising high internal phase emulsions or why polyHIPEs have an interconnected pore network structure, Wiley Online Library, pp. 19-24.
[28] R.J. Carnachan, Emulsion-derived (PolyHIPE) foams for structural materials applications, (2004).
[29] J.M. Williams, Toroidal microstructures from water-in-oil emulsions, Langmuir 4(1) (1988) 44-49.
[30] A. Barbetta, N.R. Cameron, Morphology and surface area of emulsion-derived (PolyHIPE) solid foams prepared with oil-phase soluble porogenic solvents: Span 80 as surfactant, Macromolecules 37(9) (2004) 3188-3201.
[31] P. Taylor, Ostwald ripening in emulsions, Advances in colloid and interface science 75(2) (1998) 107-163.
[32] J.M. Williams, D.A. Wrobleski, Spatial distribution of the phases in water-in-oil emulsions. Open and closed microcellular foams from cross-linked polystyrene, Langmuir 4(3) (1988) 656-662.
[33] J.M. Williams, A.J. Gray, M.H. Wilkerson, Emulsion stability and rigid foams from styrene or divinylbenzene water-in-oil emulsions, Langmuir 6(2) (1990) 437-444.

[34] S. Huš, P. Krajnc, PolyHIPEs from Methyl methacrylate: Hierarchically structured microcellular polymers with exceptional mechanical properties, Polymer 55(17) (2014) 4420-4424.
[35] J.M. Williams, High internal phase water-in-oil emulsions: influence of surfactants and cosurfactants on emulsion stability and foam quality, Langmuir 7(7) (1991) 1370-1377.
[36] P. Pakeyangkoon, R. Magaraphan, P. Malakul, M. Nithitanakul, Effect of soxhlet extraction and surfactant system on morphology and properties of poly (DVB) polyHIPE, Wiley Online Library, pp. 149-156.
[37] A.S. Kabalnov, E.D. Shchukin, Ostwald ripening theory: applications to fluorocarbon emulsion stability, Advances in Colloid and Interface Science 38 (1992) 69-97.
[38] W.I. Higuchi, J. Misra, Physical degradation of emulsions via the molecular diffusion route and the possible prevention thereof, Journal of pharmaceutical sciences 51(5) (1962) 459-466.
[39] N. Cameron, D. Sherrington, Preparation and glass transition temperatures of elastomeric PolyHIPE materials, Journal of Materials Chemistry 7(11) (1997) 2209-2212.
[40] M.P. Aronson, M.F. Petko, Highly concentrated water-in-oil emulsions: Influence of electrolyte on their properties and stability, Journal of colloid and interface science 159(1) (1993) 134-149.
[41] F.P.W. Melchels, J. Feijen, D.W. Grijpma, A review on stereolithography and its applications in biomedical engineering, Biomaterials 31(24) (2010) 6121-6130.
[42] A. Bandyopadhyay, S. Bose, S. Das, 3D printing of biomaterials, MRS Bulletin 40(02) (2015) 108-115.
[43] D.W. Johnson, C. Sherborne, M.P. Didsbury, C. Pateman, N.R. Cameron, F. Claeyssens, Macrostructuring of Emulsion-templated Porous Polymers by 3D Laser Patterning, Advanced Materials (2013).
[44] P.S. Gandhi, S. Deshmukh, A 2D optomechanical focused laser spot scanner: analysis and experimental results for microstereolithography, Journal of Micromechanics and Microengineering 20(1) (2010) 015035.
[45] F. Claeyssens, E.A. Hasan, A. Gaidukeviciute, D.S. Achilleos, A. Ranella, C. Reinhardt, A. Ovsianikov, X. Shizhou, C. Fotakis, M. Vamvakaki, Three-dimensional biodegradable structures fabricated by two-photon polymerization, Langmuir 25(5) (2009) 3219-3223.
[46] V. Melissinaki, A.A. Gill, I. Ortega, M. Vamvakaki, A. Ranella, J.W. Haycock, C. Fotakis, M. Farsari, F. Claeyssens, Direct laser writing of 3D scaffolds for neural tissue engineering applications, Biofabrication 3(4) (2011) 045005.
[47] F. Causa, P.A. Netti, L. Ambrosio, A multi-functional scaffold for tissue regeneration: the need to engineer a tissue analogue, Biomaterials 28(34) (2007) 5093-5099.
[48] Y. Lumelsky, I. Lalush-Michael, S. Levenberg, M.S. Silverstein, A degradable, porous, emulsion-templated polyacrylate, Journal of Polymer Science Part A: Polymer Chemistry 47(24) (2009) 7043-7053.
[49] I.K. Kwon, T. Matsuda, Photo-polymerized microarchitectural constructs prepared by microstereolithography (μSL) using liquid acrylate-end-capped trimethylene carbonate-based prepolymers, Biomaterials 26(14) (2005) 1675-1684.
[50] M. Bokhari, R.J. Carnachan, S.A. Przyborski, N.R. Cameron, Emulsion-templated porous polymers as scaffolds for three dimensional cell culture: effect of

synthesis parameters on scaffold formation and homogeneity, Journal of Materials Chemistry 17(38) (2007) 4088-4094.
[51] S. Prakash, S. Kumar, Fabrication of microchannels: A review, Proceedings of the Institution of Mechanical Engineers, Part B: Journal of Engineering Manufacture (2014) 0954405414535581.
[52] I.A. Choudhury, S. Shirley, Laser cutting of polymeric materials: an experimental investigation, Optics & Laser Technology 42(3) (2010) 503-508.
[53] S. Prakash, S. Kumar, Profile and depth prediction in single-pass and two-pass CO2 laser microchanneling processes, Journal of Micromechanics and Microengineering 25(3) (2015) 035010.
[54] T. Baldacchini, S. Snider, R. Zadoyan, Two-photon polymerization with variable repetition rate bursts of femtosecond laser pulses, Optics express 20(28) (2012) 29890-29899.
[55] S. Jariwala, K. Venkatakrishnan, B. Tan, Single step self-enclosed fluidic channels via two photon absorption (TPA) polymerization, Optics Express 18(2) (2010) 1630-1636.
[56] S.H. Park, T.W. Lim, D.-Y. Yang, N.C. Cho, K.-S. Lee, Fabrication of a bunch of sub-30-nm nanofibers inside microchannels using photopolymerization via a long exposure technique, Applied physics letters 89(17) (2006) 173133.
[57] N.-H. Li, Y. Hsuanyu, J.R. Benson, M. Freed, Process for Reducing Residual Surface Material from Porous Polymers, Google Patents, 2010.
[58] S. Maruo, T. Hasegawa, N. Yoshimura, Single-anchor support and supercritical CO< sub> 2</sub> drying enable high-precision microfabrication of three-dimensional structures, Optics Express 17(23) (2009) 20945-20951.
[59] J.-W. Choi, R.B. Wicker, S.-H. Cho, C.-S. Ha, S.-H. Lee, Cure depth control for complex 3D microstructure fabrication in dynamic mask projection microstereolithography, Rapid Prototyping Journal 15(1) (2009) 59-70.
[60] L.H. Han, G. Mapili, S. Chen, K. Roy, Projection microfabrication of three-dimensional scaffolds for tissue engineering, Journal of Manufacturing Science and Engineering 130 (2008) 021005.
[61] P. Tayalia, C.R. Mendonca, T. Baldacchini, D.J. Mooney, E. Mazur, 3D Cell-Migration Studies using Two-Photon Engineered Polymer Scaffolds, Advanced materials 20(23) (2008) 4494-4498.
[62] B.A.M. Venhoven, A.J. De Gee, C.L. Davidson, Polymerization contraction and conversion of light-curing BisGMA-based methacrylate resins, Biomaterials 14(11) (1993) 871-875.
[63] R. Owen, C. Sherborne, T. Paterson, N.H. Green, G.C. Reilly, F. Claeyssens, Emulsion templated scaffolds with tunable mechanical properties for bone tissue engineering, Journal of the mechanical behavior of biomedical materials 54 (2016) 159-172.
[64] W. Busby, N.R. Cameron, C.A.B. Jahoda, Emulsion-derived foams (PolyHIPEs) containing poly (ε-caprolactone) as matrixes for tissue engineering, Biomacromolecules 2(1) (2001) 154-164.
[65] C.R. Langford, D.W. Johnson, N.R. Cameron, Preparation of Hybrid Thiol-Acrylate Emulsion-Templated Porous Polymers by Interfacial Copolymerization of High Internal Phase Emulsions, Macromolecular rapid communications 36(9) (2015) 834-839.
[66] E.P. Childers, M.O. Wang, M.L. Becker, J.P. Fisher, D. Dean, 3D printing of resorbable poly (propylene fumarate) tissue engineering scaffolds, MRS Bulletin 40(02) (2015) 119-126.

[67] H. Page, P. Flood, E.G. Reynaud, Three-dimensional tissue cultures: current trends and beyond, Cell and tissue research 352(1) (2013) 123-131.
[68] G. Akay, M.A. Birch, M.A. Bokhari, Microcellular polyHIPE polymer supports osteoblast growth and bone formation in vitro, Biomaterials 25(18) (2004) 3991-4000.
[69] E. Knight, B. Murray, R. Carnachan, S. Przyborski, Alvetex®: polystyrene scaffold technology for routine three dimensional cell culture, 3D Cell Culture, Springer2011, pp. 323-340.
[70] R.S. Moglia, M. Whitely, P. Dhavalikar, J. Robinson, H. Pearce, M. Brooks, M. Stuebben, N. Cordner, E. Cosgriff-Hernandez, Injectable Polymerized High Internal Phase Emulsions with Rapid in Situ Curing, Biomacromolecules 15(8) (2014) 2870-2878.
[71] M.W. Hayman, K.H. Smith, N.R. Cameron, S.A. Przyborski, Growth of human stem cell-derived neurons on solid three-dimensional polymers, Journal of biochemical and biophysical methods 62(3) (2005) 231-240.
[72] M.W. Hayman, K.H. Smith, N.R. Cameron, S.A. Przyborski, Enhanced neurite outgrowth by human neurons grown on solid three-dimensional scaffolds, Biochemical and biophysical research communications 314(2) (2004) 483-488.
[73] P. Netti, Biomedical Foams for Tissue Engineering Applications, Elsevier2014.
[74] E. Lovelady, S.D. Kimmins, J. Wu, N.R. Cameron, Preparation of emulsion-templated porous polymers using thiol–ene and thiol–yne chemistry, Polymer Chemistry 2(3) (2011) 559-562.
[75] W. Busby, N.R. Cameron, C.A.B. Jahoda, Tissue engineering matrixes by emulsion templating, Polymer international 51(10) (2002) 871-881.
[76] L.S. Nair, C.T. Laurencin, Biodegradable polymers as biomaterials, Progress in polymer science 32(8) (2007) 762-798.
[77] Y. Lumelsky, J. Zoldan, S. Levenberg, M.S. Silverstein, Porous polycaprolactone-polystyrene semi-interpenetrating polymer networks synthesized within high internal phase emulsions, Macromolecules 41(4) (2008) 1469-1474.
[78] S.C. Baker, G. Rohman, J. Southgate, N.R. Cameron, The relationship between the mechanical properties and cell behaviour on PLGA and PCL scaffolds for bladder tissue engineering, Biomaterials 30(7) (2009) 1321-1328.
[79] V. Guarino, F. Causa, P.A. Netti, G. Ciapetti, S. Pagani, D. Martini, N. Baldini, L. Ambrosio, The role of hydroxyapatite as solid signal on performance of PCL porous scaffolds for bone tissue regeneration, Journal of Biomedical Materials Research Part B: Applied Biomaterials 86(2) (2008) 548-557.
[80] D.W. Johnson, C.R. Langford, M.P. Didsbury, B. Lipp, S.A. Przyborski, N.R. Cameron, Fully biodegradable and biocompatible emulsion templated polymer scaffolds by thiol-acrylate polymerization of polycaprolactone macromonomers, Polymer Chemistry 6(41) (2015) 7256-7263.
[81] A.L. Sisson, D. Ekinci, A. Lendlein, The contemporary role of ε-caprolactone chemistry to create advanced polymer architectures, Polymer 54(17) (2013) 4333-4350.
[82] C.X.F. Lam, M.M. Savalani, S.-H. Teoh, D.W. Hutmacher, Dynamics of in vitro polymer degradation of polycaprolactone-based scaffolds: accelerated versus simulated physiological conditions, Biomedical Materials 3(3) (2008) 034108.
[83] M.A. Woodruff, D.W. Hutmacher, The return of a forgotten polymer—polycaprolactone in the 21st century, Progress in Polymer Science 35(10) (2010) 1217-1256.
[84] H. Sun, L. Mei, C. Song, X. Cui, P. Wang, The in vivo degradation, absorption and excretion of PCL-based implant, Biomaterials 27(9) (2006) 1735-1740.

[85] N.R. Cameron, A. Barbetta, The influence of porogen type on the porosity, surface area and morphology of poly (divinylbenzene) PolyHIPE foams, Journal of Materials Chemistry 10(11) (2000) 2466-2471.
[86] K. Jerábek, I. Pulko, K. Soukupova, D. Štefanec, P. Krajnc, Porogenic solvents influence on morphology of 4-vinylbenzyl chloride based PolyHIPEs, Macromolecules 41(10) (2008) 3543-3546.
[87] D.C. Sherrington, Preparation, structure and morphology of polymer supports, Chemical Communications (21) (1998) 2275-2286.
[88] A. Barbetta, N.R. Cameron, Morphology and surface area of emulsion-derived (PolyHIPE) solid foams prepared with oil-phase soluble porogenic solvents: Three-component surfactant system, Macromolecules 37(9) (2004) 3202-3213.
[89] M.T. Gokmen, B. Dereli, B.G. De Geest, F.E. Du Prez, Complexity from Simplicity: Unique Polymer Capsules, Rods, Monoliths, and Liquid Marbles Prepared via HIPE in Microfluidics, Particle & Particle Systems Characterization 30(5) (2013) 438-444.
[90] J.B. McGlohorn, L.W. Grimes, S.S. Webster, K.J.L. Burg, Characterization of cellular carriers for use in injectable tissue-engineering composites, Journal of Biomedical Materials Research Part A 66(3) (2003) 441-449.
[91] P. Eiselt, J. Yeh, R.K. Latvala, L.D. Shea, D.J. Mooney, Porous carriers for biomedical applications based on alginate hydrogels, Biomaterials 21(19) (2000) 1921-1927.
[92] S.-W. Choi, Y. Zhang, Y.-C. Yeh, A.L. Wooten, Y. Xia, Biodegradable porous beads and their potential applications in regenerative medicine, Journal of Materials Chemistry 22(23) (2012) 11442-11451.
[93] A. Salerno, C. Domingo, A novel bio-safe phase separation process for preparing open-pore biodegradable polycaprolactone microparticles, Materials Science and Engineering: C 42 (2014) 102-110.
[94] A. Kabalnov, U. Olsson, H. Wennerstroem, Salt effects on nonionic microemulsions are driven by adsorption/depletion at the surfactant monolayer, The Journal of Physical Chemistry 99(16) (1995) 6220-6230.
[95] F.J. Bye, J. Bissoli, L. Black, A.J. Bullock, S. Puwanun, K. Moharamzadeh, G.C. Reilly, A.J. Ryan, S. MacNeil, Development of bilayer and trilayer nanofibrous/microfibrous scaffolds for regenerative medicine, Biomaterials Science 1(9) (2013) 942-951.
[96] I. Ortega, L. Dew, A.G. Kelly, C.K. Chong, S. MacNeil, F. Claeyssens, Fabrication of biodegradable synthetic perfusable vascular networks via a combination of electrospinning and robocasting, Biomaterials Science 3(4) (2015) 592-596.
[97] I. Mira, N. Zambrano, E. Tyrode, L. Márquez, A.A. Peña, A. Pizzino, J.-L. Salager, Emulsion catastrophic inversion from abnormal to normal morphology. 2. Effect of the stirring intensity on the dynamic inversion frontier, Industrial & engineering chemistry research 42(1) (2003) 57-61.
[98] A.K. Das, D. Mukesh, V. Swayambunathan, D.D. Kotkar, P.K. Ghosh, Concentrated emulsions. 3. Studies on the influence of continuous-phase viscosity, volume fraction, droplet size, and temperature on emulsion viscosity, Langmuir 8(10) (1992) 2427-2436.
[99] R.G. Richards, M. Wieland, M. Textor, Advantages of stereo imaging of metallic surfaces with low voltage backscattered electrons in a field emission scanning electron microscope, Journal of microscopy 199(2) (2000) 115-123.